A STUDY OF ZINC SEPARATION FROM AN ALKALINE LEACH LIQUOR USING FIXED AND MOVING BED ION EXCHANGE SYSTEMS

BY

SAAD ABDULKHALIK JAFAR

THESIS SUBMITTED TO THE C.N.A.A. IN PARTIAL FULFILMENT IN CANDIDATURE FOR THE DEGREE OF DOCTOR OF PHILOSOPHY

DEPARTMENT OF CHEMICAL ENGINEERING
THE POLYTECHNIC OF WALES
TREFOREST, PONTYPRIDD
MID GLAMORGAN
IN COLLABORATION WITH G.K.N. TREMORFA
STEEL WORKS, CARDIFF.

APRIL, 1984

C O N T E N T S

ACKNOWLEDGEMENTS

I would like to express my sincere thanks to the Director of Studies, Dr. M.S. Doulah for his guidance and supervision. I would like also to thank the second supervisor, Dr. G.J. Rees for his help.

The help given by Mr. R. Evans of the Department of Mathematics and Computer Science on computer programmes is appreciated and the permission of Mr. R. Scott on attending the course "Statistical Analysis and Design of Experiments" is greatly acknowledged.

My thanks also go to Dr. K. Burton of the Department of Science for giving his permission to use the instrument "Atomic Absorption Spectrophotometer" and to Dr. E. Morgan for demonstrating the instructions.

I thank all the technical staff of the Department of Chemical Engineering for their help in the construction and maintenance of the apparatus.

Thanks are also due to Miss. A.R. Anderson, the Technical Information Officer of Permutit Service Division for sending samples of ion exchange resins and writting to Rohm & Haas (UK) Ltd. and Dia-Prosium Ltd. to send samples of resin.

Finally I would like to thank Mrs. J. Winter for typing this Thesis.

DECLARATION

This is to certify that neither this thesis nor any part of it has been presented or is being concurrently submitted in candidature for any other degrees.

Candidate

Dated APRIL 1984.

CERTIFICATE OF RESEARCH

This is to certify that, except where specific reference is made, the work in this thesis is the result of the investigation of the candidate.

Candidate

Director of Studies

Dated APRIL 1984.

A STUDY OF ZINC SEPARATION FROM AN ALKALINE LEACH LIQUOR USING FIXED AND MOVING BED ION EXCHANGE SYSTEMS.

S.A. JAFAR

ABSTRACT

As far as it is known from the survey of literature this is the first study of the problem of Zn separation from NaOH solution through ion exchange. It was therefore essential to carry out a selection procedure for finding a suitable resin for the separation. Ten resins were tested from which Amberlite IRC-718 was selected. The resin was found to tolerate the high pH involving the process and give a favourable equilibrium relationship for 0.1 and 0.2M NaOH solutions.

Work concerning fixed and moving bed processes was done to determine various design parameters such as mass transfer coefficients, zone height, number and height of transfer units.

The kinetics of ion exchange was studied through fixed bed operation by obtaining breakthrough data. These data were analysed through a new method and also by the methods of Michaels, and Moison and O'Hern. For some data the methods of Michaels, and Moison and O'Hern were found to be inadequate while the new method was applicable to all the data. The kinetics of ion exchange was found to be controlled by diffusion of ions in the solution. This was also confirmed by the determination of activation energy which gave a value of 1.6 kcal/mole. Correlations for saturation time, zone height and zone velocity were established.

The extraction efficiency of 99.6% was achieved using a moving bed system with bed height of 24cm and solution flow rate of 7 ml/min. The height of transfer units was found to increase with Zn and OH ions concentration, solution flow rate, and cycle time. However, HTU was unaffected by bed height increase. Correlation of HTU with Zn concentration was established.

NOMENCLATURE

Dimensions of the symbols are given in terms of Mass (M), Length(L) and Time (T).

Symbol	Definition	Dimensions
A	frequency factor	LT^{-1}
a_p	effective interfacial area	L^{-1}
C_N	concentration of given ion after N theorectical stages or transfer units	ML^{-3}
C_o	initial ion concentration in entering stream	ML^{-3}
C_R	total concentration of ions in the regenerant solution	ML^{-3}
C_Σ	total ionic concentration of all the ions present in the solution	ML^{-3}
d_p	mean diameter of resin particles	L
D_L	effective counterdiffusivity of designated ion (with the eluting ion) in the solution phase	L^2T^{-1}
D_p	effective counterdiffusivity of designated ion (with the eluting ion) in the resin phase	L^2T^{-1}
E	slope of equilibrium line/slope of operating line	dimensionless
E_a	activation energy	ML^2T^{-2}
E_c	extraction coefficient	dimensionless
G_p	mass velocity of solid phase per unit cross section	$ML^{-2}T^{-1}$

h	height of resin bed	L
h_z	height of exchange zone	L
HTU	height of transfer units based on fluid film	L
$J(\alpha,\beta)$	$1-e^{-\beta}\int_0^{\alpha} e^{-\xi} I_0(2\sqrt{\beta\xi})\, d\xi$	dimensionless
K	chemical equilibrium constant for exchange	dimensionless
K_c	equilibrium constant in concentration terms	dimensionless
k_f	mass transfer coefficient for film diffusion	T^{-1}
k_p	mass transfer coefficient for particle diffusion	T^{-1}
L	volumetric solution flow rate in fixed bed	L^3T^{-1}
N_C	number of equilibrium contacts	dimensionless
N_R	number of reaction units	dimensionless
NTU	number of transfer units based on fluid film	dimensionless
Q	total ionic concentration of the resin or the ultimate capacity	MM^{-1}
q	concentration of given ion in ion exchanger	ML^{-3}
q_N	concentration of given ion in exchanger after N theoretical stages or transfer units	ML^{-3}
q_o	concentration of ion in exchanger at point where concentration in solution is C_o	ML^{-3}

R	separation factor for a single transition	dimensionless
R_f	volumetric solution flow rate in moving bed	L^3T^{-1}
R_p	volumetric resin flow rate in moving bed	L^3T^{-1}
R_R	volumetric flow rate of regenerant	L^3T^{-1}
S	cross-sectional area of column	L^2
T	throughput parameter based on concentration changes for transition of interest	dimensionless
t	time	T
t_{fa}	apparent residence time for fluid phase = hS/F	T
t_p	solid phase residence time = h_{p_B}/G	T
u_L	superficial liquor velocity	LT^{-1}
X	fluid phase concentration between 0 downstream and 1 upstream within a transition = $x-x_1/x_2-x_1$	dimensionless
X^*	value of X at equilibrium with Y	dimensionless
x	equivalent fraction of ion in solution with respect to the total ionic level of the solution	dimensionless
x^*	value of x at equilibrium with y	dimensionless
Y	solid phase concentration within a transition = $y-y_1/y_2-y_1$	dimensionless
y	equivalent fraction of ion on the resin with respect to the total capacity of the resin	dimensionless

y^*	equivalent fraction of ion in the resin in equilibrium with a given equivalent fraction in the solution	dimensionless

Greek symbols

γ	degree of approach to equilibrium transfer for a component in the solution phase	dimensionless
ε	external void fraction of resin bed	dimensionless
κ	rate coefficient in reaction-kinetic treatment	$L^3M^{-1}T^{-1}$
Λ	system partition ratio for a component or for total solutes = $q_o\rho_B/C_o$	dimensionless
μ	solution viscosity	$ML^{-1}T^{-1}$
ρ	density of solution	ML^{-3}
ρ_B	bulk density of resin	ML^{-3}

Dimensionless Groups

Pe	Peclet number	$d_p u_L \varepsilon / 6D_L(1-\varepsilon)$
Re	Reynolds number	$d_p u_L \rho / \mu$
Sc	Schmidt number	$\mu / \rho D_L$
Sh	Sherwood number	$k_f d_p / D_L$

CHAPTER ONE

INTRODUCTION

The ion exchange process was first observed in 1845 by Thompson[1] in studying soil fertilisation and in 1905 Gans[2], in Germany softened water industrially using natural and synthetic zeolites. The process was reversible, the zeolite being reconverted to the sodium form by means of brine. Water softening, whose application became world-wide remained the only application of ion exchange until 1934. In that year two inventions founded a new industry. The first was sulphonated coal, developed by Liebknecht in Germany. This was a tough, physically and chemically stable material, which would not only soften water but, unlike the zeolites, was also stable to acids, and could therefore be converted to the hydrogen form. It would then remove all cations, converting salts into the corresponding free acids. The second invention was the development of the first cation and anion exchange resins by Adams and Holmes[3].

The other developments in ion exchange came in 1942 when D'Alelio[4] in the USA invented the first polymeric ion exchange material, sulphonated cross-linked polystyrene, followed in 1949 by McBurney's[5] development of the corresponding anion-exchange resin, cross-linked polystyrene with quaternary ammonium groups. Polyacrylic resins, which were developed later, have advantages for some purposes, but the polystyrene materials remain by far the most widely used exchangers.

While initially ion exchange or base exchange, as it was called, was looked upon as simple exchange of ions, today it has become a unit process applicable to complex systems whether it be in biochemical laboratories for amino acid, nucleotide, and carbohydrate separations, or in industry for rare earths and radioactive nuclide separations. Exclusive of water treatment, one of the major field of applications of ion exchange has been in the processes concerning the concentration and recovery of valuable metals from solutions. In wet process metallurgy, such solutions include leach solutions, mine waters, filter washes and mother liquors and metal finishing. The removal of zinc from solution in hydro-metallurgical leach liquors is a problem which occurs in a wide range of processes. In the process of recycling of steel making dust the main contaminants are Zn and Pb. By leaching the dusts with NaOH both Zn and Pb can be taken into solution leaving behined a solid residue for recycling.

In a preceeding work Rasheed[6] studied the problem of Pb separation from the leach liquor through the technique of cementation which removes lead by adding some zinc in the liquor from a solid Zn surface. For the reuse of NaOH solution Zn must be removed. In the present work the problem of Zn removal from the leach liquor is studied through fixed and moving bed ion exchange systems. Previous work on the removal of zinc ion from aqueous solutions involved acidic, neutral and cyanide solutions. Zinc was removed by either a cation or anion exchanger. An extensive survey of literature indicates that the removal of zinc from an alkaline solution

of sodium hydroxide has not attracted the attention of many research workers. To select a resin that could give an effective separation of Zn from a solution of extreme alkalinity an elaborate search method was needed. First three resins in the sodium form were selected and tested, but, they were found unsuitable because of their physical weakness. Then seven resins were tried, amongst them Amberlite IRC-718(Na) was found to give good separation and at the same time possesses, high selectivity for Zn, stability over the entire pH range and resistivity to physical break-down.

With this resin experiments were conducted in fixed beds for kinetic studies. The kinetics of ion echange is dominated by five steps. These are (1) the diffusion of counter ions through the bulk solution to the surface of the ion exchanger, (2) diffusion of the counter ions within the solid phase, (3) chemical reaction between the counter ions and the ion exchange sites, (4) diffusion of the displaced ions out of the ion exchanger and (5) the diffusion of displaced ions from exchanger surface into the solution.

Steps (4) and (5) are the reverse processes of steps(2) and (1) respectively. Either a diffusion or a mass action mechanism depending on which is the slowest step, ultimately governs the exchange kinetics. In general, the diffusion of ions in the external solution is usually termed film diffusion control. This is a useful concept but hydrodynamically it is ill-defined. The diffusion or transport of ions within the exchanger phase is commonly termed particle diffusion control.

The chemical exchange of ions at the exchanger sites is observed in certain complex reactions. Hence, studies of ion exchange kinetics fall into three broad classifications which divide into two distinct categories.

The rate-controlling step depends primarily on the concentration of the external solution. Under ordinary conditions, i.e., moderate stirring and a moderately or highly swollen resin, diffusion through the film is the slow step with solutions of order of 0.01 N or less. Diffusion in the resin is ordinarily the slow step with solutions of the order 0.1 N or more.

Other factors having influence on the rate are

(1) Particle size of resin,

(2) Diffusion coefficient inside the resin which depends on;

  (a) The degree of swelling of the resin,

  (b) Temperature of the system,

  (c) Nature of the exchanging ions

(3) Diffusion coefficient in the aqueous film and

(4) Stirring.

For the determination of rate controlling steps an analysis of breakthrough curves is a must. Breakthrough curves can be analysed through the solution method of Thomas. This method however depends on a number of simplifying assumptions and thus reducing the range of applications. Furthermore Thomas solution assumes a rate equation expressed by the stoichiometry of the monovalent ion exchange reactions, which is more valid for reaction controlled exchange processes. In this work breakthrough curves obtained from fixed bed

operation were analysed through a new method which is described in Chapter (6). This analysis has provided the values of mass transfer coefficients, zone height and number of zones in a bed. Through this study in fixed bed useful information such as resin capacity, zone height, liquor velocity to be used and the overall mass transfer coefficients were obtained. Experience gained through the fixed bed operations has helped to select and set up a moving bed system. A moving bed system of the Higgins type was selected for further studies.

The Higgins contactor consists of two columns which are joined at the top and bottom. The solution flows in the first column are stopped after a period of several minutes, and the settings of the valves reversed. Hydraulic pressure is then suddenly applied to the top of the auxiliary column so that resin moves downwards, and up the main column. Some resin passes into the overflow pipe, where it is retained by the overflow valve. The two valves between the columns are returned to their initial settings and the solution flows are then restarted.

The apparatus used in this study are almost similar to that described above, however, there are some differences such as, auxiliary column being mounted to the supporting framework at a higher level which helped to avoid the use of hydraulic pumping and the columns were not connected at the top thus exhausted resin was collected from an overflow valve. The method of operation is a semi-continuous countercurrent and design informations on optimum resin and fluid flow rates for effective separation of Zn, number and height of transfer

units values and the optimum amount of resin in the bed were obtained.

Some work was also carried out on the regeneration process and the results are encouraging. This and the results obtained on the extraction of Zn will provide a basis for further work on a pilot plant scale.

C H A P T E R T W O

LITERATURE SURVEY

2.1 METALS REMOVAL FROM STEEL MAKING DUST

Over 2 million tons of dust containing approximately 1,100,000 tons of iron, 100,000 tons of zinc, 20,000 tons of manganese, and 10,000 tons of lead are produced by the steel-making industry each year. A 1970 Bureau of Mines survey of 95 steel mills showed average dust emission per ton of steel produced as follows: Open hearths, 25 pounds; basic oxygen furnaces; 40 pounds; and electric furnaces, 20 pounds. Based on the 1969 U.S. production of steel[7], it is estimated that 761,000 tons of open hearth dust, 1,200,000 tons of basic oxygen furnace, and 201,000 tons of electric furnace dust are emitted annually. At present these dusts are, for the most part, a wasted resource awaiting the development of suitable recycling methods.

The dusts are high in iron content. Therefore, recycling to the furnace appears to be a logical approach to the problem. To do this, however, requires that the dusts be converted to a suitable physical form. The wastes must also be sufficiently free of deleterious elements so as to neither adversely affect the subsequent melting operation nor add undesirable impurities to the steel.

Although numerous processes have been developed for removal of zinc and lead from steel furnace dustSonly a minor amount of dust is being recycled[8-12]. Most of these processes are expensive to install and operate and some of them are reported below.

Electrostatic precipitators were used by Thom[11,12] to collect iron oxide dust from the basic open hearths. The dust contained zinc and lead oxides and sulphur compounds and were removed by direct reduction in a rotary kiln.

Barnard et al[13] investigated various methods such as (1) pelletization and reduction roasting to remove lead and zinc, (2) sulphation with sulphuric acid or SO_2 followed by leaching to remove lead and metallize the iron, (3) pelletization of mixtures of dusts containing carbon, zinc, and lead followed by roasting to eliminate said elements, (4) and pelletization and roasting of mixtures of blast furnace dusts, basic oxygen furnace dusts, and mill scale.

Ikeno et al[14] in Japan treated open-hearth dust using various methods in order to remove zinc. The methods included acid leaching before or after roasting, chloridizing roasting, chloride volatilization, and reductive roasting of the dust with or without pelletizing.

A combination of leaching and ion exchange seems to be a more economical route.

Acid leaching was applied to steel making dust by Wakamatsu[15] in Japan. Zinc formed a negative charged chloride complex which was adsorbed by strongly basic anion exchange resin and the maximum adsorption of Zn was obtained from a solution of 2 N-HCl. In this medium most elements with which Zn is associated in the dust are not adsorbed by the resin. It is therefore possible to separate Zn from Fe, Al, Mn, Ca, Mg, Cr, and Ni. Zinc is then eluted from the resin with 0.3N-HNO_3. Part of Fe, Cu, Sn, Pb, and As

are adsorbed on the resin, but a subsequent EDTA titration procedure obviates their interference.

The recycling of complex heavy metal wastes using solvent extraction and ion exchange was discussed by Van Veen[16] in order to solve environmental problems. In the ion exchange process, the solid waste is treated with 6M HCl at high temperature to dissolve all metals. The residue is filtered off. The solution is treated by MIBK to remove Fe^{3+}; back extraction gives $FeCl_3$ with high purity.

The raffinate is led through an anion exchange column. The metals Cu, Pb, Zn and Cd are fixed as chloride complexes, while Cr, Ni, Mn, Ca, and Na pass through. For the separation of Ni and Cr from this eluate several techniques are available one of them is electrolysis; subsequently, Mn can be removed by precipitation.

The separation of the adsorbed metals Cu, Pb, Zn, and Cd takes place by elution with HCl solutions of decreasing strength. Recovery of HCl from Pb and Cu eluates takes place by distillation in the presence of sulphuric acid. Products are obtained as sulphates. HCl can be recycled within the process.

The Zn and Cd eluates can be treated by a cation exchanger in order to obtain sulphates. Electrolysis can be applied to obtain the materials in the metal form. Cobalt can also be recovered with this process. An aspect of this process is that liquid wastes can be introduced directly, without pretreatment (except the 6M HCl conditions). Moreover, a broad spectrum of wastes can be treated without leaving

residues that have to be considered as hazardous.

Van Veen[16] also evaluated both processes considering the revenues of the products, operating costs, separation spectrum, legislation with respect to dumping, and types and composition of wastes. Based on the revenues and operating costs, both processes were roughly equal. However, the ion exchange process showed a broader separation spectrum which was an advantage from the point of legislation. The author[16] reached the conclusion that the recycling of heavy metal wastes could be economically feasible.

The problem of lead separation from electric arc furnace (e.a.f.) steel-making dusts was studied by Rasheed[6] using a cementation process. Non-ferrous metals present in the e.a.f. dust were separated by hydrometallurgy involving alkaline leaching. During the leaching of the dust, the iron compounds remained in solid form. The non-ferrous metal fraction entered the solution and was separated from the iron compounds by filteration. Using zinc as cementing metal lead was removed from the liquor. This led to the present study which involves the removal of zinc ion from sodium hydroxide solution through ion exchange. Thus sodium hydroxide can be concentrated and reused in the process (in the leaching step).

Davies[17] discusses the unit operations involved in all hydrometallurgical processes. They are broadly classified into separation and non-separation processes. The separation processes in hydrometallurgy include leaching, filteration, centrifugation, floatation, liquid extraction, cementation, ion exchange, membrane separation and electrowinning. The

non-separation processes are usually referred to operations such as crushing, grinding, communition and conveying. The author[17] also discusses the step-wise processes found for separation and non-separation processes in hydrometallurgy with specific reference to Sherrit - Gordon cobalt/nickel process. The choice of solid-liquid separation equipment will depend on the specifications placed for solution purification. These in turn are set by the separation method used, solvent extraction, ion exchange membrane processes etc. Davies[17] also recommended the use of recycle streams to increase overall separation and recovery and to reduce entrainment and loss from the process. With respect to processing of solids it is one industry where the waste from a process is dumped and is later reworked as either economics and/or technology improves to make the processing of a lower assay material possible.

2.2 TYPES OF ION EXCHANGE RESINS

Water softening was the main application of ion exchange. The ion exchangers were either natural or synthetic inorganic alumino silicates. These ion exchangers had to be used in neutral solutions since they were unstable outside of the pH range 6.5 to 8.5. With the discovery by Adams and Holmes in 1935 that polar groups could be fixed on polymeric matrices, development began and continued on a whole series of ion exchangers to meet the needs of industry, especially the new sophisticated technologies that came after World War II, for example, nuclear, microcircuits, and pharmaceuticals. Table 1 gives a list of the ion exchangers by function that are available today. Ion exchangers derive their properties from various functional groups that are fixed to polymeric matrices. Table 2 lists the most common groups utilized for ion exchange.

The weakness of the condensation type of polymeric materials to which were attached the fixed polar groups became evident during the period of their use (1935 to 1945). The development of the sulfonated and aminated copolymers of styrene-divinylbenzene placed the ion exchange process on a firm base for large industrial uses under conditions not previously possible.

To overcome fouling of the ion exchangers by foulants present in some waters and solutions, macroporous and isoporous matrices were developed. In the former, the matrix has large fixed pores so entering foulants can diffuse out

on regeneration. In the isoporous exchangers, the pores are uniform, and the small pores which prevent the entering foulants from diffusing out are eliminated.

The ion exchangers can be made in particle, bead, powder, and membrane forms. They also have been made as fibers, cloth, tubes, and foams as well as coated on various materials.

TABLE 1 LIST OF ION EXCHANGERS BY FUNCTION

Cation exchangers
- Strong acid
- Weak acid

Anion exchangers
- Strong base
- Weak base
- Medium base

Miscellaneous
- Chelates
- Retarding exchangers
- Extracting exchangers
- Precipitating exchangers
- Specific exchangers
- Adsorbing exchangers

TABLE 2 POLAR GROUPS UTILIZED IN ION EXCHANGERS

Cation exchangers
- Sulfonic
- Carboxylic
- Phenolic
- Phosphoric
- Thiol
- Specific groups for specific ions

Anion exchangers
- Primary amines
- Secondary amines
- Tertiary amines
- Quaternary amines
- Pyridinum
- Sulfonium
- Hydroxyapatite (inorganic)
- Specific groups for specific ion removal

Chelates
- Iminodiacetic acid
- Amidoxime
- Carbamates
- Amino - phosphonic
- Isothiorunium

2.3 APPLICATION OF ION EXCHANGE PROCESS

2.3.1 PICKLING OF STEEL

Much of the pickling of steel is done today with hydrochloric acid because it reacts more rapidly, attacks the oxide in preference to the parent metal, and can be used at ambient temperature. The pickling is done with an 18% acid concentration and ends when the concentration is reduced to about 2%. The latter solution containing $FeCl_2$ and residual acid is often used for stripping zinc from galvanized rejects with the zinc accumulated in jigs during galvanizing operations.

At one time, the waste solutions were dumped after being neutralized. But due to legislation, methods have been developed to recover the iron as iron oxide, the chloride as hydrochloric acid, and the zinc as zinc sulphate.

Haines et al[18] in South Africa developed a process called "Metsep" for the removal of zinc from the pickle liquor. The process was designed to treat two streams:

(a) uncontaminated pickle liquor containing about 220g of $FeCl_2$ and 31g of hydrochloric acid per litre.

(b) contaminated pickle liquor containing about 73g of $ZnCl_2$, 230g of $FeCl_2$ and 30g of HCl per litre.

The uncontaminated material is fed direct to a spray roaster in which the ferrous chloride and small quantities of ferric chloride are decomposed to oxides of iron and HCl.

The zinc contaminated pickle liquor is fed to a continuous ion exchange plant in which the zinc chloride is pickled up as $ZnCl_4^-$ while the effluent goes to the zinc-free pickle liquor for roasting.

The zinc chloride is eluted from the anion exchanger with water. The zinc is then converted to zinc sulphate through liquid ion-exchange extraction and elution by means of H_2SO_4. Thus, this plant received a waste product and produced marketable recycle acid, marketable FeO and Fe_2O_3 and $ZnSO_4$ which could be sold to zinc refiners for electrolytic recovery. The only waste product was steam from the pyrohydrolysis reactor. The ion exchange plant was closed when the source of zinc contaminated acid ceased[19,20].

2.3.2 CYANIDE PLATING

The major problem with the removal of cyanide by ion exchange is the poisoning of anion resins by the tightly held metal cyanide complexes. As a result the anion resins are very difficult to regenerate. However, as long as the cyanide concentration is low, little or no poisoning of the resins will occur.

Early work by Bloodgood and Losson[21] on the removal of cyanide and Chromium from metal plating wastes by ion exchange revealed that,

(1) it is possible to materially reduce the cyanide content in metal plating wastes and other aqueous solutions by means of a cation and anion exchanger used in series,

(2) Chromate can be removed from solution by ion exchange,

(3) plating wastes can be purified by ion exchange with essentially demineralized water being produced from these wastes, and

(4) Adsorbed Chromate is difficult to recover.

Later Walker and Zabban[22] investigated the removal of cyanide ions from segregated dilute copper, zinc, and silver plating solutions using Dowex and Amberlite ion-exchange resins. The concentration of the dilute plating solutions varied from 20 to 1000 ppm of total CN. The ion exchange system consisted of a strong acidic cation resin in the hydrogen form in series with a strong basic anion resin in the hydroxide form. The cyanide and metal ion concentrations in the treated effluents in most cases were less than 0.1 ppm (total CN) and 0.2 ppm, respectively, while the concentrations in the regenerant wastes varied between 5 and 30 g/1. A 10% sodium hydroxide regenerant solution was passed through both exchangers. However, the cation-exchange resin had to be regenerated a second time with about 10% solution of hydrochloric acid to replace the sodium ions with hydrogen ions.

After the passage of a decade Tallmadge[23] used a mixed-bed system containing a strong acid cation resin (Amberlite IR-120) and a strong-base anion resin (Amberlite IRA-410) to treat a synthetic mixed electroplating waste containing anionic cyanide complexes of copper and zinc, and sulphuric, phosphOric, and chromic acids. The concentration of each of the metals (copper, zinc, nickel, and chromium)

did not exceed 13 mg/1, while the cyanide concentration was 18 mg/1 (as CN). The total solids content was 540 mg/1. The test data showed that over 99% of both the heavy metals and cyanides could be effected. However, because of the high selectivity of the anion-exchange resins for the anionic cyanide complex, the only effective regeneration procedure for the anion resin was a two step treatment first using sulphuric acid to break the cyanide complex and then caustic to replace CN.

Recently Kawaguchi and Imai[24] in Japan recovered zinc from synthetic cyanide rinse water using beds of a weak-acid exchanger in the hydrogen form. The total exchange capacity of Zn was 1/4∿1/12 the overall capacity.

2.3.3 TEXTILE WASTES

The textile industry has two waste waters containing valuable metals. These are as a result of the manufacture of rayon. There are two processes in general use for rayon manufacture, the xanthate and the cuprammonium, in both of which very large volumes of water are used during the rinsing of the filament, and these emerge contaminated with zinc and copper respectively. These solutions are being treated successfully by cation exchange on a large scale in U.S.A. and in Germany[25,26]. In the case of the cuprammonium wastes, the cation exchanger is operated in the hydrogen cycle, and the regenerant is recycled to build up its copper content. Eventually it is neutralized and the copper

precipitated and subsequently redissolved. In the xanthate process, rayon is manufactured by reacting the sodium salt of cellulose with carbon disulphide to form a cellulose anthate. This solution is then extruded as fibre filaments into a solution containing sulphuric acid and zinc sulphate is obtained. The solution, containing approximately 100ppm Zn, is treated with a strong-acid cation exchanger to recover the zinc. This was made possible following the development of two unique processes for metal recovery by cation exchange by Mindler and Coworkers[27].

The original sulphuric acid-zinc sulphate solution can be used as a regenerant, since the sulphuric acid concentration is sufficiently high that little of the contained zinc is adsorbed by the resin. Increasing amounts of zinc sulphate in the regenerant tends to reduce regeneration efficiency; however, the effect is not marked until the $ZnSO_4$ concentration exceeds 10%.

The findings of Mindler et al[27] were on the recovery of tin and zinc. In the tin recovery process, sodium stannate wastes are derived from the rinses of continuous sheet metal tinning mills of the electrolytic type. The waste water has a temperature of about 170°F. It contains approximately 600ppm of sodium stannate in addition to the salts in the water used for rinsing; the pH is 8.1. A typical tin plating bath of sodium stannate is diluted to 675ppm of tin with demineralized water and used as an influent. The rinse water is passed through Permutit Q and filtered by the sludge filteration principle before more than a trace of tin

is present in the effluent. The clarified water, after separation of the precipitated metastannic acid, posses 30 ppm sodium; the pH is about 3. Such water can be neutralized and re-used for rinsing tinned sheet metal; thus both the water and the heat values in the rinse water are conserved.

For the second process, the removal of zinc ion from strongly acid solutions using Permutit Q, the authors[27] found that at sulphuric acid concentration below 0.1%, the removal is virtually complete and at concentrations of 0.5 to 1.0% H_2SO_4, the removal is greater than 95% from solutions containing 500ppm of zinc. At higher concentrations, the effluent from Permutit Q bed contained high quantities of zinc slippage. The exhausted resin is regenerated using sulphuric acid and concentrations of over 10% zinc sulphate containing relatively small amounts of H_2SO_4 are recovered. These recovered solutions may often be re-used directly in the processes from which the wastes arise or they may be concentrated for the production of the zinc salts.

Bowen et al[28] conducted extensive research on the recovery of zinc from rayon plant sludge. The sludge was accumulating in basins over 25 years and had 80 million-Lb. of zinc in it. During 27 years, some 23 processes were investigated for the recovery of zinc in a usable form from the waste stream or from sludge lagoons for internal use or sale to outside concerns. Twenty two of these techniques were rejected or tried for brief periods before discarded. In general, the economics were poor or the impurity

concentration in the recovered zinc was too high for re-use. Numerous ideas were bench-scaled, and others went through fairly elaborate pilot plants. Several reached commercial production and ran for several years on a marginal basis. Amongst them was ion exchange which was tested extensively on a pilot plant and was run on a commercial scale for three years. Full recovery efficiencies and severe material of construction problems caused a shutdown. Both calcium accumulation and resin fouling were problems. Recovery cost was about the same as the newly developed heat treatment process which was described in the publication. The typical compositions of basin sludge was, solids 4.5%, zinc 34%, iron 0.5% and calcium sulphate 8% (all based on solids).

The authors[28] also suggested that of all the processes examined in the light of 1977 economics, pressure filtration of a heated sludge that has broken the gel was the most economically feasible. This process combined the two important factors of good economics with a good product: a relatively concentrated zinc sulphate solution of an acceptable purity for reuse and/or sale to others.

A chelating resin containing a hydrazide group was used in Japan by Egawa and Maeda[29] to remove Na^{+}, Zn^{++}, and Ca^{++} from waste solutions from the viscose rayon industry. Adsorption of Ca^{++} decreased with increasing amount of Na^{+} in the solution and with decreased of flow rate. The breakthrough capacity of the resin was 22.2g of Zn^{++}/1. resin. Zinc was eluted by H_2SO_4.

A process for the recovery of zinc ions from waste

solutions in the processing of viscose by ion exchange has been patented by Kollar[30]. Strongly acid cation exchangers of polystyrene cross-linked with divinylbenzene (Katex S) adsorbed Zn^{++} from strongly acidic waste solutions. Retained Zn^{++} was eluted with spent baths containing 5-15% H_2SO_4 and 10-25% Na_2SO_4, in which Na^+ ions functioned as the elution agent for Zn^{++}. The eluates were adjusted to the desired composition and recycled.

Glover and Pratt[31] in U.S.A. invented a process to recover zinc from viscose rayon production. Zinc was removed from used acidic solution by cation exchange and recovered from the ion exchanger with a solution containing 20% H_2SO_4. This acidic $ZnSO_4$ solution was returned to the rayon production solution. Thus, in the production of rayon, the used $ZnSO_4$ solution can be continuously removed, purified, and returned to the production baths.

Carboxyl cation-exchangers were used by Morgenshtern and Matorenok[32] for removing zinc from waste waters of the viscose industry. Weakly acidic ion exchange resins KB-2-14/40 or KB 2-14/50 (both based on divinylbenzene and unsaturated carboxylic acids) were more effective in removing Zn^{++} from the effluents of viscose rayon manufacture than strongly acidic resins such KU-2. The resins have 4.1-4.2 meq. Zn^{++}/g. ion-exchange capacity at pH 6.4, and remove Zn^{2+} from the effluents containing 1053mg/l Zn^{2+} and 18.5g/l salts. The desorption of Zn^{2+} from the exchangers requires 2-2.5 volumes of 10% H_2SO_4/volume resin. The desorbed concentration contains 30-5 g/l. Zn^{2+} (as $ZnSO_4$). The exchangers are regenerated

with 4% NaOH solution and 2 gequiv. are required per gram of resin.

2.3.4 BRASS MILL

The brass-mill wastes are the result of pickling and bright-dipping brass in acids during its fabrication. Sulphuric acid, chromic acid, nitric acid, and mixtures of these are used. The over-all waste therefore may contain these anions along with the cations copper, zinc, trivalent chromium, and the ions present in water sent to the rinsing tank. The most satisfactory treatment scheme involves segregation of the wastes containing chromium from the remainder. Cation exchange may be applied directly to the bright-dip bath for removal of metal cations and substitution of hydrogen cations so that this bath does not require dumping. This eliminates most of the chromium waste problem. The remainder of the brass-mill wastes, which make up by far the largest volume and most difficult disposal problem, are also treated by cation exchange. These are chiefly dilute sulphuric acid solutions containing copper and zinc.

The separation of copper from zinc by ion exchange has been studied by Breton and Schlechten[33]. Amberlite IRC-50 and Amberlite IR-120 were used and the Carboxylic resin was found to be more effective than the sulphonic one. The latter demonstrated a greater capacity over a wider pH range. The copper and zinc were removed from the saturated resin by passing 10% sulphuric acid as a regenerant for Amberlite IR-120.

Amberlite IRC-50, due to its inefficient exchange of copper for sodium, was regenerated in two steps. First, the copper and zinc were removed with 10% H_2SO_4 and then the resin was converted back to the sodium form with 4% caustic.

Later Blake and Randle[34] investigated the removal of Zn^{2+} from the ternary system Zn^{2+}-Na^+-H^+ by cation exchange. Very dilute solutions containing zinc sulphate, sodium and sulphuric acid were passed down a column of Zeo-Karb 225 cation-exchange resin. The authors[34] concluded that the absorption of zinc was decreased markedly at concentrations 0.3% $ZnSO_4$ in solutions containing 0.1% H_2SO_4, and 0.07% $ZnSO_4$ in 0.1% H_2SO_4. Blake and Randle[34] also observed competition between Zn^{2+}, H^+, and Na^+ for resin sites which were in the hydrogen form. At equilibrium, the affinity of the resin is in the order, Zn^{2+}, Na^+, H^+. However, at high flow rate, the limiting factor in the exchange will be the mobilities of the ions and therefore the affinity of the resin is then in the order H^+, Zn^{2+}, Na^+.

2.3.5 PRECIOUS METALS RECOVERY

With precious metals, there is an additional incentive for treatment of rinse waters because of the value of the metal to be recovered. A good example is to be found in a gold plating line where flowing rinses can result in loss of gold by dragout, and in drain lines. This gold is recoverable by ion exchange techniques as suggested by the patent of Nachod[35]. Ion exchange has been used for many years to

recover gold from rinse waters[36-40]. In solution, the gold is generally in the form of a gold cyanide complex and is removed by a strongly basic anion exchanger either in the hydroxide form or the chloride form. The capacity of the resins are in the range of 20 to 35 troy oz of gold per cubic foot of resin with gold recovery of over 95%. A number of techniques for eluting gold from the anion resin were tried, but the simplest approach is to burn the gold off the resin as recommended by the patent cited.

New ion exchangers have been developed with higher capacities for gold. The capacity of the Pyridinium Type I strong-base anion exchanger is in the range of 50 to 100 troy oz of gold per cubic foot of resin. A troy oz of gold is worth approximately $180 (1979 value) so that the value of gold recovered is $9,000 to $18,000 per cubic foot of resin. If the resin costs about $100 per cubic foot then the value of the recovered gold is approximately 100 to 200 times the cost of the resin.

Strafion MMRR, an isothiouronium chelating ion exchanger, is very effective for the recovery of gold and precious metals at low pH[41]. The capacity of the resin at a pH of 0.5 is 850 g/l. The resin also has a high capacity for removing mercury and methyl mercury; the capacity for ionic mercury is 545 grams Hg per litre of resin.

Another resin reported in the literature[42] is AATH-O which can be charged with HCl or H_2CO_3, is capable of taking up Au from $KAu(CN)_2$(I) solutions of acid, neutral, or strongly alkaline pH. At a pH of 3.5, 1 gram of dry AAT takes up

1.17 meq., or 23.1% of its weight in Au.

Water Management Chemicals Limited[43] is currently developing a resin specifically designed to recover precious metals in a usable form. This resin will in fact absorb any metal capable of chelation, but it is particularly effective for silver, platinum, palladium, gold and importantly rhodium which previously was extremely difficult to recover. Recovery rate of between 2-3 grams of metal/gram of resin has been reported.

2.3.6 URANIUM

By all odds one of the largest uses of ion exchange outside the field of water is in the recovery or precipitation of uranium from acid leach solution of the ores[19,26,44]. The chief uranium producing countries of the world are the U.S.A., Canada, South Africa, Nigeria and Australia. Total world production of uranium is about 30,000 tonne per annum, though these are predictions that this could increase considerably by the end of this century.

Uranium is recovered from the host mineral by leaching and subsequently the pregnant solution is clarified and purified using either ion exchange, liquid-liquid extraction or both processes in series. Pregnant solutions often contain less than 1000 ppm uranium as U_3O_8 and in the treatment of low-grade ore deposits this could be in the region 150-250 ppm U_3O_8. Purified products using both ion exchange and solvent extraction can produce a product concentrate containing

about 95% by weight U_3O_8.

The leaching is carried out using either sulphuric acid or alkaline solutions of sodium carbonate/sodium bicarbonate depending on the mineralogy of the ore. Acid leaching dissolves many elements besides uranium which are present in the ore body. Effective separation is possible from most impurities because uranium forms complex anionic species in sulphate solutions. Most of the other elements in the pregnant solution, apart from Fe^{3+}, form cations and therefore do not interfere with the separation process. The sorption of uranium from solution by a strong base anion exchange resin of the macroreticular type. Equally effective for sorption are weak base tertiary amine-type resins. Hot or cold sulphuric acid is the preferred eluant, however, nitrate ions or chloride ions can be used though these are less acceptable from an environmental point of view. Leaching with alkali requires that the uranium exists in solution in the oxidised state. In order to prevent the pH rising to a value in excess of 7.2, where the uranium will precipitate, sodium bicarbonate is used to buffer the hydroxide formed. The anionic $UO_2(CO_3)_3^{4-}$ complex will interact with an anion exchange resin in an identical way to the sulphate complex. Elution is usually performed with sodium chloride.

2.3.7 MISCELLANEOUS

This sub-section covers metal removal and recovery from various waste streams and the use of various ion exchange resins.

Early work by Berg and Truemper[45] on the separation of zinc, cadmium and mercury in aqueous and partial nonaqueous media has shown that the metal ions can be resolved as their anionic chloro complexes by an ion exchange chromatographic procedure. The metal chloro complexes were adsorbed from a 0.01M hydrochloric acid solution by an anion exchange resin Dowex 1, in the chloride form. Zinc and cadmium were eluted separately in that order with 0.01M HCl. Mercury then was removed with a 0.01 M HCl-0.1M thiorea solution. Resolutions were enhanced by the addition of a non-aqueous component to the 0.01 M HCl eluting solvent. The methods were simple and did not require a regeneration of the resin because the sample solvents and eluting solvents were hydrochloric acid mixtures and the resin was used in the chloride form.

Natural waters contain trace metals like Pb, Cu, Cd, Zn, Mo, and U. These can be absorbed by anion-exchange resins if they are negatively charged complexes[46]. There are several studies describing the use of these resins in columns to collect trace metals. The metals are stripped from the columns by reagents like 6M HCl. Selective absorption is achieved by adding an appropriate complex-forming reagent to the water before it is passed through the column; for example, Pb, Cd, and Bi are absorbed by a strong-base anion exchange resin from a solution 0.15M in HBr, while Zn and Cu are not absorbed. Selectivity is also achieved in the elution step.

Waitz[47] carried out work on the removal and recovery of heavy metals by ion exchange. Using Amberlite DP-1(Na), heavy metals such as zinc and cadmium were removed without

removing the alkaline earths such as calcium from a lagoon of one million gallons of acidic waste water with the composition = Calcium 391 ppm, Magnesium 350 ppm, Zinc 91 ppm, Sodium 57 ppm, Manganese 3.5 ppm, Cadmium 0.12 ppm, and Nickel 0.12 ppm. The principal anion was sulphate, although quantities of chloride and bicarbonate were also present. Total dissolved solids were 3550 ppm and the pH was 4.7. Regeneration was accomplished with 4 Bed volumes (BV) of 1 N-HCl followed by 4 BV of deionized water. The acid waste regenerant was treated with lime to precipitate the heavy metals as insoluble hydroxides and oxides. In this case the lime dosage had to be sufficient to reach pH of greater than 10 to effect the maximum precipitation of zinc and cadmium. The supernatant liquid from the precipitation step was recycled to the waste lagoon since the zinc concentration exceeded 0.5 ppm. The sludge was burried in a suitable land fill.

Ion exchnage resin and equipment costs were less than $3,000. Regenerant requirements were 200 pounds of acid per cycle with 225 pounds of sodium hydroxide per cycle required to return the resin to the sodium form. There were 38 cycles to treat the entire 1 million gallon lagoon. The entire operation was carried out at a cost was less than $10,000 in 1975 exclusive of labor. This included equipment start-up costs and the required analytical work. Considering the fact that during rainstorms this lagoon would overflow into local stream and cause water pollution, it was worth while. In addition, the treated water was suitable for use in spray

irrigation.

Amberlite XE-279, an acrylic strong basic anion exchange resin was used by Avery and Waitz[48], to remove cyanide from waste stream. After the cyanide complexed by the addition of ferrous ion, the waste stream was passed through a sand filter to the ion exchange vessels. The vessels were operated in a 2-bed "merry-go-round" mode.

The regeneration was effected with a total of 4 BV of 15% NaCl at a flow rate of 2 BV/hr. The first 2 BV eluted $>$ 95% of the adsorbed cyanide and were discarded. The second 2 BV completed the regeneration by eluting the last traces of cyanide from the bed. To minimize the volume of spent regenerant the last 2 BV were diverted to a recycle tank for reuse.

Following laboratory studies on a number of cyanide-containing streams, field studies were conducted and a pilot plant was set up to treat a waste stream which had varying concentrations of ferrocyanide and ferricyanide. The pilot plant consisted of a 2" diameter column containing 1,200 ml. of resin. The waste stream contained Fe, Cu, Al, Ni, Zn, Na, F, P, CO_3, TDS, and SCN. The concentration of Zn was 0.05 ppm and that of total cyanide was in the range 100-700 ppm. The pH of the waste stream was 10.5.

Quarm[49] recovered copper from mine drainage water by ion exchange. A carboxylic ion-exchange resin (Amberlite IRC 50) was employed to adsorb copper selectively from mine waters containing 0.15-0.30g of copper and 1.5-3.0g of iron per litre. In the laboratory, resin in the sodium form adsorbed over

90 percent of the copper and only 4 percent of the iron, but a further 12 percent of the iron was precipitated in the resin bed. Elution with sodium chloride solution recovered the adsorbed metals, and dilute acid dissolved the precipitate to form a middling product that could be recirculated.

At the field station, no iron was precipitated in a larger bed of resin in the calcium form, and the adsorbed metals were recovered with dilute acid. Here, treatment of a water containing 0.14g of copper per litre produced a solution containing 6.02g per litre. Exploratory tests indicated that refined copper powder could be extracted from the solution by electrolysis. Along with copper and iron, zinc, arsenic and sulphuric acid were present at concentrations of 0.2 - 0.4g, 0.01 - 0.03g and 0.0 - 0.5g per litre respectively and the pH was 2.8 - 4.0.

The advantages of using ion exchange to recover chromic acid from wastes generated during the anodizing of aluminium, chromium plating and copper stripping over a chemical disposal method have been reported by Paulson[50]. In these aforementioned processes, chromic acid becomes contaminated with metallic cations, lowering its effectiveness and requiring replacement as a certain amount is lost through dragout on the surface of the work. The wastes resulting from these sources have always been an expensive nuisance. A variety of disposal methods have been considered and installed, however, ion exchange process eliminates stream pollution and return the chromate in usable form to the

treatment tank. The system consists of a cation exchanger (Permutit Q) to remove metallic cations from the strong chromic acid anodizing solution and an anion exchanger (Permutit S) to recover the chromate from the dilute rinse solutions.

The advantages of using ion exchange process are:

(1) Initial and installation costs are reduced by 50%.

(2) Operating costs are lowered by 75%.

(3) Approximately 80% less floor space is required.

(4) Reduces consumption of strategic materials by 90%.

(5) Reduces water and steam consumption by 85%.

(6) Insures better plating and anodizing efficiency.

(7) Higher quality finished product is assured.

A new process for the separation of iron from solutions of cobalt and other base metals using recently developed resins, the methyl and ethyl esters of Poly (iminoethenedithio carboxylic acid) has been developed by Birch and coworkers[51]. This resin is capable of selectively removing ferric iron from cobalt solution. Solutions of copper sulphate and ferric sulphate of 0.1M were passed through the resin bed and hydrochloric acid or 0.2M EDTA solution were used as elutant. Fe^{3+} was stripped fairly rapidly from the resin whereas Cu^{2+} was more difficult to elute, needing stronger hydrochloric acid (3M), a longer elution time and a higher elution volume. Sodium hydroxide was used to regenerate the resin to Na-form.

Hirsch et al[52] prepared two macroreticular chelating ion exchangers, one contains the iminodiacetate group and the second contains the arsonate group as the ion exchanging site.

Chromatographic separations on the new resins are rapid and sharp. The selectivity order for the iminodiacetate resin is $K^+ < Mg^{2+} < Ca^{2+} < Mn^{2+} < Ni^{2+} < Co^{2+} < Zn^{2+} \ll Cu^{2+}$. The selectivity order for the arsonate resin is $Mg^{2+} < Ca^{2+} < Mn^{2+} < Co^{2+} < Ni^{2+} < Zn^{2+} < Cu^{2+}$.

Sziden and Fritz[53] studied the elution of Fe^{3+}, U^{6+}, Al^{3+}, Cu^{2+}, Zn^{2+}, Cd^{2+}, Ni^{2+}, Co^{2+}, and Sn^{4+} with sulfosalicylic acid, HCl, and HF or HF-NaF mixtures from an iminodiacetate-type chelating resin.

The application of ion exchange process to metal ion removal and recovery has been discussed above, however, ion exchange has other applications such as sugar refining, nicotine recovery, sorbitol desalination, and amino acid recovery and separation. An excellent paper by Gold and Calmon[54] reviews the application of ion exchange process with emphasis on food, energy, resource recovery, and pollution abatement applications.

2.4 THE KINETICS AND MECHANISM OF ION EXCHANGE

The theory of ion exchange kinetics is well covered in a book and in a publication by Helfferich[55,56] and will not be repeated.

A review on ion exchange kinetics studies has been given by Gupta and Streat[57] covering the period 1969 to 1974. The review is confined to studies using strong acid exchangers, with no complexing reactions.

The kinetics of Na^+, Cs^+, Zn^{++} and Y^{+++} were studied by Soldano[58]. The self-diffusion coefficient of Na^+ at 10% crosslinking was higher than that for Zn^{++} and Y^{+++} and the activation energy when Zn^{++} was present increased from 5.2 kcal/mole at 4% crosslinking to 10.0 kcal/kg-mole at 24% crosslinking. The author[58] also found that the capacity of the resin and the ionic environment of the exchange system strongly influenced the ion exchange rate.

Boyd and Soldano[59] determined the self-diffusion coefficient of nine cations in sulfonated polystyrene-divinylbenzene type cation exchangers as a function of temperature and polymer cross-linking. The authors[59] observed a strong dependence of the diffusion coefficient on the formal cationic charge at all cross-linkings: In Dowex-50 at 25°C values of 2.88×10^{-7} for Na^+, 2.89×10^{-8} for Zn^{++}, 3.18×10^{-9} for Y^{+++} and 2.15×10^{-10} for Th^{++++} ion were reported. Increased cross-linking resulted in a sharply lowered self-diffusion rate. The coefficient at 25°C for Zn^{++} 1% DVB was 1.06×10^{-6} compared with 2.63×10^{-9} cm^2/sec.

in a 24% DVB exchanger. The activation energies were temperature but not charge dependent, increased with crosslinking from 4.7 to 10.0 kcal/kg-mole.

In an earlier paper by Boyd et al[60], the activation energy for particle diffusion was suggested to be higher than for the film mechanism (5-10 kcal/kg-mole for 0.1M solutions). The authors[60] also observed the following:

(1) The rate of the exchange adsorption of alkali metal cations (Na^+, K^+, Rb^+ and Cs^+) by the resinous zeolite Amberlite IR-1 can be described by equations on the basis of a diffusion mechanism or according to a bimolecular chemical rate process on the law of mass action.

(2) The rate was governed by diffusion through a liquid film at the periphery of the particle with solutions of 0.003M or less and controlled by diffusion in and through the adsorbent particle with solutions of 0.1M or greater.

(3) The primary factors determining the nature of the rate controlling mechanism were shown to be distribution constant (D_c) and the particle radius (r_o). Large values of D_c and/or small values of r_o favor a rate determined by film diffusion, if the temperature and flow rate are kept constant.

The effect of the electric potential produced by diffusion in ion exchange kinetics was examined by Schlögl and Helfferich[61] for the film diffusion controlled exchange of monovalent ions, Li^+ for H^+. The authors[61] have shown

that, rather than resulting in a minor correction, the electric field as a rule makes an essential contribution to the process.

Extensive experimental rate data using a single particle radioactive tracer technique for the component binary systems and the ternary systems Mn-Cs-Na, Ba-Mn-Na and Sr-Mn-Cs-Dowex 50W-x8 for the cases where particle diffusion is rate controlling have been obtained by Gopala Rao, Bajpai and Gupta[62]. The Nernst-Planck equations were used to describe the ion exchange kinetics. Under unfavourable equilibrium conditions, this model can not disregard the effect of liquid film resistance when correlating either binary or ternary diffusion. Incorporation of the film diffusional effects enabled satisfactory correlation of all the experimental data and even in cases where the fit was not perfect, the theoretical approach adequately interpreted the trend in the results.

Turner et al[63] measured the interdiffusion coefficient in Zeo-Karb 225, 8% DVB, ion exchange resin for the exchange of H^+ and Na^+ ions from 0.1M solutions. The variation of the interdiffusion coefficient with resin composition was determined by the authors[63] and the results were in good agreement with the Nernst-Planck model for diffusion in ion-exchange resin.

A theoretical model based upon irreversible thermodynamics for the description of ternary ionic diffusion rates inside ion-exchange resins has been proposed by Viswanathan and workers[64]. The model was in good agreement with the

experimental rate data obtained with the single-particle method for the Ba-Sr-Na-Dowex 50W-X8 systems in chloride solutions of 0.1N. Viswanathan and workers[64] also suggested that the single-particle method (which measures the concentration history of the resin phase directly) can be useful for measurement of ternary rate data in ion-exchange resins.

Hering and Bliss[65] reported observations on the rate of ion exchange in Dowex-50W resin. Ion pairs Na-Zn, Na-Ag, Ag-Al, Zn-Cu, Zn-Al, Al-Ce were studied under solid diffusion control. The effects of temperature and of resin cross-linkage were studied with the first system. Exchange in both directions was studied for each pair except the last.

The diffusion coefficients were obtained for each pair using Fick's law and were greatly dependent on the direction of the exchange as well as on the particular pair. The diffusivities of each ion were obtained using Nernst-Planck model and were greatly influenced by the nature of the second ion except in the case of sodium. Numerical solution of the flux equations was obtained for valence ratios of 1/3 and 2/3 with diffusivity ratios 5, 10, and 20 and for valence ratios of 3 and 3/2 with diffusivity ratios of 1/5, 1/10, and 1/20.

The activation energies for either model were reported to be 4 to 6 kcal/mole and the diffusion values decreased by 80% when the resin cross-linkage increased from 4 to 12%. The authors[65] also recommended Fick's law for design purposes because of its simplicity.

Single particle ion exchange data for systems: Zn-Zn, Cs-Cs, Na-Na, T-Zn, Na-Cs, Rb-Cs, Na-Cu, and Na-Ba were obtained by Van Brocklin and David[66]. Using the isotopic data, a single particle j factor curve for mass transfer with no ionic migration was developed. The isotopic results were compared with ion exchange results and indicated that the mass transfer rate (or coefficient) differed by 50% or more. The authors[66] were not able to select the best mass transfer model, but attempted to predict the mass transfer rate for (Ag-H, Cu-H, and Na-H), from the available literature. The validity of the method was indicated from fair agreement between predicted and experimental results. The authors[66] also discussed several methods for treatment of laboratory single particle data particularly velocity normalized plotting is useful for determining the presence of internal resistance. The significance of variable coefficients on breakthrough curves were also discussed.

Pan and David[67] carried out experiments to determine which, if any, of the models proposed by Van Brocklin and David[66] is most appropriate for predicting the liquid phase, packed bed, exchange rates with ionic migration effects included. The single- particle method was used in exchange of Na^+ and Ba^{++}, both radioactive, with H^+ in both directions with the flow rate being 2-60 gpm/ft^2. The laminar boundary layer model described the liquid-phase exchange rates the best in the Reynolds No. range 3-120. Using this model with the model of Helfferich and Plesset (1958) for the internal mass-transfer rate enabled the excellent calculation of the

overall ion exchange rates. This approach requires only self-diffusivity data for the ions, equilibrium data, and a generalized j-factor correlation for packed-bed mass transfer.

The rates of both the liquid-phase mass transfer and the internal-diffusion steps in ion exchange were studied by means of shallow-bed experiments by Selke et al[68]. The mass transfer coefficients obtained fitted the general correlations for other packed-bed operations when the Schmidt group was evaluated with experimentally determined ionic counterdiffusivities. An incremental calculation of the diffusion rates within the particles yielded a value of the counter-diffusivity in the resin phase. The authors[68] proposed a general design procedure based on these findings. The counterdiffusivity for Cu^{++}-H^{+} and Ag^{+}-H^{+} at 25°C were reported to be 0.80×10^{-5} and 1.74×10^{-5} cm^2/sec. respectively. The self-diffusion coefficient for Cu^{++}-H^{+}-Amberlite 120, 8 to 10% DVB was 1.1×10^{-6} cm^2/sec. Copper sulphate of 0.05N was used.

Giovanni et al[69] obtained rate equations for an ion-exchange system with 3 heterovalent counterions, considering that both liquid and particle diffusion affect the mass-transfer rate of the process. The Nernst-Planck model was applied to the ion exchange system strong cationic resin and seawater or its concentrated brines. The results of the authors[69] which were obtained through the kinetic model and those derived by Donnan's hypothesis equilibrium theory were consistent. Using mass transfer coefficients from literature gave concentration profiles which were in good

agreement with the experimental breakthrough curves.

A method for calculating the constant diffusion coefficient in particle diffusion controlled ion exchange has been developed by Lee[70]. The method seems to be adequate in spite of its theoretical dependence on ionic concentration as defined by Nernst-Planck equation. The diffusion coefficient is a function of the degree of exchange and a corrective scheme for such an effect is given. The rate constant for empirical rate equations was calculated by defining the adequate average particle size of a group of particles.

The rate of removal of oxalic acid from glycol solution was studied by Tien and Thodos[71] using the ion-exchange resin Permutit SKB under the control of the combined liquid and resin phase resistances. The equilibrium relation for the system fitted a Freundlich isotherm equation over the concentration range 0-0.12 meq. of oxalic acid/cm^3 . Liquid film and diffusion coefficients were experimentally determined and the breakthrough curve predicted.

Oleinik and Korshunov[72] investigated the kinetics of ion-exchange of labeled Zn^{++} and Pm^{+++} in the initial stages of the process using resin in H-form and 0.00245N solutions of ions at 19 $\pm$ 1 ^{o}C and pH 1.6 for exchange times of 5-50 seconds. Initially the rate follows a complex law and after a certain time interval it becomes constant. The authors[72] also observed that in the initial stage of sorption some factors hinder diffusion, the effect disappeared or diminished as a certain amount of ions were adsorbed on the resin. With

the help of ultrasonics Oleinik and Korshunov[72] found that the diffusion process produced an increase in the initial rate of sorption with a clearly shown minimum surface and bulk processes being considered separately. The authors[72] experimental results were in good agreement with the theoretical data.

Two approximate analytical solutions of the Dranoff equation (which includes both concentration and potential gradients) were suggested by Petrova and Lifshits[73]. The authors[73] experienced a difficulty in the application of the Dranoff equation to evaluate the influence of individual factors on the ion exchange kinetics. The mathematical treatment was tested on the exchange of methylene blue (I) on the Na^+-form of carboxymethyl cellulose under static condition at initial concentration of $I < 1.5 < 10^{-5}N$. The agreement between experiments and theory was good over the entire x_A range (0-0.55) but with the simplified solution of the Dranoff equation, good agreement was obtained only at $x_A \leq 0.25$. The rate constant of the iodine sorption increased with the stirring velocity, with the amount of ion exchanger in the system, and with the temperature. The activation energy was 3.8 kcal/mole (film diffusion controlled process).

Kawazoe et al[74] applied Rosen's analysis to the exchange of Na^{24} at the bed of a Na^{24}-Na isotope cation exchange resin. Kawazoe et al[74] found that the intraparticle diffusivity was constant and was not affected by the liquid concentration and resin particle size. A value of 1.2×10^{-6} cm^2/sec. at 20^oC was found for Amberlite IR-120 with particles of 0.090cm.

in diameter and the activation energy was 5 kcal/mole.

Dickel and Koerner[75] suggested that the kinetics of ion exchange is not adequately described by Fick's law with a concentration dependent diffusion coefficient. For the reversible reaction, the authors[75] found different diffusion coefficients at small concentration changes.

The kinetics of the ion exchange reaction of K^+ with Cd^{++} in a phenolsulphonic acid resin membrane was studied by Hermann et al[76] using a new polarographic method. The diffusion coefficients of Cd^{++} within the membrane were determined to be 2×10^{-6} cm^2/sec. at ionic strength of 1.0 and 1×10^{-6} cm^2/sec. at ionic strength of 0.1. In both cases D_{Cd}/D_K = 0.5-0.2. The results were in good agreement with the theoretical values obtained using Nernst-Planck relations.

Dranoff and Colwell[77] investigated the effects of slightly nonlinear equilibrium and axial dispersion on the performance of a packed bed ion exchange resin using dilute aqueous solutions of acetone and ethylene glycol. The authors[77] emphasised that using a linear model will give a false estimate of the intraparticle diffusivity of the solute within the resin beads, thus a computer model was developed which gave a close agreement with data.

The mass transfer of ions at a liquid film resistance on a resin surface was treated theoretically by Kataoka[78]. Ions having various diffusion coefficients necessitate the concentration of the gradient due to electric potential, in addition to the conventional concentration gradient. Nernst-Planck equations were modified to account for particular cases

where the concentration of the external solution was either constant or variable and a simplified discussion on the case where the diffusion coefficient in the resin phase has to be taken into account.

In another publication by Kataoka et al[79] theoretical equations for the rate of ion exchange were derived using Nernst-Planck model for the diffusion of an ion in the aqueous phase. The rate of ion exchange was measured in simple anion exchange systems with a jet apparatus. The results of the rate measurement indicated that the rate was not affected by the non-counter ion (e.g. Na^+ or Zn^{++} or Zn^{++} in an exchange system $Cl^- \rightleftharpoons No_3^-$ or $Cl^- \rightleftharpoons ACo^-$), and can be expressed by quantitative theoretical equations taking into account the electric field when the diffusivities of counter ions are not equal. The authors[79] also observed that the rate of ion exchange was decreased with an increase in the diffusivity ratio and the degree of this effect may increases with an increase in the equilibrium constant.

Nativ et al[80] determined the kinetics of ion exchange processes accompanied by fast chemical reactions and characterized by a sharp moving boundary between the reacted shell and the shrinking unreacted core within each ion-exchanger bead. Protonation of the carboxylic ion exchanger Amberlite IRC-50, $PdCl_4^{--}$ - Cl^- exchange on the strong-base anion exchanger Amberlite IRA-401, and chelation of Cu^{++} on the chelating ion-exchanger Dowex A-1 were investigated. Nativ et al[80] analyzed the rate data with the theoretical model and found that all 3 processes were controlled by the

rate of diffusion of the ions penetrating the reacted layer. Diffusion coefficients were determined from the graphical representation of the proposed model.

Equations for the calculation of diffusion coefficients and breakthrough curves were developed by Froelich[81] for the case Of internal diffusion as a step determining speed (gel kinetics) in ion exchange column including parameters such as concentration, time, throughput, quantity of exchanger radius of particles, characteristic constants loading and dynamic cases. The equations were tested for Sr-cation exchange on KU-2, and for Na-cation exchange on a sulphonated styrene-divinylbenzene polymer.

Kataoka et al[82] developed a model for intraparticle mass transfer of ion exchange coupled with instantaneous irreversible reaction and theoretical equations were derived assuming that the reaction plane arises in the resin phase and that the Nernst-Planck equation is applicable for the flux of counter ions and coion. Comparison was made between the numerical solutions of the model and Nernst-Planck model without reaction. The model was supported by experiments in cation and anion exchange systems.

A method for approximate solution of kinetic equations of ion exchange on a complexing ion exchanger was proposed by Chmutov et al[83]. The method is illustrated on RNa-Ni exchange at a constant diffusion coefficient.

2.5 THE RATE OF ION EXCHANGE

The effective rate of ion exchange is determined by one or more of several diffusional steps. The performance of equipment containing large number of particles will depend both upon local particle behaviour and upon the size and overall arrangement of the apparatus-whether countercurrent, fluidized bed, fixed bed, or batch. The design methods applicable to fixed bed equipment are given in this section. Design informations are obtained by solving the concentration history or breakthrough of column effluent.

Amongst the established theories is the Thomas solution [84] which is used widely for design purposes. It takes into account the curved shape of the equilibrium relationship, which has an important bearing on the shape of breakthrough curves[85]. Thomas[84] assumed that the rate of adsorption can be represented by an expression suggested by the stoichiometry of the monovalent ion-exchange reaction

$$Na^+ + RH \longrightarrow H^+ + RNa$$

$$\rho_B \frac{\partial q}{\partial t} = \kappa Q \left[C\left(1 - \frac{q}{q_m}\right) - \frac{1}{K}\left(C_o - C\right)\frac{q}{q_m} \right] \qquad (1)$$

The expression in square brackets is called the "kinetic driving force" and κ is the corresponding "kinetic coefficient". The rest of symbols are defined in nomenclature. His solution can be expressed as

$$\frac{C}{C_o} = \frac{J(n/K,\ nT)}{J(n/K,\ nT) + (1-J(n,\ nT/K))\exp((1-K^{-1})(n-nT))} \qquad (2)$$

$$\frac{q}{q_m} = \frac{1-J(n/K,\ nT)}{J(n/K,\ nT) + (1-J(n,\ nT/K))\exp((1-K^{-1})(n-nT))} \qquad (3)$$

where

$n=\frac{\kappa Q x}{u\varepsilon}$ = dimensionless distance or number of transfer units to position x.

$T=\frac{u\varepsilon C_o t}{q_m \rho_B x}$ = moles introduced with feed/moles needed to saturate bed to distance x.

$nT=\frac{\kappa Q C_o \hat{t}}{q_m \rho_B}$ = dimensionless time

$\hat{t}$ is the time following the arrival of a fluid particle, equal to $(t - \frac{x}{u})$, u is the velocity of fluid in interstics of bed and εu is the superficial fluid velocity.

Table given in Sherwood et al[85] lists values of the J function and a program developed by Tan[86] evaluates the J function using HP-25 programmable pocket calculator. Numerical values of J have been listed by Hougen and Marshall[87].

Gilliland and Baddour[88] derived an equation for the rate of ion exchange in a rather different form given by

$$\frac{d\bar{C}}{dt} = k\left(C(1-\bar{C}) - \frac{\bar{C}}{K}(C_o - C)\right) \qquad (4)$$

where the rate constant k, is

$$k = \frac{1}{(Q/k_L) + (C_o/Kk_R)} \qquad (5)$$

where Q/k_L is liquid side resistance and C_o/Kk_R is solid side resistance.

The integrated form of equation (4) is

$$\ln \frac{1 - E(x/x_e)}{1 - (x/x_e)} = kCt \qquad (6)$$

where

$$E = \frac{a + b}{a\ b}\ x_e - 1$$

$$C = \frac{2ab - x_e(a+b)}{x_e}$$

and x = concentration of H^+ in solution

x_e = concentration of H^+ in solution at equilibrium

a = initial concentration of Na^+ in solution

b = meq. of H^+ in resin initially per cc. of solution

t = time

Equation (4) expresses the rate of exchange in terms of average concentrations in the main body of the solution and in the ion exchange particles. In the derivation of the equation some important assumptions were made and these are summarized here:

(1) Equilibrium exists at the interface.

(2) The factors limiting the rate of ion-exchange are those which limit the rate at which ions are transported to the interface between the ion exchanger particle and the liquid, by whatever mechanism this transport is accomplished.

(3) For either phase, this transfer may be described by a rate equation of the form:

$$\text{Rate} = k' A(C - C_i)$$

where k' = mass transfer coefficient; A=area; C=concentration in bulk phase of material being transferred; and C_i= concentration at interphase of material being transferred.

The authors[88] applied the above method to the exchange of Na^+ for H^+ on Dowex 50 in NaCl solution of concentrations between 0.001N and 0.1N and have found that:

(1) The rate constant for ion exchange in a packed bed is not a function of bed height or bed diameter (except as this affects solution flow rate) so long as the column diameter is sufficiently greater than particle diameter-approximately twenty times as great.

(2) Both the resistance in the liquid phase and the resistance in the solid phase are important in determining the total resistance to ion exchange in the range of concentrations (0.01-1.0N), particle diameters (0.022-0.1005cm), and flow rates (0.0207-2.32 cm^3/sec.) tested.

(3) The concentration of ion in the exchanging solution affects the value of the rate constant, and this effect can be predicted with a moderate degree of success.

(4) The elution curves for the exchange of H^+ in solution for Na^+ on the resin can be predicted successfully from the rate data for the exchange of Na^+ in solution for H^+ in the resin.

Gilliland and Baddour[88] correlated their results with an equation, which summarized all the data on rate constants determined from the exchange of Na^+ in 0.1 N-NaCl solutions for H^+ in deep beds of sized spheres of Dowex-50 for a range of particle diameters (0.022 - 0.1005 cm), column heights (12 - 50cm.), and two different column diameters (1.5 - 3.0cm.). The equation is of the form:

$$\frac{1}{kd_p^2} = \frac{1010}{Re^{0.84} + 0.049} + 720 \qquad (7)$$

The authors[88] also used the Thomas equation[84] to predict the breakthrough curves and have shown mathematically that equation (2) tends toward constant-pattern or proportionate pattern behaviour in the limit $Kx/u\varepsilon$ becomes very large.

Kelly et al[89] tested Thomas equation[84] for the exchange of Na^+ in 0.1N-NaCl and 1.0N-NaCl with H^+ on Dowex 50W-X8 and have indicated that the assumption of constant-pattern conditions for favourable equilibrium is not generally valid. Solution-side mass transfer rates appeared to be affected by bed depth. Neither Thomas equation[84], nor its proportionate pattern limit for an unfavourable equilibria, satisfactorily described their results for elution processes where the hydrogen ion was involved. This was attributed to marked variations in selectivity during the course of breakthrough. The authors[89] utilised a hybrid computer to simulate their experimental results and recommended its use since factors such as varying selectivity and diffusion coefficients, axial dispersion and

resin swelling were taken into account.

Breakthrough curves for the exchange of Na^+ ions in 0.1N-NaCl in glycerol-water mixtures for H^+ ions in a fixed bed of Dowex-50 resin for Reynolds numbers from 0.01 to 2 have been obtained by Nutt et al[90]. Solutions containing up to 75% by vol. of glycerol and having viscosities up to 30 cp at 25°C were used. The total resistances to mass-transfer were calculated from the slopes of breakthrough curves and values of the liquid film resistance were estimated by the method of Gilliland and Baddour[88]. The values of the liquid film coefficient were correlated with flow rate, solution viscosity, and ionic diffusivity by the equation

$$k_L d_p^2 / D_L = 0.5 \times Re^{0.83} \times Sc^{0.75} \qquad (8)$$

The authors[90] found that the diffusivity, D_L, decreased with increase of the viscosity and that the exponents of the Reynold and Schmidt numbers differed from those values generally accepted to hold for other mass-transfer operations in packed beds and those which were also predicted by boundary layer theories.

Shallow-bed techniques were employed by Bieber and coworkers[91], to study the rate mechanisms for silver-hydrogen on Amberlite IR-120 cation-exchange resin. The authors[91] found that both liquid and solid diffusional resistances were significant under the conditions studied and the effect of chemical kinetics was negligible. The liquid-phase mass transfer coefficients varied as the 0.56

power of the velocity and inversely as the particle diameter and were independent of C_o(0.003-0.06 N-$AgNO_3$). Bieber and coworkers[91] fitted their rate results with an empirical overall equation of the form:

$$\frac{\partial(q/Q)}{\partial Y} = \frac{k_D S\, C_o}{QV}\,(1 - Bq/Q)(C/C_o - C^*/C_o) \qquad (9)$$

where

B = an empirical constant.

Y = volume of liquid through bed.

V = volumetric liquid-feed rate (column flow rate).

$k_D S$ = liquid-phase mass transfer coefficient.

(The rest of symbols are defined in nomenclature).

The difficulty in developing exact mathematical formulas for conditions of practical interest in the operation of ion exchange columns has led to the introduction of "exchange zone" method by Michaels[92]. The portion of the bed considered the exchange zone is that in which the feed concentration is reduced from 95% of the influent value to 5%. The method is based on the fact that for exchange with favourable equilibrium, the exchange takes place in a band of nearly constant length which moves down through the bed as it is being saturated. The exchange zone is a moving frame reference which can be regarded mathematically as a continuous system in which resin and liquid flow countercurrent to each other. The assumption is made that a steady-state process is taking place within this moving zone.

The height of the exchange zone, h_z, from C/C_o=0.05 to 0.95 can be calculated from the equation which is derived by

Michaels[92]

$$h_z = h \frac{V_Z}{V_T - (1-F)V_Z} \qquad (10)$$

where

h = total bed height

F = fraction residual capacity of exchange zone

V_Z = volume of effluent collected between C/C_o=0.05 and C/C_o=0.95.

V_T = volume of effluent collected upon exhaustion.

Zone height is correlated by Michaels[92] with superficial liquor velocity for the exchange of Na^+ with H^+ on Dowex 50 by the equation $h_z = 37.4\ u_L^{0.5}$ (11)

with h_z in cm and u_L in cm/s

and the overall liquid mass transfer coefficient is correlated by

$$K_L a = 0.86\ u_L^{0.50} \qquad (12)$$

Michaels[92] also derived the following equation for the determination of number of transfer units

$$NTU = \frac{K_L a\ h_z\ S}{L} = \frac{K}{K-1} \ln(19)^2 - \ln(19) \qquad (13)$$

L is liquid flow rate, K is the equilibrium constant, and S is the cross-sectional area of the column.

The height of transfer units is given by

$$HTU = h_z/NTU \qquad (14)$$

Michaels[92] found that useful exchanger capacity decreased with increasing liquor velocity and decreasing bed height and that exchange rate increased with increasing liquor velocity but was unaffected by bed height. Zone height was

proportional to the square root of liquor velocity suggesting that liquid film diffusion was the controlling step in the system Na^+/H^+-Dowex-50.

Later, a new equation for the determination of zone height was introduced by Moison and O'Hern[93], which is

$$h_z = \frac{V_z C_o}{S(Q + \varepsilon C_o)} \qquad (15)$$

and the rate at which the exchange zone moves down through the bed is

$$u_z = \frac{u_L C_o}{Q + \varepsilon C_o} \qquad (16)$$

The authors[93] studied the exchange of 0.01 and 0.1N-NaCl with H-form Dowex-50 resin. The analysis of many data has shown an effect of the ratio of bed depth to the particle diameter on the height of transfer units. The final correlation is linear plot on log-log coordinates of

$$j_D\left(\frac{h}{d_p}\right)^{0.28} = \frac{1}{HTU}\, a\left(\frac{\mu}{\rho D_L}\right)^{2/3}\left(\frac{h}{d_p}\right)^{0.28} \quad \text{vs.} \quad Re = \frac{d_p u_L \rho}{\mu}$$

The bed depth was reported to influence to some degree the HTU which was attributed to longitudinal mixing.

The effect of resistance to diffusion in the resin on the height of a transfer unit based on the liquid film was found by plotting HTU vs. the concentration for a given flow rate. Each plot was linear, however, the resulting values of the solid phase resistance depended on the 0.3-0.4 power of the flow rate. The authors[93] suggested that a greater proportion of the surface of the particles was available to the solution as the flow rate was increased.

Moison and O'Hern[93] also investigated the reverse exchange, hydrochloric acid with the sodium resin, for which the equilibrium is unfavourable. The results were compared with those predicted from the theoretical equation of Goldstein, which is based on equilibrium operation. While the results were in fair agreement, the differences between the curves indicated the existance of diffusional resistance.

Lukchis[94] proposed a method for analysing breakthrough data. Based on the mass-transfer-zone concept, column height and diameter can be calculated. The method is simple and effective for considering rate phenomena in fixed-bed adsorption systems. It is particularly amenable to rapid determination and correlation of rate data and to simple design procedures. Simple breakthrough curves provide the data required for the correlation of rate data in dynamic systems and the basic equation used for analyzing these data is given by

$$LUB = L_o\left(\frac{\theta_s - \theta_b}{\theta_s}\right) \qquad (17)$$

LUB is the length of unused bed, L_o is the total length of adsorbent bed, θ_b and θ_s are the breakthorugh time and stoichiometric time respectively.

In the derivation of equation (17), the following assumptions were made:

(1) The bed is uniformly packed

(2) The adsorbent temperature and initial adsorbate loading are uniform throughout the bed

(3) The feed rate, feed temperature and feed composition are constant

(4) There are no radial temperature, concentration or flow rate gradients

(5) The temperature of both the fluid and adsorbent are essentially equal

(6) The fluid does not undergo a phase exchange

(7) Adsorption heat effects are negligible

(8) Chemical reactions do not occur.

The above method was applied by Moseman and Bird[95] for the comparison between molecular sieve and silica gel in the desiccant dehydration of natural gasoline. The authors[95] have found that the LUB at the same superficial velocity was shorter for silica gel than for molecular sieve and have concluded that for the same length of bed, the potential capacity of the field desiccant vessel was higher for silica gel than for molecular sieve.

Gondo and Kusunoki[96] have described a technique for calculating the number of theoretical stages required for mass transfer achieved in a fixed bed operation. The authors[96] assume that mass transfer is so rapid that equilibrium is achieved instantaneously in each stage. The bed is divided into N stages of the same depth, containing a volume of Δh of liquid and ΔH of resin. The feed solution is considered to flow in units of Δh. For stage n and feed portion r a mass balance on a stage incorporating ε and the equivalent fractions x and y gives;

$$\varepsilon C_{\Sigma}\ x_{n-1}^{r} + (1-\varepsilon)\ Qy_{n}^{r-1} = \varepsilon C_{\Sigma}\ x_{n}^{r} + (1-\varepsilon)\ Qy_{n}^{r} \qquad (18)$$

where Q is the total ion exchange capacity of the resin, and C_{Σ} the total cation concentration of the liquid.

For a uni-valent/di-valent ion exchange system with non-linear equilibrium relationship may be written:

$$y_n^r = \frac{K\, x_n^r}{1 + (K-1)\, x_n^r} \qquad (19)$$

Equations (18) and (19) were simultaneously solved by those authors by successive numerical computation for values of x and y at given n and r. Values of ε, C_{Σ}, Q, N and K were known and in addition, initial boundary conditions of the form,

$$x_n^o \text{ and } y_n^o = 0 \quad , \quad n = 1,2,\text{--------}, N$$

$$x_o^r = x_{in} = 1 \quad , \qquad r \geqslant 1$$

The theoretical breakthrough curve was obtained by plotting x_N^r (= x_{out}) against r, whereas the authors[96] experimental curve was plotted against V.

The method was employed to systems of Na^+-H^+ and Ca^{++}-H^+ exchange using Amberlite IR-120. Gondo and Kusunoki[96] have found that N depended on the ion exchange system (i.e. N is larger for Na^+-H^+ than Ca^{++}-H^+ at the same concentration and flow rate), on the concentration of the liquid phase (N is larger for 0.1N than 1N), and on the liquid flow rate (N decreased with increasing flow rate).

The validity of the method was proved by comparing the values of HETP based on N thus obtained and those of HTU obtained independently of N.

The above method was tested by Slater and Zumer[97] for conditions of extraction copper ion from very dilute solution of copper sulphate/sulphuric acid with the value of C_o less than 0.01 N under very favourable equilibrium. Slater and Zumer[97] have indicated that under those conditions the computation was very sensitive because of the very low initial liquid concentrations. The authors[97] also encountered another important problem concerning the difficulty of distinguishing between breakthrough curves for different values of the number of mixing cells and did not recommend the method for the extraction of divalent ions from a very dilute solution with resin holding a monovalent ion. In a recent publication by Slater[98], the method of Gondo and Kusunoki[96] was reported to be applicable to the exchange of ions of equal valence.

Breakthrough curve in ion exchange between divalent and monovalent ions under liquid-phase diffusion control including the effect of the electric field has been studied by Kataoka and Yoshida[99]. The authors[99] suggested that the breakthrough curve could be obtained from approximate solutions for irreversible equilibrium, $K(Q/C_o)=\infty$, (namely $C^*/C_o=0$) if β=constant (if β was set equal to 1) by the equations

$$\left.\begin{aligned} x &= \exp(-6\beta\xi) \\ \bar{y} &= 6\beta\,\tau\exp(-6\beta\xi) \end{aligned}\right\} \quad \tau \leqq 1/6\beta \qquad (20)$$

$$x = \bar{y} = \exp\left\{6\beta(\tau - \xi) - 1\right\},$$

$$1/6\beta \leqq \tau \leqq \xi + (1/6\beta) \qquad (21)$$

$$x = \bar{y} = 1 \quad , \quad \zeta + (1/6\beta) \leq \tau \qquad (22)$$

where

$x = C/C_o$, equivalent fraction of ion in the liquid phase.

$\bar{y} = q/Q$, equivalent fraction of ion in the solid phase.

$\beta = k/k_o$

k = liquid-phase mass transfer coefficient with electric field.

k_o = liquid-phase mass transfer coefficient without electric field.

$\zeta = (Sh/Re\ Sc)(h/d_p)$

$\tau = k_o\ ((t-h\varepsilon/u_L)/d_p)\ (C_o/Q)$

When the above equations were applied to the ion exchange systems R-Na-$Zn(NO_3)_2$, R-H-$Zn(NO_3)_2$ and R-H-$Ba(NO_3)_2$, resulted in good agreement between theory and experiment.

More recently Liberti and Passino[100] suggested an idealized model for cyclic operation of fixed-bed ion exchange processes with favourable and unfavourable equilibrium conditions. The model views the fixed bed as a continuous system in which the solid and fluid phases flow countercurrently to one another at their respective average concentrations.

Once the operating line and equilibrium lines for a given ion-exchange operation have been determined, the method allows fixed bed performances over a wide range of operating conditions to be predicted and the basic kinetic parameters for bed design can be calculated with acceptable precision.

In addition to two major idealizations inherent in the model, the authors[100] introduced the following simplifications:

(1) Constancy of liquid phase flow rate and of total concentration of both phases

(2) Uniform saturation of the fixed bed

(3) Uniform fluid distribution (no channelling) in the column

(4) Negligible composition gradients in the intraparticle liquid.

Liberti and Passino[100] expressed the exchange rate of film-diffusion controlled process with the use of linear driving force theory for liquid-solid mass transfer kinetics as

$$\frac{dy}{dt} = K_L a \ \frac{C}{Q} \ (x - x^*) \qquad (23)$$

K_L is the liquid phase mass transfer coefficient and a is the particle surface per unit volume. C is the total solution concentration.

The continuity condition in mixed feed system is expressed by

$$y_o \ dx = x_o \ dy \qquad (24)$$

The authors[100] suggested that by solving equations (23) and (24) simultaneously and evaluating the corresponding linear driving forces graphically from proper O.L and E.L, the breakthrough curves for exhaustion and regeneration can be calculated.

Design method for fixed beds had for some time been under evaluation by Vermeulen and Hiester[101-103]. In their paper[101], techniques for handling the full range of possible rate mechanisms were included. Chemical reaction, external diffusion, internal or pore diffusion, and longitudinal diffusion or mixing-all can be treated.

Rate relationships were represented in the form of heights of transfer or reaction units. The authors[101] made use of data from the literature and correlated the number of transfer units with the Peclet group, which is expressed by $(d_p u_L \varepsilon / 6D_L(1-\varepsilon))$. A mechanism parameter was defined and used to correct for internal diffusion resistance.

The resulting predictions of breakthrough curves for fixed beds were presented on a generalized plot of effluent concentration, x, vs. solution-capacity parameter, $N_f Z$, for N_f values of 20, 40 and 80 and r values of 0.5, 1, and 2.

The calculation of the number of transfer units, N_f, from fixed-bed data is possible from a figure of effluent concentration, x, at r=1, vs. throughput ratio Z for different values of N. An alternative procedure is to use a cross-plot of Z-1 vs. r at different values of N_R, number of reaction units. Vermeulen and Hiester[101] pointed out the manner in which the slope of a breakthrough curve at the point of 50% leakage characterizes the curve. In cases where pore diffusion was an important resistance, this was only approximate, but the use of the mid-point slope in analyzing data still was convenient.

The authors[101] demonstrated the utility of their results for calculating such aspects of bed performance as resin utilization, regenerant efficiency, and bed leakage. The inclusion of modifications of the calculation for beds which are partially presaturated removes one of the major barriers in applying this work to the design of industrial ion exchange units.

In an earlier paper by Hiester et al[104] interpretive techniques for nonlinear equilibrium cases where the rate is controlled by a combined diffusion mechanism are provided. The techniques can be applied whether or not the value of the equilibrium constant is known.

A completely general correlational method was derived for adding the mass transfer resistances under conditions of nonlinear equilibrium. The authors[104] evaluated published breakthrough results from numerous sources and from their measurements using the techniques and determined the numerical constants for the general correlation

$$\frac{h}{S_c d_p} = \frac{0.29\ (Pe')^{0.5}}{b\varepsilon} + \frac{0.06\ (Pe')}{b\varepsilon D_s D_p/D_L} \qquad (25)$$

where:

S_c = column-capacity parameter for the kinetic case

b = correction factor for computing reaction-kinetic coefficient

D_s = partition parameter, or ratio of concentrations in resin phase and solution phase at saturation

D_L, D_p = fluid and solid phase diffusivites

$$Pe' = Re \cdot Sc = \frac{d_p u_L \rho}{6(1-\varepsilon)S_\mu} \quad \frac{\mu}{\rho D_L}$$

In the derivation of equation (25), the authors[104] made use of the following rate equations for external (fluid-film) and internal (particle) diffusion respectively

$$\frac{dq}{d\tau} = k_f a \frac{\varepsilon}{\rho_B} (c - c_i) \qquad (26)$$

$$\frac{dq}{d\tau} = k_p a (q_i - q) \qquad (27)$$

Hiester et al[104] also suggested that for external diffusion controlling, the total ionic concentrations and flow rates must be low. For a constant pattern breakthrough curve, the value of the separation factor, r, must lie between zero and unity and usually between zero and 0.5.

Fleck et al[105] presented numerical solutions of the equations describing adsorption (or ion exchange) in fixed-bed columns for various combinations of mass-transfer resistances under constant pattern conditions. Breakthrough curves were developed for pore, solid, and external diffusion acting separately and in combination for adsorption equilibrium described by the Langmuir or Freundlich isotherms.

The concept of a final-form front advancing down an exchange column at high rates of flow has been satisfied experimentally by Lapidus and Rosen[106]. Data for the exchange of Na^+(0.08-0.173N-NaCl) with H^+ on Dowex were reported and the experimental conditions were chosen so that liquid film-diffusion was controlling. The authors[106] have found that the rate of diffusion was first order with respect to the bulk concentration and to the equilibrium concentration of liquid on the outer surface of the solid. The following equation was used for the reversible rate step (liquid film diffusion and a langmuir isotherm):

$$F(c,q) = k_f (c - q/Q(1-q)) \qquad (28)$$

2.6 CONTINUOUS ION EXCHANGE EQUIPMENT

The need for countercurrent equipment for ion exchange particularly but also for adsorption processes has been recognised for many years. A large number of contractor designs have been proposed but very few have met with any degree of commercial success.

Water treatment, uranium extraction from ore slurries and gold extraction are amongst the main topics of interest.

There is no one simple criterion for choosing continuous rather than fixed bed ion exchange but low annual costs and reliable operation are important factors. High flows of solute, the cost or difficulty of filteration, the cost of chemicals, the plant reliability, height and area restrictions and hold-up of high value solutes all affect the matter.

The design of continuous countercurrent ion exchange systems require close control over resin flow rates and column inventories, avoidance of excessive damage to resin, hydraulic properties of resins in the design of fluidized systems (particle size, densities, terminal velocities, fluidization characteristics), equilibrium and kinetic data, and flow patterns for scale-up.

This section is concerned mainly with several major types of continuous contercurrent resin ion exchange equipment now used on a large scale. Other designs are briefly discussed.

Several reviews on continuous systems have been published. Hiester and Phillips[107] reviewed industrial applications and techniques in 1954 and Hutcheon[108] in 1955 summarised

a few available designs, Lauer[109] reported in 1956 on the mechanical features of a larger number of contactors and Poole[110] in 1959 described more recent developments. Slater[111] reviewed the problems concerned and methods of resolving them and also compared the effectiveness of the design types in 1969 and in 1981, Slater[112] reviewed the industrial applications and particularly recent experience of plants used for water treatment and uranium extraction.

2.6.1 MOVING BED SYSTEMS

2.6.1.1 Chem-Seps or Higgins contactor[113-123]

The apparatus consists of a vertical column with appropriate tappings for feed and product solutions. A resin overflow pipe leads from the top of the column through an overflow valve, usually open, into another column alongside the first, bearing a valve, which is closed during normal operation. The two columns are joined at the base. The solution flows in the first column are stopped after a period of several minutes, and the settings of the two valves reversed. Hydraulic pressure is then suddenly applied to the top of the auxiliary column so that the resin moves downwards, and up the main column. Some resin passes into the overflow pipe, where it is retained by the overflow valve. The two valves are returned to their initial settings, allowing the overflowing resin to fall into the auxiliary column, where it may be washed, and the solution flows are then restarted, usually ten seconds is sufficient for this operation.

The advantages of such a system are that the solution downflow may be large; the arrangement of the resin particles is substantially the same throughout the cycle; and that the product flows are almost continuous.

Plants installed since 1958. Applications to water softening, de-alkalization, demineralizing, NH_4NO_3 recovery, NO_3 removal, gelatin treatment, chromate recovery, KNO_3 recovery, phosphoric acid purification, molybdenum and uranium recovery.

Units with extraction sections up to 2.44 m diameter and regeneration columns up to 1.07 m have been constructed. Liquid velocities from 70 to 200 m^3/m^2h are used for liquid film rate controlled processes. Resin damage is less than 25% pa for cation, 35% pa for anion, gel or macroporous, depending on process conditions. The maximum pressure to drive the resin is about 120 psi (830 kPa) and the downtime of 5 to 7% pa is average.

2.6.1.2 Asahi Equipment[124-127]

The Asahi Chemical Industry Co., in Japan, developed a continuous ion exchange process for the recovery of copper from a waste spinning solution in a rayon plant. Pilot plant tests were then made with this design in the refining of sugar juices, in water softening and dimineralizing. Later some large-scale continuous plants were installed in Japan and recently in the U.S.A., United Kingdom, France, Argentina and Australia[127].

The apparatus uses three vessels called service, regeneration and rinsing. The process is actually intermittent. The adsorption cycle begins with the vessel absolutely full Of resin, so that when service begins, on upflow, the bed can not break up or circulate. The pressure in the unit forces exhausted resin lying at the bottom of the vessel to pass on to the next stage, thus creating a water space under the working bed. After a relatively long service period, raw water flow is stopped, and a rapid downflow is induced in the vessel. This brings the resin column to the bottom of the vessel so quickly that the bed does not have time to break up, and the stratification of fresh and exhausted resin is preserved. At the same time, regenerated resin fills the water space now created at the top of the vessel. When this is full, the adsorption cycle begins afresh. The regeneration of the resin takes place in a vessel which operates in exactly the same way, but is typically tall and thin. The stages are connected via hoppers, each of which fills itself automatically under the static or pressure head in the preceding unit. The resin is therefore never pumped, but moves quite slowly and gently. No valve closes on resin or has to operate in chemical solutions. The technique is therefore not only very simple, but is very reliable in operation and leads to minimal resin attrition losses.

Mixed bed plants have been built for a wide variety of water treatment which require a resin separation column and separate regeneration columns. Although performance has been

good, attension to strainers and valves seems required[112].

2.6.1.3 The Avco system[128]

The Avco system is a truly continuous moving bed system consisting of one column which contains three different types of zones: reaction, driver, and wash zones. The reaction zones consist of the exchange zone and the regeneration zone where the liquids move countercurrent to the motion of the resin bed. Two driving zones are used in series to keep down the absolute pressure level in the column, the driver liquids are treated in the primary zone and the feed in the secondary zone. The wash and separation zones are inserted between the exchange and driver zones. The resin bed is driven downward, with the liquids entering or exiting under different pressures at screened ports located along the column. These screens retain all but the smallest beads and provide a mechanism for removing resin fines and particulate matter. The velocity of the liquid in any section between two adjacent ports controlled independently of those in the other section by regulating the pressure differential across the section, while the resin bed motion is controlled by a metering device at the bottom of the column.

No large scale industrial units have been built to date suggesting that the design is too complex and operating conditions too severe[112].

2.6.2 FLUIDIZED BED SYSTEMS

2.6.2.1 Cloete/Streat/NIMCIX[129-132]

This is a multistage fluidized bed containing perforated distributor plates and no downcomers. The hole size in the plates is greater than the maximum resin particle size. Countercurrent flow of resin is achieved by controlled cycling of the liquid feed. In this way, a precisely determined fraction of the resin holdup per stage can be transferred. In practice, it is desirable to transfer the entire resin holdup per cycle. The regeneration is carried out in a separate column similar to the adsorption column but of smaller diameter. No valves are used on resin flows and a small number of automatic valves is required. Attrition losses of a few per cent pa have been recorded. Resin is elutriated from column but is recovered for re-use with screens.

This system has been developed for application in the uranium industry and the greatest advances have occured in South Africa[132].

Typical liquid velocities are 13 to 15 m^3/m^2h for uranium processing; anion resins are used and the mass transfer rate is in part controlled by diffusion in resin beads. The nominal operating voidage is 0.7 and columns with diameters up to 4.85 m have been built to process 272 m^3/h each [112].

2.6.2.2 Himsley System[19,133]

The Himsley design of multistage fluidized bed column system has been adopted on a large scale for uranium extraction in Canada, U.S.A., and South Africa[112].

Liquid flow during extraction is continuous. In the extraction column a central liquid feed point for each stage induces circulation of resin and liquid such that conditions may be considered well mixed. Resin is transferred by abstracting liquid from an empty stage and pumping into the stage above so that resin is transferred through the centre feed passage to the stage below. This method of resin transfer ensures constant hold-up in each stage and controllable average resin flow rate. Resin is moved upwards in a packed bed regeneration column in a periodic manner. Downflow regeneration avoids bed expansion and the eluate being more dense than the eluant (in the case of uranium), minimal axial mixing is suffered. Rinsing is done at the top of the elution column or in a separate vessel.

Extraction columns with diameters of up to 4m processing 210 m^3/h are operating in South Africa. Valves and strainers are used on every stage and the operating procedure requires automation.

2.6.2.3 Porter/Rossing System[134]

Though most fluidized bed development is in the form of vertical columns it is also possible to operate the system in a series of horizontal tanks. Possibly the largest continuous ion exchange plant in the world operate at Rossing uranium mine in Namibia[19]. This plant, designed by Porter, comprises an array of horizontal inter connected tanks, each acting as an effective fluidized bed. The resin beads are progressively moved from tank to tank by air-lifts in countercurrent to the flow of pregnant solution. The total pregnant flow to the plant is about 3500 m^3/hr and each contacting tank is 6 m square by 3.5 m deep. The initial plant had 4 lines of 5 contacting tanks in each. Careful design of resin traps has been included in the plant; these comprised a sophisticated rotating trommel and this has now permitted a sixth contractor to be installed in each line.

Civil engineering costs tend to be high and the resin and liquid distributors are expensive; the use of gravity liquid flow would be preferable as used in a separate plant at Rossing used for tailings pond treatment[112].

2.6.2.4 Slater/CANMET System[135,136]

This is simple fluidized bed vertically partitioned to reduce axial mixing. The resin is transferred by vacuum. Pilot plant, 0.76 m by 4 m extraction column was tested by Slater et al[135] in Ottawa, Canada, for uranium removal from

mine water. They concluded that it is possible to build a large multi-section plant for the removal of uranium, but Beaverlodge mine water had high chloride and calcium and this led to high process costs because of the need to remove the calcium.

A review on the pilot-plant development of processes for the treatment of base metal mine water, cyanide waste water, uranium leach liquor and uranium mine water using the concept of single-stage fluidized bed continuous ion exchange is presented by Lucas[136].

2.6.2.5 USBM column[137,138,139]

This was developed in the U.S.A. by the U.S. Bureau of Mines. It is a multistage countercurrent fluidized bed contactor and operates by controlled cycling. In many respects it is similar to the Cloete-Streat contactor and differs only in plate design, mode of solid transfer, and resin withdrawal. This column has all the advantages of a multistage fluidized bed and has found application for uranium recovery at various locations in the U.S.A.

The resin transfer system to a continuous elution column is based on ejectors, drum screens and vibrating resin feeders. For extraction of 1 Kg/m^3 U_3O_8 an extraction specific flow of 23.4 m/h is recommended[112], for elution 4.7 to 7 m/h.

2.6.2.6 Swinton/Weiss contactor[140]

This is a vertical multistage fluidized bed contactor containing perforated distributor plates and downcomers. Ion exchange resin is supported on the distributor plate in the no-flow condition and during upward flow the particles passed over a weir and into the downcomer. Resin is moved in downflow from stage-to-stage and can be removed from the base of the column. The concept is feasible in principle, however, the operation of this column and others like it is hydraulically unstable[19]. Control of resin holdup and by-passing of the pregnant feed were problems. Start-up was not easy since the pressure drop in the downcomers was invariably less than through the resin bed and thus by-passing was readily initiated.

2.6.3 PULSED BED SYSTEMS

2.6.3.1 Arden column[141]

This is a simple type of pulsed column. Periodic fluidisation induced by pulsing or vibrating the contents of the column permits the same liquid flow rates as in moving beds at lower pressure drop and allows the free passage of turbid liquids. The flow of solids is much more easily obtained since intraparticulate friction is lessened periodically. A good distribution of liquid and solids is maintained across the contactor and pulses of 10 to 200 per minute are used.

2.6.3.2 Grimmett contactor[142]

This is a multistage contactor consisting of one column with five contact stages. Ion exchange resin flow rates up to 150 Lb/hr. ft^2 and calcined Al_2O_3 flow rates up to 300 Lb/hr. Ft^2 were reported while feeding H_2O at rates up to 2000 Lb/hr. ft^2. Stage efficiencies of greater than 27 to 62% were reported for the systems Cu-Na and Cu-H at a cationic concentration of 0.1N. Sulphate was the common ion in the first system and nitrate ion in the second system. The internal diameter of the column was 2 inches. Pulses of 600 per minute were used.

In general, the operating efficiency is poorer than in a moving bed but the operating conditions are less demanding and the overall system probably less complex[111].

2.6.4 FIXED BED SYSTEMS

2.6.4.1 Barnebl/Riker equipment[143]

This is an annular cylindrical ion exchange reactor, divided into a large number of segments by radial walls and rotating about a vertical axis. Each segment drains through an individual pipe to a common circular channel in a fixed plate on which the reactor compartment rotates. This channel is blocked by bridges corresponding to the number of operations (feed, regenerant, wash, etc.), the angular separation of the bridges being adjustable to suit the process. Pipes between the bridges lead off the various streams as

required. Feed streams are brought in above the reactor at fixed points, the angular separation of which is adjustable to match that of the take-off arrangements in the lower channel. Thus, in turn, each segment passes under the feed stream, where it receives a charge of feed, this charge being drained away under partial vacuum while the segment moves round to the first washing stream, and so on until the cycle of feed, wash, regenerant, regenerant wash and backwash is complete.

Such a device allows the relative quantity of the exchanger on each part of the cycle to be adjusted to meet the requirements of the process and it also avoids the difficulties associated with short cycle times in cyclic column systems. The resin is undergoing exchange for a higher proportion of the cycle and is therefore being more efficiently used.

The equipment described, however, is mechanically complicated and it seems probable that only in large scale operations would the saving in resin costs justify the capital expenditure[108].

2.6.4.2 Porter/Arden equipment[144]

This was developed in the late 1950's and was adopted in the uranium industry in the Blind River region of Ontario, Canada. Here, exhausted resin was transported to an empty conventional column by hydraulic conveying. The resin was then backwashed and transported to a bank of elution columns,

fresh resin having previously been transported to a vacant extraction column. The movement of resin around the fixed bed installation was essentially countercurrent though the process was not fully continuous by modern standards[19].

2.6.5 STIRRED TANK SYSTEMS

2.6.5.1 Collier system[145]

The solutions to be treated with mixed resins are mixed in agitators or mixer-pipe sections and the slurry is passed into one or more centrifuges which separate the resins from the solution and from each other, using density differences for this purpose. Alternative methods of separating the resins such as rake-wet classifiers, dry classifiers or sieves are described which utilize differences in size or shape as well as, or in addition to, differences in density, to separate the resins. The patent specification, however, gives no guidance on how the regeneration would be accomplished.

2.6.5.2 SRI contactor[146]

Stanford Research Institute has developed a batch contactor on small pilot plant scale that combines both agitation and filtration in the same unit and thus does not require movement of the resin, with possible resultant attrition. It can be used as a single unit, or group of the mixer-settlers can be operated in a countercurrent fashion by automatic cycling and sequencing techniques.

SRI's individual mixer-settler consists of a tank with a perforated plate near the bottom to retain the resin, and a top and bottom outlet fitted with three-way plug valves. Considering the operating steps in sequence, the tank, containing a given amount of exchange resin, is initially empty of solution. To start the cycle, a definite amount of contacting solution is pushed into the mixer-settler by gas pressure. The gas flow, passing through the solution, agitates it and assists in bringing about equilibrium between resin and solution. Finally, the gas flow is reversed so that the solution is forced out of the tank and the resin freed of interstitial solution. The sequence can then be repeated.

This device can be regenerated in a similar manner, using elutant instead of feed.

Stirred tank systems performance probably does not justify their complexity[111] and they are more than twice as expensive as the corresponding fixed or moving bed apparatus[108].

2.6.6 MISCELLANEOUS EQUIPMENT

At Stanford Research Institute[147,148] continuous countercurrent ion exchange was carried out in a glass column 4 in. in diameter. Two rotating valves were invented for dewatering and metering the resin to and from the column. Countercurrent was achieved by passing the liquid up the column and the resin was passed down. Contact between the two phases occured in a dense bed of resin, moving as a piston

through the column. The upper valve continually supplied resin to the top of the moving bed while the lower valve withdrawed it at the same rate, maintaining a constant bed height.

Resin entering the rotating valve was retained on a perforated glass disk at the midpoint of the bore. Free solution drained through the disk. As the bore passed under the air inlet, air pressure was applied by means of a cam-actuated solenoid valve dewatered the resin by forcing the interstitial solution through the disk. When the bore became aligned with the outer, wash solution displaced the resin and carried it out as a slurry. Any residual wash solution was forced from the bore by air pressure.

In Germany, a patent[149] claimed that liquids can be passed downward through a cylindrical vessel packed with ion exchange resin supported by an impermeable strong membrane. The membrane is alternately blown upward and withdrawn pneumatically in a pistonlike movement at regular intervals, and fresh resin is introduced at the bottom, while used resin is withdrawn at the top.

Baddour[150] invented a continuous ion exchange apparatus. A continuous bed of ion-exchange material in the form of a circle, mounted so that it rotates about its axis, moves between the treating zone and the regeneration zone; wash water is introduced between the two zones to maintain a pressure sufficient to prevent intermingling of the treated fluid with the regenerative solution.

Lomonosov[151] invented a method for continual renewal of ion-exchange materials and a continual decanting of used solution. A reservoir of solution is maintained at a constant level. It is fed into the column, which is divided into sections, which are shaped like small cones. These hold the resins and are continually refreshed by resins from another reservoir. The decantation rate is held constant by a glass tube which acts as a siphon.

A new process has been developed in Germany by Schuetze and Wetzel[152] in which the solid phase consists of several separate moving containers of packing and are open at both ends. The containers move upward, countercurrently to the liquid which trickles down. Regeneration and washing occur as the containers move down (to complete the cycle) at a lower rate. The movement can be continuous or stepwise. The authors[152] claimed that this method reduces mechanical breakage of packing, enables greater throughput, and has lower pressure drop than a single conventional column. The principle was demonstrated by separating Co-Ni solutions with granules (0.6-1.0 mm. diam.) of a cation resin in 1, 3, 6, or 10 containers 13 cm. long x 2 cm. internal diameter. The optimum number of containers was found to be 3.

Japan Organo Co.[153] patented an apparatus for continuous ion exchange treatment by a countercurrent process. The apparatus consists of one or more ion exchange units. An ion exchange resin is introduced into the system from above and sent to the lower part through a jet feeder by spraying a liquid through the feeder, which results in improving the

mixing effect between the resin and the solution to be treated. The solution is supplied from the lower part and sent to the upper part through a side path.

An apparatus consisting of two columns was invented by Yokozeki et al[154]. In the first column, fresh ion exchange resin moves downward countercurrent to the solution to be treated. At the base, the spent resin is collected and transferred to the top of the regenerator. The regenerator column is divided into two parts, the upper one for regenerating, and the lower for washing the resin. At the base of the regenerator, the resin is transferred to the top of the first column. In both columns, devices are provided to ensure uniform passage of the resin and the liquid.

Bachelart[155] described an ion exchange apparatus wherein the liquid to be purified flows through successive ion exchange columns. Each column may contain more than one ion-exchange resin and can be separated as inert layers. The columns are regenerated countercurrently and after regenerating and rinsing the resins, the liquid is removed by a flow of air. Water can be demineralized by leading it downwardly over a column, charged in the upper part with a carboxylic ion-exchanger and in the lower part with a sulphonic acid exchanger. Next, the water goes through a column with a moderately basic ion-exchanger, and after elimination of CO_2 over a strongly basic resin.

Fedulov et al[156] developed a continuous adsorption column with a compressed layer of circulating ion exchanger. This layer is dry, compressed resin which is positioned above

the liquid overflow and replenishes the resin carried out with the liquid overflow. The method was adopted to a 0.5 m diameter column packed to a height of 2 m with a type KU2 x 8 (0.3-0.8mm.) cationic resin. The apparatus handled continuously 300 l/hr. of solution at resin flow rate of 150 l/hr. Solution velocities were limited to 3 m/hr.

An apparatus for continuous ion exchange processes was patented by Goetzmann[157]. The apparatus consists of two columns with ion exchange material. The material moves downward whereas the solutions to be treated move upward through the columns. There are no valves in the column and tubes that are passed by the exchange material.

Shah et al[158] obtained ion exchange data in a fluidized-moving bed combination that has no supporting sieve or screen and in which the solid particles are continuously circulated between the fluidized and moving beds.

Waste water from fertilizer plant was treated by Arion [159] using a moving bed system. This consists of two vertical parallel tubes with their bases connected by a curved tube. Each tube contains a valve at the lower end. One of the tubes has an enlarged portion, just above the valve, in which the ion-exchange treatment takes place and an upper portion that holds regenerated ion exchanger. The other tube has a lower portion in which regeneration takes place and an enlarged upper portion in which the regenerated ion exchanger is washed. These two portions are separated by a valve. A smaller tube is connected to the upper end of the first vertical tube and passed through the upper end to a point

near the lower end of the enlarged washing portion. This connecting tube contains a valve. The ion exchanger is transferred intermittenly when it has reached a certain level of exhaustion.

Broughton et al[160] studied the extraction of p-xylene in a unit which completely reproduces the continuous, simulated-moving bed, commercial mode of operation. The technique consists essentially of simulating the movement of solids past fixed points of liquid feed and withdrawal, by moving the positions of feed and withdrawal around a stationary bed. Solid and liquid are conveyed substantially continuously and countercurrently to each other.

2.7 DESIGN OF MOVING BED SYSTEMS

An indication of the data necessary, and of the various steps in the solution of any design problem has been discussed by Poole[110], but the theory involved was not covered. The design methods applicable to truly and semi continuous moving bed systems are reviewed below.

Slater[98] suggested that continuously moving packed bed systems used under conditions of liquid film diffusion rate control can be designed on a basis of transfer units using the equation

$$h = NTU \times HTU \qquad (29)$$

The author[98] also indicated that if the bed is moving intermittently, a more complex computer calculation developed by Gondo[161] can be used and a comparison of the two calculation methods would be useful.

Gondo[161] derived a difference equation for the material balance of fixed bed operation by assuming that ion exchange column consists of equilibrium stages and also graphical and numerical methods for solving the equation were obtained. Gondo[161] has shown that the concentration distribution of the moving bed operation can be obtained for the steady state by applying the numerical method. Concentration distributions were obtained for contacting volume ratios of fluid and ion exchange resin, using equilibrium relation of the ion exchange of Na and H on a strongly acidic cation exchange resin. The results showed that the concentration distribution was pushed to the end of fluid outlet as the ratio of contacting

volume of fluid to that of exchange resin increased, the degree of ion exchange of the fluid can be determined for a given ratio of contacting volume since the concentration of exit fluid is fixed corresponding to the steady distribution of the concentration. Each concentration distribution gives its number of the exchange zone stage, accordingly, a given contacting volume ratio has its own number of the exchange zone stage and its own exchange degree of the fluid phase. The results were correlated graphically by plotting the ratio of number of equilibrium stages occupied by the ion exchange zone in the moving bed operation to that in the fixed bed operation against the degree of ion exchange of fluid. Gondo [161] also suggested that the graphical correlation may be useful for estimating the exchange zone height of the moving bed from that of the fixed bed.

A design theory on kinetic and equilibrium considerations for countercurrent ion exchange under trace conditions was developed by Hiester and coworkers[107,148]. Equipment was designed to provide continuous countercurrent contact between a moving bed of ion exchange resin and the solution to be treated and was evaluated experimentally by the separation of trace ions Li, K and gross ion H.

The authors[148] suggested the following equation for computing the number of overall mass transfer units using a dynamic method

$$NTU = \frac{E}{1-E} \ln \frac{E(1-\gamma)}{E-\gamma} = \frac{khS\varepsilon}{R_F} \qquad (30)$$

E and γ are defined in nomenclature.

By using an equilibrium method, the authors[148] have obtained the following relation for calculating the number of equilibrium stages

$$N_c = \frac{\ln\left((E-\gamma)/E(1-\gamma)\right)}{\ln E} \qquad (31)$$

The ratio between NTU and N_c is given by

$$\frac{NTU}{N_c} = \frac{E \ln E}{E-1} \qquad (32)$$

The authors[148] have correlated their results graphically using an equation which relates the height of a transfer unit to the operating variables and the characteristics of the resin-ion system. The equation is of the form

$$\frac{HTU}{d_p} = \frac{h}{NTU d_p} = \frac{1.6}{\varepsilon(Re.Sc)^{0.5}}\left[\frac{d_p R_F}{6(1-\varepsilon)SD_L}\right] + \frac{1}{E}\frac{0.6}{(1-\varepsilon)}\left[\frac{d_p R_p}{6(1-\varepsilon)SD_p}\right] \qquad (33)$$

All symbols are defined in nomenclature and the following simplifications were made:

(1) The equilibrium line is linear.

(2) The resin and solution entering and leaving have constant flow rate and constant composition.

(3) Steady state conditions.

(4) The equilibrium method assumes that the section is made up of a finite number of equilibrium contacts similar to plates in a distillation column.

In another publication by Hiester et al[162], the design of moving bed is outlined. This involves the use of relations

(30) and (33) for evaluating the number and height of transfer units respectively. The column diameter is selected from the linear solution velocity and the volumetric flow rate of the solution. With E and the volumetric flow rate, R_F, the required resin flow rate, R_p, is calculated from

$$E = \frac{M\ R_p\ \rho_B\ Q}{R_F\ C_\Sigma} \tag{34}$$

Hutcheon[108] discussed the design methods for continuous ion exchange. In all three methods were outlined, the first and second concern the determination of the NTU by the conventional graphical integration and the number of equilibrium contacts using a McCabe-Thiele diagram. The third method is for the special case where one ion is present only in trace concentration with respect to the other (an equivalent fraction less than 0.1), permits the use of a simplified analytical approaches. Solutions may be obtained in terms of the Kremser equations

$$\frac{C_o - C_N}{C_o - (q/K)} = \frac{E^{N_C + 1} - E}{E^{N_C + 1} - 1} \tag{35}$$

$$\frac{q_N - q_o}{q_N - K} = \frac{E^{N_C} - 1}{E^{N_C + 1} - 1} \tag{36}$$

Equation (35) with the assumption that the resin entering the column is initially free of the ion to be absorbed simplifies to

$$\frac{C_o}{C_N} = \frac{E^{N_c + 1} - 1}{E - 1} \qquad (37)$$

All symbols are defined in nomenclature.

An analysis for predicting the performance of the AVCO continuous moving-bed ion exchange system and detailed design calculations are presented by Gold and Sonin[128]. Emphasis is placed specifically on predicting the characteristics of the regeneration zone because the volume of this zone essentially determines the volume of the entire system because of the slow kinetics associated with particle diffusion as compared to film diffusion. The effect of resin bed volume flow rate on chemical efficiency is also presented.

The volumes of the regeneration and exchange zones can be computed using the following equations

$$V_{RZ} = \bar{V}_{RZ} \quad C_o R_F (C/C_o)/Qk_p(1-x_3) \qquad (38)$$

$$V_{EZ} = \bar{\eta}_{EZ} \; R_F/k_f \qquad (39)$$

and the ratio is given by

$$V_{RZ}/V_{EZ} = (C_o/Q)(k_f/k_p)(V_{RZ}/\bar{\eta}_{EZ})((C/C_o)/(1-x_3)) \qquad (40)$$

$\bar{V}_{RZ}$ is dimensionless volume of regeneration zone, x_3 is equivalent ionic fraction of regenerant feed, $\bar{\eta}_{EZ}$ is dimensionless length at equilibrium ($\equiv$ NTU), the rest of symbols are defined in nomenclature)

The resin bed volume flow rate is calculated from

$$R_p \sim C_o \; R_F (C/C_o)/Q \; \alpha_{RZ}(1 - x_3) \; (EFF) \qquad (41)$$

where,

α_{RZ} = is the slopeof regeneration zone operating line = $\frac{C_R R_R}{Q R_p}$

EFF = is the chemical efficiency which is the ratio of the total equivalents of ion removed from the feed to the total equivalents of regenerant ion in the regenerant solution.

The authors[128] observed the following points:

(1) The volume of the regeneration zone is directly proportional to the total number of equivalents to be removed and inversely proportional to the rate constant for particle diffusion.

(2) High chemical efficiencies can be obtained if the regeneration zone is operated in such a way that the slope of the operating line is close to the value of the regeneration isotherm at x=1.

(3) The efficiency is insensitive to values of $\bar{V}_{RZ}$ greater than 15 to 30, while the product effluent concentration is insensitive to values of $\bar{\eta}_{EZ}$ greater than 5.

(4) The volume of the regeneration zone is greater than the volume of the exchange zone.

Broughton et al[160] studied the extraction of p-xylene from its mixtures with other C_8 - hydrocarbons by adsorption from the liquid phase in the laboratory and also in a unit which completely reproduced the continuous, simulated- moving bed, commercial mode of operation.

The authors[160] derived the following relationship by assuming that axial mixing is absent, equilibrium line is linear, y = Kx, and transfer rate is directly proportional to

a driving force expressed as Kx-y.

$$HETP = \frac{L}{kK} \left(\frac{m \ln m}{m - 1} \right) \qquad (42)$$

where:

HETP = height of equivalent to theoretical tray.

L = Liquid flow rate.

K = equilibrium distribution, y/x.

y = concentration in pore liquid.

x = concentration in void liquid.

k = mass transfer coefficient.

m = adsorption factor = SK/L.

S = pore circulation rate.

At reasonable operating conditions, the bracketed term in equation (42) is close to unity and in low-selectivity systems, K does not depart greatly from unity, therefore equation (42) is approximated to

$$HETP = L/k \qquad (43)$$

The authors[160] compared the results of the continuous system with that of fixed bed operation and found that the continuous system required only 1/25 of the adsorbent inventory required in the fixed bed system. At the same time, the desorbent circulation requirement for the continuous system was about one-half of that for the fixed bed system.

Higgins and Roberts[114] conducted the separation of Li-Na on the resin Dowex 50W-X12 in the H-form in a moving bed contactor which was developed by Higgins and described in the previous section.

The Fenske equation for total-reflux was used to calculate the number of theoretical stages

$$R = {}_{\alpha}{}^{N.T.S} \qquad (44)$$

where,

α = Li-Na separation factor which was assumed to be constant = Li-Na ratio in the solution phase/Li-Na ratio in the resin phase when the phases are in equilibrium.

R = enrichment factor = Li-Na ratio in the solution phase at the point of interest/Li-Na ratio at the feed point.

The following equation for calculating the height equivalent to a theoretical stage was derived by Higgins and Roberts[114]

$$H.E.T.S = \frac{\ln \alpha}{k(\alpha-1)} \qquad (45)$$

k is empirical rate constant.

Fixed bed data was used to calculate the HTU and k by using the following assumed rate laws

$$\frac{dx}{dz} = \frac{1}{HTU} (x^* - x) \qquad (46)$$

and

$$\frac{dx}{dz} = k(\alpha y (1-x) - x(1-y)) \qquad (47)$$

x^* = equilibrium value of x corresponding to y.

x = Li-mole fraction in the solution phase at the same point.

y = Li-mole fraction in the resin phase at the point of interest in the Li-enriching section.

The following equation was also derived by the authors[114]

$$k\,(\alpha-1)z = \ln R \qquad (48)$$

(z = distance from the feed point to the point of interest). A graph of log Li/Na vs. distance down a continuous column was plotted with the data falling on a straight line.

Two rate relations for a continuous differential moving bed unit were reported by Vermeulen et al[103]. The reaction-kinetic form and the external transport form. The rate equation and the driving force for the reaction-kinetic are given by

$$\frac{dY}{dt_p} = \frac{1}{\Lambda}\,\frac{dX}{dt_{fa}} \qquad (49)$$

$$\frac{dY}{dt} = k\,\left(X(1-Y) - RY(1-X)\right) \qquad (50)$$

The column height is determined as a function of the proportion X_{out} of unsorbed feed component, with $N_R = \kappa\,\Lambda h\,S/R_F$, the result is

$$N_R = \frac{1}{T(1-R)\ell}\ln\frac{2X_{out} - m + \ell}{2X_{out} - m - \ell}\,\frac{2 - m - \ell}{2 - m + \ell} \qquad (51)$$

with $m = X_{out} + \left((1-RT)\ (T(1-R))\right)$;

$n = RX_{out}/(1-R)$;

$\ell = (m^2 + 4n)^{0.5}$

If ℓ is imaginary, the alternate integral applies:

$$N_R = \frac{2}{T(1-R)\ell}\ \tan^{-1}\frac{2-m}{\ell} - \tan^{-1}\frac{2X_{out}-m}{\ell} \qquad (52)$$

with $\ell = (-m^2-4n)^{0.5}$

The external transport form illustrate the familiar graphical technique for determining the number of transfer units when the overall kinetics of the sorption step are controlled by fluid-phase transport external to the particle. Combination of that rate equation

$$\frac{dY}{dt} = \frac{k_f a_p}{\Lambda} (X - X^*) \tag{53}$$

with the material-balance relation

$$G_p(q_2 - q_1) = - (\frac{R_F}{S}) (C_2 - C_1) \tag{54}$$

and the boundary conditions leads to the result

$$\int_1^{X_{out}} \frac{dX}{X - X^*} = NTU = k_f a_p \frac{hS}{R_F} \tag{55}$$

This is the well-known Chilton-Colburn equation relating the sorption efficiency of a countercurrent contactor to its number of transfer units. Although an analytical solution of this is possible for a given isotherm equation and material-balance relation between Y and X, the authors[103] suggested that the use of a McCabe-Thiele diagram is much more simple.

C H A P T E R T H R E E

PHYSICO-CHEMICAL PROPERTIES

3.1 RESIN BULK DENSITY DETERMINATION

The bulk density of Amberlite IRC-718 (Na) was determined by weighing the amount of resin required to fill a 10 cc measuring cylinder. Settling of the resin was achieved by hand tapping with each addition. The bulk density of the resin was found to have a typical value of 0.672 g/cc. This value agrees very well with that given in the Manufacturer's literature[163].

3.2 RESIN CAPACITY DETERMINATION

pH titration method was used in order to determine the capacity of the ion exchanger, Amberlite IRC-718 (Na). Eight samples (about 1g each) of the ion exchanger were weighed into dry 500 cc plastic bottles and different volumes of standard 0.1 M NaOH were added to each sample and then de-ionised water was added as required to keep the ratio of solution volume to resin weight constant (100 cc solution/ gram of ion exchanger). The samples in bottles were kept on a mechanical shaker (Griffin flask shaker) until the pH of the solutions attained a constant final value (About two hours were needed to reach equilibrium condition). The same procedure was followed for 0.107 M HCl solution. The titration curve was obtained by plotting the pH versus the amount of titrant added. Typical curves for 0.107 M HCl and 0.1 M NaOH

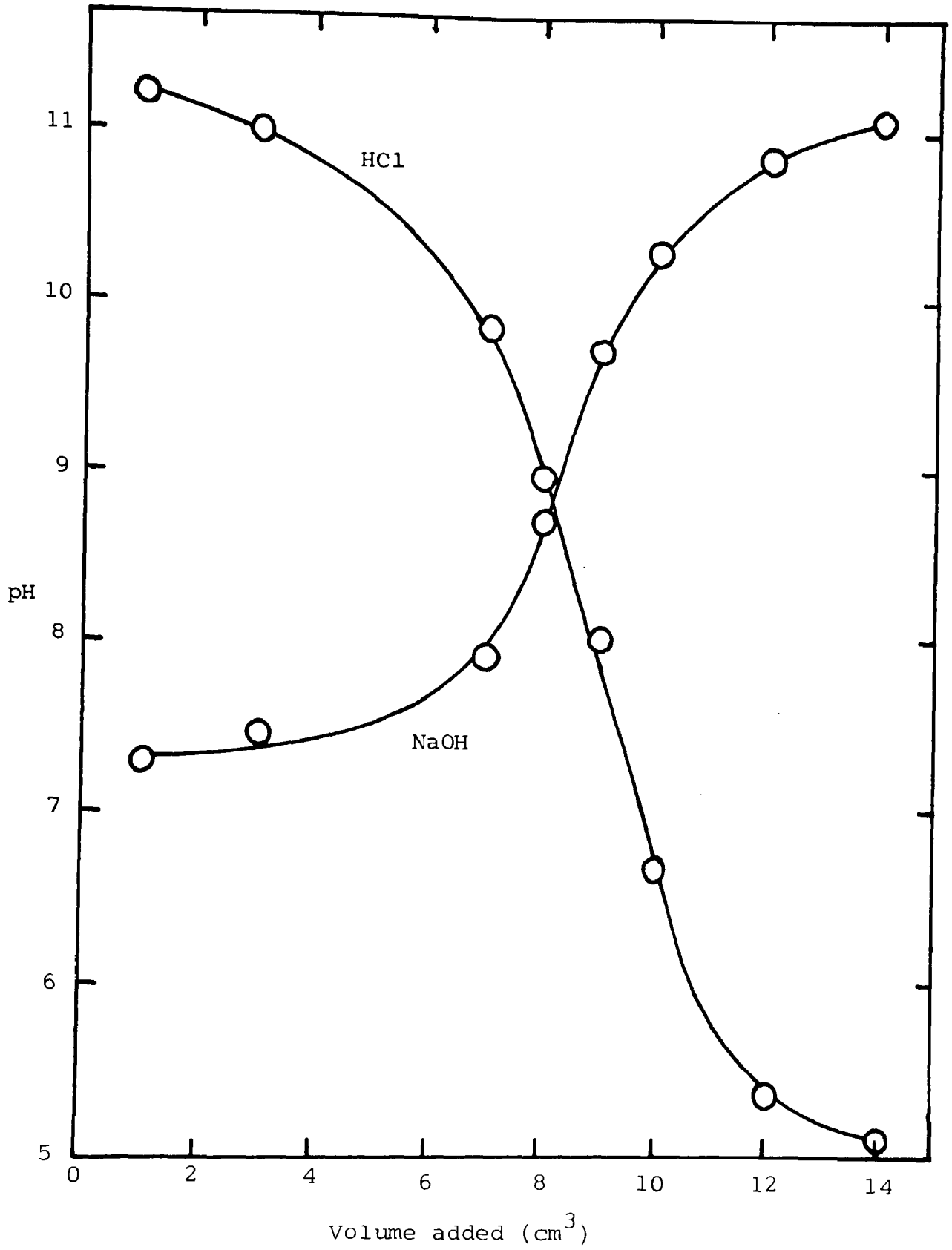

Figure 1 pH Titration curves

are shown in Figure 1.

Using resin in the Na form and 1 cc of 0.107 M HCl and 99 cc of H_2O gave a pH of 3.15 (measured using Pye model 291 pH meter, supplied by Pye Unican), however, after equilibrium the pH was measured to be 11.2. On the other hand with resin in the H form and 0.1 M NaOH, the pH decreased from 10.35 to 7.3. As can be seen from the figure Sigmoid curves were obtained and in the case of using 0.1 M NaOH, the pH increased from 7.3 with the addition of 1 cc to 11.1 with 14 cc. On the other hand the pH decreased with 0.107 M HCl from 11.2 to 5.1. In both cases the pH tends to remain unchanged after the addition of about 14 cc which gives weight capacities of 1.4 meq. Na^+/g of resin and 1.498 meq. H^+/g. These values are in close agreement with that given in the Manufacturer's literature[163,164] of 1.0 meq./cc. which is equivalent to 1.488 meq./g.

The variation between the values obtained in this study and the Manufacturer's value can be attributed to the nature of ion used, its concentration and the pH of the solution[47].

3.3 PARTICLE SIZE DETERMINATION

Since the ion exchange reactions are nearly always conducted in aqueous media in which the particles are fully hydrated, the hydrated particle diameter is the value that is most desired. Although there are several methods for determining the particle size of a comminuted solid, for the particle

range that is usually encountered, a wet - sieve analysis is the method usually prefered[165], although several mechanical procedureshave been suggested. The procedure for conducting a wet-sieve analysis is described below.

A sample of 152.22 grams of Amberlite IRC-718(Na) was placed on the top of a nest of screens. The screens were then placed in the sink, and a slow stream of water from a length of rubber tubing attached to the tap was played over the resin for 5 minutes. The No. 18 screen was then carefully removed and placed in a 12-inch dish pan. Tap water was poured into the pan until the water depth was about one-half the height of the sieve. The sieve was then gently raised and lowered so as alternately to lift the particles on the screen and float them off again. In this manner the resin was swished about over the surface of the screen, and the smaller particles were pulled through the screen by the upward movement. This operation (raising and lowering) was repeated twenty times. Care was taken to retain the coarse material in the screen and not float or jar it over the edge. The No. 18 screen, plus the coarse resin, was carefully removed from the dishpan and set a side. The contents of the dishpan were then washed (by means of the stream of water from the rubber tubing) onto the No. 20 screen on top of the nest of screens. The No. 18 screen was then replaced in the dishpan, water added as before, and the swishing operation repeated. The washing, were poured again over the No. 20 screen, and the entire operation repeated until no more than a dozen or so particles were seen to come through after a

single washing.

When the No. 18 screen had been washed free of particles finer than No. 18, it was inverted into the dishpan and all the coarser resin washed free from the sieve. The resin was then brushed into a beaker and dried to constant weight in an oven at 105°C. The samples were then weighed and recorded as "retained on No. 18 screen". This operation was repeated for all other screens. The results of this analysis are given in Table 3 and plotted on log-probability paper as shown in Figure 2.

The effective size, which is defined as that sieve opening which will retain 90 percent of the sample is obtained from the best straight line and found to be 0.43 mm. The uniformity coefficient, which is the ratio of the sieve openings that will retain 90 and 40 percent of the sample is found to be 1.44 and the mean particle size is 0.521 mm.

The screen analysis is used to find sauter mean size which can be defined by

$$\frac{1}{D_p} = \sum \frac{x}{d_p} \qquad (3.1)$$

where,

D_p = sauter mean size,

x = fraction of size in mixture,

$d_p = \sqrt{d_1 d_2}$

(d_1, d_2 = adjacent sieve openings)

The sauter mean diameter is found to be 0.628 mm.

TABLE 3 PARTICLE SIZE ANALYSIS

U.S. Standard screen series	Sieve Opening mm	Weight dried resin g	% Retained	% Cumulative
18	1.00	0.0695	0.116	0.116
20	0.85	3.1893	5.327	5.443
25	0.71	7.4849	12.502	17.945
30	0.60	14.4808	24.187	42.132
37	0.50	20.1465	33.651	75.783
50	0.30	14.1902	23.702	99.485
60	0.25	0.3083	0.515	100.000
		59.8695	100.000	

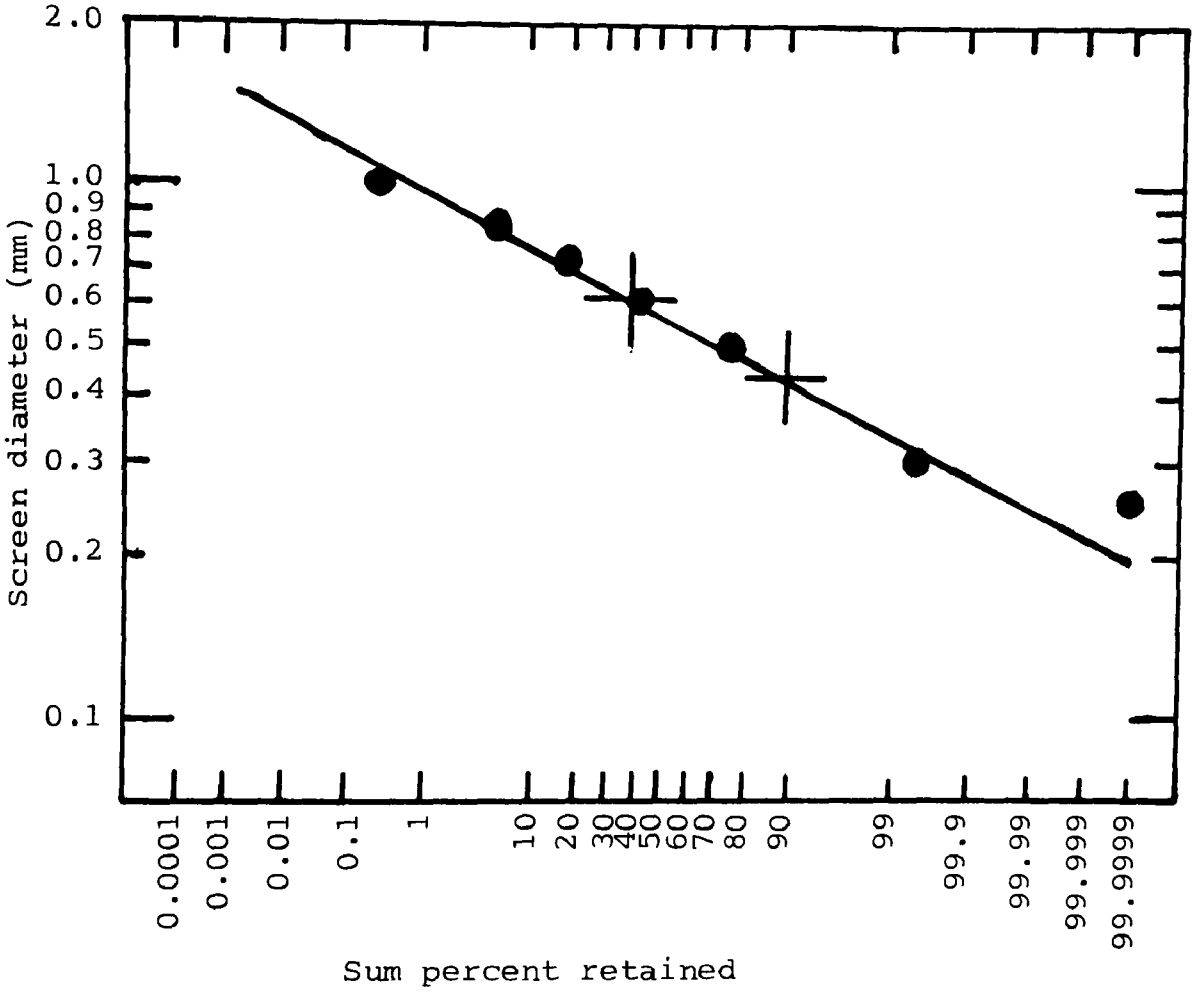

Figure 2 Particle size distribution

3.4 SURFACE AREA MEASUREMENT

Surface area was measured using the following method.

The method is based on the use of two glass adsorption vessels of the same volume; one of them was filled with the sample (measuring vessel) while the other remained empty (reference vessel). Both vessels were filled at ambient temperature with nitrogen gas at the same pressure (atmospheric pressure), they were then cooled in the cold bath to the temperature of liquid nitrogen. The adsorption of the nitrogen on the sample resulted in a pressure difference between measuring and reference vessel which was indicated on the differential manometer.

The surface area of the particles was computed using the following relation

$$S_g = \frac{A \cdot \Delta h}{m} \qquad (3.2)$$

where,

S_g = specific surface area (m^2/g).

Δh = pressure difference on manometer (mm)

A = coefficient determined fromanomogram

m = dry sample weight (g)

The surface area of particles with mean diameter of 0.55 mm is found to be 19.81 m^2/g and for particles of mean diameter of 0.925 mm. is 14.81 m^2/g.

3.5 LIQUOR DENSITY DETERMINATION

The density of 0.2M NaOH with 550 p.p.m. zinc ion

concentration was determined at room temperature using 50 cc density bottles. The average value obtained was 1.007 g./cc. which agrees very well with the value 1.0072 g/cc given by Perry[166] and Weast[167].

3.6 LIQUID VISCOSITY MEASUREMENT

Attempts were made to measure the viscosity of 0.2 M NaOH with zinc ion concentration of 550 p.p.m. at different temperatures using HAAKE Rotovisco RV2[168]. This instrument consists of coaxial cylinder and plate and cone viscosity sensor systems (Searle type) which allows viscosity measurement of Newtonian and non-Newtonian substances over an extremely wide range of shear stress and shear rate. The measuring principle is to contain the substance in the annular space between a rotating cylinder (called the rotar) and a fixed cylinder. The rotar rotates at a defined r.p.m. and the resulting shear stress is an accurate measure for the viscosity of the substance to be measured.

This instrument seems to be insensitive to dilute solutions of sodium hydroxide of low viscosity and therefore the value of the viscosity of 0.2 M NaOH given in Weast[167] (1.042 cp at 20^{o}C) is used in the calculations.

C H A P T E R F O U R

DESCRIPTION OF APPARATUS

Ion exchange was conducted using the ion exchange resin Amberlite IRC-718(Na) to remove zinc ions present in a solution of sodium hydroxide. In the present study a typical laboratory ion exchange column and a burette were used to investigate the rate of ion exchange in a fixed bed. These are represented in Figures 3 and 4. The effect of temperature on the rate of ion exchange led to the use of a water jacket system as shown in Figure 5. A semi-continuous countercurrent moving bed ion exchange system was also constructed and the overall flow sheet is presented in Figure 6. This is also illustrated by the photograph attached. The detailed arrangements of the apparatus are considered under the following headings.

4.1 FIXED BED ION EXCHANGE SYSTEMS

4.1.1 a Ion exchange column

This column is of 2.40cm. internal diameter (measured with a Vernier calipus, supplied by Chesterman, Sheffield), 0.20cm. wall thickness (measured with a micrometer, supplied by Moore & Wright, Sheffield), and 150cm. height. It was held in a vertical position by means of screw clamps mounted on a framework. Two 500ml. separatory funnels, one for feed solution and the other one for regenerant solution were installed over the column at both sides and connected to the

top of the column with rubber tubes. Backwash outlet was connected with a T-junction glass tube and led to the sink via a rubber tube. Backwash inlet was connected from the tap to the bottom of the column via a rubber hose. The other bottom end was the outlet for the effluent from the column. Glass wool plug was used for the bed support which was resting on a tightly fitted rubber stopper with a glass tube of 0.6cm. internal diameter inserted through it. The overall flow sheet of this system is shown in Figure 3.

4.1.1b Burettes

A typical set-up of a burette and a separatory funnel mounted over it is represented in Figure 4. Five burettes of 2.06cm. internal diameter, 0.25cm. wall thickness, and 65cm. height were used and 5x500ml. separatory funnels were mounted over the burettes through a tightly fitted rubber stopper. All burettes and separatory funnels were held in a vertical position by means of screw clamps fixed on one stand. Again glass wool plug was used for the bed support. Constant hydrostatic level of liquid in the burettes was maintained using this arrangement. It was found that results can be obtained much faster as sets of 5 and it was more convenient to handle this arrangement than the previous one described in section 4.1.1a and therefore most of the fixed bed results were obtained using this assembly.

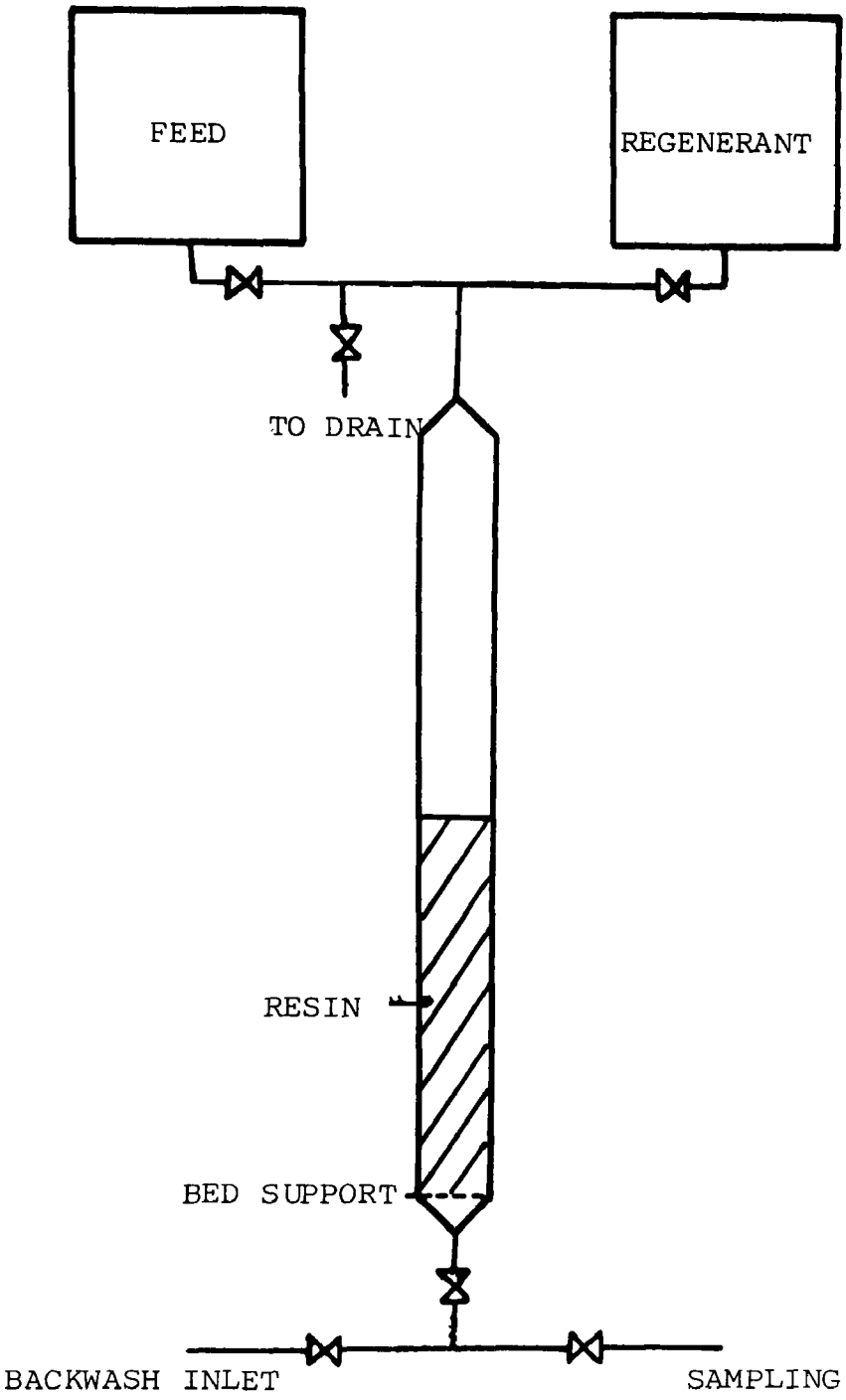

Figure 3 Ion exchange column

Figure 4 Fixed bed ion exchange apparatus

4.1.2 Apparatus for the study of Temperature effect

Figure 5 shows the different units used in this study and they are described below.

4.1.2.1 Water jacket column

This consists of two columns, the inner column is made of glass and of 2.54cm. internal diameter, 0.2cm. wall thickness and 100cm. length. The outer column is made of plastic and of three sections, each section is of 3.6cm. internal diameter, 0.3cm. wall thickness, and 30cm. length. There are screw groves at both ends of each piece and are mounted together with 2 circular rings of 2.5cm. width. Both ends of this column have a circular ring of 2cm. width with inlet/outlet hose of 0.4cm. internal diameter. The two columns are held together with two rounded pieces of 3cm. width screwed to the outer column. The top piece contains a cone which is narrow at its lower end, internal diameter of 2.54cm. and this is in line with the inner column. The lower end of the inner column is closed with a rubber stopper with a glass tube of 0.6cm. internal diameter fitted through it to provide an outlet for the effluent from the column. A perforated circular disc made of perspex and of 2.4cm. internal diameter and 0.3cm. thickness with holes of 1mm. diameter was placed inside the column and two layers of 6mm. and 2mm. in diameter glass beads were packed over the perforated plate to act as means of bed support.

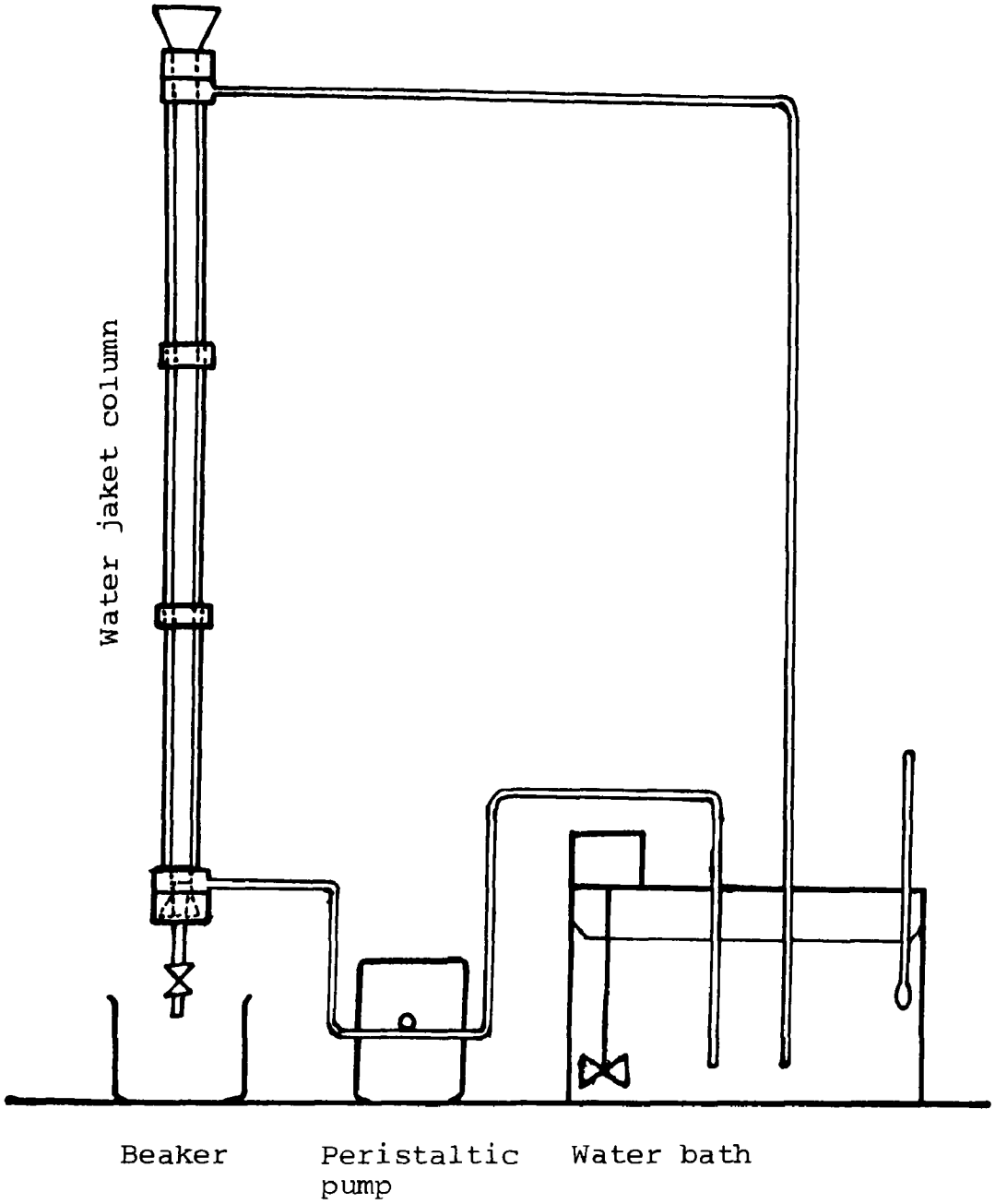

Figure 5 Apparatus used to study the effect of Temperature on BT.C

4.1.2.2 Temperature control and measurement

The temperature of the water used for recirculation was controlled by a glass-fronted water bath (supplied by Grants Instruments-Cambridge, Ltd.). The thermostat was set to the required temperature and after the temperature has reached the required value, the water was pumped into the annulus by means of peristaltic pump (supplied by Watson Marlow Ltd., Marlow, Bucks.). After about 30 minutes, the temperature in the inner column reached values of -0.5 to -2.0^{o}C from the set value, this was achieved through the use of maximum flow rate with tubes of 0.7cm. internal diameter and also heat and water evaporation from the thermostatically controlled water bath were minimised using small insulating plastic spheres (supplied by Gallenkamp, Ltd.) which covered the surface of the water. The temperature in the inner column was measured using a thermometer (supplied by Gallenkamp, Ltd. and graduated from -10^{o}C to 110^{o}C) inserted through a rubber stopper and placed at the top of the column in the liquid. The temperature was also checked at the end of each run by allowing the effluent to flow at high flow rate. The range of temperatures used in this study was 24-60^{o}C, the water bath was set to 62^{o}C in order to give a temperature of 60^{o}C in the inner column. At a lower temperature the deviation was small (at 32^{o}C, a temperature of 31.5^{o}C was recorded in the inner column).

4.2 SEMI-CONTINUOUS MOVING BED ION EXCHANGE APPARATUS

The different parts of this apparatus are described below.

4.2.1 Extraction column

It consists of a cylindrical borosilicate Q.V.F. (Quickfit) glass column(E) as shown in Figure 6. The column has an internal diameter of 2.54cm., 0.5cm. wall thickness, and 30.5cm. in height. Two T-junctions of 14cm. length were fixed to the top and bottom ends of the column with the help of two parallel circular metal fittings and five equally spaced galvanized bolts. The side arm of the bottom piece was filled with glass wool and closed with rubber stopper with a bend glass tube of 0.7cm. internal diameter inserted through it and provided an exit for the processed liquor. A control valve (C) was fixed to the bottom T-junction. This valve provided support to the resin bed and ensured a uniform ascending of resin up the column. The top T-junction was for the inlet and outlet of liquid and resin respectively. The liquid entered the column through a T-junction of 0.6cm. internal diameter inserted through a rubber stopper, the top end kept open to act as a vent (V). The side arm was joined to a bend tube with the help of metal fittings and bolts and a control valve was fixed to the bottom end of the bend tube. This assembly was held in position by means of four horizontal clamps fixed to the supporting framework.

B Beaker for D.I.H_2O
F Feed reservoir
W Drainage valve
P Peristaltic pump
FM Flowmeter
V Vent
E Extraction column
R Resin sampling valve
L Liquid exit valve
M Measuring cylinders

D Resin drainage valve
A Auxiliary column
Flow direction of liquid
Flow direction of resin
On/off valve
Control valve

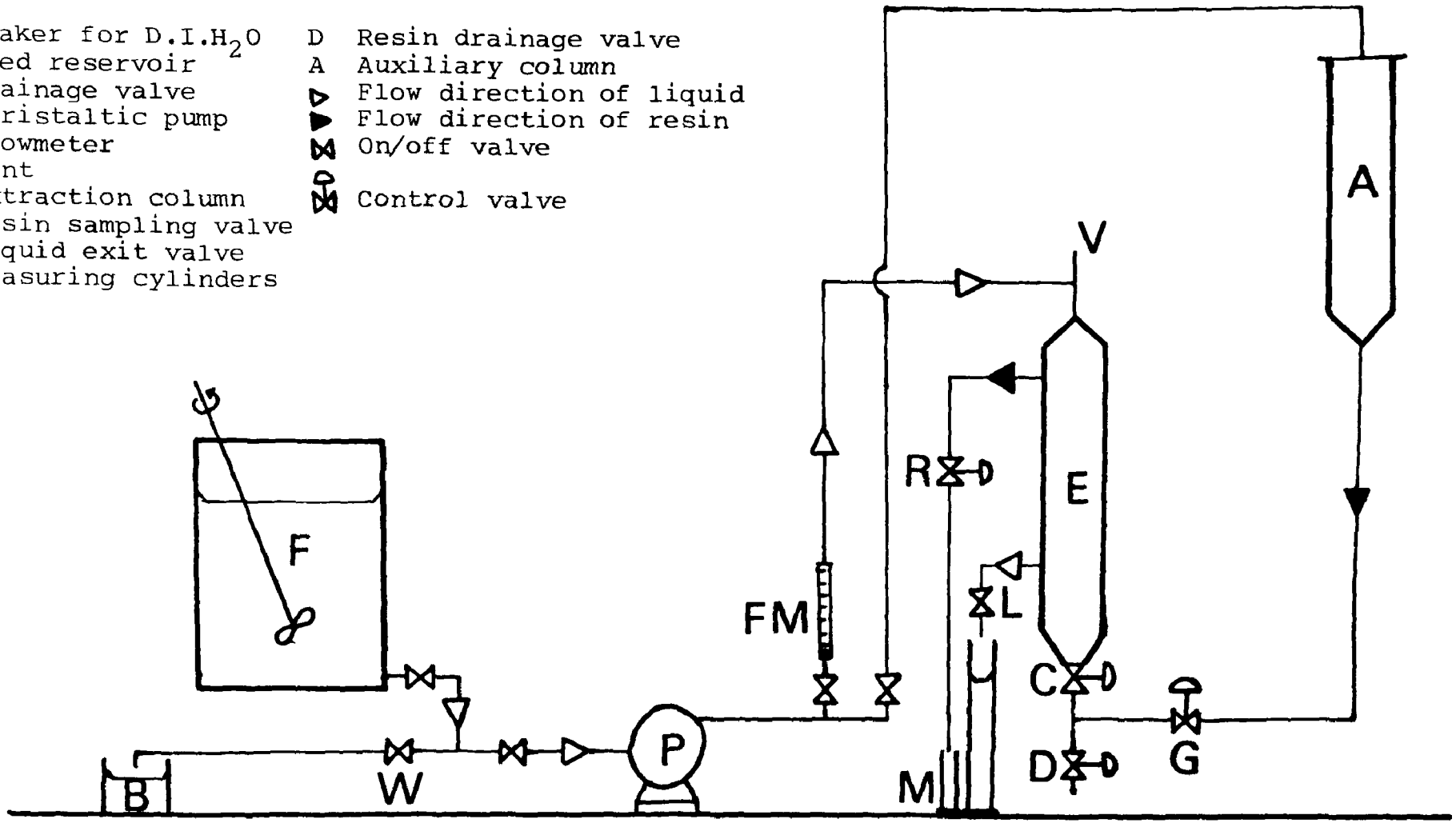

Figure 6 Flowsheet of the apparatus for moving bed ion exchange

4.2.2 Auxiliary column

This column is made off the same material and of the same diameter as for the extraction column but of 61cm. in height.

It is fixed to a tapering of 9cm. in length and the outlet is positioned at 110cm. from bench level. A pvc tube of 1.6cm. internal diameter, 0.34cm. thickness, and 94cm. in length is fixed to the tapering and at the bottom to a control valve (G) which is positioned horizontally and fixed with a clamp to the framwork. It is joined to a T-junction of 1.2cm. internal diameter by means of pvc tubing. Valve G is of 15cm. length and 4cm. away from the T-junction. The bottom end of the T-junction contains a small control valve (D) of 0.85cm. internal diameter. This was installed to provide means of emptying the whole content of the extraction and auxiliary columns and all the tubes and valves connected to the column and also to remove excess resin from the extraction column. The top end of this T-junction is connected to the control valve (C).

The auxiliary column (A) was open to the atmosphere and when not in use was covered with a stopper to prevent any dust from getting into resin slurry since metals such as zinc are found in various dusts.

4.2.3 Feed reservoir

A borosilicate glass container (F) of 20cm. internal diameter, and 33cm. in height with a total volumetric capacity of 10.5 litres was used to contain the feed solution. The solution was stirred continuously at constant speed using an electromagnetic stirrer. A wooden stand of dimensions 20x20x6.5cm. was used to support and raise the level of the feed reservoir to 19cm. The container was graduated with a sticker to read up to 10 litres and periodic topping of solution maintained the level of liquid to within $\pm$ 0.5 litre. This reservoir was covered with an inverted plastic bottle to prevent any dust contamination. The outlet stream was controlled with on/off valve, during operation the valve was fully open and was closed on other occasions.

When working with low flow rates of the order 7-10 ml./min., it was suitable to use a 500 ml. separatory funnel fitted on top of the extraction column through a tightly mounted rubber stopper instead of the feed reservoir. This also helped to avoid stirring and pumping of the solution.

4.2.4 Resin flow arrangement

A beaker (B) of volumetric capacity of 1000 ml. was used to pump de-ionised water to the auxiliary column in order to create a hydrostatic head which helped to force the resin move down the tubing and up the extraction column. On one occasion the resin was poured into this beaker and pumped using the peristaltic pump to the top of the auxiliary column

but unfortunately this caused to considerable attrition of the resin particles and therefore the resin was replenished manually by standing on the bench. This end of the apparatus was also used to drain the solution from the feed reservoir and from the tubings connected to the extraction and auxiliary columns by opening the on/off valve (W) and by reversing the pump flow direction.

4.2.5 Feed flow arrangement

When the feed reservoir was in use a two-way flow peristaltic pump (P) capable of delivering liquids up to flow rates of 830 ml./min. was used. This pump was installed between the Feed reservoir and the flow meter as shown in Figure 6. The flow rate was controlled with a selector dial which regulates the speed of the rotor, at a speed of 2.40, a flow rate of 60 ml./min. was recorded.

4.3 Flow rate measurement

The flow rate of the feed solution was measured with the help of a flow meter (FM). This meter has a plastic coated glass float and is graduated from 0 to 150 mm. in height and gives calibrated flow rates of water in the range 0-150 ml./min. A calibration curve is included in the appendix (Figure A 3.1). The flow rate of the effluent from the extraction column which was the same flow rate as for the feed was also checked using a measuring cylinder and a

stopclock. The latter method of measuring the flow rate was also adapted when the feed solution was supplied through a 500 ml. separatory funnel fitted at the top of the extraction column and at the top of each burette in fixed bed runs.

The flow meter is of 25cm. length and is fixed to the supporting framework by means of two wires. It is at distances of 27cm. and 64cm. from the peristaltic pump and the T-junction fitted to the top of the extraction column respectively.

4.4 Pressure drop measurement

The pressure drop due to the liquid flow alone was found to be in the range 3.4-42.0cm. CCl_4 for flow rate ranged from 8 ml./min. to 130 ml./min. There was an additional pressure drop of 35.5cm. CCl_4 created by the weight of resin and de-ionised water filling a total height of 46cm. The pressure drop for various flow rates is plotted in Figure A 3.2 (in the appendix) and the attached photograph illustrates the apparatus construction for this measurement.

4.5 Bed voidage determination

The voidage of the packed bed for the fixed and moving bed systems was determined by the following method.

Amberlite IRC-718 (Na) was slurried into the burette/ column and the level of de-ionised water was adjusted in such a way that it coincided with the upper surface of the

resin. The de-ionised water was then allowed to drain into a graduated cylinder and finally air was blown through the burette/column. This method gives results 5% less than the real value[169] because of the adsorption of water on the surface of the resin particles. The void fraction is simply given by the following relation

$$\varepsilon = \frac{\text{volume of the collected water}}{\text{volume of the packed bed}}$$

Using the burette the voidage ranged from 0.38 for particles of mean size diameter 0.521 mm. (in the range 0.297-1.19mm.) to 0.44 for particles of mean diameter 0.855mm. The voidage of particles of mean diameter 0.655mm. is 0.40. For the moving bed a column of 2.54cm. internal diameter and 50cm. in length was used with a nylon mesh and a circular perspex perforated plate placed at the base for the bed support. A mean value of 0.3 was obtained for bed heights ranged from 8 to 30cm. and mean particle diameter size of 0.521mm.

4.6 Superficial liquor velocity

The superficial liquor velocity was calculated by dividing the volumetric flow rate by the cross-section area of the packed burette/column.

4.7 Effective interfacial area

The effective transfer area per unit volume of bed is calculated from the equation

$$a = \frac{6\ (1 - \varepsilon)}{d_p} \qquad (4.1)$$

where,

a = effective transfer area per unit volume

ε = bed voidage

d_p = mean diameter of resin particles

Using the values of ε and d_p, the effective transfer area, a, is in the range 39.3-97.5 cm^2/cm^3 for particles of mean diameter 0.0855cm. and 0.040cm. respectively.

C H A P T E R F I V E

EXPERIMENTAL STUDY

5.1 LEACH LIQUOR

The leach liquor was provided in 5 litres well covered plastic containers from the previous investigation on lead separation[6]. The concentration of sodium hydroxide solution ranged from 40 gm./l. to 400 gm./.l. (10N). Zinc and lead ions concentration were measured using atomic absorption spectrophotometer. Zinc concentration ranged from 5500 p.p.m. to 48300 p.p.m. while lead concentration was much lower (250-1875 p.p.m.). Since ion exchange kinetics are enhanced in dilute solutions this led to the dilution of the leach liquor (40 gm./l. concentration) down to concentrations of 4 gm./l. and 8 gm./l. which contained zinc and lead ions concentration in the range 55-550 p.p.m. and 2.5-25 p.p.m. respectively. The level of lead ion in the solution was accepted in the present study and its effect on the breakthrough curves investigated.

The other reagents which were needed in this study are listed below

1. Hydrochloric acid about 36% HCl for atomic absorption spectroscopy.
2. Nitric acid about 70% HNO_3 for atomic absorption spectroscopy.
3. Lead nitrate standard solution for atomic absorption spectroscopy.

4. Zinc nitrate standard solution for atomic absorption spectroscopy.
5. Sodium hydroxide 400 gm./l.
6. Lead monoxide.

Reagents (1) and (2) are specific for atomic absorption spectroscopy since the concentration of the metal ions present are in the range 0.02-1.0 p.p.m. All the reagents are obtained from BDH Chemicals.

5.2 SAFETY PRECAUTIONS

When handling concentrated acids, rubber gloves, goggles and a laboratory coat were worn. Distillation of HCl was carried out in a fume cupboard. Care was taken when handling caustic solutions since they can cause severe burns and also they are poisoneous. Borosilicate glass columns although their wall thickness is 0.5cm. they are found to be fragile and could break easily and therefore care was needed during the construction of the apparatus and maintenance. Every effort was made to insure that the pressure did not build up during the operation of the apparatus.

5.3 PREPARATION OF LEACH LIQUOR

The solutions used for the separation of zinc ion using fixed and moving bed ion exchange systems were prepared from the stock caustic solutions provided by the following dilution procedure.

A tenfold dilution of 40 gm./l. NaOH with 5500 p.p.m. zinc ion concentration using de-ionised water followed by a tenfold dilution with 4 gm./l. NaOH to give a diluted solution of 4 gm./l. NaOH with zinc ion concentration of 55 p.p.m. Solutions of 8 gm./l. NaOH with zinc ion concentration of 550 p.p.m. were obtained by a fivefold dilution of 40 gm./l. NaOH followed by a twofold dilution with 8 gm./l. NaOH. The dilution with sodium hydroxide solution of the required strength was necessary since precipitation of zinc ion in solution of pH $<$ 13 or even at pH $\geqslant$ 13 was observed. The stability of the zincate complex is low and under these circumstances zincate complex tends to combine with the hydroxide ions to form a precipitate of zinc hydroxide.

5.4 EXPERIMENTAL PROCEDURE

The equilibrium data for zinc-sodium exchange on Amberlite IRC-718 were obtained using a mechanical shaker and the separation of zinc ion from sodium hydroxide solution was studied in fixed and moving bed ion exchange systems.

5.4.1 Batch ion exchange

The hydrated ion exchange resin was weighed accurately using a unimatic balance (supplied by Stanton instruments) which gives readings up to 5 decimal places. Eight samples each of approximately 1 gm. (0.99532-1.02448 gm.) were placed in plastic bottles (supplied by Gallenkamp) of

volumetric capacity 500 ml. Sodium hydroxide solution was diluted using de-ionised water in such away to give eight different zinc ion concentrations of 55-550 p.p.m. but of the same caustic strength (8gm./l.). The solutions from eight 100 ml. volumetric flasks were than added to the samples of resin and the bottles were covered. The covered bottles were mounted on an 8-pin Griffin flask shaker (supplied by Gallenkamp) and left shaking at a speed of 3 for four hours.

The concentration of zinc ion in the liquid phase was followed by withdrawing a 1 ml. sample at intervals ranged from 15 min. to 60 min. for 240 min. The samples were then diluted with 0.05 M HNO_3 and analysed for their zinc ion content using atomic absorption spectrophotometer and the concentration of zinc ion in the resin phase was obtained by difference.

The ion exchange equilibrium of zinc was also investigated using sodium hydroxide solutions of concentrations 4-40 gm./l. with zinc concentration of 55 p.p.m. and exchange resin weights 0.06-2.0 gm.

The analytical procedures for zinc and lead measurements are given in section (5.6).

5.4.2 FIXED BED ION EXCHANGE

Fixed bed ion exchange was carried out in five burettes with glass wool plugs placed at the bottom for the beds support. The hydrated resin was transferred to a 1000 ml. beaker and de-ionised water added. The required amount of

resin was then measured using a 50 ml. measuring cylinder and slurried into the burette with the help of a funnel and de-ionised water from a wash bottle. The remaining steps followed are described under the following headings.

5.4.2.1 Backwash

The resin bed was backwashed with 500 ml. of water at a rate of about 50 ml./min. For this, plastic tubes of 0.9 cm. internal diameter were connected from the bottom of the burette to the tap water and from the top via a bend glass tube of 0.7 cm. internal diameter fitted through a rubber stopper to a 1000 ml. measuring cylinder.

Backwashing was necessary in order to wash light particles adhered to the resin during manufacturing and to loosen the bed and also to free trapped air bubbles.

5.4.2.2 Exhaustion

The resin was rinsed with about 100 ml. of de-ionised water and the static head lowered to a level just covering the resin bed. Sodium hydroxide solution containing zinc ion was poured into the burette carefully in order not to disturb the resin bed and the separatory funnel was then mounted over the burette and filled with the solution. The funnel valve was then fully released and the apparatus was ready for use.

The solution was allowed to flow by opening the burette valve slowly and measuring the flow rate with a measuring

cylinder and a stopclock and also by measuring the amount of effluent collected in a regular time interval. Samples of 1 ml. were taken at regular time intervals until the concentration of zinc ion in the effluent reached its initial value. The samples were diluted with 0.05 M HNO_3 and analysed chemically for their zinc content using atomic absorption spectrophotometer.

The resin bed was then stored and the burette flushed with water followed by de-ionised water. Fresh resin was introduced and backwashed, it was then ready for use. In this study the stored resin was not used again, however, some runs were treated further by rinsing the resin beds with de-ionised water at the same flow rate until the pH of the effluent was neutral.

5.4.2.3 Regeneration

The rinsed resin beds were regenerated with hydrochloric acid. The regeneration was continued until there was no trace of zinc ion in the effluent when analysed using atomic absorption spectrophotometer. The effects of hydrochloric acid strength, flow rate and particle size of resin were investigated. After regeneration the resin was rinsed with de-ionised water until the pH of the effluent was neutral.

5.4.2.4 Conversion

The conversion of the ion exchange resin, Amberlite IRC-718 from the hydrogen form to the sodium form was accomplished using sodium hydroxide. Samples of 1 ml. were taken at regular intervals, diluted and titrated with 0.107 M HCl using methyl orange as an indicator. The process of conversion was continued until the original 1 M NaOH titration volume with 0.107 M HCl, was reached. During the titration the colour changed from orange to pink.

Two breakthrough curves were obtained using re-conditioned resin.

5.4.3 Moving bed ion exchange

Moving bed runs were carried out using the apparatus illustrated in Figure 6 (page 109). Initially the extraction column (E) was calibrated using measured volumes of the ion exchange resin. The ion exchange resin Amberlite IRC-718 (Na) was then slurried with streams of de-ionised water from a wash bottle into the auxiliary column (A), tubings and the extraction column (E) until the required volume was reached. Extreme care was taken to insure that no air bubbles were trapped since this lead to channelling and poor results. Excess resin was removed from the extraction column (E) by opening the valve (D) and the static head of de-ionised water was lowered to a level just covering the top of the resin bed by opening the liquid outlet on/off valve (L). The apparatus was then ready for use.

Sodium hydroxide solution containing zinc ion was stirred at constant speed in the feed reservoir (F) or in the case of using a separatory funnel mounted over the extraction column (E), the solution was well mixed in 1000ml. volumetric flask. The solution was then pumped into the extraction column at the selected flow rate (the measurement of flow rate is described in chapter four). Samples of 1ml. were taken at regular time intervals, diluted and analysed chemically for their zinc content using atomic absorption spectrophotometer. After a pre-determined time period the pumping was stopped and the excess liquid covering the resin bed was siphoned using a plastic tube of 0.3 cm. internal diameter. A small amount of the resin was removed by opening valves (C) and (G) and by pumping de-ionised water to the auxiliary column (A). The ion exchange resin was observed descending down the auxiliary column (A) and ascending up the extraction column with the resin particles moving relatively to each other and keeping their position constant in the bed. The volume of the resin removed via the control valve (R) was measured with 50ml. measuring cylinder. The amount of the resin removed was monitered with the control valve (G). The excess resin in the extraction column was removed through valve (D) and recycled to the auxiliary column. Any excess resin on the outlet valve (R) was withdrawn and re-added to the extraction column by removing the T-junction. The valves (C) and (R) were then closed and the pumping of the solution re-started. A time period of ten minutes was sufficient for each shutdown. The procedure was repeated until the required number of cycles

achieved. At the end of each run the whole working volume of resin was transferred and fresh resin replaced it. The exhausted resin is treated by the following procedure.

The resin samples were filtered by transferring them from the 125ml. plastic bottles onto a 2 litre filteration flask with Whatman filter paper of size 9 cm. as the porous medium. Filtration was continued (for about 10 minutes) and the resin was rinsed properly with de-ionised water. After filtration the resin was transferred to a 500ml. plastic bottle with the help of a spatula. Hydrochloric acid of 0.5M was added to each sample in quantities of 100ml. and the covered bottles were mounted onto the 8-pin flask shaker and left shaking at constant speed of 3 for 90 minutes. After the regeneration with hydrochloric acid, 1ml. samples were taken, diluted and analysed chemically for their zinc content. This procedure measured the concentration of zinc in the exit stream.

5.5 ACID RECOVERY

The effluent leaving the burette from the regeneration step consisted of hydrochloric acid and zinc chloride. Sodium chloride was also present. An attempt was made to recover the hydrochloric acid by the process of distillation. The whole assembly was set-up in a fume cupboard. The water inlet of the condenser was connected to the tap and the water outlet immersed in the sink. A conical filtration flask of volumetric capacity 1000ml. was used as a receiver and was

connected to a filtration pump. This pump provided a vacuum which was controlled with on/off valve. The liquid mixture was poured into a 1000ml. quickfit distillation flask and a thermometer inserted through a quickfit cover. Anti-bumping chips were added and the heating started with the help of a bunson fire. Distillation was continued until most of the hydrochloric acid was collected in the receiver. Heating was then stopped and sodium hydroxide was added to the cold residue in order to raise the pH of the solution and thus precipitate zinc hydroxide. Sodium hydroxide was added in small aliquot and the mixture was stirred at constant speed with a magnetic stirrer. The pH of the equilibrated solution was measured with a pH meter (supplied by Unican, Model 291). Zinc hydroxide precipitated at a pH of 9.5 and was dried in a thermostatically controlled oven at a temperature of 125^{o}C over three hours period. At this temperature zinc hydroxide decomposes to zinc oxide. The dried zinc oxide was weighed and stored in a covered plastic container.

5.6 ANALYTICAL PROCEDURE

The samples containing zinc and lead ions were analysed using atomic absorption spectrophotometer. The underlying principle of atomic absorption spectroscopy is discussed in the following paragraph.

If a solution containing a metallic salt (or some other metallic compound) is aspirated into a flame (e.g. of acetylene burning in air), a vapour which contains atoms of the metal

may be formed. A large number of the gaseous metal atoms will normally remain in an unexcited state or, in other words, in the ground state. These ground state atoms are capable of absorbing radiant energy of their own specific resonance wavelength, which in general is the wavelength of the radiation that the atoms would emit if excited from the ground state. Hence if light of the resonance wavelength is passed through a flame containing the atoms in question, then part of the light will be absorbed, and the extent of absorption will be proportional to the number of ground state atoms present in the flame.

The procedure by which gaseous metal atoms are produced in the flame may be summarised as follows.

When a solution containing a suitable compound of the metal to be investigated is aspirated into aflame, the following events occur in rapid succession:

(a) evaporation of solvent leaving a solid residue;

(b) vaporisation of the solid with dissociation into its constituent atoms, which initially, will be in the ground state;

(c) some atoms may be excited by the thermal energy of the flame to higher energy levels, and attain a condition in which they radiate energy.

The resulting emission spectrum thus consists of lines originating from excited atoms or ions.

The essential components of an atomic absorption spectrophotometer are discussed briefly under the following headings and are shown in Figure 7.

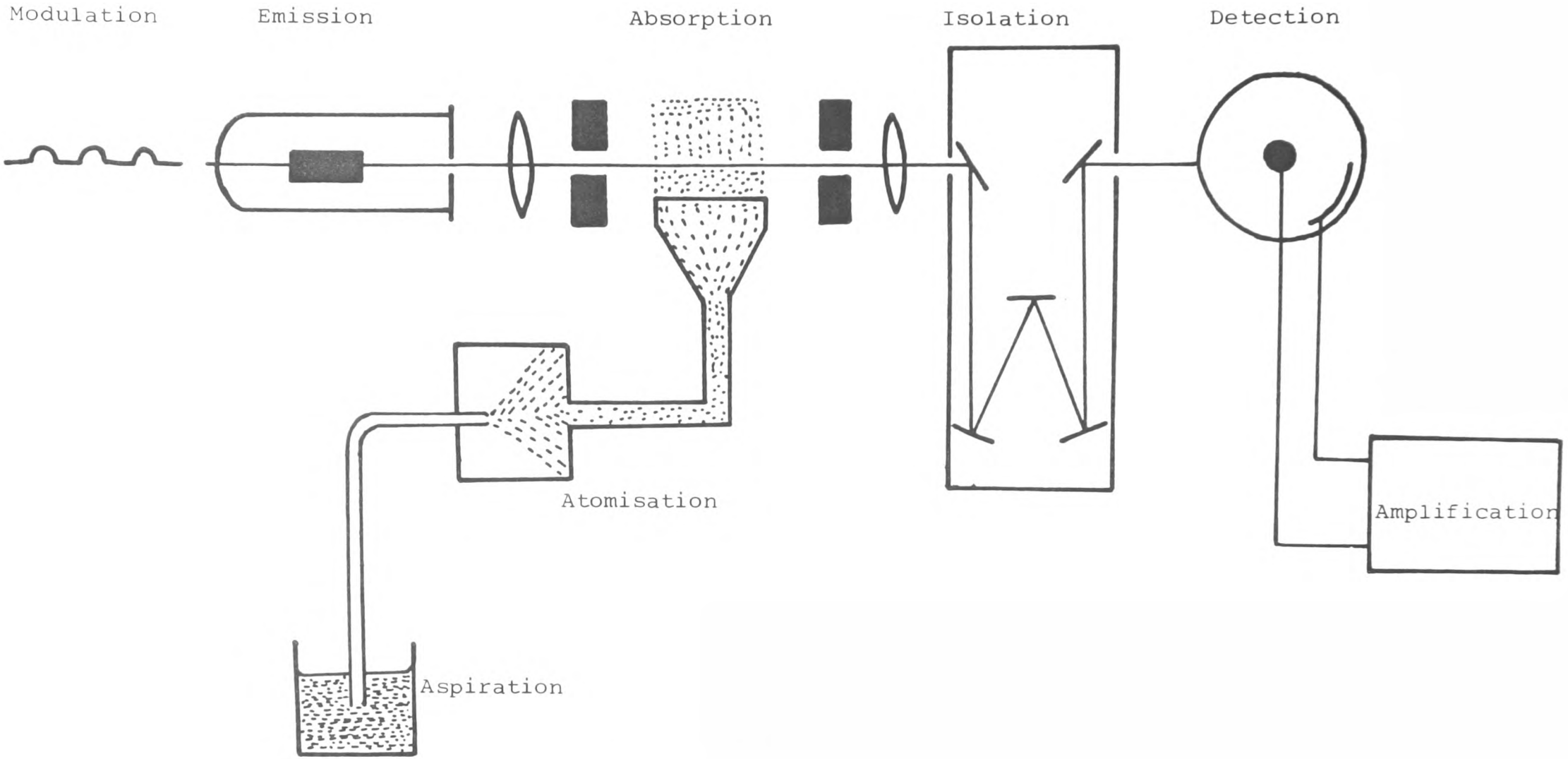

Figure 7 Schematic Diagram of Atomic Absorption Spectrophotometer

1. Combustion flames

Flames which produce temperatures in excess of 2000K are used. This is achieved by burning the fuel gas in an oxidant which is usually air, nitrous oxide, or oxygen diluted with either nitrogen or argon.

2. Nebuliser/Burner system

The purpose of this system is to convert the test solution to gaseous atoms. The function of the nebuliser is to produce a mist or aerosol of the test solution. The solution to be nebulised is drawn up a capillary tube by the Venturi action of a jet of air blowing across the top of the capillary; a gas flow at high pressure is necessary in order to produce a fine aerosol[170]. In the burner, the aerosol is produced in a vapourising chamber where the larger droplets of liquid fall out from the gas stream and are discharged to waste. The resulting fine mist is mixed with the fuel gas and the carrier (oxidant) gas, and the mixed gases then flow to the burner head.

3. Resonance line source

A hollow cathode lamp is the resonance line source. For any given determination the hollow cathode lamp used has an emitting cathode of the same element as that being studied in the flame. The cathode is in the form of a cylinder, and the electrodes are enclosed in a borosilicate or quartz envelope which contains an inert gas (neon or argon) at a pressure of approximately 5 torr. The application of a high potential across the electrodes causes a discharge which

creates ions of the noble gas. These ions are accelerated to the cathode and on collision, excite the cathode element to emission.

4. Monochromator

The function of the monochromator is to isolate the resonance line from all non-absorbed lines emitted by the radiation source. In most commercial instruments diffraction gratings are used because the dispersion provided by a grating is more uniform than that given by prisms.

5. Detectors

In view of the improved spectral sensitivity required, photomultipliers are employed. The output from the detector is fed to a suitable read-out system.

In this study two AAS instruments were used, the AAS 1100 and AAS 1275 (both supplied by Varian Techtron). Moving bed ion exchange samples were analysed using the recent installation (late 1982) of the AAS 1275 with digital read-out display.

The following is an outline of the preparation of samples and standards and the procedure adapted.

Due to the high zinc content of the samples, these samples had to be diluted with 0.05 M HNO_3 in order to bring down the concentration of zinc ion within the range 0-2 p.p.m. and also to bring down the pH of the solution to 1.5 since zinc ion will remain in solution at low and high pH. Standards were needed in order to calibrate the instrument. The working

standards for zinc are of concentrations of 0.5, 1.0, 1.5 and 2.0 ppm and that of lead are of 5, 10, 15 and 20 ppm. The standards were prepared from a stock solution of zinc nitrate spectrosol with zinc ion concentration of 1000ppm by two dilution procedures. The first dilution procedure was to pipette 10ml. into 100ml. volumetric flask and make up with de-ionised water and the second procedure was to pipette 0.5, 1.0, 1.5 and 2ml. from the 100ppm solution into four 100ml. volumetric flasks and to make up 100ml. mark using 0.05 M HNO_3. Similar dilution procedures were employed in the case of lead ion. The operating instructions followed are described below.

The required lamp was inserted into the instrument followed by switching on the Varian and power. The lamp current, the wavelength and the spectral band pass were selected and the instrument was left to warm up for 15 minutes. After warming up the air was turned on and the cylinder pressure was raised to 40 p.s.i. which gave a reading of 7 on the support gauge. The fuel acetylene was then turned on and the cylinder pressure was increased to 10 p.s.i. followed by pressing the ignition button and switching the fan on. The flame was blue and the fuel gauge indicated a reading of 2.5. De-ionised water was used for aspiration and the instrument was optimized by adjusting the wavelength and the positions of the lamp and burner. The burner was adjusted vertically and horizontally in order to give 0% absorbance and 100% transmission. The instrument was then

ready for use. The standards were aspirated and the absorbance values were recorded followed by the aspiration of the samples. The concentration of the metal ion was determined from a calibration curve of Absorbance vs. Standards concentration. The calibration curves for zinc and lead are shown in Figures A3.3 and A3.4 in appendix III.

For zinc the absorbance mode was employed and the concentration mode was used for lead[171] which gave as expected a straight line relationship. During the aspiration of the samples, the instrument was checked with the standards after every three samples. At the end of the measurement, the instrument was flushed with de-ionised water and the following were turned/switched off:

(1) Acetylene, (2) Air, (3) Lamp, (4) Power,(5) Varian and (6) Fan.

The above procedure is relevant to the AAS 1100 and that applicable to the AAS 1275 is given in appendix III.

The operating instrument conditions (fixed) for zinc are as follows:-

Lamp current	= 5 mA
Fuel	= acetylene
Support	= air
Flame stoichiometry	= oxidising

The zinc ion can be measured at two wavelengths

(1) at 213.9 nm and spectral band pass 0.2 nm for optimum working concentration range of 0.4-1.6 p.p.m. (sensitivity 0.009 p.p.m. ; and

(2) at 307.6 nm and spectral band pass 0.5 nm for optimum working concentration range of 3500-14000 p.p.m. (sensitivity 76 p.p.m.)

The detection limit at 213.9 nm wavelength is 0.002p.p.m. using air-acetylene flame.

The lamp current for lead is 6 mA and the wavelengths are:

(1) at 217.0 nm and spectral band pass 1.0 for optimum working concentration range of 5-20 p.p.m. (sensitivity 0.11 p.p.m. ; and

(2) at 283.3 nm and spectral band pass 0.2 for optimum working concentration range of 10-40 p.p.m. (sensitivity 0.23 p.p.m.)

The detection limit at 217.0 nm wavelength is 0.02 p.p.m. using air-acetylene flame.

C H A P T E R S I X

INTERPRETATION OF DATA

6.1 FIXED BED ION EXCHANGE

Kinetic informations of ion exchange processes are revealed through concentration history or breakthrough curves of effluent of fixed bed columns.

Many theories on ion-exchange kinetics differing widely in their simplifying assumptions and their results, have been advanced. For successful application it is vital to choose, in each particular case, the most appropriate theory. This requires a thorough general understanding of the phenomena and a precise knowledge of the consequences of the simplifying assumptions.

In many theories a linear isotherm has been assumed and this is applicable in a situation where the ion exchanger has no preference for one ion over the other. In other theories local equilibrium condition is assumed. This assumption is justified only if the finite ion-exchange rate does not cause significant deviations. This condition is met if equilibrium is unfavourable and the non-sharpening boundary has become sufficiently diffuse. In contrast, if equilibrium is favourable; the boundary shape continues to depend decisively on the ion exchange rate, and equilibrium theories are inapplicable.

In most theories "plug flow" in the column is assumed. In reality, however, some deviations from ideality occur such

as eddy dispersion, channelling and hydrodynamic instabilities (due to differences in density and viscosity between adjacent bands).

Amongst the well known theories is the Thomas solution [84] for non-equilibrium conditions and a non-linear isotherm. Thomas assumes a constant separation factor and a rate law which formally corresponds to a reversible chemical reaction of second order (equation (1), p. 45). As ion exchange process in most cases is controlled by ionic diffusion rather than by chemical reaction rate, Thomas solution thus fails to represent the true state of the process.

In this study breakthrough data have been analysed by the methods of Michaels[92], Moison and O'Hern[93] and also by a new method.

6.1.1 Michaels method[92]

A simple treatment of the kinetics of fixed bed ion exchange was developed by Michaels. The treatment is applicable to high exchange rate reactions and is based on the concept of an exchange zone in which the majority of the exchange occurs, and descends through the exchanger bed at constant velocity. By the use of the method, it is possible to correlate laboratory data obtained from small columns and employ the correlation for the design of large ion exchange units. This method is applicable to systems exhibiting favourable equilibrium with symmetrical breakthrough curves. Through

this method zone height, bed capacities, liquid side mass transfer coefficient, and the height and number of transfer units can be calculated.

Zone height is computed from rate data using the equation

$$h_{z1} = h_T \frac{V_Z}{V_T - (1-F)V_Z} \qquad (6.1)$$

where:

h_{z1} = zone height

h_T = mean bed height

V_Z = volume of effluent collected between breakthrough and exhaustion of bed.

V_T = volume of effluent collected upon exhaustion of bed.

F = the fraction of the exchanger present in the zone which still possesses the ability to remove ions.

and from capacity data

$$h_{z2} = \frac{Q_Z}{(1-F)C_T S} \qquad (6.2)$$

where:

Q_Z = quantity of metallic cations removed by the exchange zone from the breakthrough point to exhaustion of the bed (i.e. total cations removed by the exchange zone).

C_T = specific total capacity of the exchanger (i.e. metallic ion content per unit volume when the exchanger is exhausted).

S = total column cross-sectional area.

The total bed capacity, C_T, is calculated from the breakthrough curve according to the relation

$$C_T = \frac{\int_o^{V_T} (C_o - C)\,dV}{V_{RA}} \qquad (6.3)$$

C_o is the concentration of metallic cation in influent, C its concentration in the effluent and V_{RA} is the average volume occupied by the solid in the bed.

Similarly, the effective or working capacity of the exchanger is determined by calculating the area above the breakthrough curve up to the breakthrough point (Figure 8)

$$C_E = \frac{\int_o^{V_E} (C_o - C)\,dV}{V_{RA}} \qquad (6.4)$$

(V_E is the volume of effluent collected up to breakthrough).

The breakthrough capacity can also be determined using the zone height method.

$$C_E = C_T \left(\frac{h_T - (1-F)h_Z}{h_T} \right) \qquad (6.5)$$

The overall liquid side mass transfer coefficient can be obtained from the correlation

$$K_L a = 0.86 \; u_L^{0.5} \qquad (6.6)$$

and the number of transfer units from the equation

$$NTU = \frac{K_L a \, h_Z \, S}{L} = \frac{K}{K-1} \ln (19)^2 - \ln (19) \qquad (6.7)$$

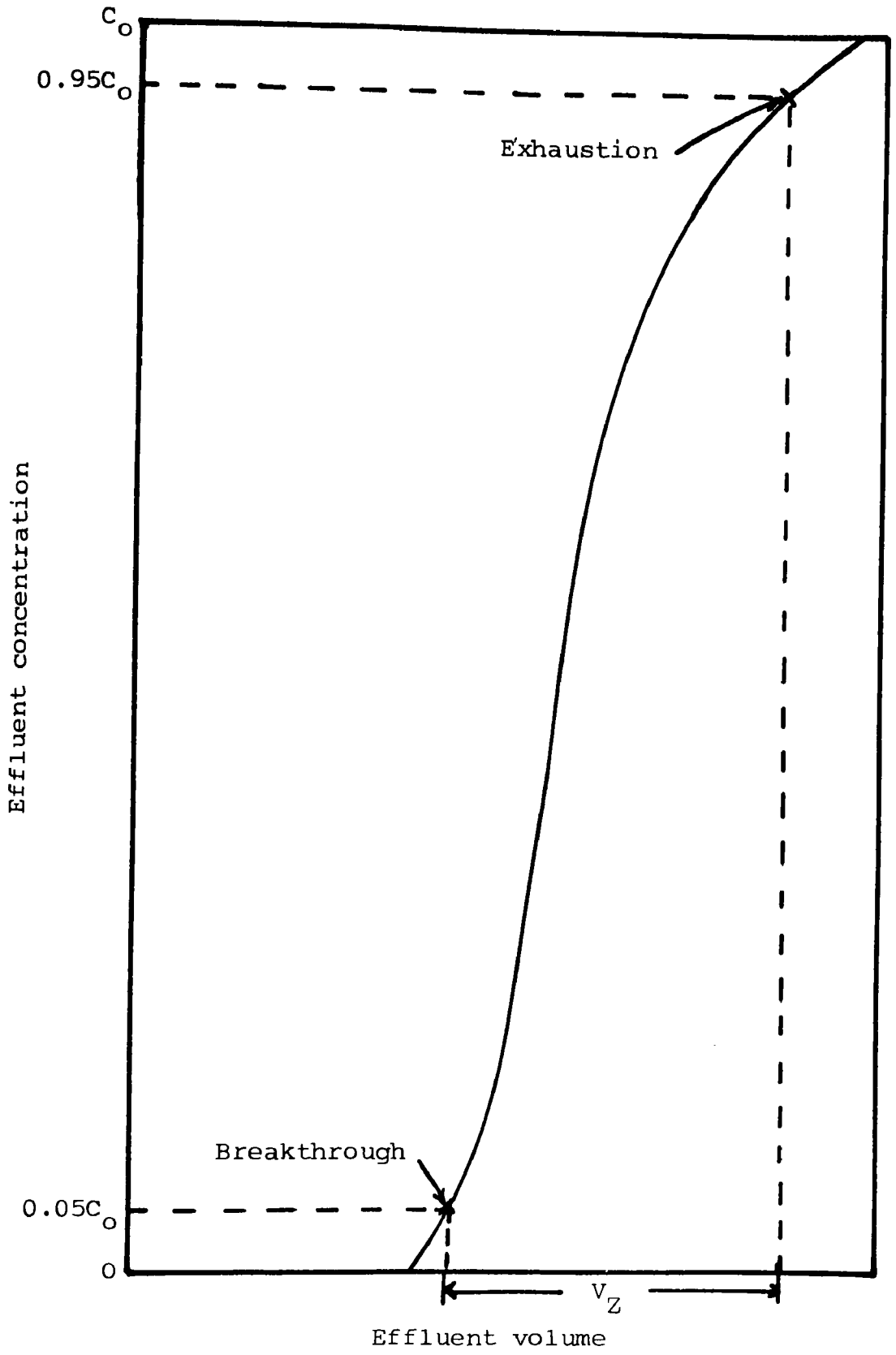

Figure 8 Typical experimental breakthrough curve

The height of transfer units is calculated from the relation

$$HTU = \frac{h_z}{NTU} = \frac{L}{K_L a\ S} \qquad (6.8)$$

6.1.2 Moison and O'Hern method[93]

Moison and O'Hern presented a simple method for correlating ion exchange data for favourable equilibria and both the resin and solution phases resistance were considered. Their correlation was compared with correlations of other packed-bed mass transfer data. The authors also interpreted data for ion exchange with unfavourable equilibria.

The method is based on the concept of exchange zone suggested by Michaels and the same assumptions were made, however, a rather different approach was employed for the derivation of equations for the calculation of zone height and the number of transfer units. Zone height is calculated from the equation

$$h_{z3} = \frac{V_z\ C_o}{S(Q + \varepsilon C_o)} \qquad (6.9)$$

and the rate of descent of the exchange zone, u_z, is given by

$$u_z = \frac{u_L\ C_o}{Q + \varepsilon\ C_o} \qquad (6.10)$$

The number of transfer units within the exchange zone is calculated following the assumption that a fixed bed ion exchange process is analogous to a countercurrent ion

exchange process in which the resin bed moves upward countercurrent to the liquid stream and by using the rate equation of Baddour and Gilliland[88].

$$NTU = \frac{K_L a\ Sh_z}{L} = \frac{K}{K-1} \ln\left(\frac{x_2}{x_1}\right)\left(\frac{1-x_1}{1-x_2}\right) \qquad (6.11)$$

where:

x_1 = equivalent fraction of ion corresponding to the lower limit of the exchange zone; for example, $x_1 = 0.05$.

x_2 = equivalent fraction of ion corresponding to the upper limit of the exchange zone, for example, $x_2 = 0.95$.

K = equilibrium selectivity coefficient.

L = flow rate of solution.

The height of transfer unit is calculated from Equation (6.8). The data can be correlated using the j factor of Colburn[172] which is a dimensionless parameter for relating the height of transfer units (based on the liquid phase) to the physical properties and particle sizes defined as

$$j_D = \frac{1}{HTU\ a}\left(\frac{\mu}{\rho D_L}\right)^{2/3} \qquad (6.12)$$

where:

D_L = liquid phase diffusivity.

μ = solution viscosity.

ρ = solution density.

a = interfacial area of particles.

HTU = overall height of a transfer unit (based on the liquid phase).

The solid phase resistance can be determined according to the equation

$$HTU = \frac{u_L}{K_L a} + \frac{C_o\, u_L}{K\, k_R\, a\, Q} \qquad (6.13)$$

A plot of HTU (at constant liquid flow rates) against solution concentration, C_o, gives a straight line, the intercept of the line indicates the liquid phase diffusion resistance, and the slope governs the resistance in the solid phase.

6.1.3 The New method

A method for the solution of breakthrough curves is developed by us. Through this method breakthrough data are analysed to obtain mass transfer coefficient, zone height and number of zones in a bed. The method is based on a function that is found to describe breakthrough curves of all shapes. The function is of the form

$$C/C_o = 1 - \exp\left(-\left(\frac{t - t_o}{t_m}\right)^{\beta}\right) \qquad (6.14)$$

Where t_o is the time corresponding to break point at $C/C_o = 0.05$, t_m is the mean of the function and β is a shape factor.

The function is applied to breakthrough data in a linear form which is given by

$$\log \ln\left(C_o/(C_o - C)\right) = \beta \log (t - t_o) - \beta \log t_m \qquad (6.15)$$

A plot of $\ln(C_o/(C_o-C))$ vs. $(t-t_o)$ on logarithmic coordinates gives a straight line from which β is obtained as a slope and t_m is calculated through a least square method. By knowing t_m saturation time, t_s is calculated from

$$t_s = t_o + t_m \tag{6.16}$$

and

$$N_z = t_s / t_m \tag{6.17}$$

The height of a transfer zone is given by

$$h_{z4} = h_T/N_z \tag{6.18}$$

Therefore

$$u_z = h_{z4}/t_m \tag{6.19}$$

The overall coefficients of mass transfer in both the stationary and mobile phases can be found through a rate expression obtained by differentiating the function

$$\frac{d}{dt}(1-C/C_o) = -\left(\frac{\beta}{t_m}\right)\left(\frac{t-t_o}{t_m}\right)^{\beta-1} \exp\left(-\left(\frac{t-t_o}{t_m}\right)^{\beta}\right) \tag{6.20}$$

This gives a rate that is dependent on time. A time independent rate is obtained at a point of time when $(t-t_o) = t_m$ and $C/C_o = 0.632$ and this is given by

$$\frac{d\ C/C_o}{dt} = (\beta/t_m)(0.37) \tag{6.21}$$

In order to obtain mass transfer coefficient this rate is related with a conventional rate of mass transfer. Since the loss of material from the fluid is a gain for the solid phase, the rate of mass transfer can be expressed by

$$\frac{d}{dt}(1-C/C_o) = Ka_x \; q_o \; \rho_B \left(\frac{\Delta q}{q_o}\right)_m \qquad (6.22)$$

where $(\Delta q/q_o)_m$ represents the mean value of concentration driving force $(q^*/q - q/q_o)$. This mean value of the driving force can be ascertained by considering mass transfer process over a zone. At the start of a zone the resin is unsaturated $q=0$ and $q^*=q_o$. The driving force is (1-0). When the zone becomes saturated the driving force expressed by $(q^*-q)/q_o$ approaches to zero. The mean of these two values in this case is represented by 0.37 since the driving force is an exponential function of zone saturation time.

Thus $$\frac{d(1-C/C_o)}{dt} = Ka_x \; q_o \; \rho_B \quad (0.37) \qquad (6.23)$$

The overall mass transfer coefficient in solid phase side can therefore be obtained from equations (6.21) and (6.23) and is given by

$$Ka_x = (C_o/q_o \; \rho_B)(\beta/t_m) \qquad (6.24)$$

Similarly fluid side mass transfer coefficient can be obtained from the equation

$$C_o \frac{d}{dt} (1-C/C_o) = Ka_y \; C_o (\Delta C/C_o)_m \qquad (6.25)$$

where $(\Delta C/C_o)_m$ represents the mean of the driving force $(C/C_o - C^*/C_o)$. Like the mean driving force of solid phase this driving force has also a mean value of 0.37. Putting this into equation (6.25), the mass transfer coefficient Ka_y from equations (6.21) and (6.25) is

$$Ka_y = (\beta/t_m) \qquad (6.26)$$

6.1.4 Regeneration data

The regeneration curves or elution curves are analysed by calculating the amount of zinc ion eluted from the column, m, from the area under the elution curve:

$$m = \int_o^{\infty} C_{Zn} \, dV \qquad (6.27)$$

V is the volume of eluate.

6.2 MOVING BED ION EXCHANGE

Moving bed ion exchange results are analysed using the two methods developed by Hiester et al[148] and also by McCabe - Thiele graphical method.

In continuous countercurrent practice, a stream of ion-exchange resin of constant composition, y_o is fed into the top/bottom of a countercurrent contacting section at a constant volumetric rate of flow R_p and is removed from the bottom/top of the section at the same rate. Simultaneously, a solution stream of constant composition, x_o, is introduced into the bottom/top section at a constant volumetric rate of flow R_F and at this same rate passes up through the column countercurrent to the resin and leaves the top. Diagrammatically this is shown in Figure 9.

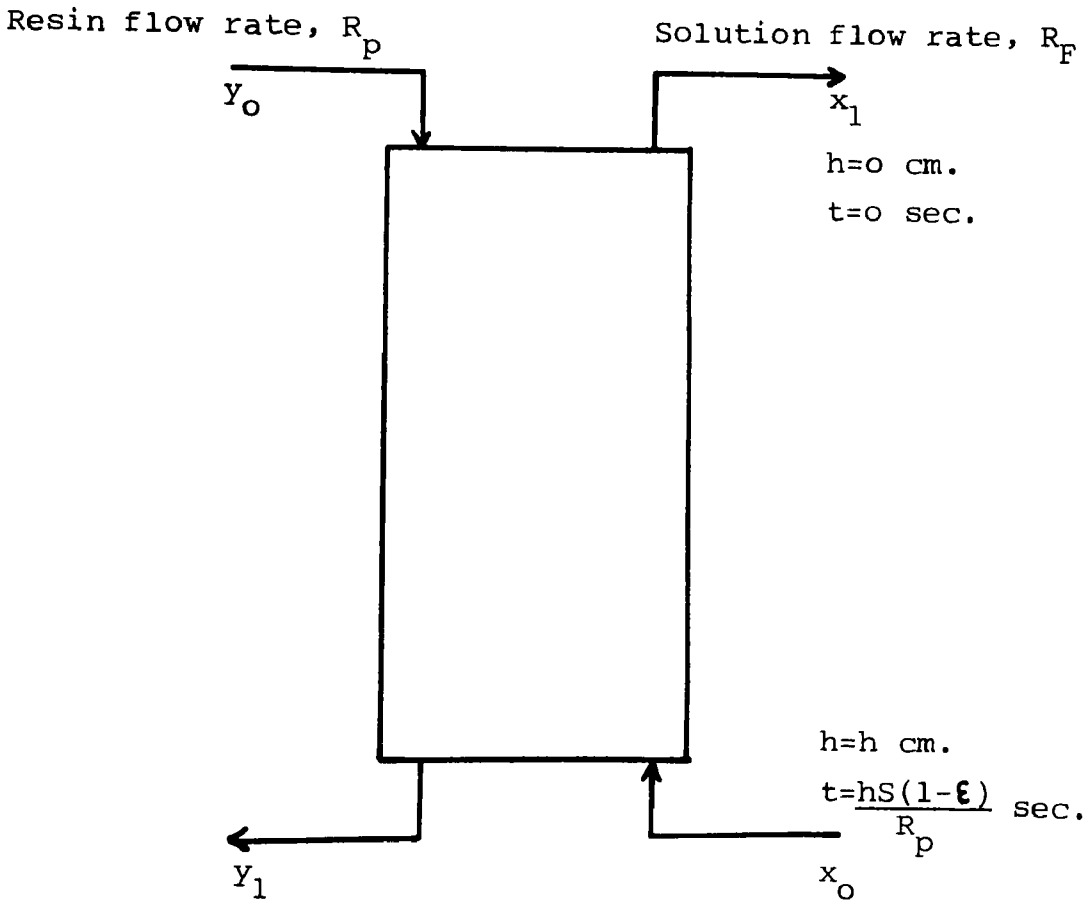

Figure 9 Simple countercurrent operations

Hiester et al[148] suggested two methods for predicting the exit compositions, the first, or dynamic, method based on a rate equation and the second based on the assumption that the section is made up of a finite number of equilibrium contacts (similar to plates in a distillation column).

6.2.1 Dynamic method

For the dynamic approach, a conservation equation and boundary conditions are needed in addition to the rate equation. At steady state, i.e., no accumulation or depletion of ions at any cross section in the column, the following differential material balance equation applies:

$$R_p \rho_B Q \frac{dy}{dt} = R_F C_\Sigma \frac{dx}{dt} \qquad (6.28)$$

The result of solving this equation with the generalized rate equation

$$\left(\frac{dy}{dt}\right)_{particle} = Ka \frac{M}{D_C}\left(x - \frac{y}{M}\right) \qquad (6.29)$$

and the boundaries indicated in Figure 9 gives

$$NTU = \frac{E}{1-E} \ln \frac{E(1-\gamma)}{E-\gamma} = \frac{Ka \cdot h \, S\varepsilon}{R_F} \qquad (6.30)$$

where:

E = ratio of the slope of the equilibrium line to the slope of the operating line $= \frac{M}{R_F C_\Sigma / R_p \rho_B Q} = D_C \frac{R_p/(1-\varepsilon)}{R_F/\varepsilon}$

γ = degree of approach to equilibrium transfer of a component $= \frac{x_o - x_1}{x_o - x_1^*} = E \frac{y_o - y_1}{y_o - y_1^*}$

D_c = distribution or partition parameter = $\frac{M\ Q\ \rho_B(1-\varepsilon)}{C_\Sigma\ \varepsilon}$

M = slope of the equilibrium line.

6.2.2 Equilibrium contanct method

Under the assumption that complete equilibrium is attained in each discrete stage, the relation for the number of equilibrium contacts between the two phases is

$$N_C = \frac{\ln\left[\frac{E - \gamma}{E(1-\gamma)}\right]}{\ln E} \qquad (6.31)$$

The exact relation between NTU and N_C is given by

$$\frac{NTU}{N_C} = \frac{E \ln E}{E - 1} \qquad (6.32)$$

6.2.3 McCabe - Thiele graphical method

The McCabe - Thiele graphical method is applied to the analysis of the results and a typical McCabe - Thiele diagram for trace countercurrent ion exchange is shown in Figure 10.

The number of equilibrium contacts required to reduce the concentration of ion from its feed value to the desired exit concentration is found graphically by stepping off the stages in the conventional manner.

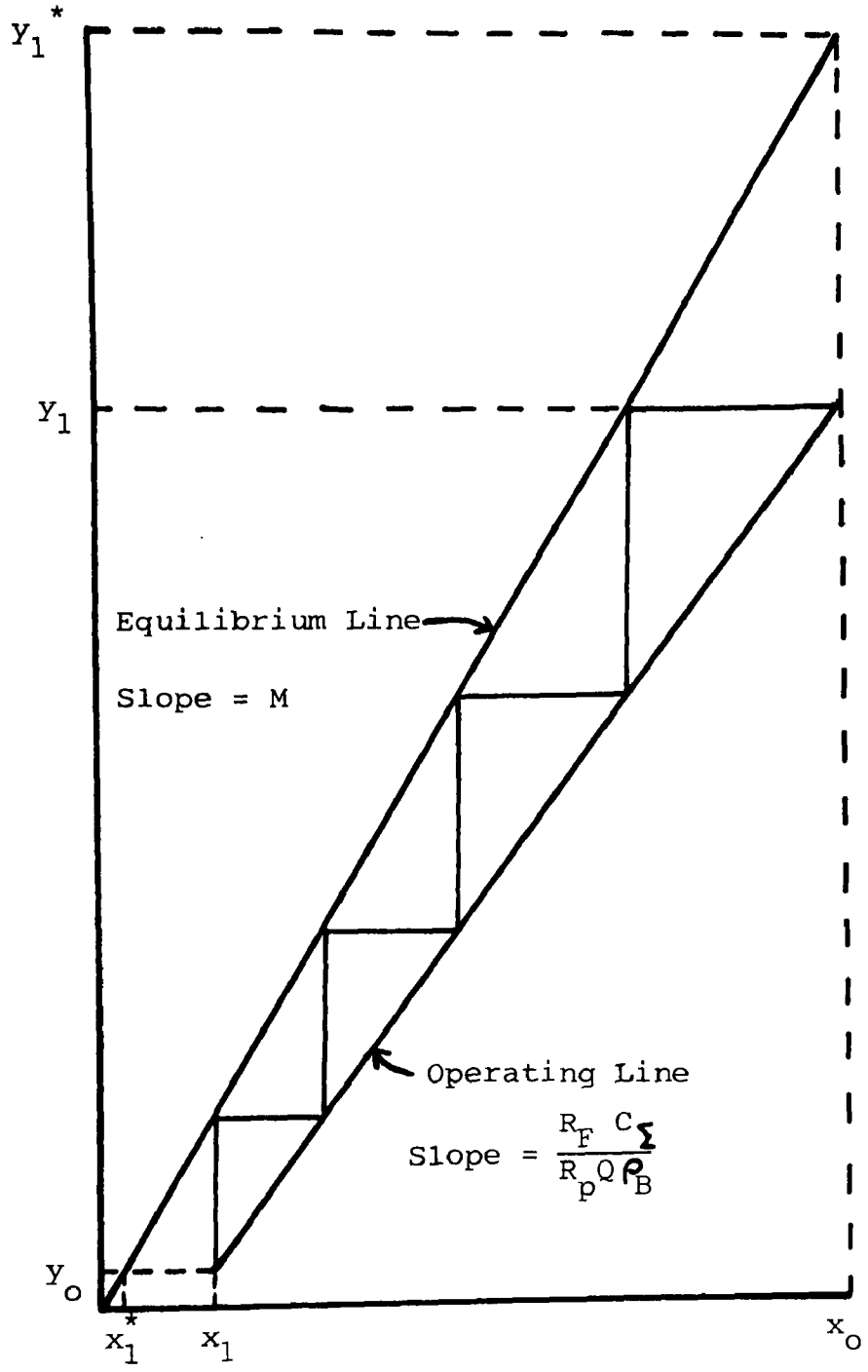

Figure 10 McCabe-Thiele diagram for trace countercurrent ion exchange

6.2.4 Number of transfer units

The number of transfer units is determined graphically as indicated in Figure 11 by the procedure suggested by Selke and Bliss[173].

6.3 ACTIVATION ENERGY

The activation energy of the system is calculated using the Arrhenius equation and the method is outlined below:

$$Ka_x = A.\ e^{-E_a/RT} \qquad (6.33)$$

where

A = frequency factor

Ka_x = solid phase mass transfer coefficient.

E_a = activation energy.

R = universal gas constant, 1.98 cal/g-mol °K

T = temperature, degree kelvin.

Taking log of both sides of equation (6.33) gives

$$\ln Ka_x = \ln A - E_a/RT \qquad (6.34)$$

A plot of $\ln Ka_x$ vs. 1/T gives straight line with slope of $-E_a/R$. Ka_x is calculated from equation (6.24).

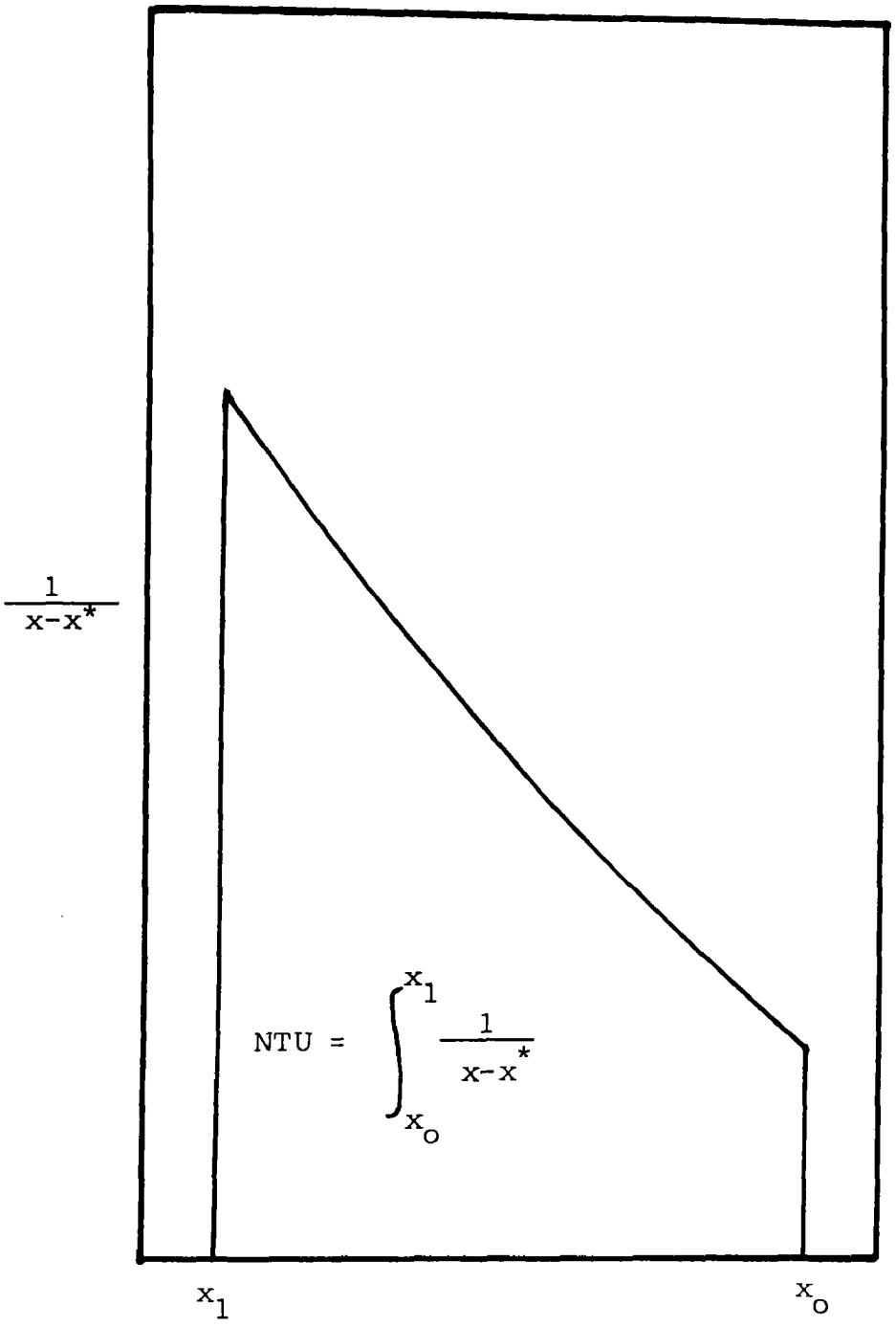

Figure 11 Graphical determination of number of transfer units

6.4 SELECTIVITY COEFFICIENT

The equilibrium constant, K, for the ion exchange reaction

$$Zn^{++} + R\ Na^{+} \longrightarrow R\ Zn^{++} + Na^{+}$$

is given by

$$K = \frac{\left(\bar{a}_{Zn}\right)^{Z_{Na}} \left(a_{Na}\right)^{Z_{Zn}}}{\left(\bar{a}_{Na}\right)^{Z_{Zn}} \left(a_{Zn}\right)^{Z_{Na}}} \qquad (6.35)$$

where:

a = activity in the solution phase = $C\gamma$

$\bar{a}$ = activity in the resin phase = $\bar{C}\ \bar{\gamma}$

Z_{Na}, Z_{Zn} = charge of Na and Zn.

Expression (6.35) is simplified to the following relation by taken the value of the activity coefficients, γ and $\bar{\gamma}$, to be unity

$$K_{C\ Na^{+}}^{Zn^{++}} = \frac{\left(\bar{C}_{Zn^{++}}\right)^{1} \left(C_{Na^{+}}\right)^{2}}{\left(\bar{C}_{Na^{+}}\right)^{2} \left(C_{Zn^{++}}\right)^{1}} \qquad (6.36)$$

K_C is selectivity coefficient.

In terms of equivalent ionic fractions

$$K_{C\ Na}^{Zn} \left(\frac{\bar{C}}{C}\right)^{2-1} = \frac{\left(y_{Zn}\right)^{1} \left(x_{Na}\right)^{2}}{\left(y_{Na}\right)^{2} \left(x_{Zn}\right)^{1}} \qquad (6.37)$$

where:

$$x_{Zn} + x_{Na} = 1$$

$$y_{Zn} + y_{Na} = 1$$

x = equivalent ionic fraction in solution.

y = equivalent ionic fraction in resin.

C = total solution concentration.

$\bar{C}$ = resin phase ionic concentration or capacity.

C H A P T E R S E V E N

RESULTS AND DISCUSSION

7.1 SELECTION OF ION EXCHANGE RESIN

Ten ion exchange resins as listed in Table 4 were tested for their tolerance for high pH values, their selectivity for Zn ions in alkaline solutions, physical strength and particle size.

Resins Duolite C225(Na), Dowex HCR(Na), Dowex HCR-W2, and Zerolite 225(Na) were found deficient in selectivity. With Duolite 255(H) a pH change from 12 to 6 was observed. Although Dowex 50x8(Na) and Amberlite IR-120(Na) are strong cation exchangers, they however were partially dissolved in solutions of sodium hydroxide of concentration 4g/l. and pH 13.

Out of the ten resins only three have shown good selectivity for Zn ions. From these Amberlite IRC-718(Na) was chosen for this work because it was found to give positive results on all points of selection.

7.2 ION EXCHANGE EQUILIBRIA

Equilibrium relationships for the exchange of zinc ion with sodium ion on Amberlite IRC-718 were determined for different zinc and sodium hydroxide concentrations.

The equilibrium isotherm (in the form of a plot of equivalent fraction of zinc on resin against equivalent fraction of zinc in solution) is presented in Figure 12. For this

TABLE 4 List of ion exchange resins tested

	RESIN	MANUFACTURER
1.	Dowex 50x8(Na)	Dow Chemical Co.
2.	Dowex HCR-S	Dow Chemical Co.
3.	Dowex HCR-W2	Dow Chemical Co.
4.	Decalso (Na)	Dia-Prosium
5.	Duolite C225 (Na)	Dia-Prosium
6.	Duolite 255 (H)	Dia-Prosium
7.	Amberlite IR-120 (Na)	Rohm & Haas Co.
8.	Amberlite IRC-718 (Na)	Rohm & Haas Co.
9.	Zerolit (Na)	Permutit Co.
10.	Zerolit 225 (Na)	Zerolit Ltd.

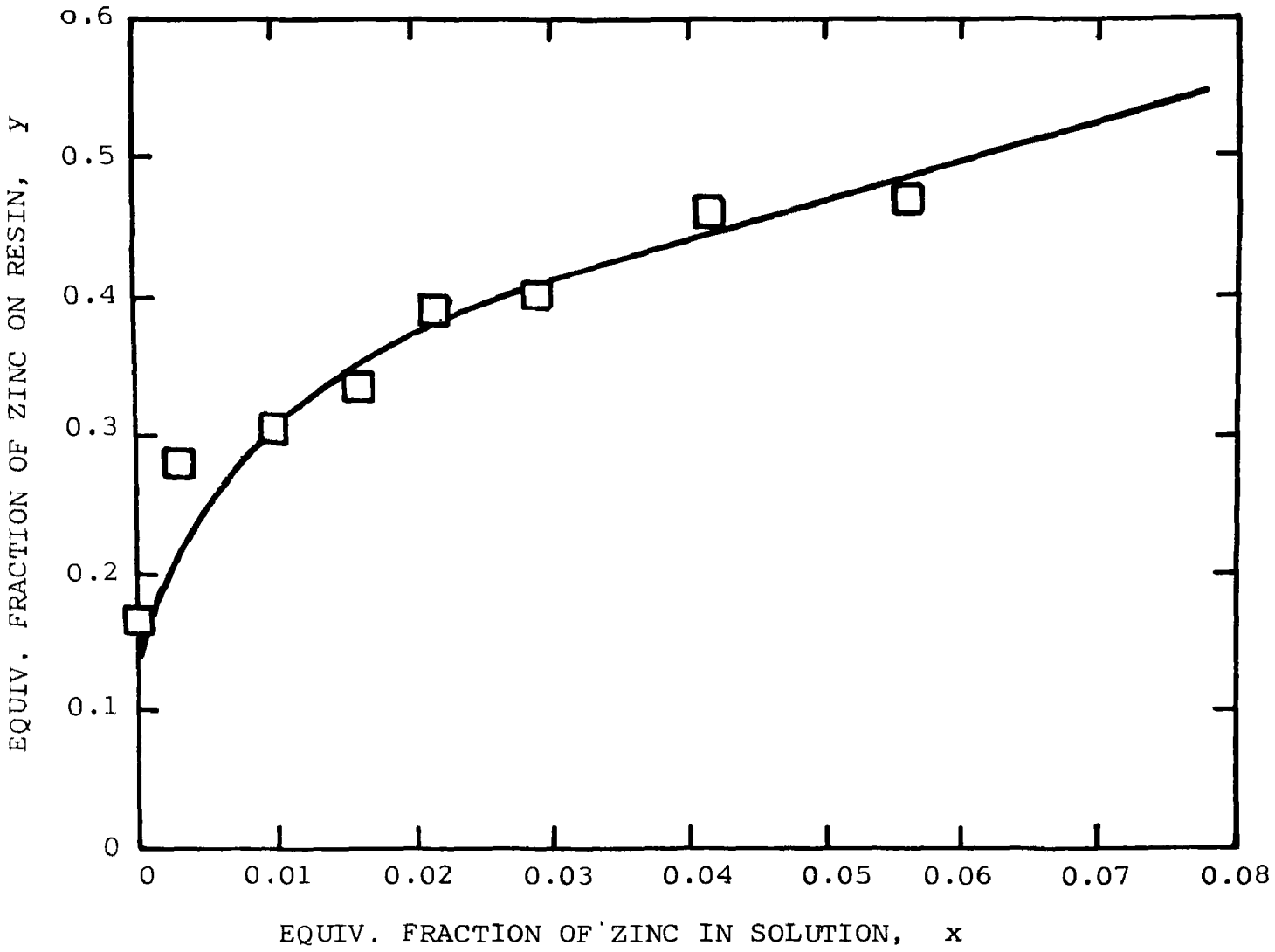

FIGURE 12 EQUILIBRIUM ISOTHERM

zinc ion concentrations ranging from 55 to 550 ppm and sodium hydroxide solution of 8 g/l. were used. The weight of resin was the same for each sample (approximately 1g) and the equilibration was conducted at room temperature (about 20°C). It is expected that sodium hydroxide solutions with these concentrations of zinc ion should exhibit favourable equilibria, the results obtained just confirm this. Table 5 gives the values of the selectivity coefficient, K_c, which were calculated using equation (6.37) and were found to decrease from 318.10 to 5.82 corresponding to C_o of 55 and 550 ppm respectively.

7.2.1 Effect of caustic concentration on isotherms

The effect of sodium hydroxide concentration on the isotherms was studied for the caustic concentrations of 4, 8, 20 and 40 g/l keeping zinc concentration at 55ppm. For this the weight of resin used was varied from 0.06 to 2.41 g. The equilibrium isotherms (in the form of g Zn/g resin against g Zn/g solution) are presented in Figure 13. As can be seen the isotherms for 0.1 and 0.2 M NaOH are favourable while for 0.5 and 1 M are unfavourable.

7.2.2 Equilibration time

The time required to reach equilibrium was also recorded with the various zinc ion concentrations (55-550ppm). Figure 14 shows the change of zinc concentration in solution with time. Apparently high Zn concentration gave low equilibration time.

TABLE 5 ION EXCHANGE EQUILIBRIUM DATA

Amberlite IRC-718 (Na) + 0.2 N Sodium Hydroxide

Initial concentration of Zn p.p.m.	Equilibrium concentration of Zn p.p.m.	Equivalent fraction in solution x_{Zn}	Equivalent fraction in resin y_{Zn}	Equilibrium selectivity coefficient K_c
55	1	0.00015	0.16500	318.10
110	19	0.00286	0.27800	37.71
165	65	0.00969	0.30583	13.17
220	110	0.01627	0.33641	8.18
275	148	0.02174	0.38841	9.52
330	200	0.02913	0.39758	7.44
440	290	0.04155	0.45874	7.38
550	396	0.05585	0.47097	5.82

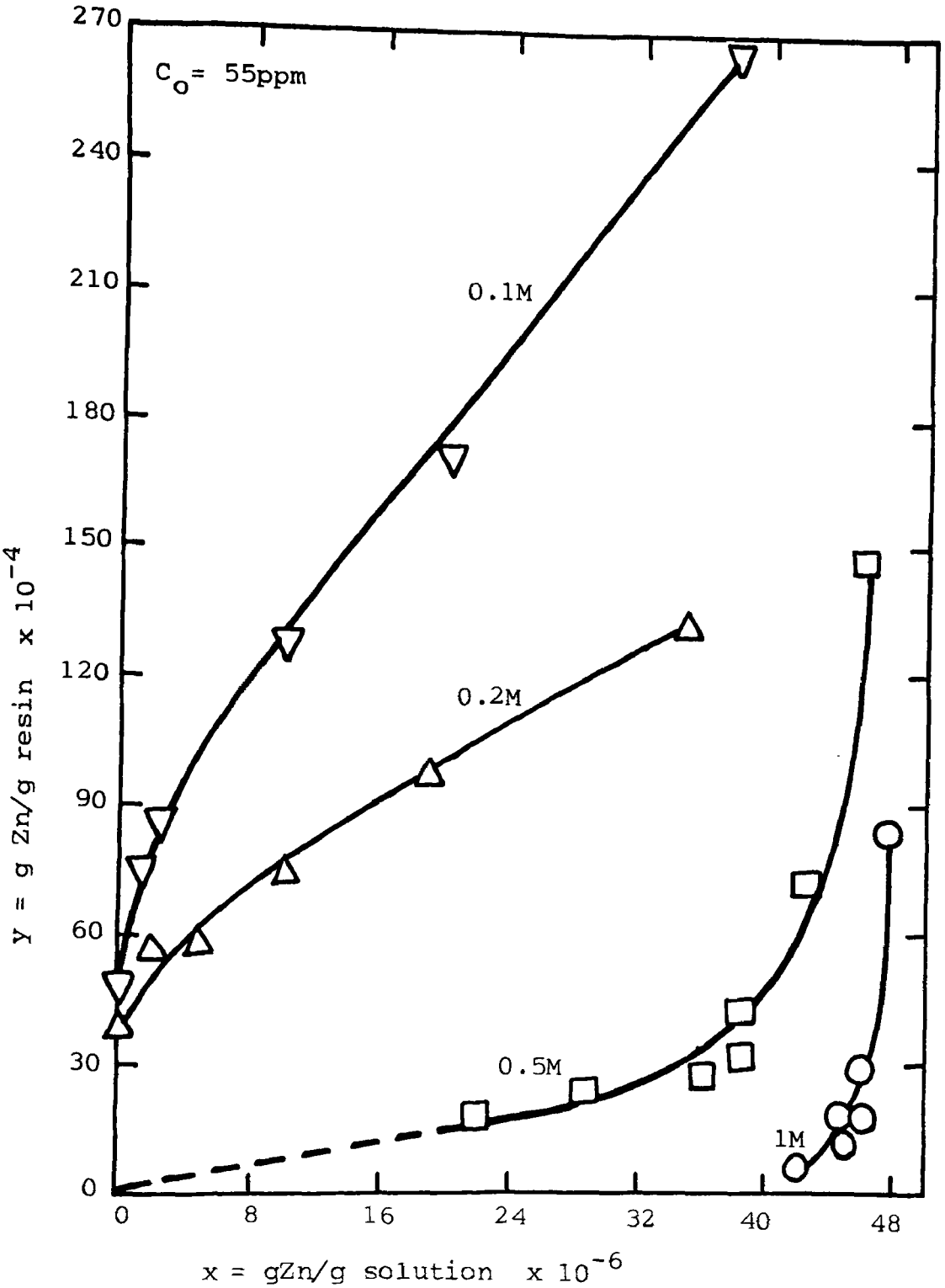

Figure 13 Effect of caustic concentration on equilibrium isotherm.

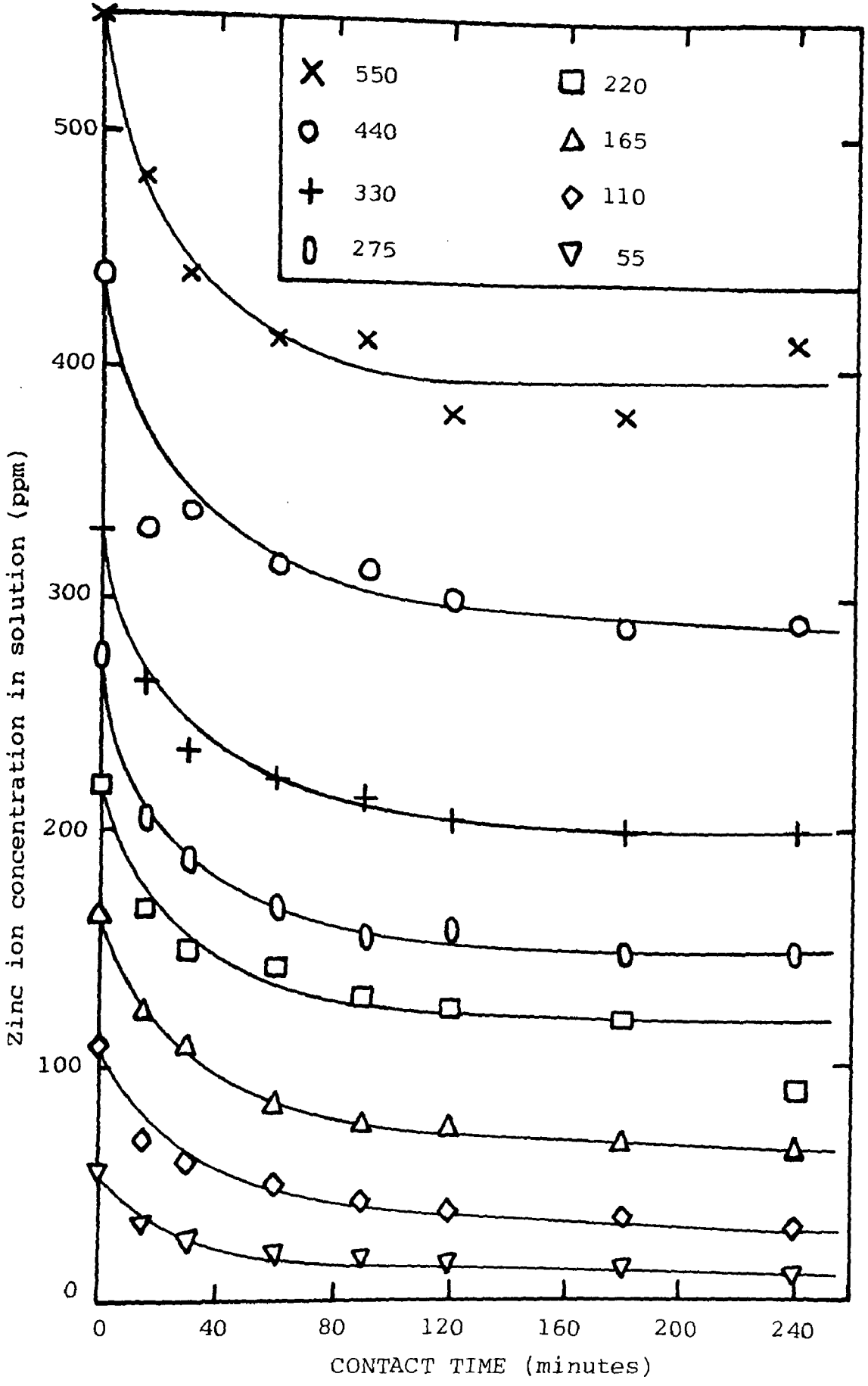

Figure 14 Change of zinc ion concentration in solution with time during equilibration.

7.3 Breakthrough data

Breakthrough data were obtained for different bed heights, flow rates, Zn concentrations, caustic concentrations, Pb concentrations, resin particle size and temperatures. Figure 15 shows a typical set of breakthrough data plotted as C/C_o vs. time.

All breakthrough data were possible to analyse through the New method. The plots of log. ln $(C_o/C_o-C))$ against log $(t-t_o)$ are linear. The slope, intercept, and the correlation coefficient were calculated using Commodore M55 calculator. For a perfect fit of the data, the correlation coefficient should equal to 1. The values obtained were in the range 0.98-0.9999 which are almost perfect. A typical set of three straight lines obtained are shown in Figure 16. These lines are for different initial zinc and NaOH concentrations, bed height, temperature, and flow rate. From the graph values of β (=slope) and t_m were obtained. The value of t_o was obtained by a trial and error procedure until the point at which C/C_o= 0.05 fell on the line. During the analysis of data it was found that for some experimental conditions negative values of t_o were obtained. Under those conditions a complete zone height was not formed as shown by N_z values (number of zones) in the tables of calculated results. Tables A(1-7) show the calculated values of β, t_m, Ka_x, Ka_y, N_z, h_z, and u_z. Using the calculated values of β, t_o, and t_m comparisons between equation (6.14) and experimental breakthrough data could be

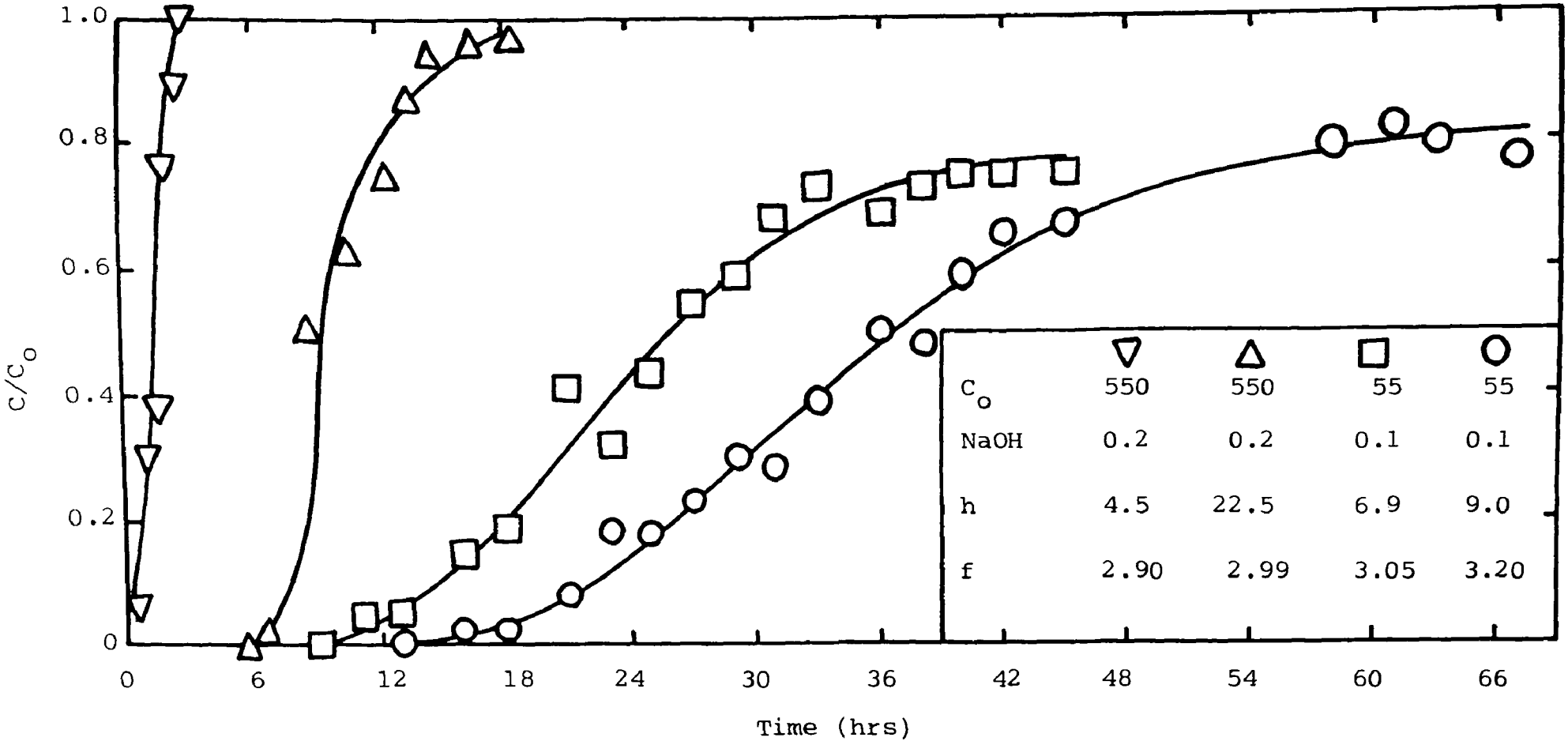

Figure 15 Breakthrough curves.

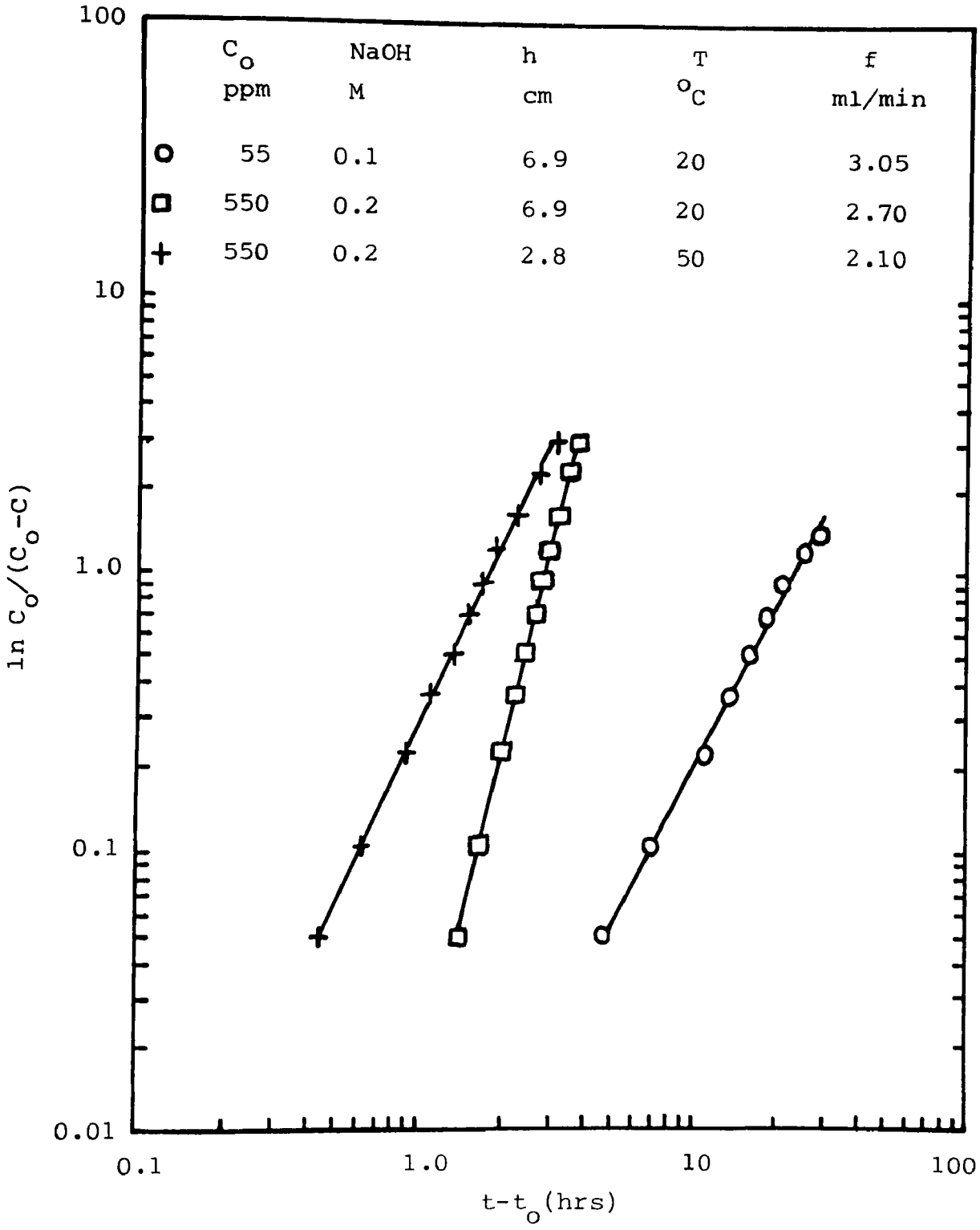

Figure 16 Breakthrough data in a linear form.

made. Figure 17 shows this comparison indicating an excellent agreement between the predicted and experimental data.

The effect of various parameters on saturation time, t_s, mass transfer coefficients , zone height, h_z, number of zones, N_z, and zone velocity, u_z are now discussed under the following headings.

7.3.1 Saturation Time

7.3.1.1 Effect of bed height

The effect of bed height on t_s was investigated with twenty sets of breakthrough data obtained for flow rates of 2.8±0.1 and 3.35±0.3 cc/min. and by varying bed height from 4.5cm. to 22.5cm. Initial zinc concentrations were at 55, 275, and 550 ppm, and NaOH concentrations were at 4 and 8 g/l. Unscreened resin was used with particles of mean diameter, d_p=0.521mm. and of size range from 0.297 to 1.19mm. The temperature was at around 20°C, but not controlled.

The saturation time, t_s, is plotted as a function of bed height in Figure 18. As can be seen from the figure, t_s increases with bed height, h and is found to be directly proportional to h. This seems to be reasonable in that as h increases time required for the saturation of a relatively longer bed should be higher.

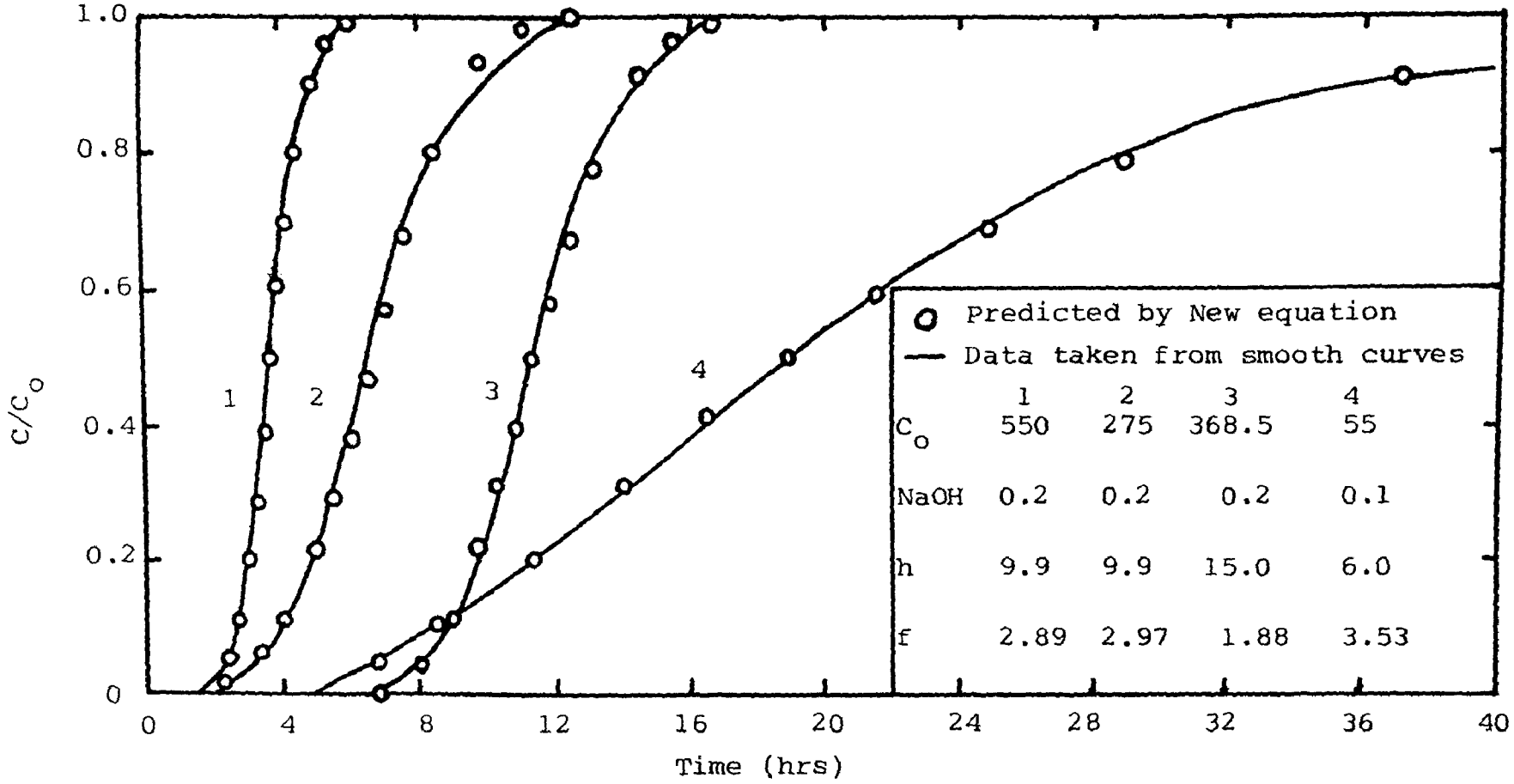

Figure 17 Comparison between experimental and predicted breakthrough curves

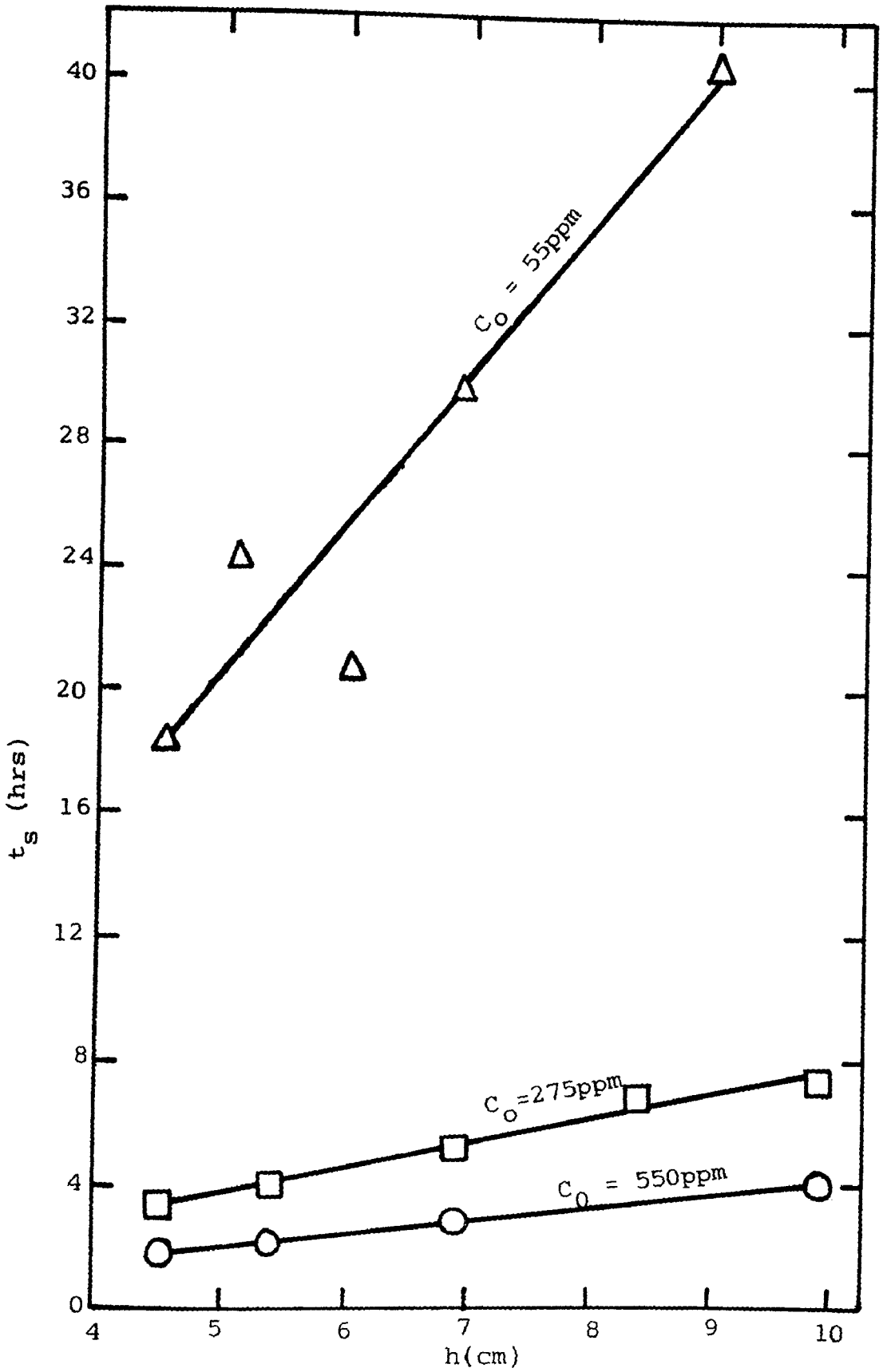

Figure 18 Saturation time as a function of bed height.

7.3.1.2 Effect of flow rate

The effect of flow rate was investigated with seventeen breakthrough data using zinc concentrations of 550, 368.5 and 55 ppm and bed heights of 4.5, 15 and 9cm. The flow rates used fall into three ranges 2.02-4.12, 1.88-20.89 and 3.20-8.26 cc/min.

The saturation time was found to decrease with flow rate as shown in Figure 19. This effect can be seen to be due to an increase of mass transfer coefficient with flow rate.

7.3.1.3 Influence of initial zinc concentration

A series of experiments in which zinc concentration ranged from 275 to 550 ppm was carried out at two bed heights of 4.5 and 22.5 cm. Sodium hydroxide solutions of 0.2M were used and the flow rates were at 2.36 $\pm$ 0.09 and 3.00 $\pm$ 0.08 cc/min.

It is expected that NaOH solutions with high zinc concentrations should give a relatively lower saturation time, the results obtained just confirm this. An increase in C_o decreases t_s and this decrease could be due to the increase of mass transfer driving force.

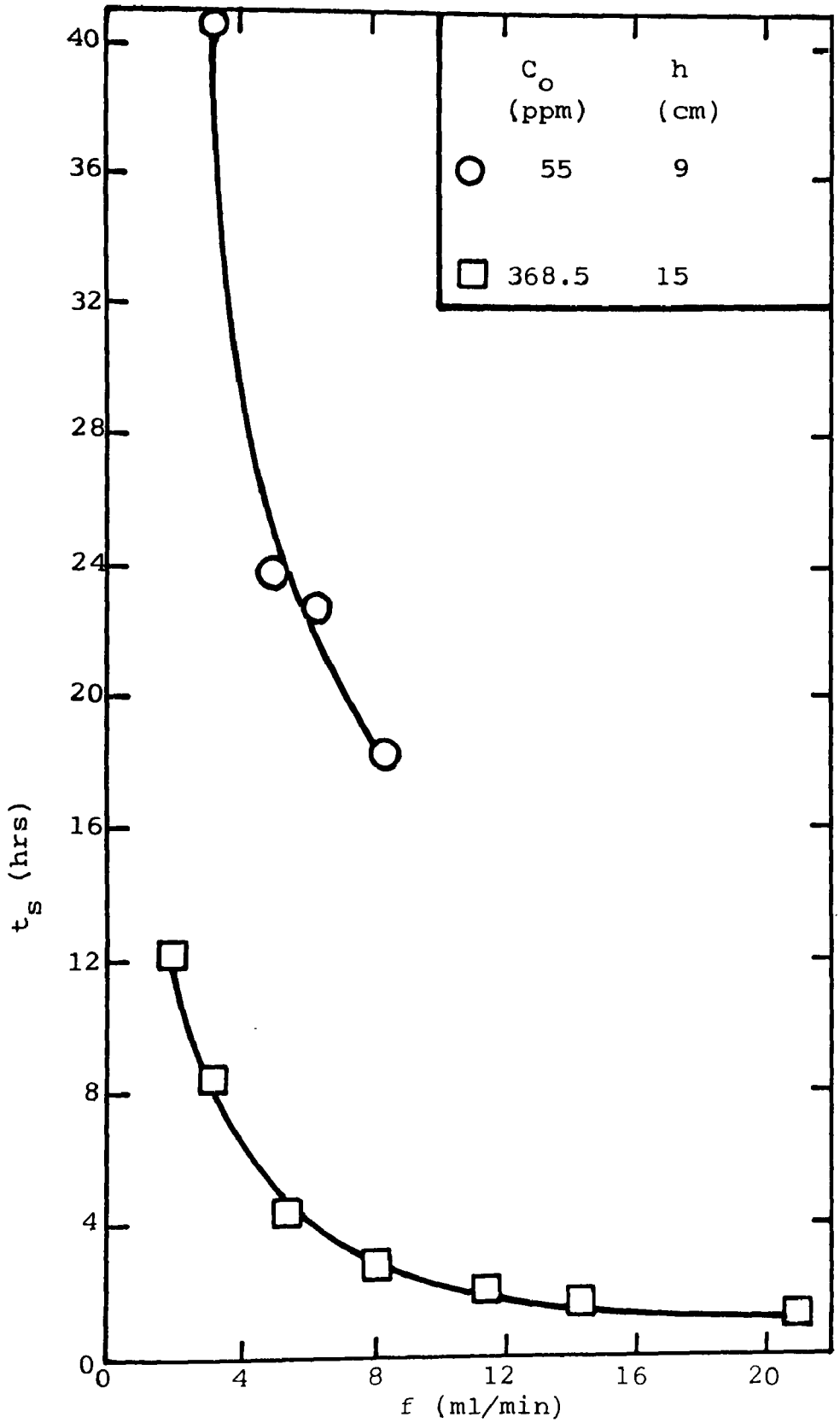

Figure 19 Saturation time as a function of flow rate.

7.3.1.4 Effect of initial lead concentration

The effect of lead concentration as an added impurity was studied with five runs using Zn concentration of 483 ppm and NaOH of 0.4M. The concentration of Pb ions was varied from 75 to 694 ppm keeping the bed height and flow rate at 4.5cm. and 2.19 $\pm$ 0.16 cc/min. respectively.

In this case both lead and zinc ions are taken by the resin. Because of the higher distribution coefficient of Pb with respect of Zn ($K^{(47)}$ for Pb/Ca is 1200 at pH 4 and $K^{(47)}$ for Zn/Ca is 17 at the same pH value) it is expected that saturated resin will have more lead than zinc. The overall saturation time is found to decrease with the increase of Pb concentration.

7.3.1.5 Influence of caustic concentration

To study the influence of caustic concentration solutions of 0.3, 0.35, 0.4, 0.45, and 0.5M were used with Zn concentration of 412.5ppm. The bed height and flow rates were 15cm. and 2.96 $\pm$ 0.14 cc/min. respectively.

The experimental data indicate a fall in saturation time with an increase in caustic concentration as shown in Figure 20. The reduction of t_s in this case is rather different from that of other situations. In this case equilibrium is unfavourable indicating that Zn is prevented from being taken up fully by the resin. As the resin remains unsaturated with

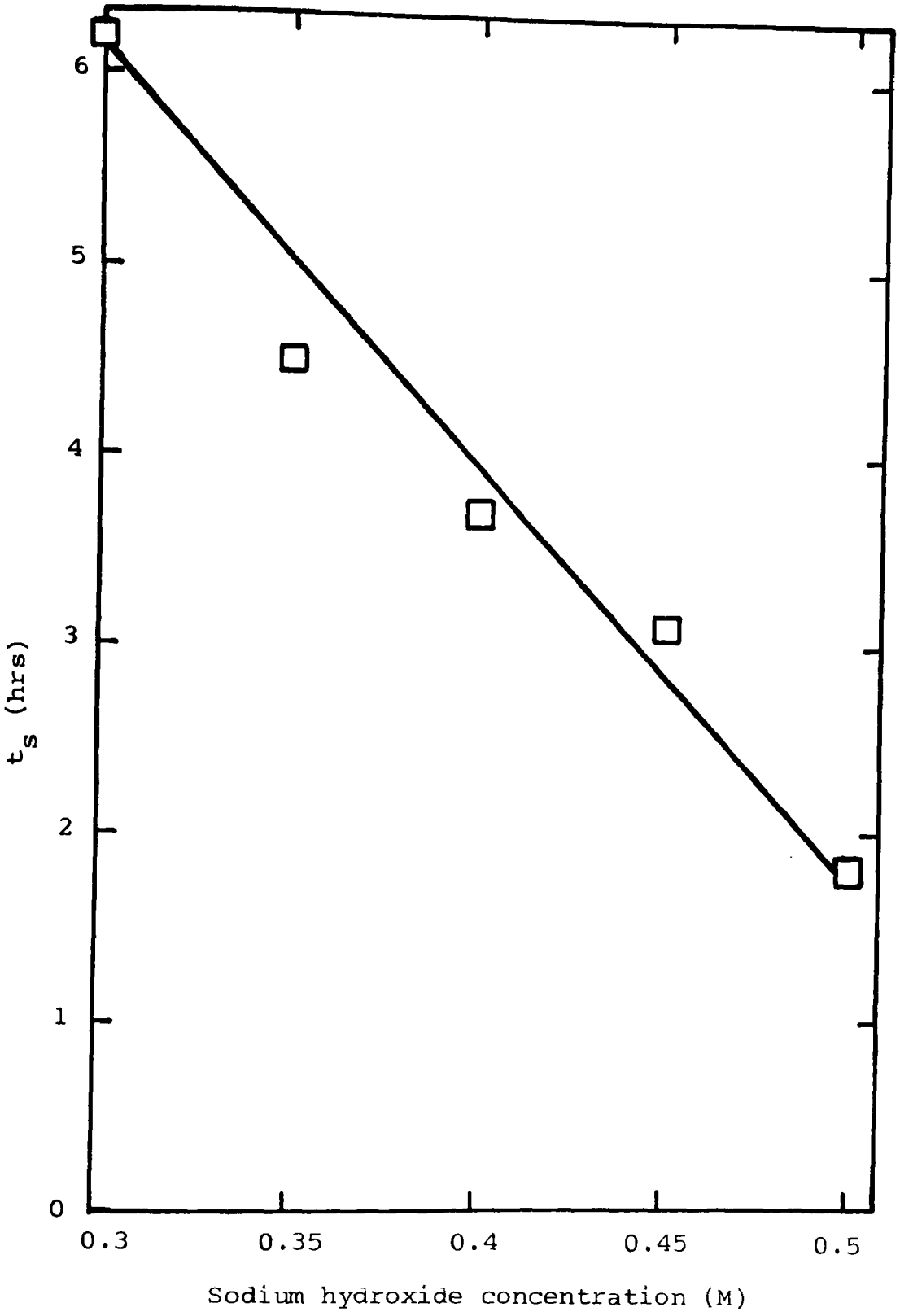

Figure 20 Saturation time as a function of caustic concentration.

respect to Zn at the time of breakthrough the saturation time becomes smaller than t_m.

7.3.1.6 Influence of resin particle size

In this study resin particle size ranging from 0.4 to 0.855 mm were used and two different bed heights of 6 and 4.5cm were employed. The initial Zn concentrations were at 55 and 550 ppm and NaOH concentrations were 0.1 and 0.2M. Flow rates of 4.84 $\pm$ 0.31 and 2.71 $\pm$ 0.19 cc/min were selected.

Results of saturation time obtained for different particle sizes do not show any definite trend.

7.3.1.7 Effect of temperature

The effect of temperature was investigated with five runs at temperatures of 24, 32, 41, 50, and 60^{o}C. The bed height was 2.8cm and NaOH of 0.2M containing 550 ppm Zn was used at a flow rate of 2.16 $\pm$ 0.06 cc/min. At 60^{o}C zinc precipitation was observed.

In this study the saturation time was found to increase with temperature - a result which contradicts the expected effect of temperature on ion exchange kinetics. The reason for this lies in the stability of the zincate complex which becomes unstable with the increase of temperature and thereby giving the precipitation of Zn.

7.3.1.8 Correlation of Saturation Time

The saturation time is finally correlated with bed height,

h, and initial zinc concentration, C_o. Figure 21 shows the correlation of t_s with h/C_o which follows the equation.

$$t_s = 242 \frac{h}{C_o} \qquad (7.1)$$

7.3.2 Mass Transfer Coefficients

Liquid side mass transfer coefficient, Ka_y, was calculated by equation (6.26) and solid side coefficient, Ka_x, was computed from equation (6.24). As can be seen from the tables A (1-7) Ka_x values are much smaller than Ka_y. This may be attributed to the factor $C_o/\rho_B\ q_o$.

Since $Ka_x = Ka_y(C_o/\rho_B\ q_o)$, the effect of various parameters on mass transfer coefficients are discussed only for Ka_y.

7.3.2.1 Effect of bed height

Mass transfer coefficient, Ka_y, is plotted against bed height in Figure 22. As can be seen from this figure Ka_y is independent of bed height. There is some scatter of data which could be due to flow rate variations and fluctuations.

7.3.2.2 Influence of flow rate

Ka_y values for different flow rates are plotted in Figure 23. The data for Zn concentration, 55ppm almost fall on a straight line with slope of 0.5. For 368.5ppm the data gives two straight lines with different slopes whereas Ka_y values for 550ppm do not show any variation with respect of

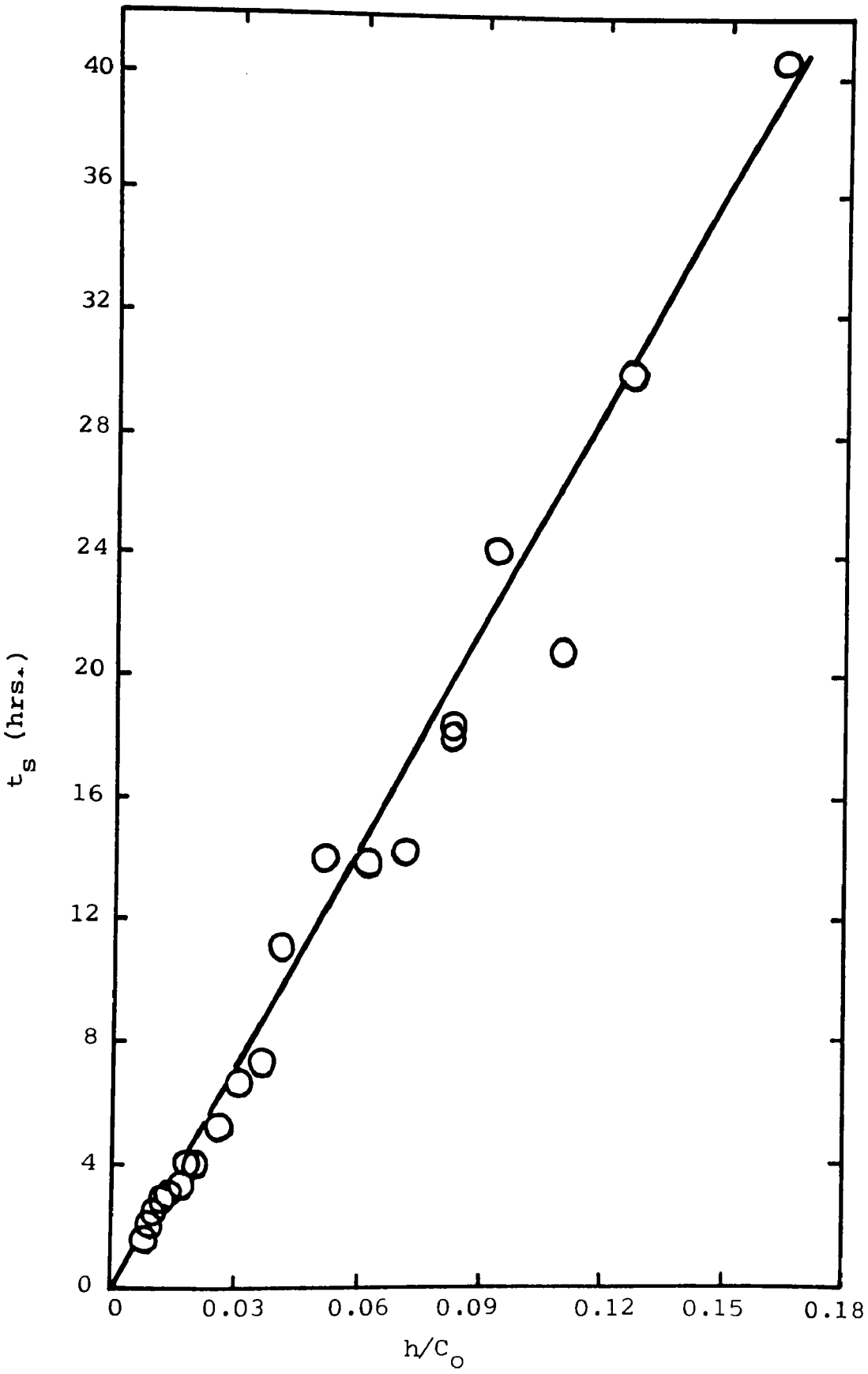

Figure 21 Correlation of saturation time with bed height and zinc concentration.

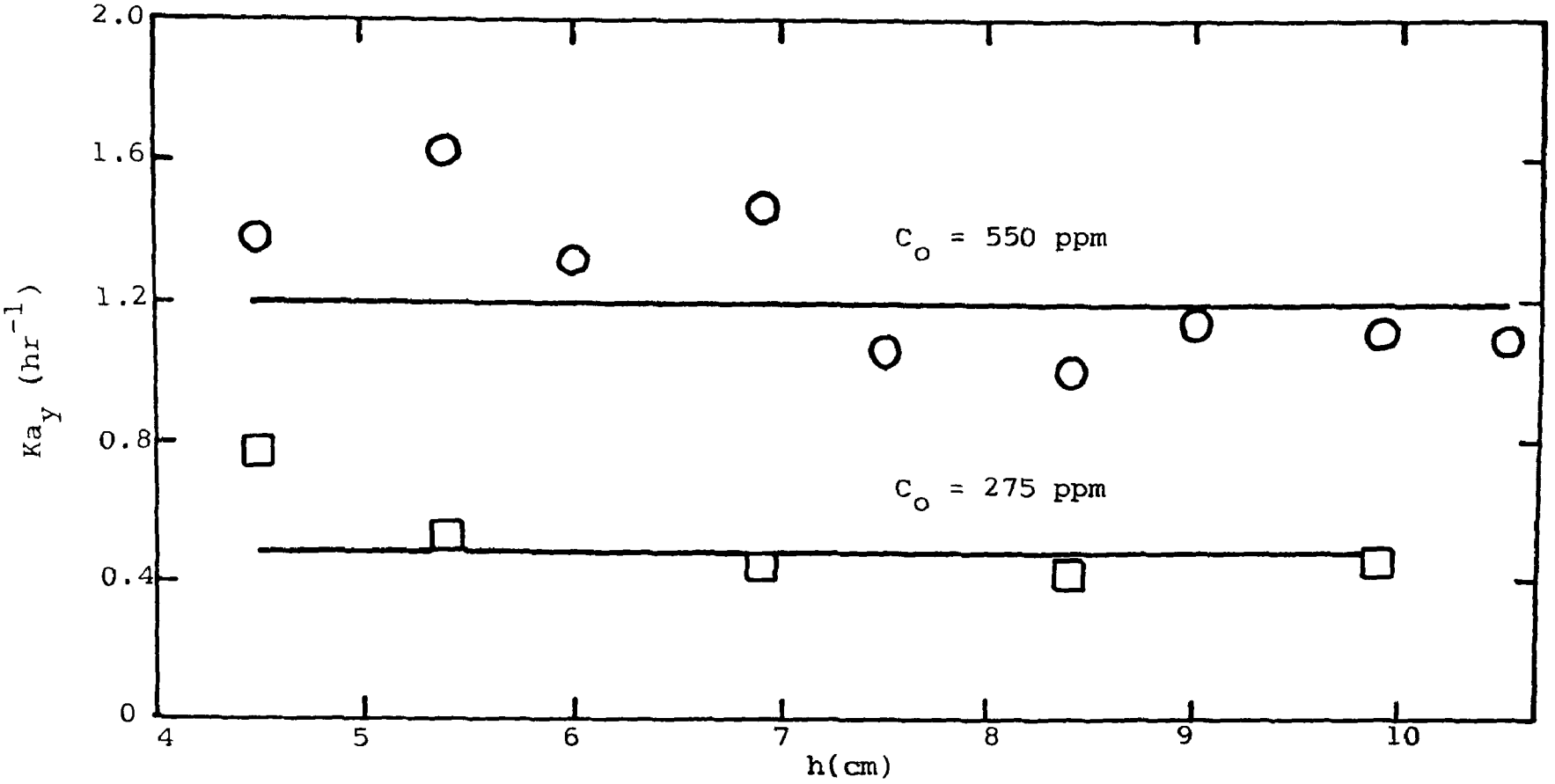

Figure 22 Mobile phase mass transfer coefficient as a function of bed height

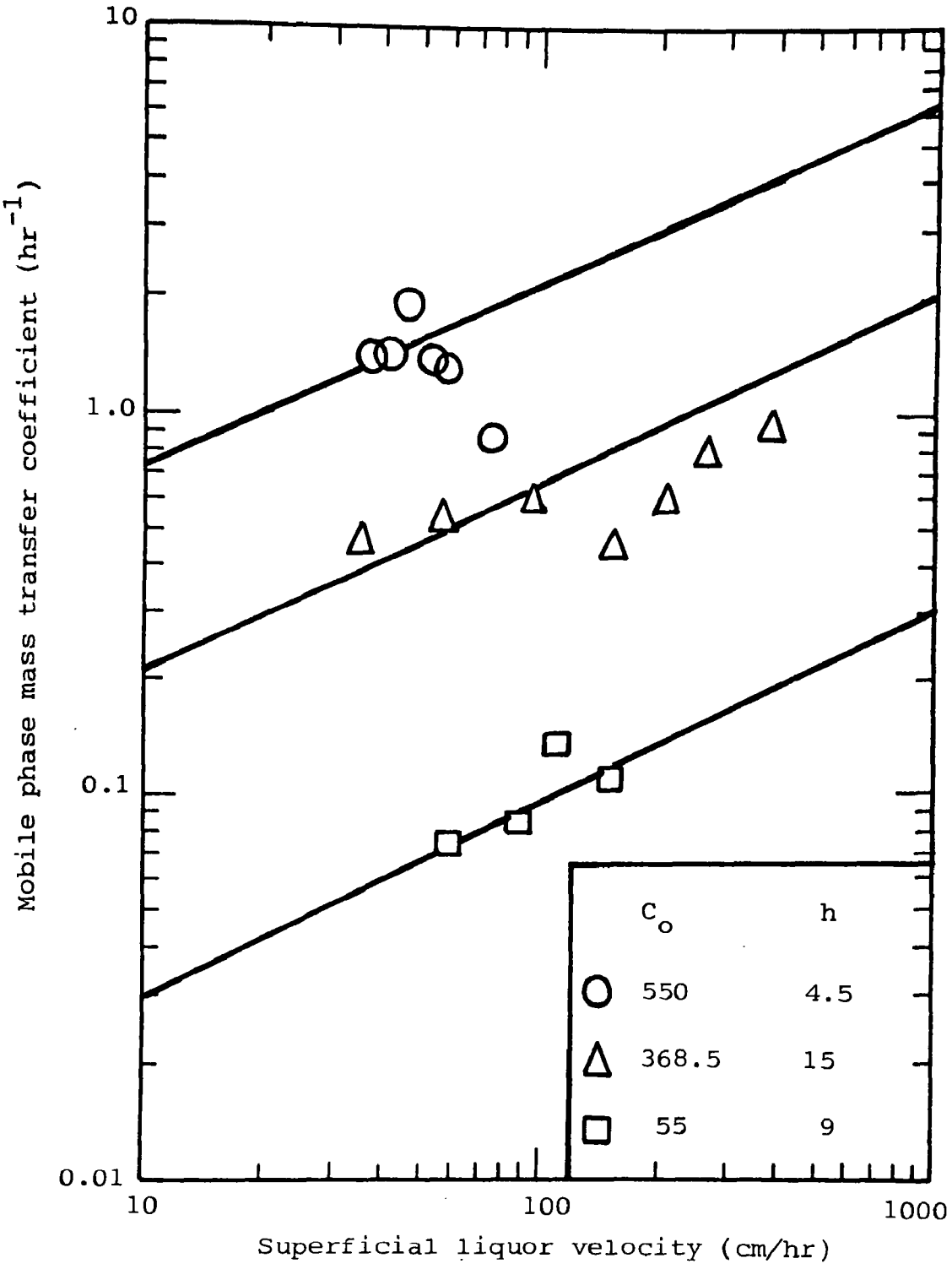

Figure 23 Mobile phase mass transfer coefficient as a function of liquor velocity

liquor velocity. The data for 55ppm indicate that the mass transfer process is controlled by the diffusion of Zn ions. This seems to be the mechanism of mass transfer in the case of concentration 368.5ppm since most of the points fall on a straight line having a slope of 0.5. For 550ppm concentration the range of flow rate is small and thus one can not establish the mechanism of mass transfer from these data.

7.3.2.3 Effect of particle size

The results of particle size varying from 0.4 to 0.855mm do not show any definite trend in Ka_y values.

7.3.2.4 Influence of zinc concentration

The influence of zinc concentration was studied with the concentration ranging from 275 to 550ppm. Ka_y values are found to increase with these values.

7.3.2.5 Effect of caustic concentration

The effect of caustic concentration on Ka_y values given in Table A5 is difficult to ascertain due to the incomplete zone formation. However, in general, Ka_y is found to decrease with caustic concentration.

7.3.2.6 Influence of lead concentration

The presence of lead ions had hampered the Zn exchange and mass transfer coefficient for Zn was not possible to evaluate from breakthrough data as zone formation was not

complete. However, Ka_y for Pb shows an increase with Pb concentration.

7.3.2.7 Effect of temperature

It is expected that the kinetics of ion exchange should be enhanced with the increase of temperature. However, in this study Ka_y values were found to decrease with temperature and this could be due to Zn precipitation which is found to occur at higher temperatures.

7.3.3 Number of zones

The number of zones, N_z, was computed from equation (6.17) and the results are given in Tables A(1-7). The values of N_z are found to increase with bed height and temperature, however, N_z decreased with flow rate, Pb and NaOH concentrations. Zn concentration and size of resin particles seem to have no effect on N_z.

7.3.4 Zone height

The height of the exchange zone is a measure of the rate of ion exchange under a fixed average concentration driving force. The factors that could influence zone height are flow rate, exchanger particle size, various ions concentration, and temperature. The effects of these factors are discussed below.

7.3.4.1 Influence of flow rate

Zone height values appear to increase with flow rate as

shown in Figure 24 from which it can be seen that there is some scatter of data. These are for zones which gave negative t_o. Zone height results for bed height of 15cm and zinc concentration of 368.5ppm were found to follow the equation.

$$h_z = 88.7\ u_L^{0.5} \quad , \quad 0.94\times10^{-2} \leqslant u_L \leqslant 10.45\times10^{-2} \qquad (7.2)$$

However, the results of h_z for C_o of 55 and 550 ppm were found to give a different correlation which can be represented by

$$h_z = 37.4\ u_L^{0.5} \quad , \quad 0.97\times10^{-2} \leqslant u_L \leqslant 3.62\times10^{-2} \qquad (7.3)$$

A similar equation was also obtained by Michaels[92] for the ion exchange of Na^+ with H^+ on Dowex 50.

Equations (7.2) and (7.3) indicate that zone height increases with the square root of the velocity thus pointing to a diffusion controlled process.

7.3.4.2 Effect of resin particle size.

The zone height has been found to be unaffected by particle size in the size range of 0.4 to 0.855 mm.

7.3.4.3 Influence of zinc concentration

Zinc concentration did not show any significant influence on zone height.

7.3.4.4 Effect of caustic concentration

Sodium hydroxide concentration influenced the exchange process by increasing Na^+ ions and viscosity. Sodium ions in

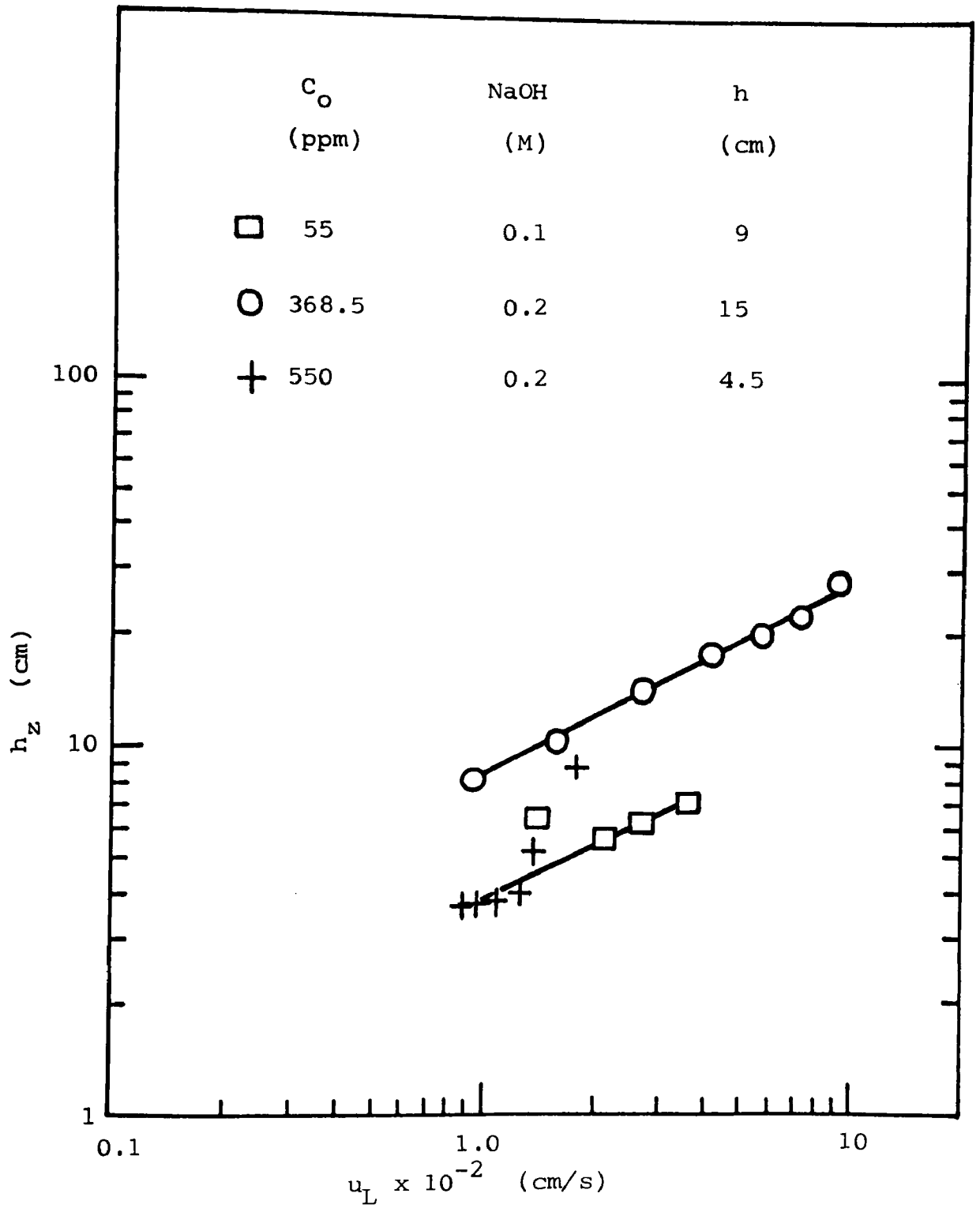

Figure 24 Correlation of zone height with liquor velocity

the solution resisted the flow of Na^+ from the resin and the viscosity affects the diffusion of Zn^{2+} ions to the resin. Moreover with caustic concentration greater than 0.2M zone formation was found to be incomplete.

7.3.4.5 Influence of lead concentration

Zone height results obtained for various lead ion concentrations remained fixed at an average value of 4.5cm.

7.3.4.6 Effect of temperature

In this study h_z was found to decrease with temperature - a result which contradicts the expected effect of temperature on ion exchange kinetics. This can be attributed to the precipitation of Zn which has occured at higher temperatures.

7.3.5 Zone velocity

Zone velocity data for the effect of various parameters are given in Tables A(1-7).

7.3.5.1 Correlation of zone velocity with Zn concentration

In Figure 25 zone velocity is plotted against Zn concentration and the data show a good correlation by falling on a straight line which is represented by

$$u_z = 4.78 \times 10^{-3} \; C_o \qquad (7.4)$$

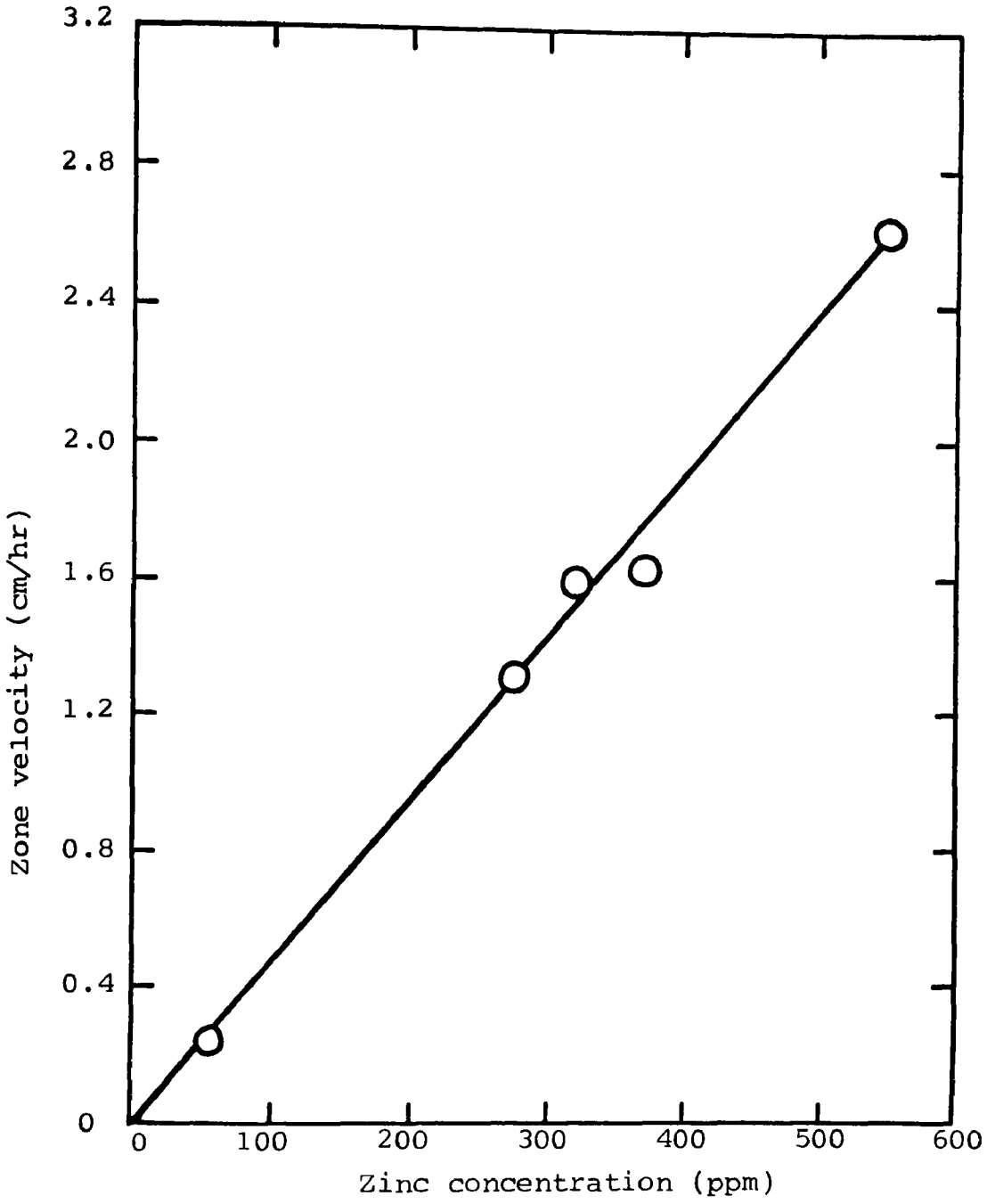

Figure 25 Correlation of zone velocity with zinc concentration

7.3.5.2 Correlation of zone velocity with flow rate

Zone velocity data are plotted against flow rate in Figure 26 which shows that data fall on straight lines corresponding to C_o values of 55, 368.5, and 550ppm. These lines can be represented by

$$u_z = 6.17 \times 10^{-2} f \quad \text{for} \quad C_o = 55 \qquad (7.5)$$

$$u_z = 6.25 \times 10^{-1} f \quad \text{for} \quad C_o = 368.5 \qquad (7.6)$$

$$u_z = 9.47 \times 10^{-1} f \quad \text{for} \quad C_o = 550 \qquad (7.7)$$

Attempts were made to bring all the points on one line by the use of equation (7.4). As can be seen in Figure 27 that data for C_o values of 368.5 and 550ppm fall on a line while data for 55ppm give a separate line. This is most probably due to the caustic concentration which is 0.1M instead of 0.2M in the other cases.

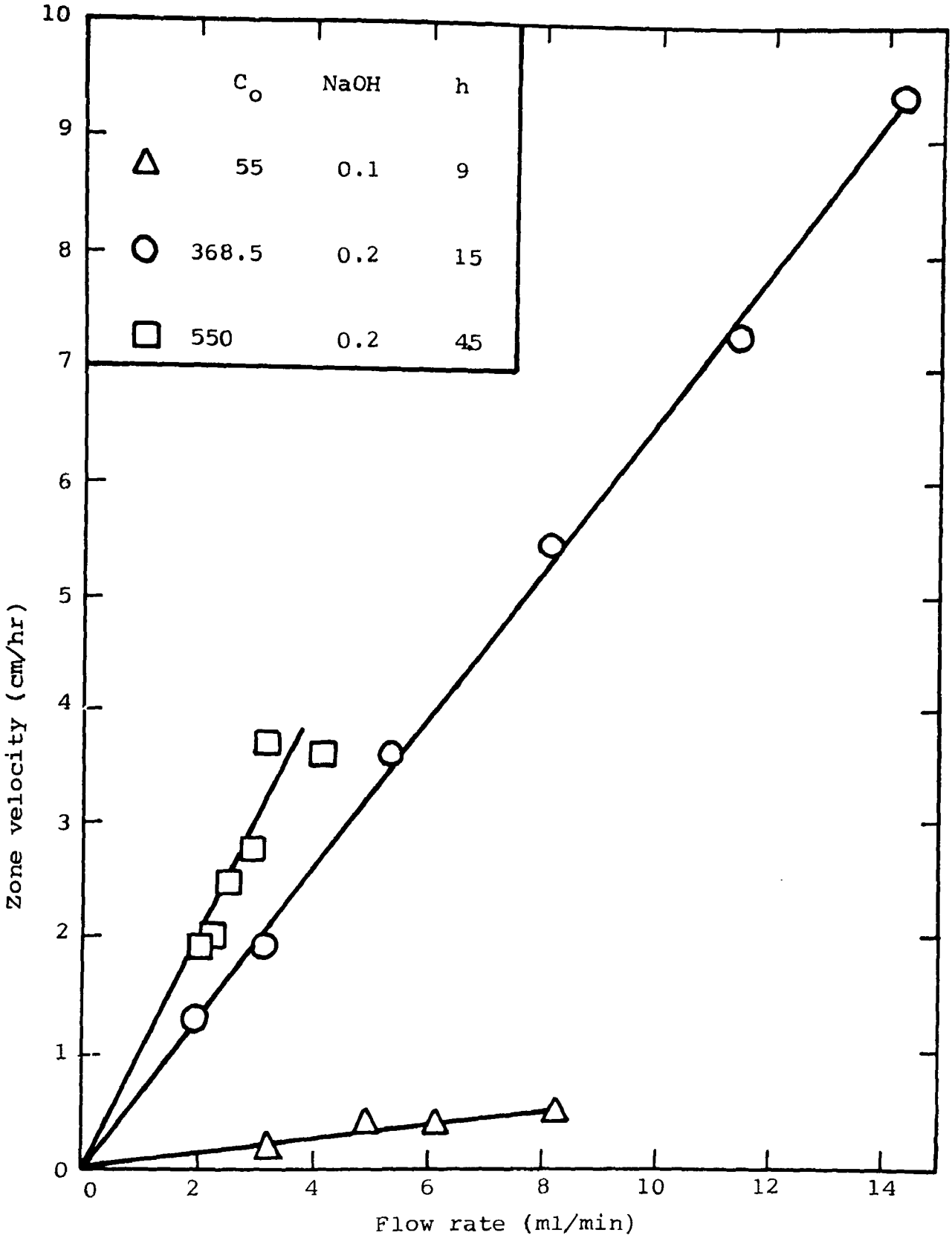

Figure 26 Zone velocity as a function of flow rate

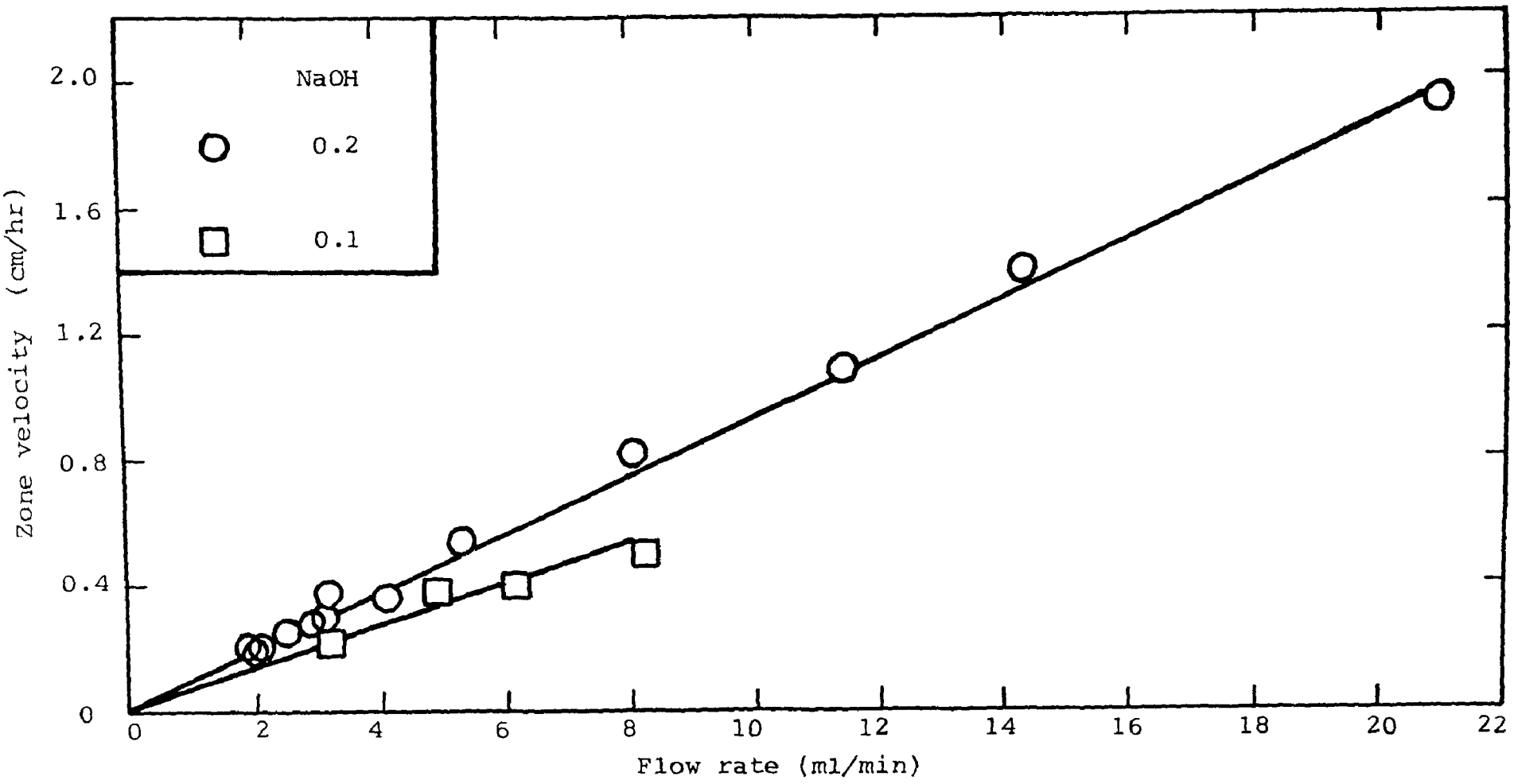

Figure 27 Correlation of zone velocity with flow rate

7.4 Application of the New method to other works

To check on the New method, the breakthrough data of Michaels[92] who studied the exchange of Na^+ with H^+ on Dowex 50 were taken and analysed through the New method. Table 6 shows the data read from his breakthrough curves along with the operating conditions. The results of h_z and u_z calculated through the New method and the Michaels results on these two parameters are given in Table 7 . As can be seen, the results show that there is an excellent agreement between the two sets of data. Most of the values of zone height calculated through the New method fall within the range of Michaels zone height values calculated using equations (6.1) and (6.2). Like the h_z values the zone velocity agree equally well Michaels results.

The New method was also applied by Clark[174] for the analysis of his data on the recovery of valuable vapour phase solvent using activated charcoal cloth.

TABLE 6 Data read from Michaels breakthrough curves

h , cm	22.5	22.5	22.5	33.5	33.5	33.5	43.8	43.8	43.8	43.8
u_L , cm/s	0.05	0.19	0.38	0.08	0.31	0.62	0.13	0.26	0.51	0.77
X/X_o	V, Effluent volume, cubic centimeters									
0.05	1111.1	785.7	714.0	1777.8	1464.5	1142.9	2259.3	2185.2	1740.7	1592.6
0.10	1185.2	892.9	857.7	1888.9	1642.9	1285.7	2370.4	2370.4	1851.9	1740.7
0.20	1237.0	1071.4	1074.3	2000.0	1892.9	1571.4	2518.5	2555.6	2111.1	1963.0
0.30	1259.3	1128.6	1213.0	2111.1	2074.0	1714.3	2592.6	2666.7	2222.2	2111.1
0.40	1296.3	1178.6	1286.1	2185.2	2142.9	1857.1	2666.7	2740.7	2333.3	2259.3
0.50	1333.3	1250.0	1356.9	2222.2	2214.3	1964.3	2740.7	2814.8	2407.4	2481.5
0.60	1370.4	1300.0	1429.5	2274.1	2285.7	2071.4	2777.8	2911.1	2518.5	2644.4
0.70	1407.4	1357.1	1498.9	2318.5	2392.9	2214.3	2851.9	2963.0	2629.6	2851.9
0.80	1429.6	1428.6	1643.2	2407.4	2535.7	2357.1	2963.0	3074.1	2814.8	3000.0
0.90	1459.3	1535.7	1820.8	2518.5	2740.0	2607.1	3148.2	3296.3	3211.1	3259.3
0.95	1592.6	1714.3	2000.0	2629.6	3000.0	2857.1	3296.3	3496.3	3407.4	3444.4

(X = Effluent Sodium ion concentration, meq/cc., X_o = Influent Sodium chloride concentration, 0.12 meq/cc, S = 3.80 sq.cm., d_p = 0.06 cm)

TABLE 7 Comparison between the New method and Michaels method

u_L	B	t_o	t_m	Ka_y	h_{z4}	$u_{z3} \times 10^3$	h_{z1}(6.1)	h_{z2}(6.2)	$u_{z1} \times 10^3$
0.05	5.80	65	55.55	0.104	10.4	3.1	7.7±0.8	6.4±0.6	3.3±0.3
0.19	4.04	7	23.89	0.169	17.4	12.1	17.2±1.7	15.4±1.5	13.8±1.4
0.38	4.13	0	17.23	0.240	22.5	21.8	20.5±2.1	20.4±2.0	25.0±2.5
h = 22.5 cm									
0.08	3.58	77	49.25	0.073	13.1	4.4	12.8±1.3	11.3±1.1	4.8±0.5
0.31	3.90	10	23.63	0.165	23.5	16.6	23.8±2.4	21.3±2.1	18.6±3.4
0.62	3.03	4	11.13	0.272	24.6	36.9	29.2±2.9	28.6±2.9	39.4±3.9
h = 33.5 cm									
0.13	5.38	47	49.44	0.109	21.4	7.2	15.5±1.6	15.9±1.6	7.8±0.8
0.26	4.18	25	24.98	0.167	21.9	14.6	20.3±2.0	24.0±2.4	15.2±1.5
0.51	3.06	10	12.64	0.242	24.5	32.2	27.4±2.7	23.5±2.9	33.6±3.4
0.77	3.09	5	10.25	0.301	29.4	47.9	31.8±3.2	30.5±3.1	52.0±5.2
h = 43.8 cm									

($t = \sqrt{u_L} \times S \times 60$ mins)

7.5 Analysis through Michaels method[92]

Through Michaels method two sets of breakthrough data were analysed. As described previously the method is applicable only to systems with favourable equilibria and symmetrical breakthrough curves. In the present work, although some equilibria are favourable but all breakthrough data do not give symmetrical breakthrough curves.

7.5.1 Zone height

Zone height was calculated using two equations of Michaels, eqs. (6.1) and (6.2). As can be seen from Tables B1 and B2 that the values of h_{z1} obtained from eq.(6.1) and h_{z2} from eq. (6.2) are not in agreement except in the case when F=0.5 representing a symmetrical breakthrough curve. Even though the calculated zone height is higher than the actual bed height. For the same run the new method gives a zone height of 3.95cm (Table A2) in a bed of 4.5cm and this appears to be reasonable.

7.5.2 Specific total capacity

The specific total capacity was calculated using equation (6.3) and is found to be unaffected by liquor velocity. The maximum deviation from the mean of 0.25 meq/ml is computed to be 8%. However, the calculated values fall short of experimental values.

7.5.3 Effective capacity

Specific effective capacity, C_E, was computed from

equation (6.4) and found to decrease with liquor velocity.

7.5.4 Number of transfer units

The number of transfer units for the two different Zn concentrations was computed using equation (6.7). Values of 4.17 and 3.79 were obtained corresponding to C_o of 550 and 368.5ppm respectively. As these results are calculated from a method using a concept which is different from that of the new method, comparison between number of transfer units and number of zones is not possible.

7.5.5 Height of transfer units

The height of transfer units is required to be obtained from the zone height. As the method does not give true zone height values, no attempts were made to find HTU values.

7.5.6 Overall liquid phase mass transfer coefficient

Liquid phase mass transfer coefficient was calculated from correlating equation (6.6) and the values are found to increase with liquid velocity. These values are however, much greater than those obtained through the new method.

7.6 Analysis through Moison and O'Hern method[93]

Moison and O'Hern gave equations for the determination of zone height, zone velocity, and number of transfer units. With some runs the method was tried to find those parameters.

7.6.1 Zone height

Zone height was computed using equation (6.9) and as can be seen from Tables C(1-3) the values obtained are much lower than those found through equations (6.1), (6.2) of Michaels and (6.18) of the present method.

7.6.2 Zone velocity

Like zone height the values of zone velocity, u_{z2}, calculated through equation (6.10) are much lower than those obtained through the other methods. In fact in some cases they were found to be three times smaller than the values of u_z obtained through the new method.

7.6.3 Number of transfer units

The number of transfer units was obtained from equation (6.11) and the results are given in Tables C(1-3). The NTU values ranged from 5.93 corresponding to C_o of 55ppm to 7.11 for C_o of 550ppm and these are greater than those computed through equation (6.7) of Michaels.

7.6.4 Height of transfer units

Using the calculated values of h_z and NTU, HTU was obtained

from equation (6.8). As the values are obtained from h_z by dividing with a large NTU, it is expected that the HTU values will be small.

7.6.5 Liquid and solid phase resistances

Attempts were made to estimate the resistances in the liquid and solid phase according to equation (6.13) which requires a plot of HTU versus C_o. As the calculated values of HTU are doubtful, the plot as given in Figure 28 does not show straight lines representing the equation which suggests straight lines with a positive slope.

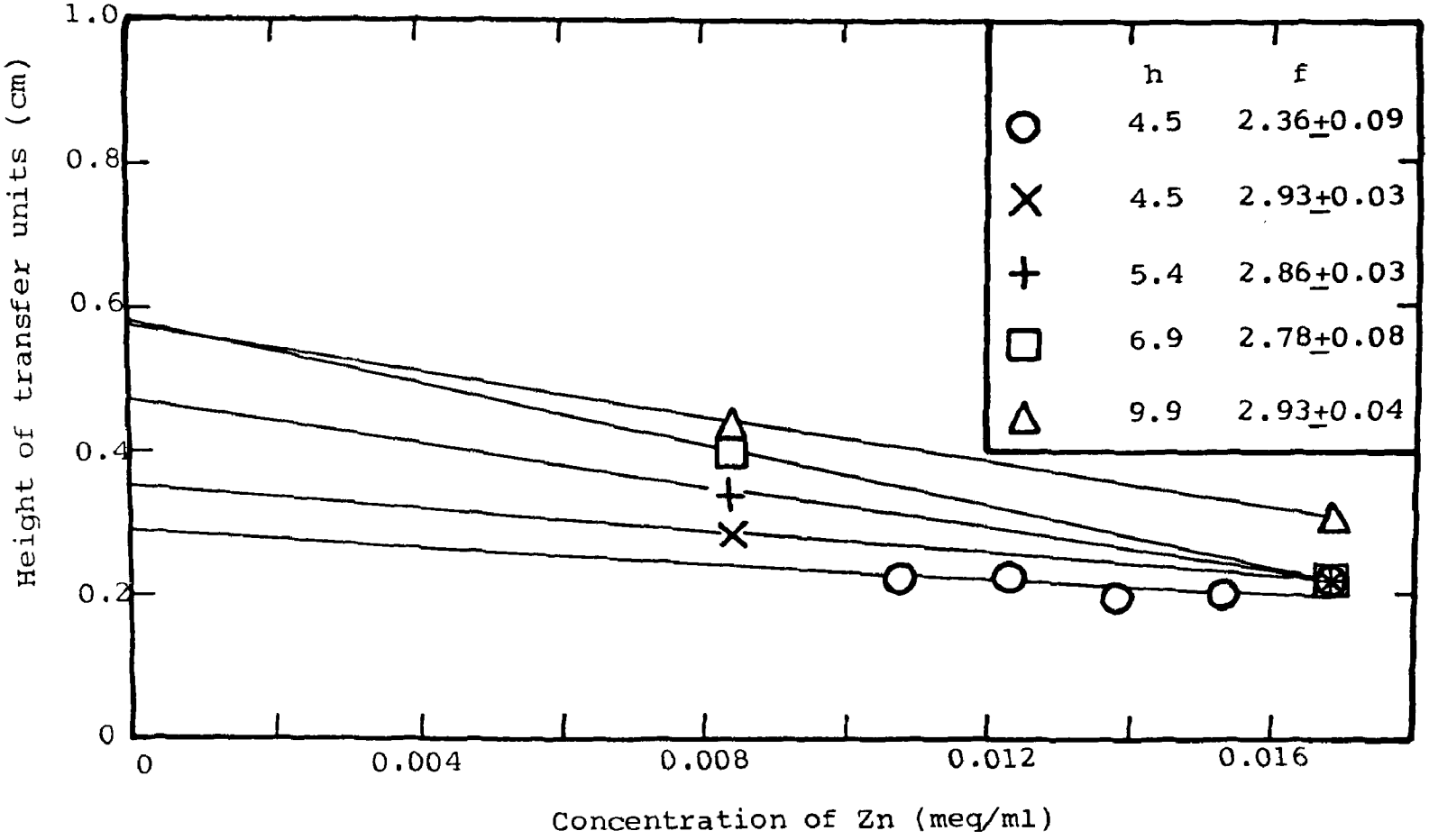

Figure 28 Effect of feed concentration on the height of a transfer unit.

7.7 Activation energy

To check whether the process of mass transfer is diffusion or chemical reaction controlled, the activation energy was calculated using Arrhenius equation. Following this equation a plot of ln Ka_x versus $\frac{1}{T}$ in Figure 29 gave a straight line. The slope of this line gives a value of 1.6 k cal/mole for the activation energy indicating a transfer process that is controlled by a diffusion mechanism.

7.8 Regeneration tests

The regeneration of Amberlite IRC-718 was accomplished by using HCl. A typical plot showing the effect of flow rate is presented in Figure 30 and the operating conditions together with the calculated data are given in Table 8. The results of this Fig.(30) show an increased Zn elution with the increase of flow rate. The acid concentration and the particle size do not show definite variation in Zn removal.

7.8.1 Acid recovery

Attempts were made to recover the spent regenerant (HCl) by distillation from which it was found that the acid was not fully recovered when 1340ml of distillate was collected from a batch feed of 1400ml. It is therefore recommended that the distillation should be continued until dryness so that all the acid comes out as a distillate.

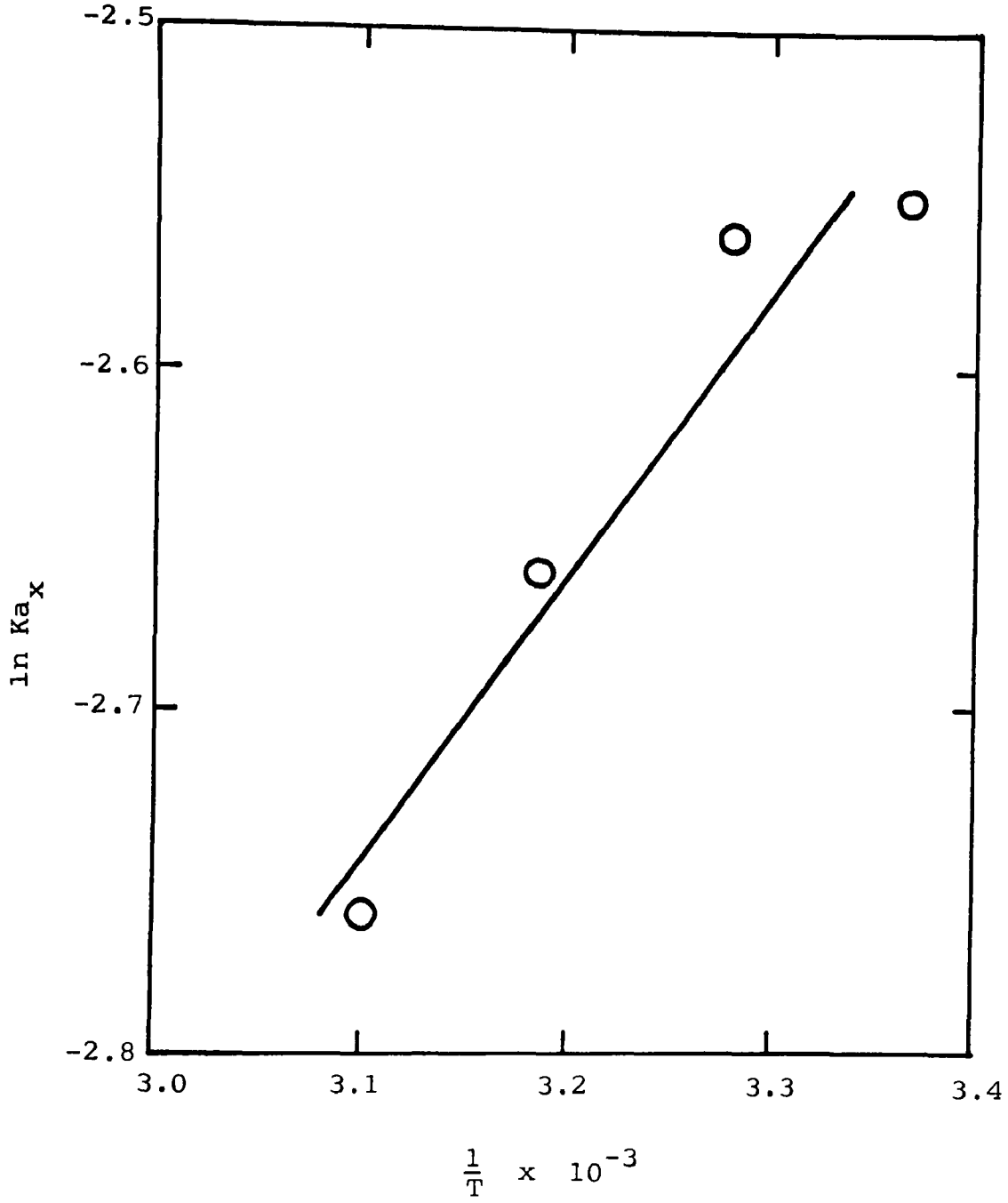

Figure 29 Arrhenius plot

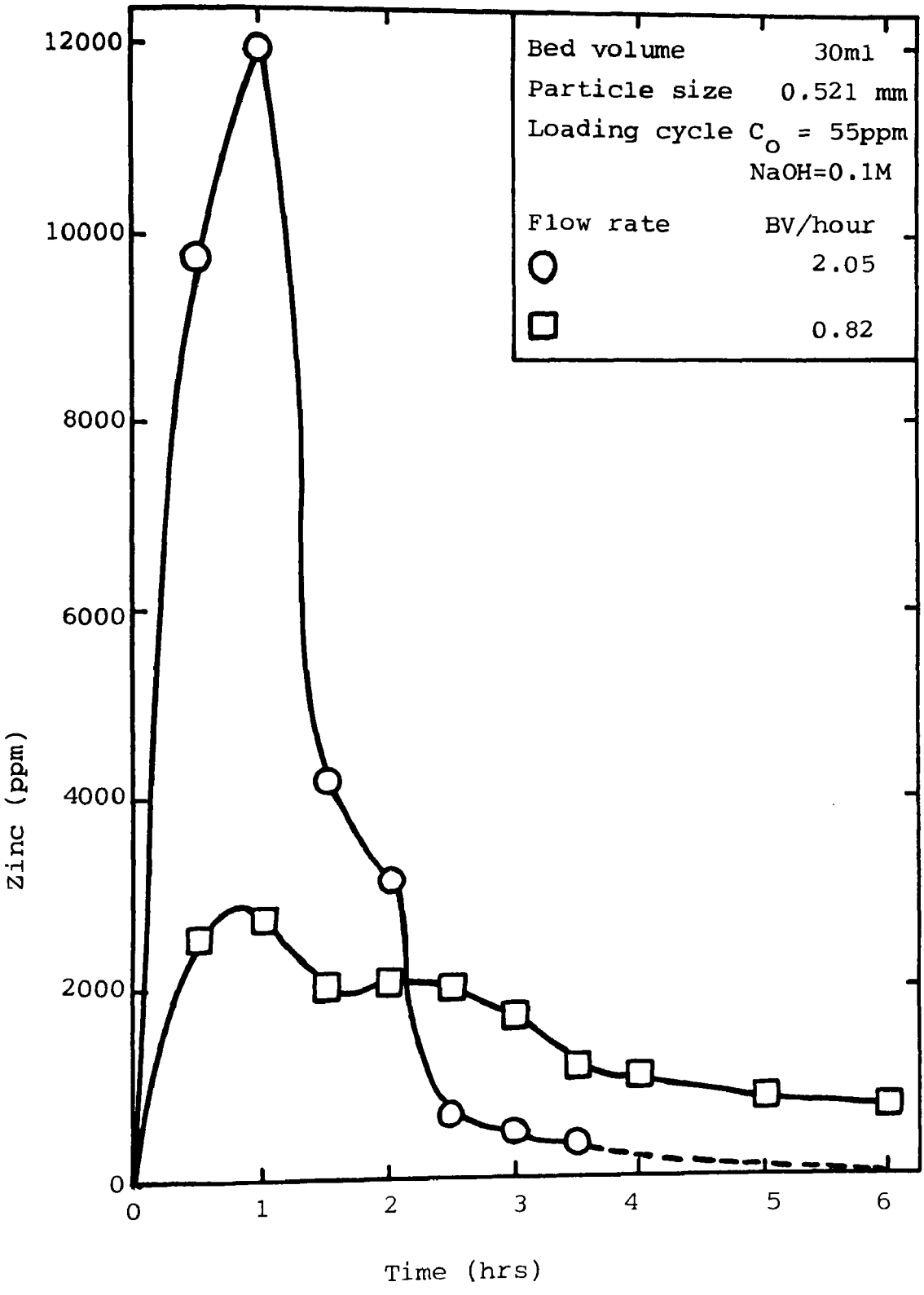

Figure 30 Effect of flow rate on the regeneration of Amberlite IRC-718 with 4M HCl.

TABLE 8 Amberlite IRC-718 regeneration

Run No.	Bed height cm.	Flow rate ml/min	Particle diameter mm	HCl concn. M	Zn^{++} removed meq.	Effective Capacity meq./ml.
3.1	6	1.00	0.855	1	12.48	0.624
3.2	6	1.09	0.855	2	8.44	0.422
3.3	6	0.75	0.550	2	8.41	0.420
3.4	6	0.78	0.521	2	10.24	0.512
3.5	6	0.69	0.521	1	9.48	0.474
3.6	6	0.88	0.550	1	9.79	0.489
3.7	6	0.79	0.655	1	10.86	0.543
3.8	9	0.85	0.521	1	7.49	0.250
3.9	9	0.41	0.521	4	18.35	0.612
3.10	9	1.02	0.521	4	28.53	0.951

7.9 Conversion tests

Sodium hydroxide was used to convert the resin from the hydrogen form to the sodium form and the operating conditions along with the calculated results are given in Table 9. Refering to this table, there are several points deserve comments, the conversion efficiency was found to vary from 95 to 99.4% and complete conversion (100%) can be achieved if sufficient amount of NaOH is used. The conversion efficiency was found to increase with flow rate as shown in Figure 31. Larger volume of NaOH and longer conversion time are required if 0.1M NaOH is used instead of 1M.

The resin after being regenerated and converted was tested for the acceptance of Zn and it was found to be satisfactory.

7.10 Zinc precipitation

In some solutions Zn was found to precipitate out. In order to overcome this problem, the solutions were diluted with sodium hydroxide solution instead of de-ionised water. However, precipitation still occured in some solutions with lower concentration of NaOH. In some solutions zinc precipitated instantly whereas with the others precipitation has occured after few hours or even few days. Table 10 shows the expected and determined zinc ion concentrations.

TABLE 9 Conversion to Na form

Run No.	Bed height (Cm)	Particle diameter (Cm)	Flow rate (ml/min)	Volume used (ml.)	Conversion time (hrs.)	Conversion efficiency
4.1	6	0.0521	0.37	134	6.00	95.2
4.2	6	0.0550	0.93	168	3.00	98.8
4.3	6	0.0650	0.43	153	6.00	99.4
4.4	6	0.0855	1.82	572	6.25	97.9 *
4.5	6	0.0550	1.31	138	1.75	98.0
4.6	6	0.0521	1.73	182	1.75	99.0
4.7	6	0.0855	1.02	122	2.00	99.0
4.8	9	0.0521	1.18	212	3.00	98.2
4.9	9	0.0521	0.89	107	2.00	95.0
4.10	9	0.0521	1.43	172	2.00	99.0

* using 0.1 M NaOH

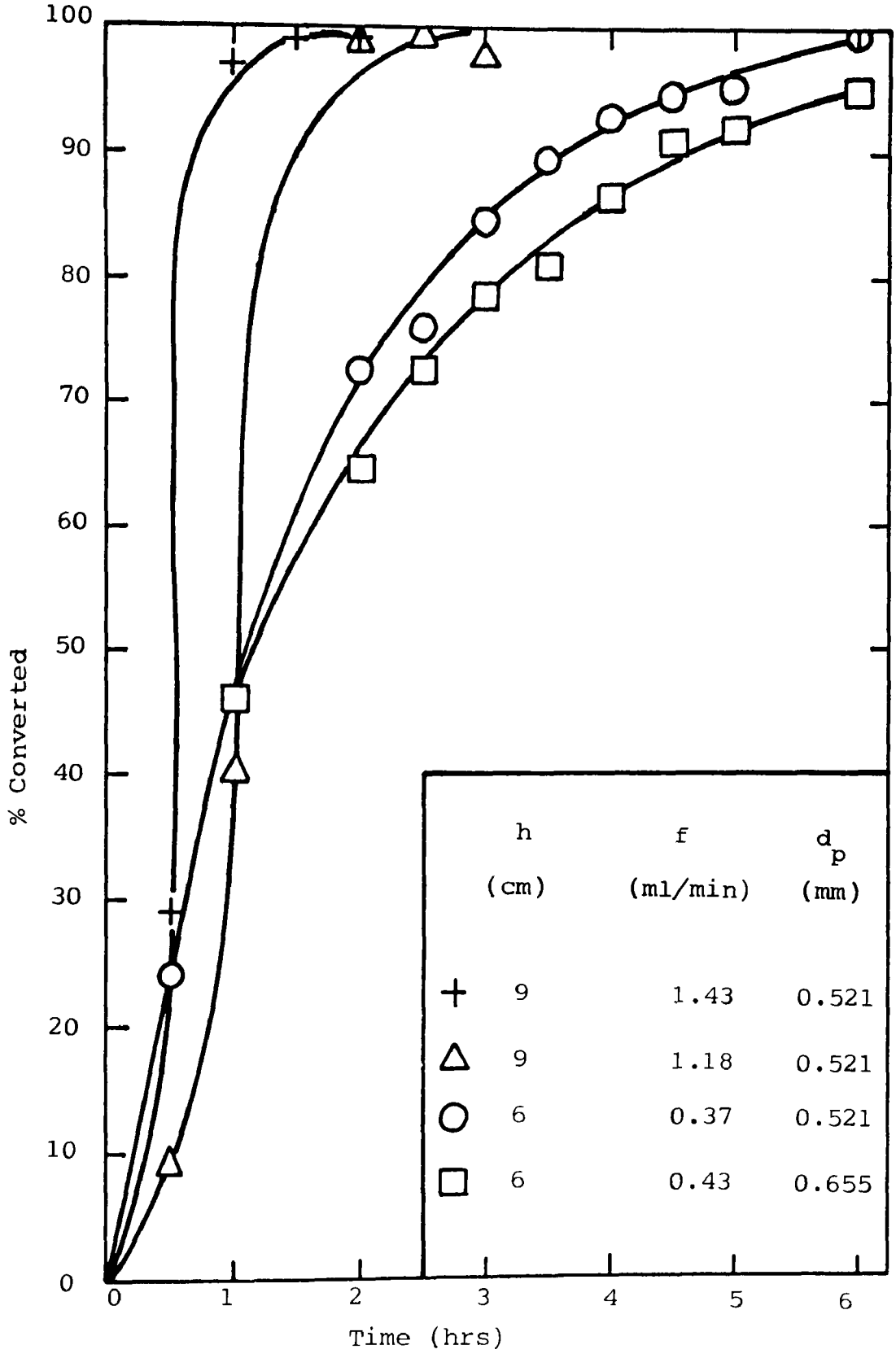

Figure 31 Conversion of Amberlite IRC-718 from H-form to Na-form using 1M NaOH

TABLE 10 Zinc precipitation

Concentration of NaOH (M)	Dilution fold using NaOH	Expected Zn^{++} concentration (ppm)	Determined Zn^{++} concentration (ppm)
0.1	-	550	195.00
0.1	2	275	195.00
0.15	2	412.5	178.5
0.2	-	1100	380.5
0.2	2	550	245.8
0.2	3	366.7	212.1
0.2	4	275	262.6
0.3	-	1650	599.3
0.3	2	825	818.2
0.5	-	2775	1508.4
1.0	-	5500	5500

7.11 MOVING BED

In this study twenty five runs were carried out in order to find the optimum operating conditions. To achieve this the bed height was varied from 8 to 30cm and Zn concentration from 55 to 550ppm. Solution flow rates ranging from 3.19 to 19.45 ml/min were used and the resin flow rates were much lower (0.083-0.328 ml/min). Sodium hydroxide concentration of 0.2M was treated in all runs except for run 5.1 for which the concentration was 0.1M. With the preliminary experiments, zinc leakage up to 25% was found to occur and later the operating conditions were modified to maintain lower Zn leakage. This was achieved using a bed height of 24cm and solution flow rate of 7ml/min with extraction efficiency around 99.5%.

7.11.1 Extraction efficiency

7.11.1.1 Effect of caustic concentration

With the first run (5.1) a bed height of 12cm was used and the solution flow rate was 19.45 ml/min. Sodium hydroxide solution of 0.1M containing 55ppm of Zn was treated and the results are shown in Figure 32 which indicates that a time of 8 hours was needed for the exit Zn concentration to reach 25% of its initial value. On the basis of this finding run 5.2 was designed in which a smaller bed was employed and NaOH concentration was raised to 0.2M. This run was operated for a period of 6 hours and later it was found that after the first 3 hours the concentration of Zn in the exit stream reached a

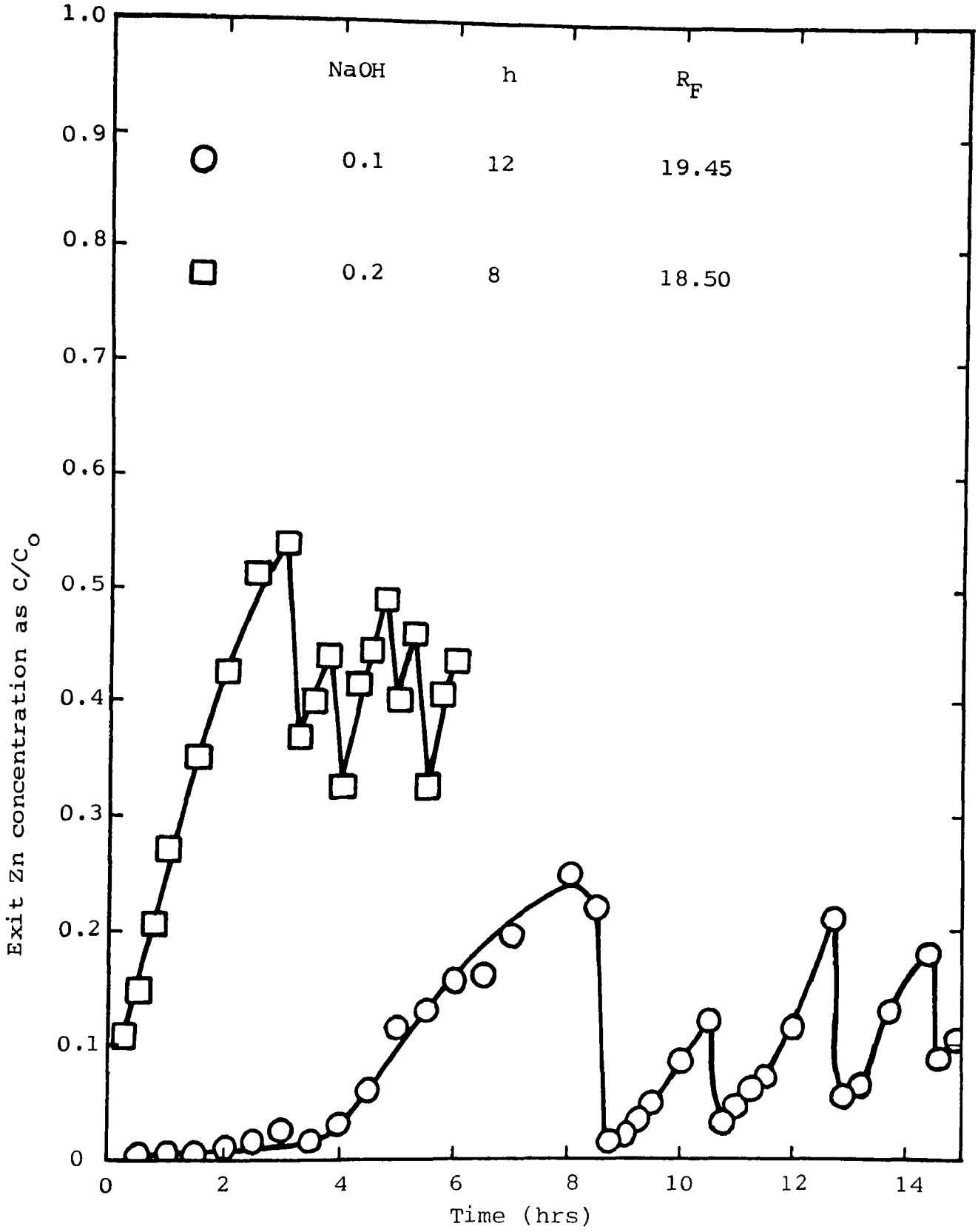

Figure 32 Exit Zn concentration as a function of time at different caustic concentrations.

value of 30ppm (54%) indicating an adverse effect of NaOH concentration.

7.11.1.2 Influence of solution flow rate

Runs 5.5, 5.6 and 5.7 were carried out with flow rates of 3.62, 5.55 and 7.05 ml/min respectively. The bed height was kept constant at 8cm and Zn concentration was raised to 550ppm. As can be seen from Table D2 that extraction efficiencies of 94% 95% &89.6% were obtained from which it is difficult to assess the true effect of flow rate. However, the effect of flow rate in general is found to decrease the efficiency.

7.11.1.3 Effect of bed height

The effect of bed height on the extraction efficiency was studied with runs 5.8, 5.9, 5.10 and 5.11 using bed heights of 12, 16, 20 and 24cm while the flow rate was kept constant at 7 ml/min. The results are given in Figure 33 which shows that the extraction efficiency increased by 10% over a three-fold increase of bed height.

In order to ensure that the combination of h=24cm and R_F=7ml/min were the conditions of maximum efficiency it was essential to carry out further investigation with R_F=9.14ml/min. The result of this investigation is shown in Figure 34 . The extraction efficiency was found to decrease from 99.6% to 98.2%.

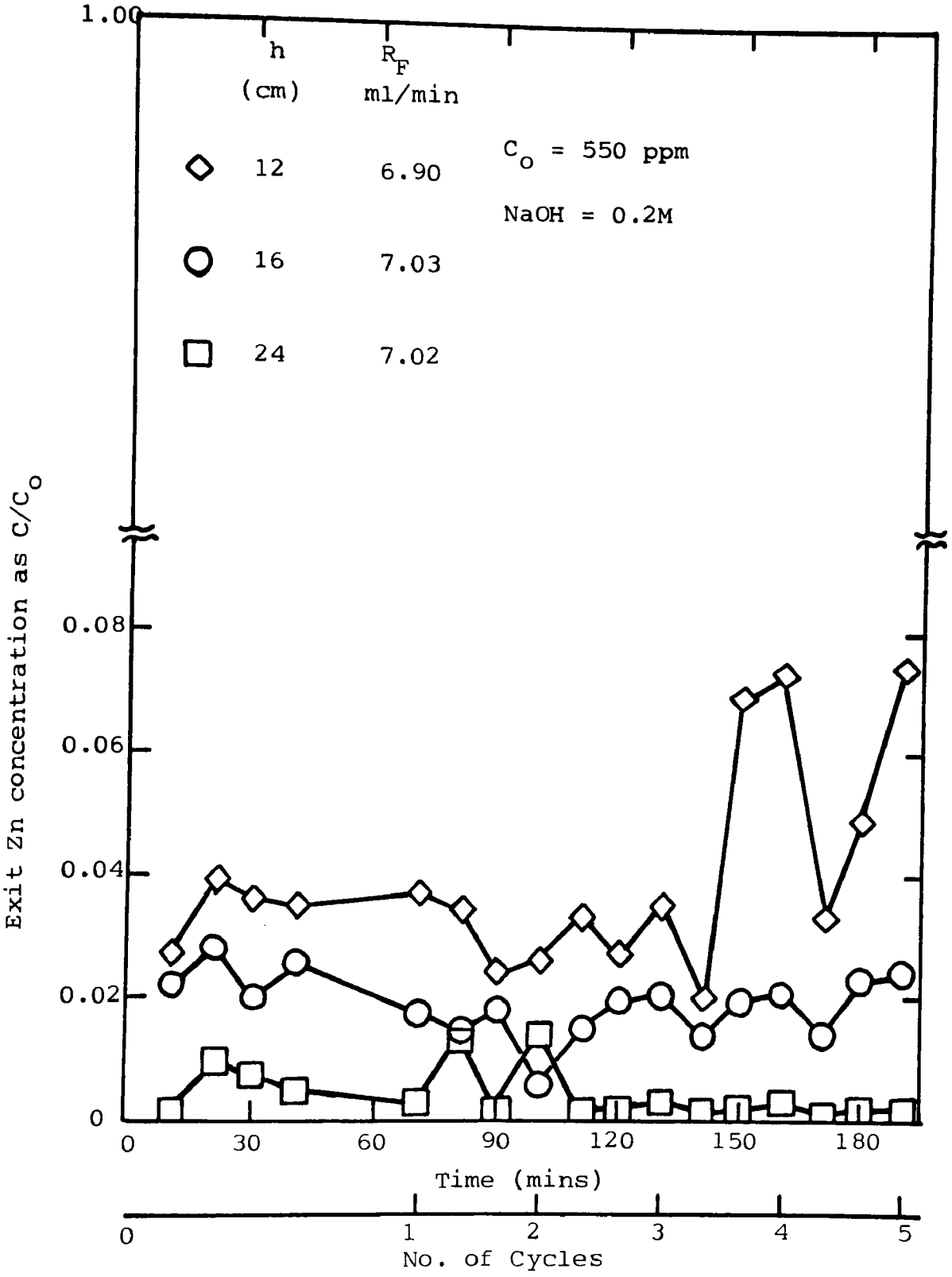

Figure 33 Exit Zn concentration as a function of time and number of cycles at different bed heights.

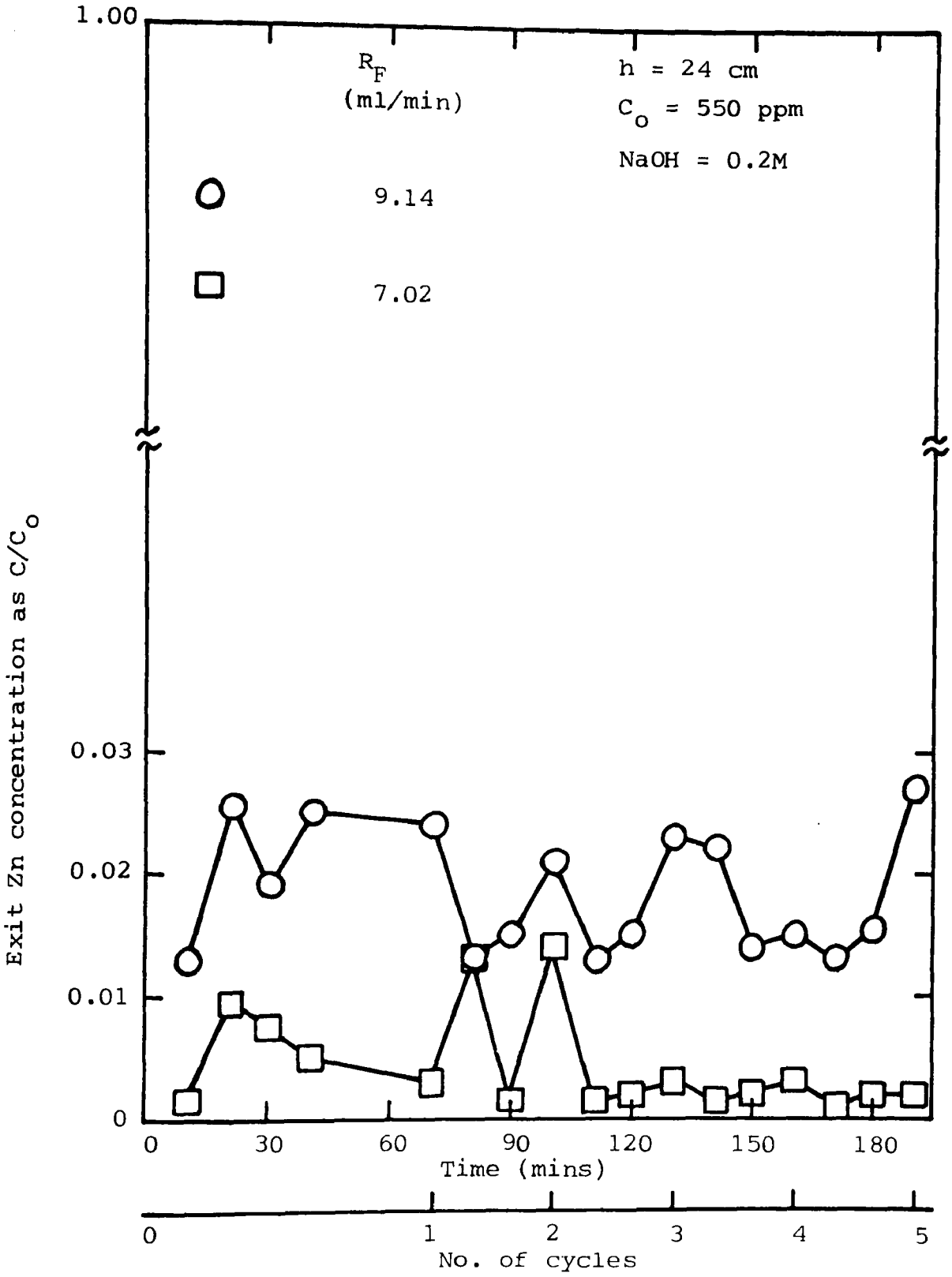

Figure 34 Exit Zn concentration as a function of time and number of cycles at different flow rates.

7.11.1.4 Influence of zinc concentration

To investigate the influence of Zn concentration on the extraction efficiency, experiments were carried out with Zn concentrations of 275, 330, 412.5 and 550 ppm with a bed height of 20cm and solution flow rate of around 10 ml/min. The bed height was selected at 20cm instead of 24cm to observe the variation of efficiency with the Zn concentration. The experimental data for C_o of 275 and 550ppm are plotted in Figure 35 and the calculated results are given in Table D4. As expected low Zn concentration gave better separation. The extraction efficiency was found to decrease by 20% over a twofold increase in Zn concentration. Figure 36 shows the relationship between the extraction efficiency and Zn concentration indicating this effect.

7.11.1.5 Effect of cycle time

In this study cycle times of 30, 45, 100 and 120 minutes were used and their effects were observed through the extraction efficiency. The bed height and the solution flow rate were kept constant at 24cm and 7ml/min respectively. Figure 37 shows the effect of cycle time on the exit Zn concentration which indicates that cycle times of 100 and 120 minutes are not desirable. The extraction efficiency decreased from 99.6% to 93.7% corresponding to cycle times of 30 and 120 minutes respectively. It can be expected that with a cycle time of 120 minutes and a relatively longer bed the extraction efficiency should

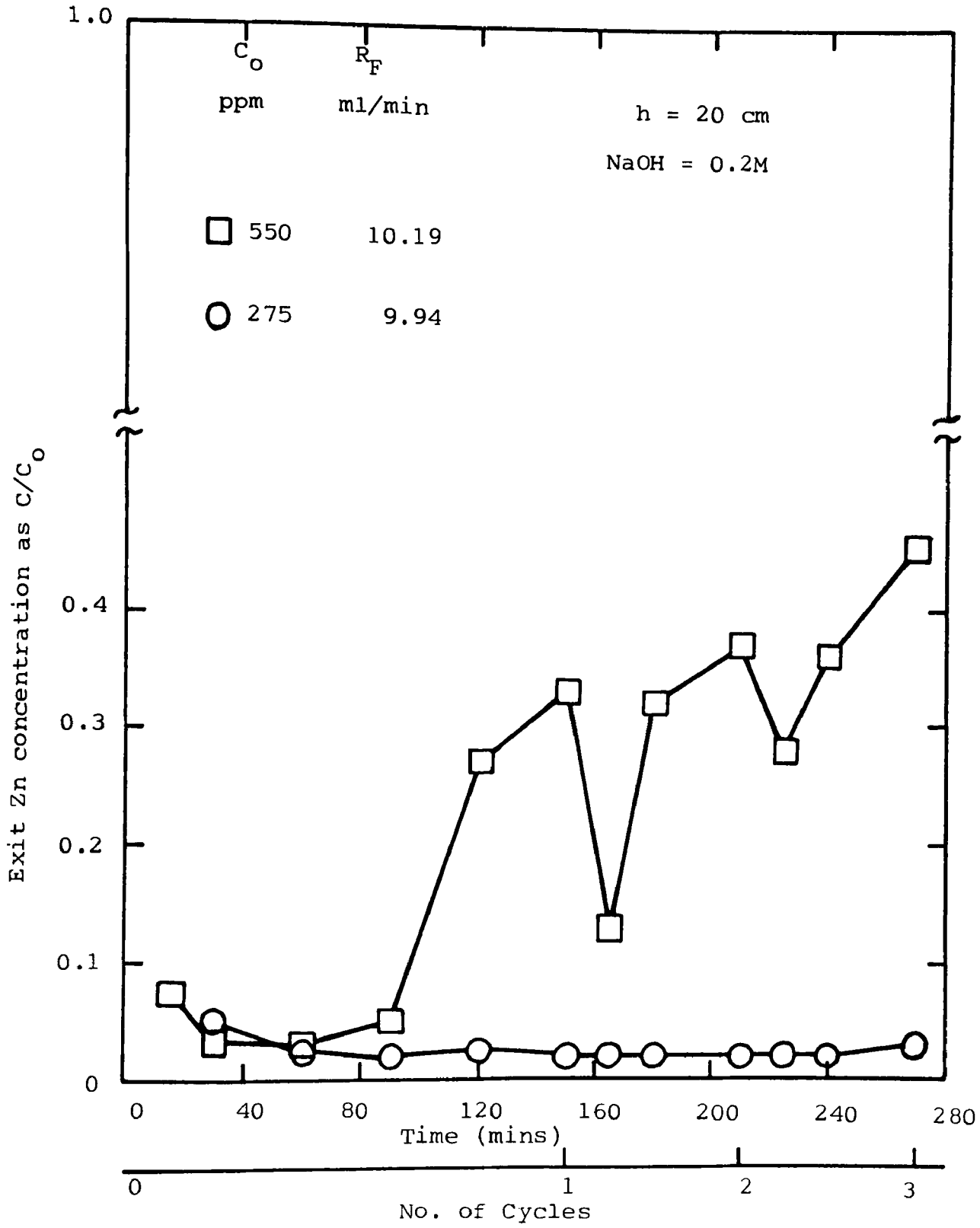

Figure 35 Exit Zn concentration as a function of time and number of cycles at different concentrations.

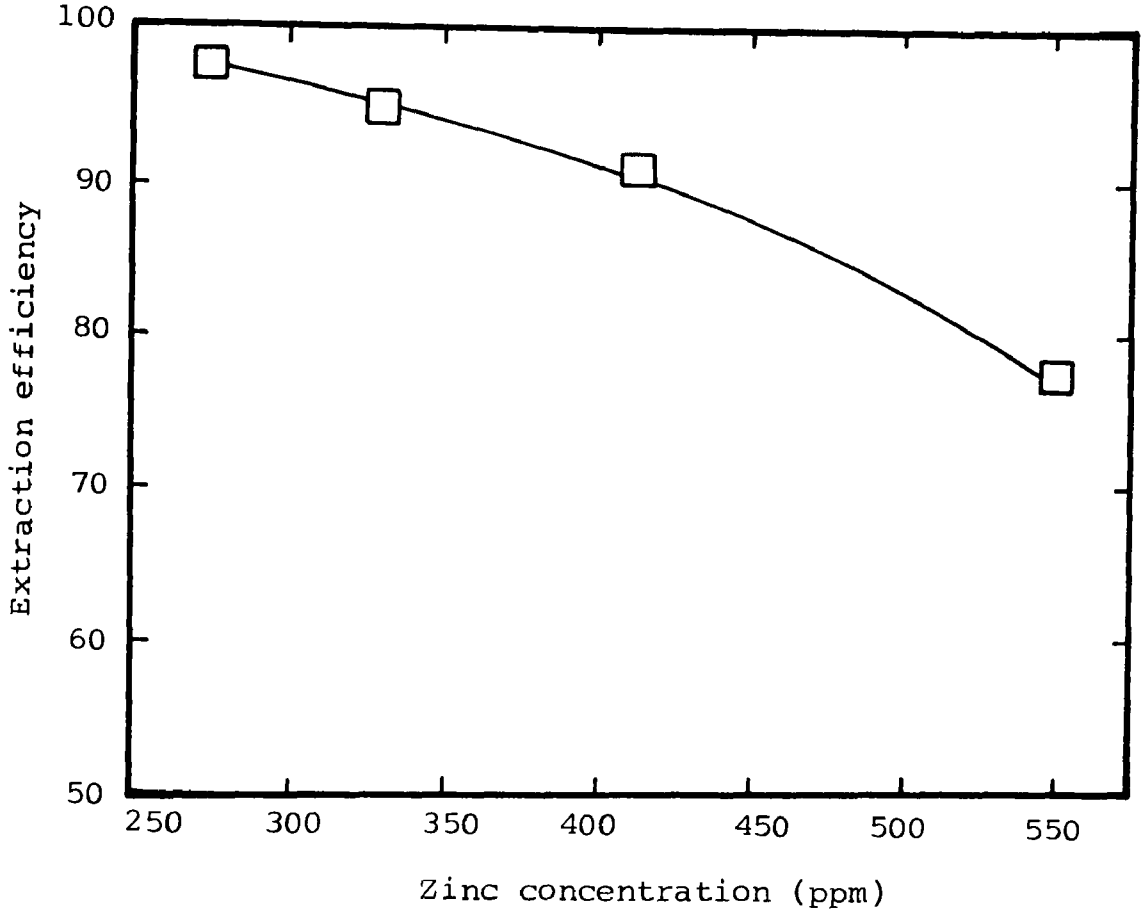

Figure 36 Extraction efficiency as a function of zinc concentration

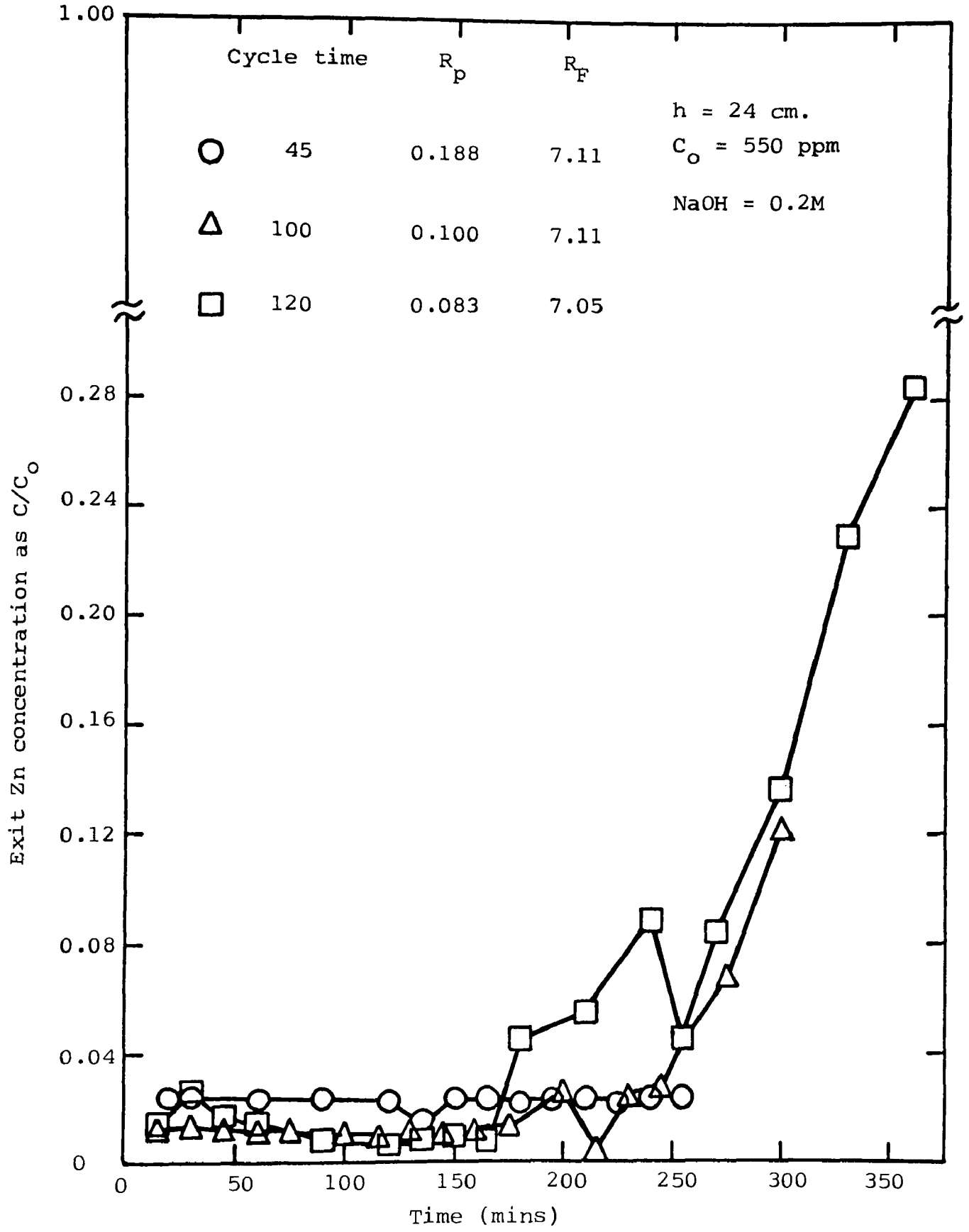

Figure 37 Exit Zn concentration as a function of time at different cycle times.

increase. This was confirmed when a bed height of 30cm was employed, the extraction efficiency was found to increase from 93.7% to 99.3%. Effective separation of Zn can also be achieved if the concentration of Zn ion is reduced and the cycle time is increased. When Zn concentrations of 412.5 and 495ppm with cycle time of 100 minutes duration were used, the extraction efficiency was found to increase from 97.7% to 99.6% corresponding to C_o of 550 and 412.5 ppm respectively.

The selection of cycle time for the moving bed operations was based on the results of a breakthrough study carried out in the same column. As can be seen from Figure 38 the time for break point (t_o) is 3.6 hrs. and all cycle times were kept lower than this value.

7.11.1.6 Influence of resin renewal

One would expect that by replacing larger volumes of resin at the end of each cycle will improve the separation of Zn. To do this three runs were conducted in which the volume of resin renewed was varied from 5 to 20 ml. With runs 5.12 and 5.13 bed height of 20cm was employed and the solution flow rate was increased to 10.19ml/min in order to compensate for the removal of larger volumes of resin. The experimental results of this investigation are presented in Figure 39 and the calculated data are given in Table D6. As can be seen from the figure that the separation of Zn was slightly improved when 20ml of resin was replaced. This surprising result could

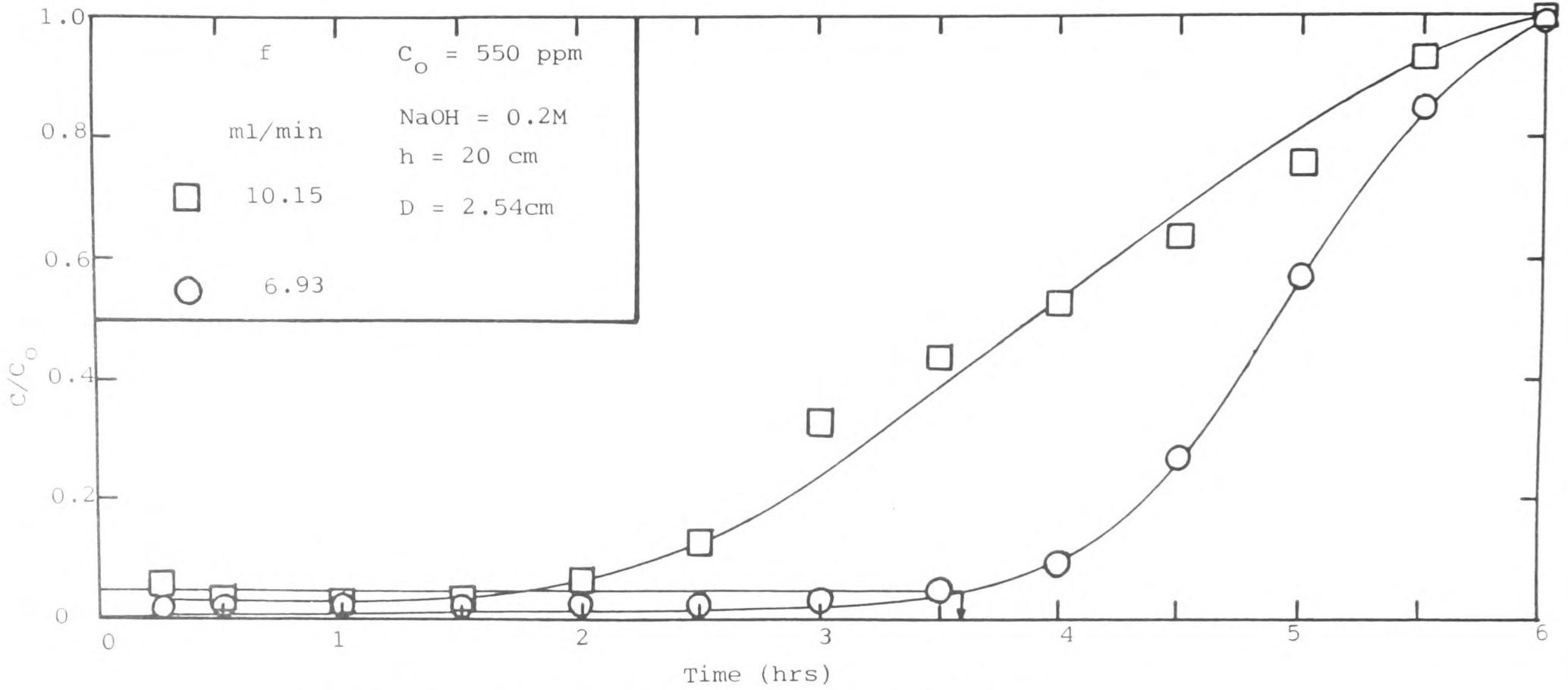

Figure 38 Breakthrough curves for moving bed column

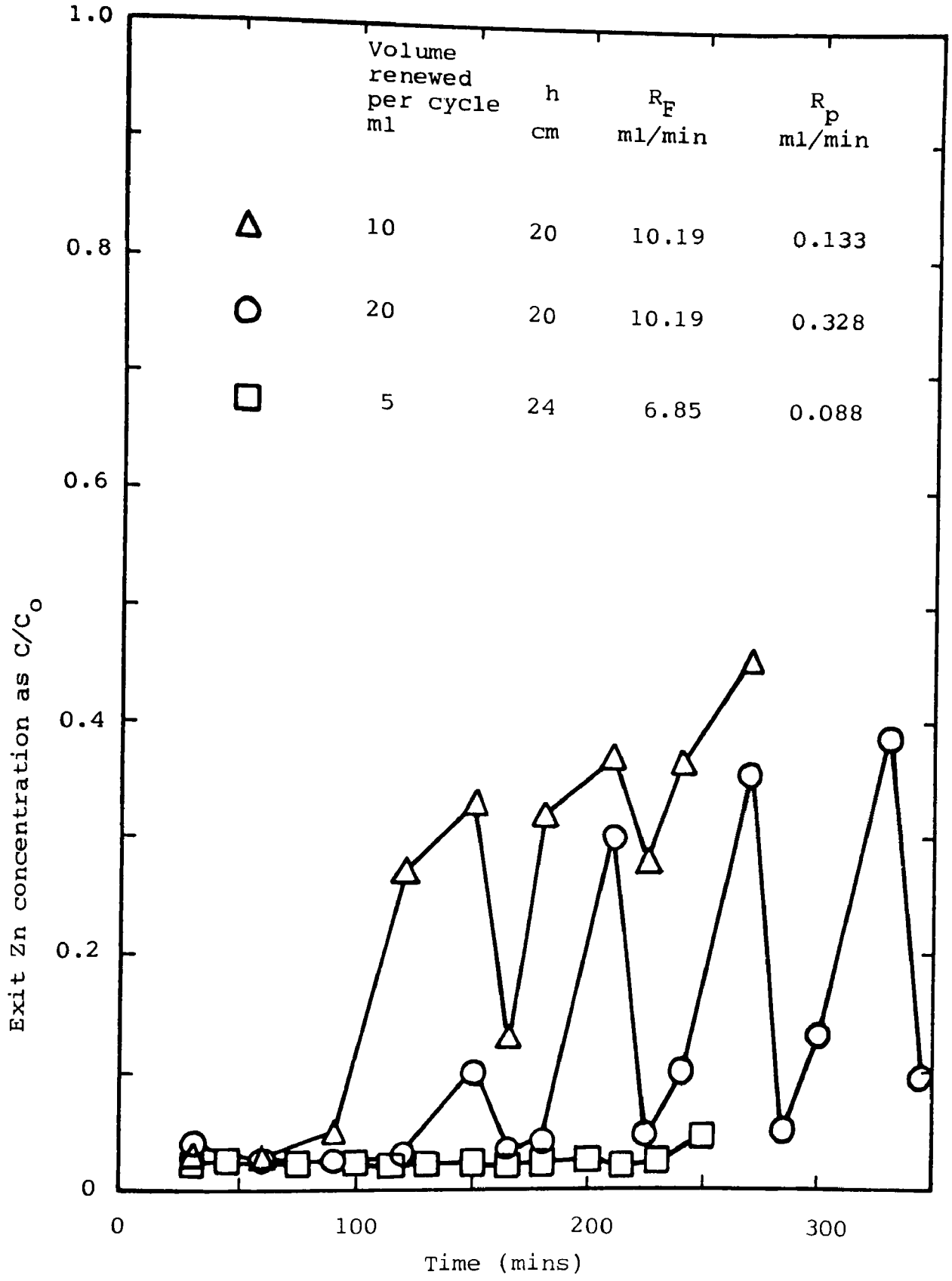

Figure 39 Effect of resin renewal on exit Zn concentration with time.

be due to the use of high flow rate. In run 5.20 the flow rate was reduced to 6.85ml/min in a bed of 24cm and the results show a 20% increase in the extraction efficiency as shown in Table D6.

7.11.2 Number of transfer units

The number of transfer units, NTU, was determined by graphical integration according to the procedure suggested by Selke and Bliss[173] as shown in Figure 11 and also was computed using Hiester et al[148] equation (6.30). The number of equilibrium contacts (stages), N_c, was obtained using McCabe Thiele procedure as shown in Figure 10 and also was calculated using Hiester et al[148] equation (6.31). Table 11 gives the comparison between NTU and N_c which indicates that results obtained through eqs. (6.30) and (6.31) are much higher than those obtained by the other methods. These equations were obtained for systems with linear equilibrium relationship and as the present systems exhibit non-linear equilibria, it is not surprising that these results are not in line with the other results. However, these results highlight the influence of equilibrium relationship on the values of NTU and N_c.

It was suggested[148] that moving bed adsorption could be treated through McCabe-Thiele procedure to obtain the number of equilibrium contacts between the phases. This procedure should give N_c equalling NTU for those systems in which the slopes of equilibrium and operating line are the same. The

TABLE 11 Comparison between NTU and N_C

Run No	C_o	h	R_F	R_p	NTU	NTU (6.30)	N_C	N_C (6.31)
5.1	55	12	19.45	0.102	3.06	7.31	1.81	6.97
5.2	55	8	18.50	0.184	1.00	2.58	0.64	0.98
5.3	550	8	3.67	0.260	3.12	4.46	1.00	3.11
5.4	550	8	3.19	0.270	2.93	3.80	0.95	2.44
5.5	550	8	3.62	0.300	2.96	3.89	0.96	2.53
5.6	550	8	5.55	0.290	3.10	5.50	1.58	4.36
5.7	550	8	7.05	0.300	2.35	5.77	1.73	5.38
5.8	550	12	6.90	0.298	3.49	7.75	1.86	6.73
5.9	550	16	7.03	0.297	4.64	10.87	1.94	9.52
5.10	550	20	7.00	0.292	5.43	15.79	1.94	14.44
5.11	550	24	7.02	0.294	10.49	17.32	2.00	15.23
5.12	550	20	10.19	0.328	2.16	5.45	1.83	5.45
5.18	550	24	9.14	0.295	5.70	50.08	3.90	50.02

present system does not meet this condition and therefore NTU values can be considered to be more representative compared with N_c values.

7.11.3 Height of transfer units

The height of transfer units, HTU, was calculated by dividing the bed height, h, by NTU. The effect of various parameters on the HTU are discussed under the following headings.

7.11.3.1 Effect of caustic concentration

By increasing the caustic concentration the separation of Zn was reduced which resulted in an increase in the HTU values from 3.92 to 8 cm corresponding to 0.1 and 0.2M NaOH respectively. This effect can be seen through the mass transfer resistance caused by the increased concentration of caustic.

7.11.3.2 Influence of solution flow rate

With a bed height of 8cm and solution flow rates of 3.62, 5.55 and 7.05 ml/min the HTU was found to decrease from 2.70 to 2.58 followed by an increase to 3.40cm. This indicates that for the bed height of 8cm a flow rate of about 5.5 ml/min would be the optimum since HTU value is at a minimum. Similar observation applies in the case of using a bed of 24cm in depth, a flow rate of 7.02 ml/min gave a lower HTU value than that of 9.14.

7.11.3.3 Effect of bed height

The HTU values seem to be unaffected by bed height increase which was varied from 8 to 20cm. However, with a bed height of 24cm the HTU was found to have a low value and this is because of a high NTU value which in turn depends on the nature of equilibrium relationship.

7.11.3.4 Effect of Zn concentration

The effect of Zn concentration was studied using bed heights of 20 and 24cm and solution flow rates of 10 and 7ml/min. In both cases the HTU values were found to increase with Zn concentration which ranged from 275 to 550ppm.

7.11.3.5 Influence of cycle time

A cycle time of 30 minutes was found to give low value of HTU when a bed height of 24cm was employed. However, the HTU value decreased with an increase of NTU when a bed of 30cm in depth was used with cycles time of 120 minutes.

7.11.3.6 Influence of resin renewal

The volume of resin replaced seemed to influence the HTU values as shown in Table D6. As HTU values depend on NTU and the bed height it is rather difficult to decipher the nature of this influence.

7.11.3.7 Correlation of HTU

The height of transfer units is finally correlated with zinc concentration as shown in Figure 40. The data follow a straight line represented by

$$HTU = 3.19 \times 10^{-2} C_o - 5.4 \qquad (7.8)$$

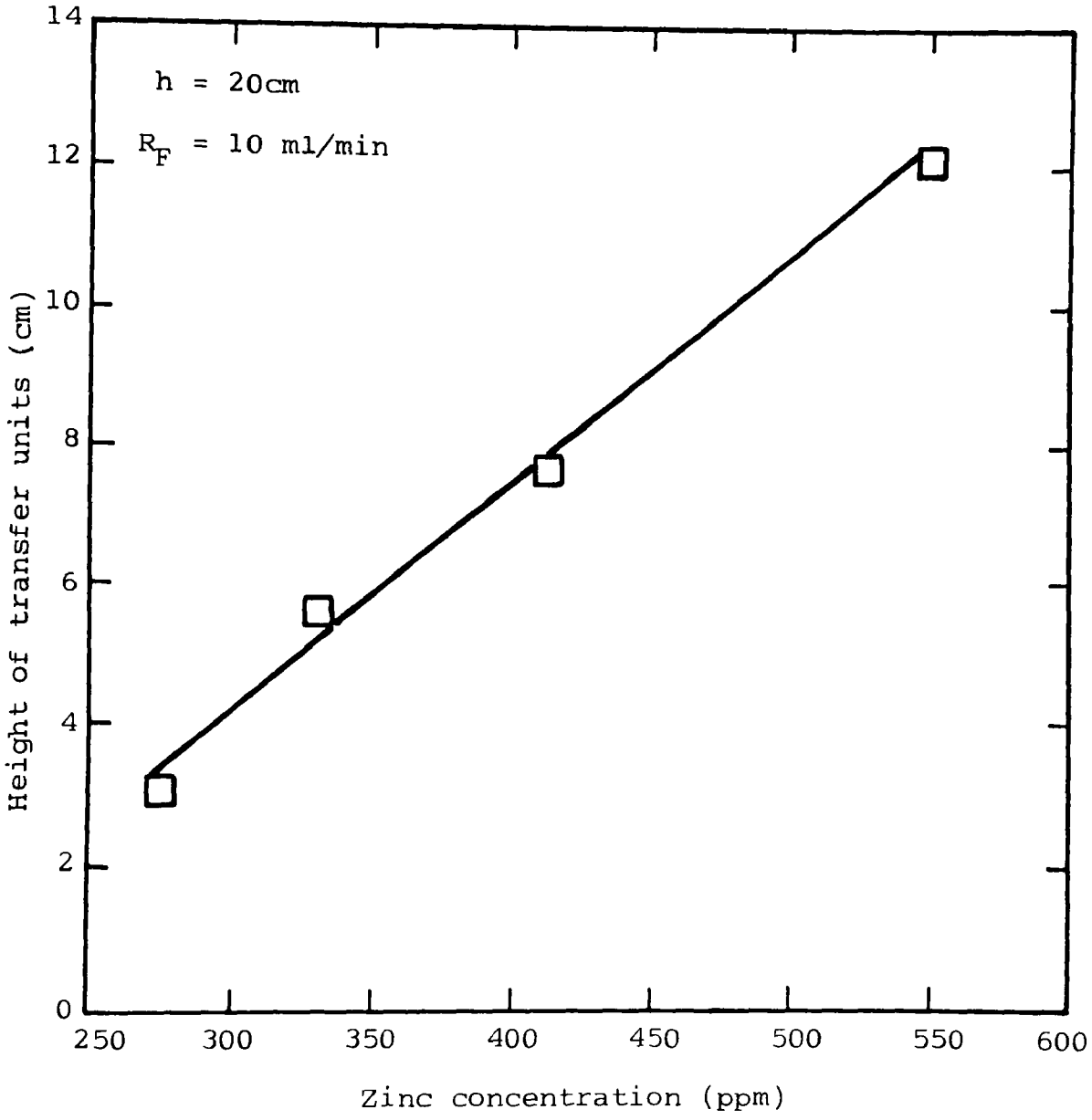

Figure 40 Correlation of HTU with C_o

CHAPTER EIGHT

CONCLUSIONS

The separation of zinc from an alkaline leach liquor of pH 13 has been possible through the use of Amberlite IRC-718 ion exchange resin. With this resin the equilibrium relationship is found to be favourable for 0.1 and 0.2M NaOH solutions. The resin is amenable to regeneration to Na - form through HCl and NaOH.

Breakthrough studies have been done in fixed beds and the data are analysed to determine mass transfer coefficients, saturation time, number of zones, zone height and velocity, number of transfer units and capacity. The activation energy of the process has been determined.

Further studies have been done with a moving bed system and the data are obtained for the determination of extraction efficiency, and number and height of transfer units.

Based on the results obtained in this work the following conclusions can be drawn.

1. Ka_y increases with $u_L^{0.5}$ (for u_L values ranging from 0.94×10^{-2} to 10.45×10^{-2} cm/s) This is confirmed by the results of zone height which also increases with the square root of the velocity indicating that the major resistance to ion transfer is diffusion in the liquid phase.

2. For the ion exchange process the activation energy has a value of 1.6 kcal/mole - a result that also

indicates a diffusion controlled process.

3. High temperature operations favour the exchange kinetics but also help the precipitation of zinc. This behaviour has a prominent effect on saturation time which is found to follow an increase rather than a decrease.

4. Caustic concentration above 0.2M reduces the rate of exchange due to the increase in solution viscosity and sodium ions concentration.

5. The presence of lead ions in the solution has a detrimental effect on the exchange kinetics of zinc.

6. The extraction efficiency in moving bed operation is found to increase with bed height and decrease with solution flow rate, Zn and OH ions concentration.

7. The conditions of maximum extraction efficiency are found to be at h of 24cm and R_F of 7 ml/min.

8. The cycle time of 30 minutes duration is found to give high extraction efficiency when the bed height and solution flow rate are 24cm and 7 ml/min respectively.

9. The height of transfer units has been found to increase with Zn and OH ions concentration, solution flow rate, and cycle time. However, HTU is unaffected by bed height increase.

8.1 Future investigations

The present study indicates a number of possible areas of interest which demands further investigations.

The selection of a cheap and effective resin is important. Claims have been made recently that chelate ion exchange resins such as Amberlite DP-1, Duolite ES-467, and Duolite ES-346 are selective for heavy metals and also have high capacity. Amberlite DP-1 is cheaper than Amberlite IRC-718 and this could lead to a better economy for the process.

The kinetics of regeneration is required for the full design of the separation process.

Work is needed on the recovery of Zn and HCl in addition to the concentration of NaOH in order to find out whether the process is economically viable.

It will be interesting to study this problem in several columns of moderate height arranged in series.

Recently advances have been made in continuous fluidized bed systems, this can be tried using a resin having faster kinetics than the present one.

Future work is also needed with moving bed system using a micro processor to control the sequences of the operation.

REFERENCES

1. THOMPSON, H.S., Absorbent power of soils, J. Roy. Agr. Soc., 11, p. 68-74, 1850.

2. GANS, R., Zeolites and similar compounds (their constitution and significance for technology and agriculture), Jahrb. Kgl. Preuss. Geol. Landesantalt (Berlin) 25, p. 2 , 1905.

3. ADAMS, B.A. and HOLMES, E.L., Adsorptive powers of synthetic zeolites, J. Soc. Chem. Ind (London), 54, 1-6T, 1935.

4. D'ALELIO, G.F., U.S. Patent 2,340,110, 1944.

5. MCBURNEY, C.H., U.S. Patent 2,591,573, 1952.

6. RASHEED, A.C.M., A study of lead separation from electric arc furnace steel making dusts using a cementation process, Ph.D (CNAA) thesis, The Polytechnic of Wales, Dec., 1981.

7. BRANTLEY, F.E., Iron and Steel, BuMines Minerals Yearbook, V. 1-2, p. 598, 1969 and 1971.

8. BAN, T.E., U.S. Patent 3,262, 771, 1966.

9. LARPENTEUR, B.J. and JOSEPH, W.P., U.S. Patent 3,547,623, 1970.

10. STIRLING, H.T., and KINSEY, F.W., Improved techniques for processing steel plant fines, J. of Metals, V.19, p. 83-7, May, 1967.

11. THOM, G.G.W., and SCHULDT, A.A.F., The collection of open hearth dust and its reclamation using SL/RN process, Canadian Min. and Metallurgical Bull., V. 59, p. 1229-33, 1966.

12. THOM, G.G.W., U.S. Patent 3,403,018, 1968.

13. BARNARD, P.G., STARLIPER, A.G., DRESSEL, W.M., and FINE, M.M., Proc. of the third Mineral Waste Utilization Symp., Chicago, p. 63-8, 1972.

14. IKENO, T., OTA, M., YAMAD, K., and NAGANO, K., Study of the removal of zinc from open-hearth furnace dust. I. The characteristics of open-hearth furnace dust and various zinc removal processes, Tetsu To Hagane, 51(10), p. 1777-9, 1965, Chem. Abstr. 21211 x, 66, 1967.

15. WAKAMATSU, S., Determination of zinc in steel-making dust, Tetsu To Hagane, 54(7), p. 787-95, 1968, Chem. Abstr. 56804 g, 69, 1968.

16. VAN VEEN, F., Recycling of complex heavy metal wastes by solvent extraction and ion exchange as a contribution to solve environmental problems, Congr. Proc. Recycling World Congress 2nd. IV/6/135-45, 1979.

17. DAVIES, G.A., Unit operations in hydrometallurgy, Chemistry and Industry, No. 12, p. 402-7, 1981.

18. HAINES, A.K.,TUNLEY, T.H., TE RIELE, W.A.M., and CLOETE, F.L.D., Recovery of zinc from pickle liquors by ion exchange, J.S. Afr. Inst. Mining Metall., 74(4), p. 149-57, 1973.

19. THE INSTITUTION OF CHEMICAL ENGINEERS, Ion Exchange Technology short course, Imperial College, March, 1981.

20. CALMON, C., Removal of zinc from pickle liquor, in Ion Exchange for Pollution Control, V.1, CRC Press, Boca Raton, Fla, p. 207-210, 1979.

21. BLOODGOOD, D.E., and LOSSON, F.J.,Jr., Removal of toxic substances from metal-plating wastes by ion exchange, Proc. Ind. Waste Conf. Extension Series 64, p. 196-208, 1947.

22. WALKER, C.A., and ZABBAN, W., Disposal of plating room wastes, Plating (N.J.) 40, p. 165-8 and p. 269-78, 1953.

23. TALLMADGE, J.A., Ion exchange treatment of mixed electroplating wastes, Ind. Eng. Chem. Process. Des. Dev. 6(4), p. 419-23, 1967.

24. KAWAGUCHI, A., and IMAI, Y., Studies on mass transfer in ion exchangers. I. The exchange adsorption of zinc ion from zinc cyanide solutions in weak acid cation exchange resin beds, Denki Kagaku Oyobi Kogyo Butsuri Kagaku, Japan, 45(3), p. 144-9,1977 Chem. Abstr. 247752 88, 1978.

25. PAULSON, C.F. and MINDLER, A.B., Use of ion exchange in the waste-treatment field, Chem. Eng. Prog. Symp. Ser., 50(14), p. 93-6, 1954.

26. MINDLER, A.B., Application in hydrometallurgy, in ion exchange technology by Nachod, F.C., and Schubert, p. 286-309, Academic Press, N.Y. 1956.

27. MINDLER, A.B., GILWOOD, M.E., and SAUNDERS, G.H., Metal recovery by cation exchange, Ind. Eng. Chem., 43(5), p. 1079-81, 1951.

28. BOWEN, L.B., MALLINSON, J.H., and COSGROVE, J.H., Zinc recovery from rayon plant sludge, Chem. Eng. Prog. p. 50-4, May, 1977.

29. EGAWA, H., and MAEDA, H., Studies on selective adsorption resin. VIII. Selective adsorption of zinc ion on a chelating resin containing hydrazide groups, Nippon Kagaku Kaishi, 7, p. 1043-8, 1978, Japan, Chem. Abstr. 153207k, 89, 1978.

30. KOLLAR, I., Czech 136, 147, 1970.

31. GLOVER, G.E., and PRATT, J.B., U.S. Patent 3,380,804, 1968.

32. MORGENSHTERN, V.S., and MATORENOK, L.N., Use of carboxyl cation-exchangers for removing zinc from waste waters of the viscose industry, Khim. Volvkna (Russia), 1, p. 66-7, 1970.

33. BRETON, E.J., Jr., and SCHLECHTEN, A.W., Separation of copper from zinc by ion exchange, J. of Metals, p. 517-21, 1951.

34. BLAKE, W.E.,and RANDLE, J., Removal of Zn^{2+} from the ternary system Zn^{2+}- Na^{+}- H^{+} by cation-exchange resin column, J. Appl. Chem., 17, p. 358-60, 1967.

35. NACHOD, F.C., U.S. Patent 2,371,119, 1945.

36. THOMPSON, J., and MILLER, V.J., Role of ion exchange in treatment of metal finishing wastes, Plating (N.J.), 58, p. 809-12, 1971.

37. PRITCHARD, E.J., and PCIHODA, W.W., Recovery of gold from rinse waters using ion-exchange techniques, Plating (N.J.), 56, p. 1044-6, 1969.

38. ANON, Gold conservation pays for platers, Plating(N.J.), 65, p. 20-2 , 1976.

39. CALMON, C., Precious metal recovery, in ion exchange for pollution control, Vol. 1, p. 213-5, 1979.

40. GOLD, H., Metal finishing wastes, ibid, p. 173-89

41. GOLDSTEIN, S., SILBERT, M., and SCHMUCKLER, G., The chelating properties of a polyisothioronium ion exchanger, Ion. Exch. Membr., 1, p. 225-9, 1974.

42. DAVANKOV, A.B., and LAUFER,V.M., Ion exchange distribution of gold ions on resin adsorbers, Tsvetnye Metal, 29(11), p. 1-6, 1956.

43. ROLINSON, P.L., Metals recovery by chelation and ion exchange, paper presented at a meeting on metals recovery arranged by the Institution of Chemical Engineers, Sheffield, March, 1983.

44. DORFNER, K., Ion exchangers: properties and applications, Ann Arbor science publishers Inc. 1972.

45. BERG, E.W., and TRUEMPER, J.T., Ion exchange separation of zinc,cadmium, and mercury in aqueous and partial nonaqueous media, Anal. Chem., 30, p. 1827-30, 1958.

46. WALTON, H.F., Ion exchange as an analytical tool in pollution control, in ion exchange for pollution control, Vol. 1, p. 111-13, 1979.

47. WAITZ, W.H., Jr., Ion Exchange in heavy metals removal and recovery, Amber-hi-lites, No. 162, Fall 1979.

48. AVERY, N.L., and WAITZ, W.H., Ion exchange treatment process for selective removal of cyanide, Amber-hi-lites, No. 155, Summer 1977.

49. QUARM, T.A.A., Recovery of copper from mine drainage water by ion exchange, Bull. Inst. Mining Metallurgy, p. 109-17, 1954.

50. PAULSON, C.F., Wastes recovery by ion exchange, Wastes Engineering, 23, p. 208-9, 1952.

51. BIRCH, M.E.J., CHARLTON, J.R., HUDSON, M.J., and GIWA, C.O., A new process for the separation of iron from other base metals, Soc. Chem. Ind. Symp., Oslo, p. I/49-60, 1982

52. HIRSCH, R.F., GANCHER, E., and RUSSO, F.R., Macroreticular chelating ion-exchangers, Talanta, 17(6), p. 483-9, 1970 Chem. Abstr. 51889 m, 73, 1970.

53. SZIDEN, R.D., and FRITZ, J.S., Separation of metal ions on chelating resin, U.S. At. Comm. IS-340, 1961. Chem. Abstr. 6687a, 56, 1962.

54. GOLD, H., and CALMON, C., Ion Exchange: present status, needs, and trends, AIChE Symposium series, 76(192), p. 60-7, 1980.

55. HELFFERICH, F.G., Ion exchange, McGraw-Hill, N.Y. 1962.

56. HELFFERICH, F.G., Ion exchange kinetics, Ion exchange, Vol. 1, p. 65-100, 1966.

57. GUPTA, A.K., and STREAT, M., Ion exchange equilibrium and kinetics studies, Rep. Prog. Appl. Chem., 59, p. 262-5, 1975.

58. SOLDANO, B.A., The Kinetics of ion exchange process, Annals N.Y. Academy of Sciences, 57, p. 116-24, 1953.

59. BOYD, G.E., and SOLDANO, B.A., Self-diffusion of cations in and through sulfonated polystyrene cation-exchange polymers, J. Am. Chem. Soc., 75, p. 6091-9, 1953.

60. BOYD, G.E., ADAMSON, A.W., and MYERS, L.S., Jr., The exchange adsorption of ions from aqueous solutions by organic zeolites. II. Kinetics, J. Am. Chem. Soc., 69, p. 2836-48, 1947.

61. SCHLÖGL, R., and HELFFERICH, F., Comment on the significance of diffusion potentials in ion exchange, J. Chem. Phys., 26, p. 5-7, 1957.

62. GOPALA RAO, M., BAJPAI, R.K., and GUPTA, A.K., Single particle studies of binary and ternary cation exchange kinetics, A.I.Ch. E.J., 20(5), p. 989-95, 1974.

63. TURNER, J.C.R., CHURCH, M.R., JOHNSON, A.S.W., and SNOWDON, C.B., An experimental verification of the Nernst-Planck model for diffusion in an ion-exchange resin, Chem. Eng. Sci., 21(4), p. 317-25, 1966.

64. VISWANATHAN, S., RAO, D.P., KEKRE, S.Y., and GOPALA RAO, M., Ternary ionic diffusion in ion-exchange resin, Soc. Chem. Ind. London, p. 281-4, 1969 (pub. 1970).

65. HERING, B., and BLISS, H., Diffusion in ion exchange resins, A.I. Ch.E.J., 9(4), p. 495-502, 1963.

66. VAN BROCKLIN, L.P., and DAVID, M.M., Ionic migration effects during liquid phase controlled ion exchange, A.I.Ch.E. Symp. ser. on adsorption and ion exchange, 71(152), p. 191-20, 1975.

67. PAN, S.H., and DAVID, M.M., Model identification for liquid-phase mass transfer rates in packed-bed ion exchange, Rec. Dev. Sep. Sci., 5, p. 199-211, 1979.

68. SELKE, W.A., BARD, Y., PASTERNAK, A.D., and ADITYA, S.K., Mass transfer rates in ion exchange, A.I.Ch.E.J., 2(4) p. 468-70, 1956.

69. GIOVANNI, D.R., FRANCO, E., and UGO, F.P., Simulation of fixed bed ion exchange columns: Mathematical model and its verification, Adv. Sep. Sci. (Proc. Symp.), p. 52-61, 1978.

70. LEE, C.S., Prediction of rate constants for particle diffusion controlled ion exchange, Hwahak Konghak, 17(1), p. 41-6, 1979(Korean), Chem. Abstr. 41307c, Vol. 91, 1979.

71. TIEN, C., and THODOS, G., Ion exchange kinetics: the removal of oxalic acid from glycol solutions, Chem. Eng. Sci., 13, p. 120-9, 1961.

72. OLEINIK, A.W., and KORSHUNOV, I.A., The kinetics of ion-exchange in its initial stage, Tr. poKhim. iKhim. Teknol, 4, p. 430-5, 1962, Chem. Abstr. 2883e, 57(1962).

73. PETROVA, L. Ya., and LIFSHITS, P.A., Approximate analytic solution of an equation on the film kinetics of ion exchange, Zh. Fiz. Khim., 40(12), p. 2947-52, 1966 (Russ), Chem. Abstr. 47526 z, 67, 1967.

74. KAWAZOE, K., et.al., Mass transfer in ion exchange Na^{24}-Na exchange in a resin bed, Kagaku Kogaku, 31(1), p. 49-55, 1967, Japan, Chem. Abstr. 85308 n, 67, 1967.

75. DICKEL, G., and KOERNER, D., A paradox of ion exchange in resin exchangers, Z. Phys. Chem. 58(1-4), p. 64-74, 1968, Germany, Chem. Abstr. 70098m,69, 1968.

76. HERMANN, H., et. al., Kinetics of ion exchange processes, Helv. Chim. Acta. 52(7), p. 2137-43, 1969, Germany, Chem. Abstr. 129149 a, 71, 1969.

77. DRANOFF, J.S., and COLWELL, C.J., Nonlinear equilibria and axial mixing effects in intraparticle diffusion-controlled sorption by ion exchange resin beds. Experimental study, Ind. Eng. Chem. Fundam. 10(1), p. 65-70, 1971.

78. KATAOKA, T., Liquid film mass transfer with or without resistances at liquid film and resin phase in ion exchange, Kogyo Yosui, 155, p. 27-32, 1971 Japan, Chem. Abstr. 28134 q, 76, 1972.

79. KATAOKA, T., NISHIKI, T., and UEYAMA, K., Mass transfer in ion exchange by liquid anion exchanger, J. Chem. Eng. Jpn., 6(4), p. 320-4, 1973.

80. NATIV, M., GOLDSTEIN, S., and SCHMUCKLER, G., Kinetics of ion exchange process accompanied by chemical reactions, J. Inorg. Nucl. Chem. 37(9), p. 1951-6, 1975.

81. FROELICH, P., Calculation of diffusion coefficients and breakthrough curves for the case of internal diffusion as a step determining speed (gel kinetics) in ion-exchange column, Acta. Hydrochim. Hydrobiol. 4(5), p. 495-9, 1976, Germany, Chem. Abstr. 149474 V, 85, 1976.

82. KATAOKA, T., YOSHIDA, H., and OZASA, Y., Intraparticle ion exchange mass transfer accompanied by instantaneous irreversible reaction, Chem. Eng. Sci. 32(10), p. 1237-40, 1977.

83. CHMUTOV, K.V., KALINIOHER, A.I., and SEMENOVSKAYA, T.D., Approximate solution of equations of the kinetics of ion exchange on complexing ion exchangers, Dok. Akad. Nauk SSSR, 239(3), p. 650-3, 1978, Russia, Chem. Abstr. 177721 d, 88, 1978.

84. THOMAS, H.C., Heterogeneous ion exchange in a flowing system, J. Am. Chem. Soc. 66, p. 1664-6, 1944.

85. SHERWOOD, T.K., PIGFORD, R.L., and WILKE, C.R., Mass transfer, McGraw-Hill, New York, 1975.

86. TAN, H., Calculation of J functions by a pocket calculator, Chemical Engineering, p. 158, October, 1977.

87. HOUGEN, O.A., and MARSHALL, W.R., Jr., Adsorption from a fluid stream flowing through a stationary granular bed, Chem. Eng. Prog. 43, p. 197-208, 1947.

88. GILLILAND, E.R., and BADDOUR, R.F., The rate of ion exchange, Ind. Eng. Chem. 45(2), p. 330-7, 1953.

89. KELLY, E.G., ALLEN, R.M., and KENNEDY, A.M., Interpretation of fixed-bed ion exchange data, Chemeca 70 Proc. Conf. No. 6B. Australia 1970, p. 18-34, 1971.

90. NUTT, C.W., SHARIFI, S., and TONGE, F., Influence of solvent viscosity on the kinetics of the exchange of sodium for hydrogen ions in fixed beds of Dowex-50, J. Appl. Chem. 10, p. 505-11, 1960.

91. BIEBER, H., STEIDLER, F.E., and SELKE, W.A., Ion exchange rate mechanism, Chem. Eng. Prog. Symp. Ser. 50(14), p. 17-21, 1954.

92. MICHAELS, A.S., Simplified method of interpreting kinetic data in fixed-bed ion exchange, Ind. Eng. Chem. 44(8), p. 1922-30, 1952.

93. MOISON, R.L., and O'HERN, H.A., Jr., Ion exchange kinetics, Chem. Eng. Prog. Symp. Ser. 55(24), p. 71-85, 1959.

94. LUKCHIS, G.M., Adsorption systems, Part I: Design by mass-transfer-zone concept, Chem. Eng. p. 111-6, June, 1973.

95. MOSEMAN, M.H., and BIRD, G., Desiccant dehydration of natural gasoline, Chem. Eng. Prog., p. 78-83, February, 1982.

96. GONDO, S., and KUSUNOKI, On the estimation of equilibrium stages of ion exchange fixed bed, J. Nucl. Sci. Technol. 6(10), p. 567-72, 1969.

97. SLATER, M.J., and ZUMER, M., Ion exchange in deep fluidized beds, Inst. Chem. Eng. Symp. Ser., 42, p. 23.1-12, 1975.

98. SLATER, M.J., Continuous ion exchange plant design methods and problems, Hydrometallurgy, 4, p. 299-316, 1979.

99. KATAOKA, T., and YOSHIDA, H., Breakthrough curve in ion exchange between divalent ion and monovalent ion-liquid-phase diffusion control, J. Chem. Eng. Japan, 10(3), p. 245-7, 1977.

100. LIBERTI, L., and PASSINO, R., Simplified method for calculating cyclic exhaustion regeneration operations in fixed-bed adsorbers, Ind. Eng. Chem. Process. Des. Dev., 21, p. 197-203, 1982.

101. VERMEULEN, T., and HIESTER, N.K., Kinetic relationships for ion exchange processes, Chem. Eng. Prog. Symp. Ser. 24(55), p. 61-9, 1959.

102 MONET, G.P., and VERMEULEN, T., Progress in separation by sorption operations- Adsorption, Dialysis, and ion exchange, Chem. Eng. Prog. Symp. Ser. 55(25), p. 109-33, 1959.

103. VERMEULEN, T., KLEIN, G., and HIESTER, N.K., Adsorption and Ion exchange in Chemical Engineer's Handbook by Perry, R.H., and Chilton, C.H., fifth edition, McGraw-Hill, 1973.

104. HIESTER, N.K., RADDING, S.B., NELSON, R.L., Jr., and VERMEULEN , T., Interpretation and correlation of ion exchange column performance under nonlinear equilibria, A.I.Ch.E.J., 2, p. 404-11, 1956.

105. FLECK, R.D., KIRWAN, D.J., and HALL, K.R., Mixed-resistance diffusion kinetics in fixed-bed adsorption under constant pattern conditions, Ind. Eng. Chem, Fundam. 12(1), p. 95-9, 1973.

106. LAPIDUS, L., and ROSEN, J.B., Experimental investigations of ion exchange mechanisms in fixed beds by means of an asymptotic solution, Chem. Eng. Prog. Symp. Ser. 50(14), p. 97-102, 1954.

107. HIESTER, N.K., and PHILLIPS, R.C., Ion exchange; A Chemical Engineering report, Chem. Eng., p. 161-80, Oct. 1954.

108. HUTCHEON, J.M., Continuous ion-exchange, Proc. Soc. Chem. Ind. (London), p. 101-11, 1955.

109. LAUER, B.E., Mechanical features of a continuous ion exchange unit, U.S.A.E.C. report HW-45149, 1956.

110. POOLE, K.R., Ion Exchange reviewed as a continuous process, A.E.R.E. - R3022 (Harwell), 1959.

111. SLATER, M.J., A review of continuous countercurrent contactors for liquids and particulate solids, Brit. Chem. Eng. 14(1), p. 41-6, 1969.

112. SLATER, M.J., Recent industrial scale applications of continuous resin ion exchange systems, J. Sep. Proc. Technol., 2(3), p. 2-12, 1981.

113. HIGGINS, I.R., A contercurrent solid-liquid contactor for continuous ion exchange, Oak Ridge, Tennessee, ORNL-1310, 1952.

114. HIGGINS, I.R., and ROBERTS, J.T., A countercurrent solid-liquid contactor for continuous ion exchange, Chem. Eng. Prog. Symp. Ser. 50 (14), p. 87-92, 1954.

115. HIGGINS, I.R., Mechanical features of the Higgins continuous ion exchange column, ORNL-1907, 1955.

116. HIGGINS, I.R., Use of the Higgins continuous ion exchange contactor in recovering uranium from aqueous slurries, ORNL-1918, 1956.

117. HIGGINS, I.R., U.S. Patent 2,815,322, 1957.

118. HIGGINS, I.R., and MESSING, A.F., Development of a continuous ion exchange process for the removal and recovery of cesium from alkaline solution, ORNL-2491, 1958.

119. HIGGINS, I.R., and ROBERTS,J.T., A countercurrent solid-liquid contactor for continuous ion exchange, AECU-2546.

120. HIGGINS, I.R., and CHOPRA, R.C., Chem-Seps continuous ion exchange contactor and its applications to demineralisation processes, Soc. Chem. Ind. London, p. 121-6, 1969 (pub. 1970).

121. AREHART, T.A., BRESEE, J.C., HANCHER, C.W., and JURY, S.H., Countercurrent ion exchange, Chem. Eng. Prog. 52(9), p. 353-9, 1956.

122. CRONAN, C.S., Ion exchange runs continuously, Chem. Eng. p. 184-5, July, 1957.

123. ROBERTS, J.T., Developments in continuous ion exchange equipment for AEC application, ORNL-2504, 1958.

124. ASAHI CO., Brit. Patent 1,062,943, 1962.

125. LEVENDUSKY, J.A., LIMON, L., and RYAN, L.F., An innovation in ion exchange, Ind. Water. Eng. 2(38), p. 11-15, 1965.

126. BOUCHARD, J., Development of the Degremont-Asahi continuous ion exchange process, Soc. Chem. Ind. London, p. 91-7, 1970.

127. SOLT, G.S., New techniques for carrying out ion exchange processes, Soc. Chem. Ind. London, p. 85-9, 1970.

128. GOLD. H., and SONIN, A.A., Design consideration for a truly continuous moving-bed ion exchange process, AIChE. Symp. Ser. 71(152), p. 48-57, 1975.

129. CLOETE, F.L.D., STREAT, M., and MILLER, A.I., A new solids-fluid contacting techniques, AIChE-IChemE. Symp. Ser.(1), p. 54-9, 1965.

130. CLOETE, F.L.D., and STREAT, M., Brit. Patent 1,070,251, 1967.

131. STEVENSON, D.G., Development of a continuous ion exchange process, Soc. Chem. Ind. London, p. 114-20, 1970.

132. HENDRIKSZ, A.R., Modifications to the conventional NIMCIX system for different industrial applications, Proc. of Hydrometallurgy, 81, U.M.1.S.T, U.K., Soc. Chem. Ind. Symp., p.-E 2/1-E2/9, 1981.

133. HIMSLEY, A., Performance of Himsley continuous ion exchange system, ibid. p. E 3/1-E3/14

134. PORTER, R.R., U.S. Patent 2,973,319, 1961.

135. SLATER, M.J., LUCAS, B.H., LAKSHMANAN, V.I., and JOHNCOX, B.A., Uranium recovery from minewater using a continuous fluidized bed ion exchange system, Soc. Chem. Ind. Symp. Oslo, p. IV/27-IV/40, 1982.

136. LUCAS, B.H., Separation processes by single-stage deep fluidized bed continuous ion exchange, Canada cent. miner. energy technol. Ottawa, CIM Bull., 73, p. 195-200, 1980.

137. GEORGE, D.R., ROSS, J.R., and PRATER, J.D., Byproduct uranium recovered with new ion-exchange techniques, Mining Engng., 20(1) p. 73-7, 1968.

138. RITCEY, G.M., SLATER, M.J., and LUCAS, B.H., A comparison of the processing and economics of uranium recovery from leach slurries by continuous ion exchange or solvent extraction, Int. Symp. Hydrometallurgy. AIMME, Chicago, p. 419-74, 1973.

139. SLATER, M., Continuous ion exchange in fluidized beds, Can. J. Chem. Eng. 52(2), p. 43-51, 1974.

140. WEISS, D.E. and SWINTON, E.A., U.S. Patent 2,742,381, 1956.

141. ARDEN, T., Brit. Patent 904,184, 1958.

142. GRIMMETT, E.S., Physical and operational features of a pulsed, continuous countercurrent liquid-solid contactor, U.S. At. Energy-Comm. IDO - 14541, 1961.

143. BARNEBL, A.C., and RIKER, W.J., U.S. Patent 2,595,627, 1952.

144. PORTER, R., and ARDEN, T., Brit. Patent 835,568, 1957.

145. COLLIER, D., U.S. Patent 2,563,006, 1951.

146. HIESTER, N.K., PHILLIPS, R.C., and FIELDS, E.F., Continuous separations of ions by countercurrent ion exchange, Stanford Research Institute, U.S.A.E.C., COO-59, 1952.

147. HIESTER, N.K., PHILLIPS, R.C., and FIELDS, E.F., ibid, COO-41, REV (1951).

148. HIESTER, N.K., FIELDS, E.F., PHILLIPS, R.C., RADDING, S.B., Continuous countercurrent ion exchange with trace components Chem. Eng. Prog. 50(14) p. 139-50, 1954.

149. PERMUTIT AKT-GES, Ger. Patent 1,051,808, 1959 Chem. Abstr. P24152 e, 61, 1961.

150. BADDOUR, R.F., U.S. Patent 3,002,922, 1962.

151. LOMONOSOV, M.V., Fr. Patent 1,436,296, 1966 Chem. Abstr. P12283 V, 66, 1967.

152. SCHUETZE, H., and WETZEL, K., New process for continuous mass separation by solid-liquid countercurrent exchange, Chem. Tech. (Berlin), 19(3), p. 175-8, 1967, Chem. Abstr, 13255V, 67, 1967.

153. JAPAN ORGANO CO., LTD., Japan Patent 15,680(60), 1960, Chem. Abstr. 11407 e, 56, 1962.

154. YOKOZEKI, Z., et.al., Fr. Patent 1,507,717, 1967, Chem. Abstr. B59209 Y, 70, 1969.

155. BACHELART, A., Fr. Patent 1,547,468, 1968, Chem. Abstr. 95324m, 71, 1969.

156. FEDULOV, YU.N., ALEKSEEVA, V.V., VODOLAZOV, L.I., and LASKONIN, B.N., Tsvetl. Metal (USSR). 43(2), p. 49-51, 1970, Chem. Abstr. 113101 P, 72, 1970.

157. GOETZMANN, K., Ger. Patent 1,303,056, 1971, Chem. Abstr. 89484 e, 75, 1971.

158. SHAH, K., LELE, P.S., and WILKINSON, W.L., Ion exchange in continuous liquid fluidized beds, Chem. Age. India, 26(1), p. 9-17, 1975.

159. ARION, N.M., Belg. Patent 818,559, 1974, Chem. Abstr. 133985 k, 83, 1975.

160. BROUGHTON, D.B., NEUZIL, R.W., PHARIS, J.M., and BREARLEY, The Parex process for recovering paraxylene, Chem. Eng. Prog. 66(9), p. 70-5, 1970.

161. GONDO, S., Concentration distribution and its numerical calculation in semi-continuous countercurrent operation of ion exchange moving bed, Mem. Fac. Eng. Kyushu University Japan, 2, p. 103-19, 1967.

162. HIESTER, N.K., COHEN, R.K., and PHILLIPS, R.C., Engineering and economic evaluation of moving and fixed bed ion exchange processes, Chem. Eng. Prog. Symp. Ser. 50(14), p.23-42, 1954.

163. ROHM AND HAAS, Amberlite ion exchange resins: Summary chart of properties and applications.

164. ROHM AND HAAS, Amberlite IRC-718, 1979.

165. KUNIN, R., Ion exchange resins, Krieger publishing Co., Huntington, New York, 1972.

166. PERRY, R.H., and CHILTON, C.H., Chemical Engineer's Handbook, fifth edition, McGraw-Hill, 1973.

167. WEAST, R.C., Handbook of Chemistry and Physics, 61st. edition, CRC Press 1980-81.

168. INSTRUCTION MANUAL OF HAAKE VISCOMETER

169. INCZEDY, J., Analytical applications of ion exchangers, Pergamon, London, 1970.

170. VOGEL'S, Textbook of quantitative inorganic analysis, fourth edition, Longman, 1978.

171. VARIAN TECHTRON-Manual, Analytical Methods for Flame Spectroscopy.

172. COLBURN, A.P., A method of correlating forced convection heat transfer data and a comparison with fluid friction, Trans. Am. Inst. Chem. Engrs., 29, p. 174-210, 1933.

173. SELKE, W.A., and BLISS, H., Continuous countercurrent ion exchange, Chem. Eng. Prog. 47(10), 529-33, 1951.

174. CLARK, J.A., The recovery of valuable vapor phase solvent using activated charcoal cloth, Ph.D. thesis, University of Aston, 1983.

A P P E N D I X I

EXPERIMENTAL DATA

TABLE I.1 Effect of caustic concentration on isotherms (Data for Figure 12.)

Weight of resin g	Equilibrium Concentration of Zn in solution ppm	Concentration of Zn on resin ppm	$x=\frac{gZn}{g\ solution}$ x 10^{-6}	$y=\frac{gZn}{g\ resin}$ x 10^{-4}
Run No. 6.1, NaOH = 0.1 M				
0.06585	37.5	1750	37.5	265.76
0.20491	20.0	3500	20.0	170.81
0.35524	10.0	4500	10.0	126.67
0.61750	2.5	5250	2.5	85.02
0.72300	1.2	5380	1.2	74.41
1.17228	0.0	5500	0.0	46.92
1.69686	0.0	5500	0.0	32.41
2.02043	0.0	5500	0.0	27.22
Run No. 6.2, NaOH = 0.2 M				
0.15089	35.0	2000	35.0	132.55
0.37196	19.0	3600	19.0	96.78
0.59565	10.0	4500	10.0	75.55
0.86431	5.0	5000	5.0	57.85
0.94967	2.0	5300	2.0	55.81
1.42935	0.0	5500	0.0	38.48
1.79678	0.0	5500	0.0	30.61
2.41385	0.0	5500	0.0	22.79
Run No. 6.3, NaOH = 0.5 M				
0.06080	46.0	900	46.0	148.03
0.17340	42.5	1250	42.5	72.09
0.37546	39.0	1600	39.0	42.61
0.51985	39.0	1600	39.0	30.78
0.71100	36.0	1900	36.0	26.72
1.08870	29.0	2600	29.0	23.88
1.91818	22.0	3300	22.0	17.20
Run No. 6.4, NaOH = 1 M				
0.08886	47.5	750	47.5	84.40
0.30926	46.0	900	46.0	29.10
0.48114	46.0	900	46.0	18.71
0.58337	45.0	1000	45.0	17.14
0.69131	45.0	1000	45.0	14.47
0.88439	45.0	1000	45.0	11.31
1.02920	45.0	1000	45.0	9.72
1.95782	42.0	1300	42.0	6.64

HCl	M	1.04	1.04	1.04	1.07	1.07	2	2	2	4	4
BV	ml	20	20	20	20	20	20	20	20	30	30
f	BV/hour	2.38	2.64	3.02	2.07	1.70	2.25	2.33	3.21	2.05	0.82
d_p	mm	0.655	0.550	0.855	0.521	0.521	0.55	0.521	0.855	0.521	0.521
Time (hours)				PPM	Zinc	in	Column	Effluent			
0.25	0	0	400	0	27		-	-	-	-	-
0.50	-	-	-	-	-		4203	3297	2391	9819	2573
1.00	3122	3054	2700	-	-		1123	4022	942	11993	2754
1.50	-	-	-	2600	933		761	1486	942	4203	2029
2.00	1600	850	1502	2700	3349		652	507	580	3116	2101
2.50	-	-	-	633	985		616	290	399	652	2029
3.00	366	415	450	266	600		236	290	200	468	1707
3.50	-	-	-	266	400		207	243	178	346	1163
4.00	272	-	245	204	264		196	214	160		1073
4.50	-	-	-	180	220		-	-	-		-
5.00	208	261	175				178	171	134		837
6.00	158	208	138				182	142			728
7.00	88	170	56								
8.00	60	88	33								
9.00	45	57	25								
10.00	36	38	20								

Loading cycles : C_o = 55 ppm, NaOH = 0.1M

TABLE 1.3 Amberlite IRC-718 conversion-Experimental conditions and titration results.

Run No		4.1	4.2	4.3	4.4	4.5	4.6	4.7	4.8	4.9	4.10
NaOH	M	0.9	0.9	0.9	0.1	1.0	1.0	1.0	0.9	1.0	1.0
h	cm	6	6	6	6	6	6	6	9	9	9
f	ml/min	0.37	0.93	0.43	1.82	1.31	1.73	1.02	1.18	0.89	1.43
d_p	mm	0.521	0.550	0.650	0.855	0.550	0.521	0.855	0.521	0.521	0.521
HCl	M	0.107	0.107	0.107	0.107	0.1	0.1	0.1	0.107	0.1	0.1
Time	hrs.	Volume of HCl used in the titrations (mls)									
0.50		3.80	4.80	2.00	0	5.70	7.60	8.70	0.80	3.40	2.90
1.00		3.85	7.10	5.10	0	9.70	9.90	9.60	3.40	7.80	9.80
1.50		-	-	-	0	9.80	10.00	9.80	-	9.30	10.00
1.75		-	-	-	0.20	9.90	10.00	-	-	-	-
2.00		5.40	8.40	5.90	4.75			10.00	8.30	9.60	10.00
2.50		6.10	8.40	6.40	5.50				8.35		
3.00		6.60	8.30	7.10	7.60				8.25		
3.50		6.80		7.50	8,65						
4.00		7.25		7.80	8.90						
4.50		7.65		7.95	9.05						
5.00		7.70		8.00	9.10						
6.00		8.00		8.35							

TABLE 1.4 Breakthrough data

TABLE 1.4a1 Effect of bed height, C_o = 55ppm., 0.1M NaOH.

h, cm	4.5	5.1	6.0	6.9	9.0
f, ml/min	3.65	3.05	3.53	3.05	3.20
Run No / t(hrs)	2.3	2.15	2.1	2.16	2.2
0.5	0.018	0.000	0.000	0.000	0.000
1.0	0.000	0.000	0.000	0.000	0.000
2.0	0.082	0.000	0.000	0.000	0.058
4.0	0.210	0.000	0.000	0.000	0.032
6.0	0.295	0.000	0.045	0.000	0.000
8.0	0.340	0.000	0.068	0.000	0.000
9.0	0.361	0.068	0.164	0.000	0.000
11.0	0.372	0.205	0.216	0.045	0.000
13.0	0.386	0.318	0.318	0.051	0.000
16.0	0.545	0.341	0.432	0.145	0.018
18.0	0.568	0.362	0.500	0.186	0.018
21.0	0.750	0.523	0.520	0.409	0.082
23.0	0.773	0.547	0.727	0.322	0.182
25.0	0.750	0.591	0.727	0.436	0.182
27.0	0.864	0.682	0.727	0.545	0.227
29.0	0.886	0.750	0.795	0.591	0.300
31.0	0.864	0.800	0.886	0.682	0.284
33.0	0.909	0.818	0.909	0.727	0.386
36.0	0.977	0.855	0.909	0.693	0.500
38.0	0.909	0.891	0.909	0.727	0.477
40.0	0.909	0.891	0.909	0.750	0.591
42.0	0.977	0.923	0.909	0.750	0.659
45.0		0.891		0.750	0.667
58.0					0.795
61.0					0.818
63.0					0.795
67.0					0.773

TABLE 1.4 a2 Effect of bed height

C_o = 275ppm., NaOH = 0.2 M

h , cm.	4.5	5.4	6.9	8.4	9.9
f ,ml/min	2.97	2.89	2.87	2.77	2.97
t(hrs) Run No	2.44	2.45	2.46	2.47	2.48
0.25	0.095	0.145	0.073	0.082	0.000
0.50	0.095	0.182	0.145	0.118	0.000
1.00	0.109	0.059	0.109	0.045	0.004
2.00	0.227	0.182	0.082	0.055	0.004
3.00	0.555	0.573	0.227	0.036	0.027
4.00	0.800	0.664	0.400	0.182	0.113
5.00	0.936	0.800	0.627	0.318	0.227
6.00	0.909	0.836	0.727	0.518	0.400
7.50	0.945	0.991	0.909	0.745	0.664
10.50	0.909	1.000	1.000	0.991	1.000
12.50	0.908	0.936	0.964	0.991	1.000
15.00	0.936	1.000	1.000	1.000	1.000

TABLE 1.4a3 Effect of bed height.

C_o = 550 ppm , NaOH = 0.2 M

h cm	4.5	5.4	6.9	9.9	22.5
f ml/min	2.90	2.83	2.70	2.89	2.99
t(hrs) Run No	2.73	2.74	2.75	2.77	2.19
0.25	0.060	0.106	0.000	-	-
0.50	0.060	0.088	0.197	0.000	0.000
0.75	0.115	0.060	0.042	-	-
1.00	0.297	0.069	0.297	0.000	0.000
1.25	0.434	0.389	0.024	-	-
1.50	0.380	0.380	0.224	0.000	-
1.75	0.489	0.398	0.115	0.000	-
2.00	0.763	0.580	0.243	-	0.000
2.25	0.881	0.735	0.325	-	-
2.50	0.890	0.708	0.453	0.060	-
2.75	1.000	0.982	0.562	-	-
3.00	1.000	1.000	0.772	0.279	-
4.00			0.735	0.599	0.000
5.00			1.000	0.973	-
5.50				0.982	0.000
6.00				1.000	-
6.50					0.020
8.50					0.510
10.50					0.630
12.50					0.750
13.50					0.870
14.50					0.947
16.50					0.960
18.50					0.970

TABLE 1.4b1 Effect of flow rate

C_o = 55ppm , NaOH = 0.1 M, h = 9cm.

f , ml/min	4.90	6.16	8.26
t(hrs) Run No	2.5	2.17	2.18
0.5	0.000	0.000	0.000
1.0	0.000	0.000	0.000
2.0	0.000	0.000	0.000
3.0	0.000	0.000	0.000
4.0	0.000	0.000	0.000
5.0	0.000	0.000	0.000
6.0	0.000	0.000	0.045
7.0	0.000	0.000	0.091
9.0	0.000	0.000	0.342
11.0	0.068	0.091	0.614
12.0	0.092	0.045	0.342
14.0	0.250	0.145	0.386
16.0	0.400	0.309	0.591
18.0	0.432	0.385	0.591
20.0	0.432	0.482	0.659
22.0	0.573	0.727	0.818
24.0	0.591	0.750	0.845
26.0	0.545	0.750	0.845
28.0	0.682	0.818	0.818
20.0	0.724	0.845	0.909
31.0	0.773	0.936	0.909
32.0	0.800	0.800	0.845
34.0	0.850	0.845	0.845
36.0	0.886	0.891	0.845
38.0	0.886	0.891	0.909

TABLE 14 b2 Effect of flow rate

C_o = 368.5ppm , NaOH = 0.2 M, h = 15cm.

f , ml/min	1.88	3.12	5.30	8.11	11.42	14.28	20.89
t(hrs) Run No	2.29	2.31	2.33	2.24	2.25	2.26	2.28
0.25	0.000	0.000	0.000	0.107	0.150	0.183	0.269
0.50	0.000	0.000	0.000	0.107	0.172	0.204	0.332
1.00	0.000	0.000	0.000	0.269	0.376	0.462	0.720
1.50	0.000	0.000	0.000	0.376	0.591	0.763	0.763
2.00	0.000	0.000	0.102	0.581	0.613	0.796	0.806
2.50	0.000	0.000	0.160	0.624	0.720	0.806	0.806
3.00	0.000	0.000	0.280	0.656	0.806	0.882	0.914
3.50	0.000	0.000	0.408	0.763	0.860	0.871	0.978
4.00	0.000	0.000	0.534	0.806	0.871	0.914	0.989
4.50	0.000	0.000	0.621	0.871	0.925	0.936	
5.00	0.000	0.068	0.753	0.934	1.000		
6.50	0.000	0.237	0.848				
8.50	0.076	0.704	0.899				
10.50	0.339	0.873	0.933				
13.00	0.789	0.848	0.899				
18.00	1.000	0.814					

TABLE 1.4c Effect of initial zinc ion concentration. NaOH = 0.2 M, h = 4.5cm.

C_o , ppm	550	500.5	451	401.5	352
f , ml/min	2.39	2.45	2.27	2.34	2.44
t(mins) Run No	2.49	2.50	2.51	2.52	2.53
10	0.010	0.011	0.025	0.112	0.032
20	0.044	0.067	0.067	0.084	0.158
40	0.027	0.011	0.025	0.061	0.112
60	0.157	0.030	0.133	0.098	0.158
80	0.252	0.150	0.154	0.271	0.112
100	0.450	0.312	0.274	0.364	0.213
120	0.709	0.412	0.474	0.308	0.330
140	0.695	0.527	0.702	0.504	0.443
160	0.818	0.527	0.612	0.486	0.618
180	0.818	0.862	0.823	0.616	0.650
210	1.000	0.974	0.823	0.831	0.763
300	1.000	1.000	0.890	0.906	1.000

TABLE 1.4d Effect of initial lead ion concentration

C_o = 483ppm , NaOH = 0.4 M , h = 4.5cm.

Pb concen.,ppm.	75	169	300	394	694	75	169	300	394	694
f , ml/min.	2.35	2.04	2.03	2.30	2.24	2.35	2.04	2.03	2.30	2.24
t(mins) Run No	2.82	2.79	2.78	2.80	2.81	2.82	2.79	2.78	2.80	2.81
Metal			Zinc					Lead		
15	0.425	0.257	0.163	0.257	0.236	0.075	0.033	0.013	0.014	0.011
30	0.216	0.310	0.289	0.195	0.299	0.050	0.033	0.013	0.024	0.162
45	0.550	0.519	0.268	0.362	0.446	0.200	0.067	0.038	0.124	0.284
60	0.320	0.362	0.414	0.519	0.519	0.100	0.111	0.113	0.281	0.397
75	0.498	0.561	0.456	0.644	0.728	0.275	0.244	0.225	0.457	0.703
90	0.624	0.770	0.644	0.676	0.781	0.325	0.367	0.338	0.619	0.865
105	0.770	0.770	0.613	0.812	0.833	0.450	0.500	0.488	0.729	0.973
120	0.728	0.822	0.822	0.749	0.791	0.575	0.589	0.625	0.905	1.000
135	0.895	0.875	0.770	0.875	0.948	0.750	0.689	0.763	0.905	1.000
150	0.979	0.885	1.000	0.927	0.937	0.800	0.789	0.869	1.000	1.000
165	0.854	0.948	0.979	0.948	1.000	0.875	0.844	0.931	1.000	1.000
240	1.000	0.979	0.937	0.895	1.000	1.000	0.922	1.000	1.000	1.000

TABLE 1.4e Effect of caustic concentration.

C_o = 412.5ppm , h = 15cm.

NaOH Concen., M	0.3	0.35	0.4	0.45	0.5
f , ml/min	2.82	2.93	2.84	2.87	3.10
t(hrs) Run No	2.34	2.35	2.36	2.37	2.38
0.25	0.000	0.000	0.000	0.121	0.121
0.50	0.227	0.000	0.151	0.030	0.000
1.50	0.303	0.000	0.227	0.061	0.545
3.50	0.212	0.258	0.576	0.706	0.909
5.50	0.485	0.864	0.970	0.947	1.000
7.00	0.864	0.927	0.970	0.970	0.992
8.50	1.000	1.000	1.000	1.000	1.000
10.50	0.970	1.000	1.000	0.947	1.000
12.50	0.927	0.970	1.000	1.000	0.970
13.50	0.970	1.000	0.992	0.927	1.000
15.00	1.000	1.000	0.992	0.927	1.000
16.00	0.970	1.000	1.000	1.000	0.947

TABLE 1.4f Effect of resin particle size.

	NaOH = 0.1 M				NaOH = 0.2 M			
Particle size,mm.	0.5-0.6	0.6-0.7	0.71-1.0		0.3-0.5	0.5-0.6	0.6-0.7	0.71-1.0
Bed height, cm.	6	6	6		4.5	4.5	4.5	4.5
Flow rate,ml/min	4.54	4.59	5.05		2.66	2.76	2.52	2.86
C_o , ppm	55	55	55		550	550	550	550
t(hrs) Run No	2.6	2.7	2.8	Run No t(mins)	2.54	2.55	2.56	2.57
1	0.125	0.125	0.091	10	0.116	0.010	0.044	0.082
2	0.125	0.155	0.155	20	0.252	0.082	0.181	0.252
4	0.125	0.155	0.245	40	0.273	0.211	0.245	0.355
6	0.200	0.218	0.309	60	0.467	0.409	0.344	0.488
8	0.159	0.200	0.327	80	0.607	0.597	0.566	0.648
10	0.345	0.345	0.455	100	0.920	0.764	0.709	0.675
13	0.545	0.500	0.591	120	0.968	0.982	0.729	0.818
16	0.636	0.545	0.659	140	0.989	0.989	0.784	0.784
19	0.773	0.682	0.727	160	1.000	1.000	0.989	1.000
20	0.773	0.705	0.750	180	1.000	1.000	1.000	1.000
23	0.841	0.750	0.795	210	1.000	1.000	1.000	1.000
26	0.891	0.818	0.841	240	1.000	1.000	1.000	1.000

TABLE 1.4g Effect of temperature.

h = 2.8cm., C_o = 550ppm., NaOH = 0.2 M.

Temperature, ^oC	24	31.5	41	50
f ml/min	2.22	2.09	2.12	2.10
t(mins) Run No	2.63	2.60	2.61	2.62
10	0.017	0	0	0
20	0.017	0	0.034	0
40	0.027	0	0.044	0
60	0.153	0.017	0.027	0
80	0.126	0.061	0.027	0
100	0.266	0.126	0.089	0
120	0.470	0.225	0.198	0.283
150	0.576	0.545	0.539	0.170
180	1.000	0.624	0.641	0.324
200	1.000	0.675	0.702	0.395
220	1.000	0.886	0.750	0.729
240	1.000	0.886	0.852	0.989
270	1.000	0.886	0.859	0.859
300	1.000	0.971	0.948	1.000
330	1.000	0.955	1.000	0.995

TABLE 1.5 Moving bed

TABLE 1.5.1 Effect of caustic concentration

C_o = 55 ppm.

NaOH	M	0.1	0.2
h	cm	12	8
R_F	ml/min	19.45	18.50
R_p	ml/min	0.102	0.184
No of cycles		6	5

Run No		5.1		5.2	
t(mins)	C/C_o	t(mins)	C/C_o	t(mins)	C/C_o
15	0.0045	600	0.0855	15	0.1073
30	0.0054	630	0.1200	30	0.1473
45	0.0054	645	0.0291	45	0.2055
60	0.0054	660	0.0436	60	0.2691
90	0.0045	675	0.0600	90	0.3509
120	0.0118	690	0.0691	120	0.4255
150	0.0145	720	0.1145	150	0.5127
180	0.0236	760	0.2090	180	0.5400
210	0.0127	775	0.0545	195	0.3568
240	0.0291	790	0.0655	210	0.4000
270	0.0609	820	0.1291	225	0.4391
300	0.1155	865	0.1782	240	0.3255
330	0.1318	880	0.0873	255	0.4145
360	0.1564	895	0.1036	270	0.4445
390	0.1582	910	0.1236	285	0.4909
420	0.1945	925	0.1545	300	0.4009
450	0.1873	940	0.0873	315	0.4609
480	0.2491	955	0.1036	330	0.3255
510	0.2182	970	0.1273	345	0.4064
525	0.0164	985	0.1309	360	0.4364
540	0.0218				
555	0.0327				
570	0.0473				

TABLE 1.5.2 Influence of solution flow rate

h = 8cm, C_o = 550ppm, NaOH = 0.2M

R_F	ml/min	3.67	3.19	3.62	5.55	7.05
R_p	ml/min	0.26	0.27	0.30	0.29	0.30
	Run No	5.3	5.4	5.5	5.6	5.7
Cycle	t(mins)					
	10	0.0055	0.0683	0.0655	0.0373	0.0445
	20	0.0436	0.0855	0.0791	0.0318	0.0382
1	30	0.0436	0.0600	0.0755	0.0291	0.0564
	40	0.0409	0.0491	0.0573	0.0364	0.1155
	70	0.0518	0.0718	0.0800	0.0964	0.1909
	80	0.0373	0.0364	0.0336	0.0200	0.1155
2	90	0.0809	0.0509	0.0591	0.0455	0.1727
	100	0.0736	0.0482	0.0509	0.0655	0.2000
	110	0.0382	0.0664	0.0691	0.0300	0.0782
3	120	0.0800	0.0764	0.0836	0.0555	0.1682
	130	0.0673	0.0800	0.0555	0.0764	0.1955
	140	0.0382	0.0373	0.0327	0.0091	0.0700
4	150	0.0600	0.0591	0.0673	0.0618	0.0964
	160	0.0600	0.0800	0.0609	0.0700	0.1429
	170	0.0355	0.0655	0.0318	0.0382	0.0318
5	180	0.0582	0.0527	0.0555	0.0573	0.0273
	190	0.0582	0.0518	0.0527	0.0891	0.0300

TABLE 1.5.3 Effect of bed height

C_o = 550 ppm, NaOH = 0.2M

h	cm	12	16	20	24	24
R_F	ml/min	6.90	7.03	7.00	7.02	9.14
R_p	ml/min	0.298	0.297	0.292	0.294	0.295
	Run No	5.8	5.9	5.10	5.11	5.18
Cycle	t(mins)					
	10	0.0273	0.0218	0.0189	0.0015	0.0131
	20	0.0391	0.0284	0.0225	0.0095	0.0256
1	30	0.0364	0.0204	0.0182	0.0073	0.0188
	40	0.0345	0.0255	0.0182	0.0051	0.0248
	70	0.0373	0.0175	0.0160	0.0029	0.0239
	80	0.0336	0.0145	0.0138	0.0131	0.0130
2	90	0.0236	0.0182	0.0124	0.0015	0.0153
	100	0.0264	0.0058	0.0036	0.0138	0.0208
	110	0.0327	0.0153	0.0007	0.0015	0.0129
3	120	0.0273	0.0196	0.0116	0.0022	0.0147
	130	0.0355	0.0204	0.0160	0.0029	0.0233
	140	0.0200	0.0138	0.0138	0.0015	0.0221
4	150	0.0691	0.0196	0.0182	0.0022	0.0139
	160	0.0727	0.0211	0.0182	0.0029	0.0148
	170	0.0327	0.0138	0.0015	0.0007	0.0129
5	180	0.0491	0.0233	0.0065	0.0022	0.0155
	190	0.0745	0.0240	0.0095	0.0022	0.0270

TABLE 1.5.3 Continued

C_o=550ppm, NaOH=0.2M

Bed height	cm.	24	30
Solution flow rate	ml/min.	7.05	7.09
Resin flow rate	ml/min.	0.083	0.083
	Run No	5.22	5.25
Cycle	t(mins)		
	15	0.0136	0.0016
	30	0.0264	0.0164
1	45	0.0173	-
	60	0.0145	0.0037
	90	0.0082	0.0027
	120	0.0064	0.0053
	135	0.0082	0.0045
	150	0.0091	0.0065
2	165	0.0073	-
	180	0.0445	0.0057
	210	0.0545	0.0055
	240	0.0882	0.0053
	255	0.0445	0.0050
	270	0.0836	0.0061
3	300	0.1364	0.0028
	330	0.2300	0.0080
	360	0.2850	0.0265

TABLE 1.5.4 Influence of initial zinc ion concentration

h=20cm., R_p=0.133ml/min.

C_o	ppm	275	330	412.5	550
R_F	ml/min	9.94	9.97	10.6	10.19
	Run No	5.15	5.16	5.17	5.13
Cycle	t(mins)				
	15	0.0487	0.0182	0.0315	0.0755
	30	0.0487	0.0164	0.0174	0.0327
1	60	0.0233	0.0152	0.0150	0.0309
	90	0.0211	0.0182	0.0174	0.0500
	120	0.0262	0.0254	0.0339	0.2727
	150	0.0189	0.0558	0.0674	0.3273
	165	0.0182	0.0230	0.0373	0.1318
2	180	0.0211	0.0406	0.1891	0.3182
	210	0.0218	0.0836	0.2085	0.3727
	225	0.0204	0.0376	0.0528	0.2818
3	240	0.0204	0.0685	0.1939	0.3636
	270	0.0269	0.2303	0.2424	0.4545

TABLE 1.5.4 Continued

h=24cm., R_p=0.100 ml/min.

C_o	ppm	412.5	495	550
R_F	ml/min	7.07	7.00	7.11
	Run No	5.23	5.24	5.21
Cycle	t(mins)			
	15	0.0026	0.0017	0.0118
	30	0.0152	0.0055	0.0127
1	45	0.0085	0.0036	0.0118
	60	0.0064	0.0030	0.0109
	75	0.0053	0.0027	0.0109
	100	0.0039	0.0025	0.0100
	115	0.0015	0.0012	0.0091
	130	0.0040	0.0027	0.0118
2	145	0.0033	0.0024	0.0100
	160	0.0030	0.0033	0.0109
	175	0.0025	0.0022	0.0127
	200	0.0024	0.0024	0.0245
	215	0.0016	0.0012	0.0036
	230	0.0025	0.0032	0.0236
3	245	0.0024	0.0039	0.0273
	275	0.0032	0.0112	0.0682
	300	0.0048	0.0282	0.1218

TABLE 1.5.5 Influence of resin flow rate

h=20cm, C_o=550ppm, NaOH=0.2M.

R_p	ml/min	0.328		0.130	
R_F	ml/min	10.19		10.19	
Run No		5.12		5.14	
Cycle	t(mins)	C/C_o	Cycle	t(mins)	C/C_o
	15	0.1236		15	0.0782
	30	0.0400		30	0.0327
1	60	0.0264		60	0.0300
	90	0.0236	1	90	0.0555
	120	0.0309		120	0.1291
	150	0.1027		150	0.3182
				180	0.3727
	165	0.0345			
2	180	0.0418		195	0.1345
	210	0.3000	2	210	0.3364
				240	0.4364
	225	0.0436			
3	240	0.1000	3	260	0.4091
	270	0.3545		290	0.4364
	285	0.0482			
4	300	0.1300			
	330	0.3364			
	345	0.0936			
5	360	0.3273			
	390	0.4182			
	405	0.0545			
6	420	0.2727			
	450	0.3455			

TABLE 1.5.5 Continued

h=24cm, C_o=550ppm, NaOH=0.2M

R_p	ml/min	0.188		0.088	
R_F	ml/min	7.11		6.85	
Run No		5.19		5.20	
Cycle	t(mins)	C/C_o	Cycle	t(mins)	C/C_o
	20	0.0235		15	0.0218
	30	0.0244		30	0.0229
1	60	0.0229	1	45	0.0237
	90	0.0228		75	0.0232
	120	0.0216		100	0.0228
	135	0.0151		115	0.0217
2	150	0.0226	2	130	0.0228
	165	0.0225		150	0.0223
	180	0.0214		165	0.0215
3	195	0.0221	3	180	0.0223
	210	0.0226		200	0.0239
	225	0.0213		215	0.0215
4	240	0.0228	4	230	0.0249
	255	0.0234		250	0.0437

TABLE 1.5.6 Influence of resin renewal

C_o = 550ppm, NaOH = 0.2M

Volume renewed	ml	20	10		5	
R_p	ml/min	0.328	0.133		0.088	
R_F	ml/min	10.19	10.19		6.85	
h	cm	20	20		24	
Run No		5.12	5.13		5.20	
Cycle	t(mins)	C/C_o	C/C_o	Cycle	t(mins)	C/C_o
	15	0.1236	0.0755		15	0.0218
	30	0.0400	0.0327		30	0.0229
1	60	0.0264	0.0309	1	45	0.0237
	90	0.0236	0.0500		75	0.0232
	120	0.0309	0.2727		100	0.0228
	150	0.1027	0.3273			
	165	0.0345	0.1318		115	0.0217
2	180	0.0418	0.3182	2	130	0.0228
	210	0.3000	0.3727		150	0.0223
	225	0.0436	0.2818		165	0.0215
3	240	0.1000	0.3636	3	180	0.0223
	270	0.3545	0.4545		200	0.0239
	285	0.0482			215	0.0215
4	300	0.1300		4	230	0.0249
	330	0.3364			250	0.0439
	345	0.0936				
5	360	0.3273				
	390	0.4182				
	405	0.0545				
6	420	0.2727				
	450	0.3455				

TABLE 1.6 Equivalent fractions of zinc in exit resin

Run No. \ Cycle	1	2	3	4	5	6
5.1	0.2564	0.2294	0.2373	0.2888	0.2963	-
5.2	0.1966	0.1869	0.2446	0.1699	-	
5.3	0.2463	0.2428	0.2159	0.2124	-	
5.4	0.1784	0.2621	0.2217	0.1529	-	
5.5	0.2548	0.2209	0.2650	-	-	
5.6	0.2433	0.2656	0.2393	0.2676	-	
5.7	0.2523	0.2905	0.2780	0.2829	-	
5.8	0.2711	0.2905	0.3135	0.3135	-	
5.9	0.2817	0.3422	0.3364	0.3364	-	
5.10	0.2905	0.4047	0.2612	-	-	
5.11	0.3957	0.2985	0.3287	-	-	
5.12	0.3096	0.3096	0.3364	0.3364	0.3007	-
5.13	0.3364	0.3670	-			
5.14	0.3287	0.3364	-			
5.15	0.2752	0.2829	-			
5.16	0.2905	0.2905	-			
5.17	0.3058	0.3287	-			
5.18	0.3287	0.2982	0.3135	0.3364	-	
5.19	0.3364	0.3440	0.3364	-		
5.20	0.3517	0.3976	0.3976	-		
5.21	0.3364	0.3593	0.1930			
5.22	0.3517	0.3823	0.1937			
5.23	0.3211	0.3287	0.1376			
5.24	0.3364	0.3670	0.0937			
5.25	0.4969	0.2523	0.1764			

- Sodium chloride interference

A P P E N D I X II A

Analysis through the New method

TABLE A1 Effect of bed height

h	f	β	t_m	t_o	$Ka_x \times 10^{-2}$	Ka_y	N_z	h_{z4}	u_{z3}
4.5	2.90	1.96	1.43	0.2	7.31	1.38	1.14	3.95	2.76
5.4	2.83	2.85	1.74	0.3	8.66	1.63	1.17	4.61	2.64
6.0	3.15	2.65	2.01	0.4	7.01	1.32	1.20	5.00	2.49
6.9	2.70	3.45	2.35	0.5	7.81	1.47	1.21	5.69	2.42
7.5	2.83	2.48	2.34	0.6	5.63	1.06	1.26	5.95	2.54
8.4	3.09	2.28	2.27	0.8	5.31	1.00	1.35	6.22	2.74
9.0	3.23	2.32	2.04	1.0	6.06	1.14	1.49	6.04	2.96
9.9	2.89	2.81	2.54	1.5	5.88	1.11	1.59	6.22	2.45
10.5	2.90	2.57	2.36	1.7	5.79	1.09	1.72	6.10	2.59
22.5	2.98	2.20	6.03	5.0	1.91	0.36	1.83	12.30	2.04

C_o = 550ppm (8.41×10^{-6}mol/cc), q_o = 2.355×10^{-4}mol/g, NaOH = 0.2M

TABLE A1 Continued

h	f	β	t_m	t_o	$Ka_x \times 10^{-2}$	Ka_y	N_z	h_{z4}	u_{z3}
4.5	2.97	2.21	2.86	0.40	2.62	0.77	1.14	3.95	1.38
5.4	2.89	1.89	3.55	0.45	1.81	0.53	1.13	4.79	1.35
6.9	2.87	1.97	4.47	0.70	1.50	0.44	1.31	5.25	1.18
8.4	2.77	2.14	5.10	1.50	1.43	0.42	1.29	6.51	1.28
9.9	2.97	2.46	5.36	1.90	1.57	0.46	1.36	7.31	1.36
C_o = 275ppm (4.205×10^{-6} mol/cc), $q_o = 1.835 \times 10^{-4}$ mol/g, NaOH = 0.2M									
4.5	3.65	1.52	15.20	3	0.152	0.100	1.20	3.75	0.25
5.1	3.05	1.60	20.17	4	0.120	0.079	1.20	4.26	0.21
6.0	3.53	1.49	14.74	6	0.153	0.101	1.41	4.26	0.29
6.9	3.05	1.94	22.00	8	0.134	0.088	1.36	5.06	0.23
9.0	3.20	2.14	28.63	12	0.113	0.075	1.42	6.34	0.22
C_o = 55 ppm (0.841×10^{-6} mol/cc), $q_o = 0.826 \times 10^{-4}$ mol/g, NaOH = 0.1M									

TABLE A2 Effect of flow rate

f	β	t_m	t_o	$Ka_x x10^{-2}$	Ka_y	N_z	h_{z4}	u_{z3}
2.02	2.70	1.91	0.45	7.52	1.42	1.24	3.64	1.91
2.20	2.63	1.86	0.4	7.51	1.41	1.22	3.70	1.99
2.50	2.91	1.54	0.3	10.04	1.89	1.20	3.77	2.45
2.90	1.96	1.43	0.2	7.31	1.38	1.14	3.95	2.76
3.14	1.84	1.41	-0.2	6.96	1.31	0.86	5.23	3.71
4.12	2.17	2.47	-1.2	4.68	0.88	0.51	8.82	3.57
C_o = 550ppm ($8.41x10^{-6}$ mol/cc), q_o = $2.355x10^{-4}$ mol/g, NaOH = 0.2M, h = 4.5cm.								
3.20	2.14	28.63	12	0.114	0.075	1.42	6.34	0.22
4.90	1.26	14.80	9	0.129	0.085	1.61	5.60	0.38
6.16	2.11	15.67	7	0.204	0.135	1.45	6.22	0.40
8.26	1.57	14.14	4	0.168	0.111	1.28	7.02	0.50
C_o = 55ppm ($0.841x10^{-6}$ mol/cc), q_o = $0.826x10^{-4}$ mol/g, NaOH = 0.1M, h = 9cm.								

TABLE A2 Continued

f	β	t_m	t_o	$Ka_x x10^{-2}$	Ka_y	N_z	h_z	u_{z3}
1.88	2.85	6.14	6.0	1.86	0.46	1.98	8.09	1.32
3.12	2.82	5.37	3.0	2.10	0.53	1.56	10.26	1.91
5.30	2.35	3.95	0.5	2.38	0.60	1.13	14.20	3.60
8.11	1.46	3.24	-0.5	1.80	0.45	0.85	17.74	5.47
11.42	1.67	2.76	-0.7	2.40	0.60	0.75	20.10	7.28
14.28	1.87	2.40	-0.8	3.12	0.78	0.67	22.50	9.38
20.89	1.98	2.16	-1.0	3.68	0.92	0.54	27.93	12.93

C_o = 368.5ppm ($5.635x10^{-6}$ mol/cc), q_o = 2.095×10^{-4} mol/g, NaOH = 0.2M, h = 15cm.

TABLE A3 Effect of particle size

d_p	f	β	t_m	t_o	$Ka_x x10^{-2}$	Ka_y	N_z	h_{z4}	u_{z3}
0.521	5.15	1.36	13.63	2.0	0.15	$9.95x10^{-2}$	1.15	5.23	0.38
0.550	4.54	1.48	14.75	0.5	0.15	$10.05x10^{-2}$	1.03	5.80	0.39
0.655	4.59	1.26	17.35	0.0	0.11	$7.37x10^{-2}$	1.00	6.00	0.35
0.855	5.05	1.06	14.54	0.0	0.11	$7.29x10^{-2}$	1.00	6.00	0.41
C_o = 55 ppm, NaOH = 0.1M, h = 6 cm.									
0.400	2.66	3.13	2.38	-1.0	7.01	1.32	0.58	7.76	3.26
0.521	2.90	1.96	1.43	0.2	7.31	1.38	1.14	3.95	2.76
0.550	2.76	1.97	1.40	0.0	7.49	1.41	1.00	4.50	3.21
0.655	2.52	1.99	1.70	-0.2	6.22	1.17	0.88	5.10	3.00
0.855	2.86	1.55	1.43	-0.1	5.74	1.08	0.93	4.84	3.38

C_o = 550 ppm, NaOH = 0.2M, h = 4.5 cm.

TABLE A4 Effect of initial zinc ion concentration

C_o	f	β	t_m	t_o	$Ka_x x10^{-2}$	Ka_y	N_z	h_{z4}	u_{z3}
352.0	2.44	1.86	2.39	0.55	4.15	0.78	1.23	3.66	1.53
401.5	2.34	1.79	2.33	0.40	3.77	0.77	1.17	3.85	1.65
451.0	2.27	1.91	2.14	0.35	3.98	0.89	1.16	3.87	1.81
500.5	2.45	2.20	1.95	0.35	4.68	1.12	1.18	3.32	1.70
550.0	2.39	2.02	1.78	0.30	4.44	1.14	1.34	3.37	1.89
h = 4.5cm, NaOH = 0.2M.									
275.0	2.96	2.03	7.49	10.5	0.92	0.27	2.40	9.37	1.25
319.0	3.03	1.21	5.15	9.0	0.87	0.24	2.75	8.19	1.59
368.5	2.94	2.35	5.30	8.5	1.76	0.44	2.60	8.65	1.63
440.0	3.09	1.35	7.47	6.5	0.79	0.18	1.87	12.00	1.61
550.0	2.98	2.20	6.03	5.0	1.91	0.36	1.83	12.30	2.04

h = 22.5 cm., NaOH = 0.1M.

TABLE A5 Effect of Caustic concentration

NaOH (M)	f (ml/min)	β	t_m (hrs)	t_o (hrs)	Ka_y (hr^{-1})	N_z	h_{z4} (cm)	u_{z3} (cm/hr)
0.30	2.82	2.80	6.2	0	0.45	1	15.0	2.42
0.35	2.93	4.45	4.5	0	0.99	1	15.0	3.33
0.40	2.83	3.77	5.7	-2	0.66	0.65	23.1	4.05
0.45	2.87	2.57	5.1	-2	0.50	0.61	24.6	4.82
0.50	3.10	2.37	3.3	-1.5	0.72	0.55	27.3	8.26

C_o = 412.5 ppm, h = 15 cm.

TABLE A6 Effect of impurity (lead ion concentration)

a. For Zn

Pb concen.	f	β	t_m	t_o	Ka_y	N_z	h_{z4}	u_{z3}
75	2.35	2.49	1.83	-0.3	1.36	0.84	5.36	2.93
169	2.04	1.75	2.02	-0.6	0.87	0.70	6.43	3.18
300	2.03	1.73	2.08	-0.5	0.83	0.76	5.92	2.85
394	2.30	1.70	2.04	-0.6	0.83	0.71	6.34	3.11
694	2.24	2.25	2.32	-1.0	0.97	0.57	7.89	3.40

b. For Pb.

75	2.35	2.91	2.11	0.0	1.37	1.00	4.50	2.13
169	2.04	2.68	2.07	0.0	1.30	1.00	4.50	2.17
300	2.03	2.94	1.89	0.1	1.56	1.03	4.35	2.30
394	2.30	2.97	1.49	0.0	1.99	1.00	4.50	3.01
694	2.24	3.42	1.68	-0.5	2.04	0.70	6.43	3.83

C_o = 483 ppm, NaOH = 0.4M, h = 4.5 cm.

TABLE A7 Effect of temperature

T (^{o}C)	f (ml/min)	β	t_m (hrs)	t_o (hrs)	$Ka_x X10^{-2}$ (hr^{-1})	Ka_y (hr^{-1})	N_z	h_{z4} (cm.)	u_{z3} (cm/hr)
24	2.22	3.56	2.43	-0.10	7.81	1.47	0.96	2.92	1.20
32	2.10	2.99	2.05	0.50	7.75	1.46	1.24	2.26	1.10
41	2.12	2.80	2.13	0.75	6.99	1.32	1.35	2.07	0.97
50	2.10	2.15	1.81	1.50	6.31	1.19	1.83	1.53	0.85

C_o = 550 ppm, NaOH = 0.2M, h = 2.8 cm.

TABLE A8 Data for Figure 16

C_o	ppm	55	550	550
NaOH	M	0.1	0.2	0.2
h	cm	6.9	6.9	2.8
T	^oC	20	20	50
f	ml/min	3.05	2.70	2.10
C/C_o	$\ln C_o/C_o-C$	$t-t_o$	$t-t_o$	$t-t_o$
0.05	0.050	4.75	1.43	0.45
0.10	0.105	7.00	1.67	0.63
0.20	0.223	11.00	2.00	0.91
0.30	0.357	13.50	2.22	1.12
0.40	0.511	16.00	2.43	1.33
0.50	0.693	18.25	2.59	1.52
0.60	0.916	21.00	2.75	1.70
0.70	1.200	25.00	2.99	1.91
0.75	1.386	29.25	-	-
0.80	1.61	-	3.20	2.25
0.90	2.30	-	3.50	2.75
0.95	3.0	-	3.80	3.20

A P P E N D I X II B

Analysis through Michaels method

TABLE B 1 Effect of flow rate, h=4.5cm and C_o=550ppm.

$U_L x 10^{-2}$	F	C_T	C_E	h_{z1}	h_{z2}	$u_z x 10^{-4}$	u_L/u_z
1.10	0.42	0.27	0.13	5.30	4.03	4.76	23.1
1.25	0.46	0.26	0.11	5.70	4.95	5.83	21.4
1.45	0.50	0.28	0.08	6.34	6.42	6.25	23.2
1.57	0.28	0.20	0.03	13.40	5.41	7.23	21.7
1.95	0.36	0.24	0.025	11.20	6.27	7.18	27.2
2.06	0.38	0.25	0.02	10.90	6.57	7.54	27.3

V_R = 15 ml., d_p = 0.521mm., R.T. = 20°C

TABLE B 2 Effect of flow rate, h=15cm and C_o=368.5ppm.

$u_L x10^{-2}$	F	C_T	C_E	h_{z1}	h_{z2}	$u_z x10^{-4}$	u_L/u_z
0.94	0.43	0.26	0.193	10.2	8.2	2.83	33.2
1.56	0.30	0.30	0.192	17.4	7.9	3.28	47.6
2.65	0.20	0.28	0.109	43.4	11.3	3.41	77.6
4.06	0.31	0.23	0.021	36.9	14.1	10.10	40.2
5.71	0.33	0.24	0.029	40.7	21.6	9.41	60.7
7.14	0.28	0.26	0.037	47.1	20.7	9.98	71.5
10.45	0.23	0.24	0.027	60.6	18.2	15.53	67.3

(V_R = 50 ml., d_p = 0.521 mm., R.T. = 20°C).

A P P E N D I X II C

Analysis through Moison and O'Hern method

TABLE C 1 Effect of bed height on the height of transfer unit

h	f	C_o	u_L	V_z	h_{z3}	NTU	HTU	$K_L a x 10^{-2}$
4.5	2.90	550	0.01272	359.6	1.58	7.11	0.222	5.73
5.4	2.83		0.01241	336.8	1.48		0.208	5.97
6.0	3.15		0.01382	548.1	2.41		0.339	4.08
6.9	2.70		0.01184	364.5	1.61		0.226	5.24
7.5	2.83		0.01241	506.6	2.23		0.314	3.95
8.4	3.09		0.01355	599.5	2.64		0.371	3.65
9.0	3.23		0.01417	532.9	2.35		0.331	4.28
9.9	2.89		0.01267	497.1	2.19		0.308	4.11
10.5	2.91		0.01276	439.4	1.94		0.273	4.67
22.5	2.98		0.01307	1611.9	7.09		0.997	1.31

TABLE C 1 Continued

h	f	C_o	u_L	V_z	h_{z3}	NTU	HTU	$K_L a x 10^{-2}$
4.5	2.97	275	0.01303	854.1	1.89	6.58	0.287	4.54
5.4	2.89		0.01268	1011.5	2.23		0.339	3.74
6.9	2.87		0.01259	1206.9	2.66		0.404	3.12
8.4	2.77		0.01215	1267.3	2.88		0.426	2.85
9.9	2.97		0.01303	1314.3	2.90		0.441	2.95
4.5	3.65	55	0.01601	2956.5	1.31	2.79	0.470	3.41
5.1	3.05		0.01338	3522.7	1.56		0.559	2.39
6.0	3.53		0.01548	3685.3	1.63		0.584	2.65
6.9	3.05		0.01338	5856.0	2.59		0.928	1.44
9.0	3.20		0.01404	6528.0	2.88		1.032	1.36

TABLE C 2 Effect of flow rate on the height of transfer unit

Re $x10^{-2}$	h	f	u_L	C_o	V_z	h_{z3}	NTU	HTU	$K_L a x10^{-2}$
4.86	4.5	2.20	0.00965	550	300.3	1.32	7.11	0.186	5.19
5.28		2.39	0.01048		351.3	1.55		0.218	4.81
5.52		2.50	0.01096		302.5	1.33		0.187	5.86
6.40		2.90	0.01272		358.1	1.58		0.222	5.73
6.93		3.14	0.01377		436.5	1.92		0.276	4.99
8.61		3.90	0.01710		573.3	2.52		0.355	4.82
9.10		4.12	0.01807		556.2	2.45		0.345	5.24
7.22	9.0	3.20	0.01404	55	10752.0	4.75	5.926	0.802	1.75
11.05		4.90	0.02149		13156.5	5.81		0.980	2.19
13.89		6.16	0.02702		14691.6	6.49		1.095	2.47
18.63		8.26	0.03623		20443.5	9.03		1.524	2.38

TABLE C 2 Continued

$Rex10^{-2}$	h	f	u_L	C_o	V_z	h_{z3}	NTU	HTU	$K_L ax10^{-2}$
4.15	15.0	1.88	0.00825	368.5	823.4	2.43	6.73	0.362	2.28
6.89		3.12	0.01368		1628.6	4.81		0.715	1.91
11.17		5.30	0.02325		3625.2	10.71		1.591	1.46
17.91		8.11	0.03557		2676.3	7.91		1.175	3.03
25.22		11.42	0.05009		3368.9	9.96		1.479	3.39
31.53		14.28	0.06263		4041.2	11.94		1.775	3.53
46.17		20.89	0.09162		4052.7	11.98		1.780	5.15

TABLE C 3 Effect of feed concentration on the height of transfer unit

C_o	h	f	u_L	V_z	h_{z3}	NTU	HTU	$K_L a \times 10^{-2}$
0.01682	4.5	2.39	0.01048	351.3	1.55	7.11	0.218	4.81
0.01531	4.5	2.45	0.01075	352.8	1.41	6.94	0.203	5.30
0.01379	4.5	2.27	0.00996	370.0	1.34	6.83	0.196	5.08
0.01228	4.5	2.34	0.01026	472.7	1.52	6.79	0.224	4.58
0.01076	4.5	2.44	0.01070	540.5	1.52	6.79	0.224	4.78
0.01682	4.5	2.90	0.01272	359.6	1.58	7.11	0.222	5.73
0.00841	4.5	2.97	0.01303	854.1	1.89	6.58	0.287	4.54
0.01682	5.4	2.83	0.01241	336.8	1.48	7.11	0.208	5.79
0.00841	5.4	2.89	0.01268	1011.5	2.23	6.58	0.339	3.74
0.01682	6.9	2.70	0.01184	364.5	1.61	7.11	0.226	5.24
0.00841	6.9	2.87	0.01259	1206.9	2.66	6.58	0.404	3.12
0.01682	9.9	2.89	0.01267	497.1	2.19	7.11	0.308	4.11
0.00841	9.9	2.97	0.01303	1314.3	2.90	6.58	0.441	2.95

C_o in meq./ml.

A P P E N D I X II D

Moving bed

TABLE D1 Influence of caustic concentration

Run No	h (cm)	NaOH (M)	R_f (ml/min)	R_p (ml/min)	Percent removed	NTU	HTU (cm)	N_C	Ka_M (min^{-1})
5.1	12	0.1	19.45	0.102	91.20	3.06	3.92	1.81	3.26
5.2	8	0.2	18.50	0.184	62.76	1.00	8.00	0.64	1.53

C_o = 55 ppm

TABLE D2 Influence of solution flow rate

Run No	R_F	R_p	Percent removed	NTU	HTU	N_C	Ka_M
5.5	3.62	0.300	94.06	2.96	2.70	0.96	0.88
5.6	5.55	0.291	95.00	3.10	2.58	1.58	1.41
5.7	7.05	0.302	89.57	2.35	3.40	1.73	1.36
h = 8 cm, C_o = 550 ppm							
5.11	7.02	0.294	99.57	10.49	2.29	2.00	2.02
5.18	9.14	0.295	98.16	5.70	4.21	3.90	1.43
h = 24 cm, C_o = 550 ppm							

TABLE D3 Influence of bed height

Run No.	h	R_F	R_p	Percent removed	NTU	HTU	N_C	Ka_M
5.7	8	7.05	0.302	89.57	2.35	3.40	1.73	1.36
5.8	12	6.90	0.298	96.05	3.49	3.44	1.86	1.32
5.9	16	7.03	0.297	98.10	4.64	3.45	1.94	1.34
5.10	20	7.00	0.292	98.71	5.43	3.68	1.94	1.25
5.11	24	7.02	0.294	99.57	10.49	2.29	2.00	2.02

C_o = 550 ppm, C_Σ = 0.21682 meq/ml.

TABLE D4 Influence of initial zinc ion concentration

Run No	C_o	R_F	R_p	Percent removed	NTU	HTU	N_c	Ka_M
5.15	275	9.94	0.315	97.57	6.56	3.05	1.82	2.15
5.16	330	9.97	0.315	94.73	3.56	5.62	1.73	1.17
5.17	412.5	10.06	0.314	90.78	2.61	7.66	1.72	0.86
5.13	550	10.19	0.315	77.40	1.65	12.12	1.48	0.55
h = 20 cm.								
5.23	412.5	7.07	0.331	99.57	21.41	1.12	2.00	4.15
5.24	495	7.00	0.331	99.52	16.78	1.43	2.00	3.22
5.21	550	7.11	0.317	97.70	4.89	4.91	1.90	0.95
h = 24 cm.								

TABLE D5 Influence of cycle time

Run No	Cycle time	R_p	R_F	h	Percent removed	NTU	HTU	N_C	Ka_M
5.11	30	0.294	7.02	24	99.57	10.49	2.29	2.00	2.02
5.19	45	0.417	7.11	24	97.79	4.59	5.23	1.75	0.89
5.21	100	0.317	7.11	24	97.70	4.89	4.91	1.90	0.95
5.22	120	0.276	7.05	24	93.66	3.05	7.87	1.82	0.59
5.25	120	0.335	7.09	30	99.30	11.28	2.66	2.00	1.75

C_o = 550 ppm.

TABLE D6 Influence of resin renewal

Run No	Volume renewed per cycle	R_p	R_F	h	Percent removed	NTU	HTU	N_c	Ka_M
5.12	20	0.328	10.19	20	84.53	2.16	9.26	1.83	0.72
5.13	10	0.315	10.19	20	77.40	1.65	12.12	1.48	0.55
5.20	5	0.383	6.85	24	97.58	3.96	6.06	1.77	0.74

C_o = 550 ppm.

A P P E N D I X III

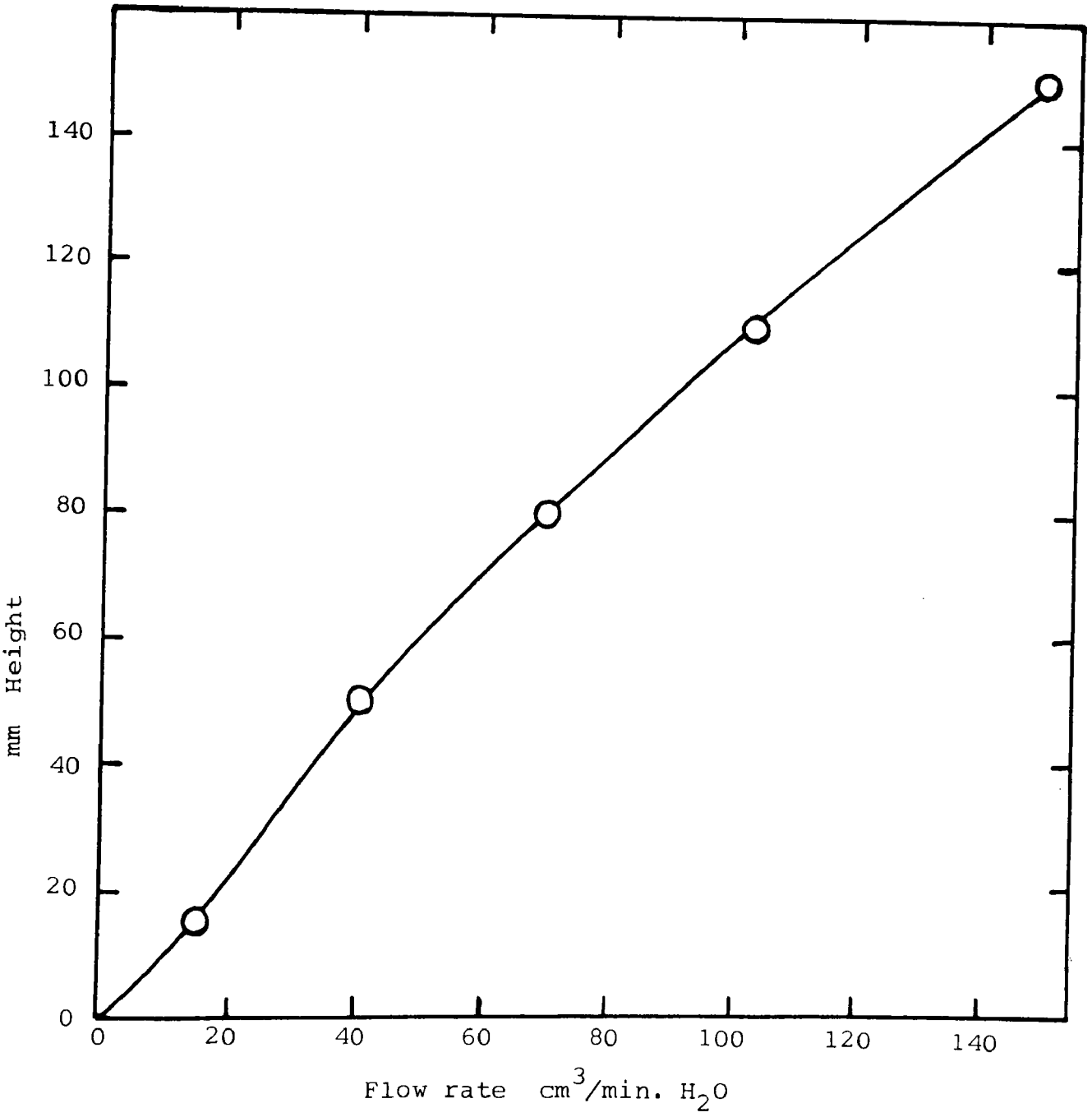

Figure A3.1 Flowmeter calibration graph

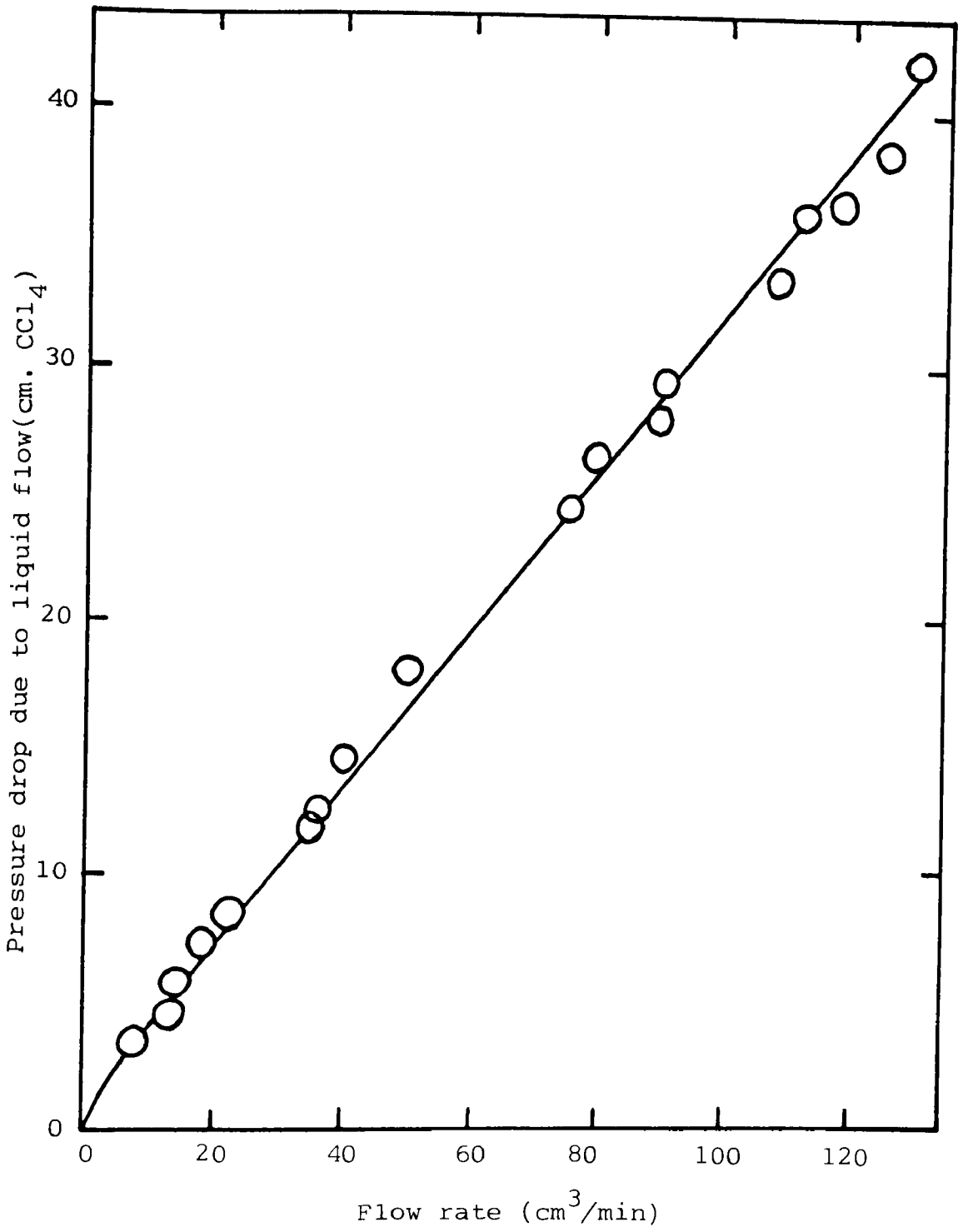

Figure A3.2 Pressure drop as a function of flow rate

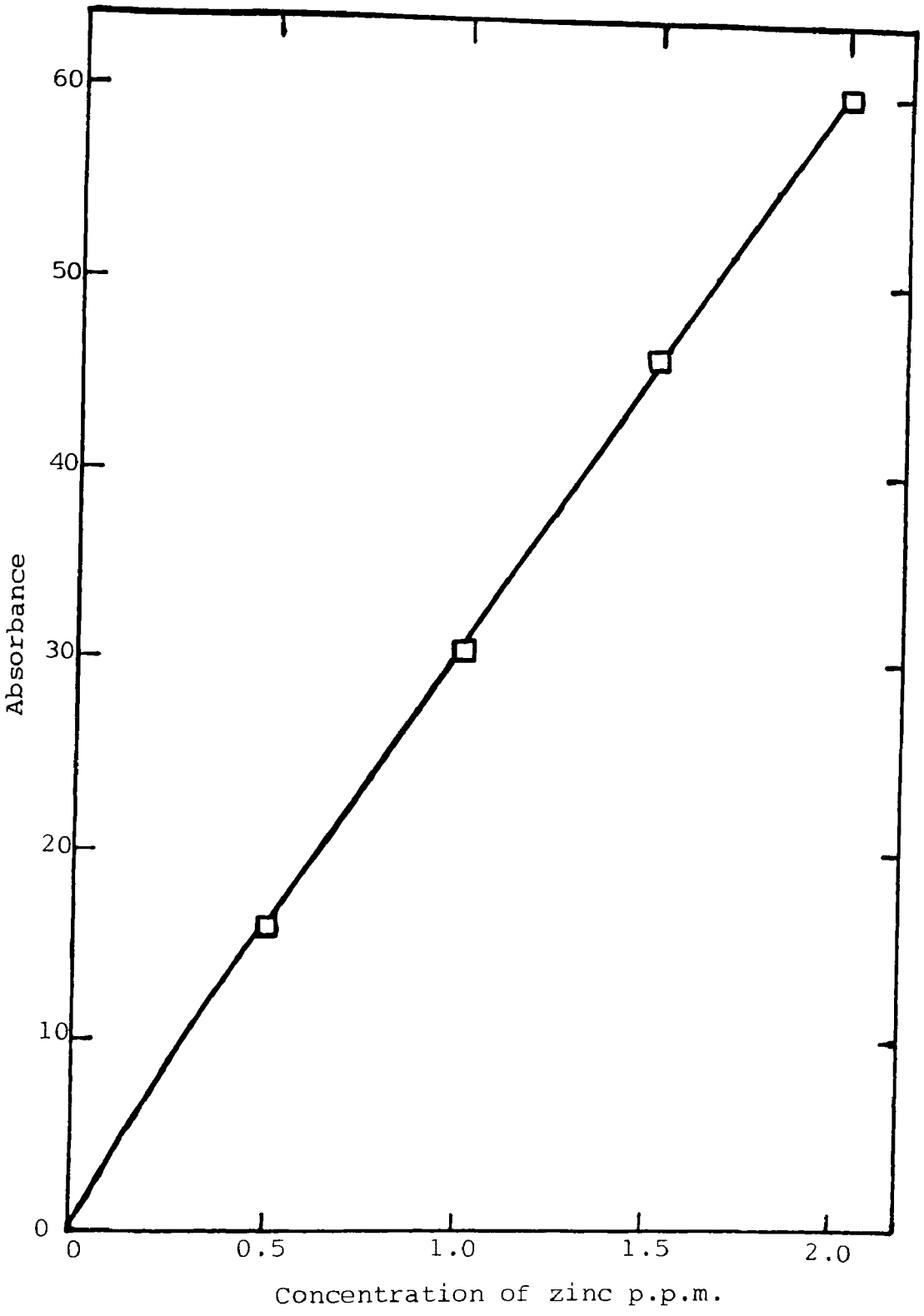

Figure A3.3 Calibration curve for zinc analysis by atomic absorption spectroscopy

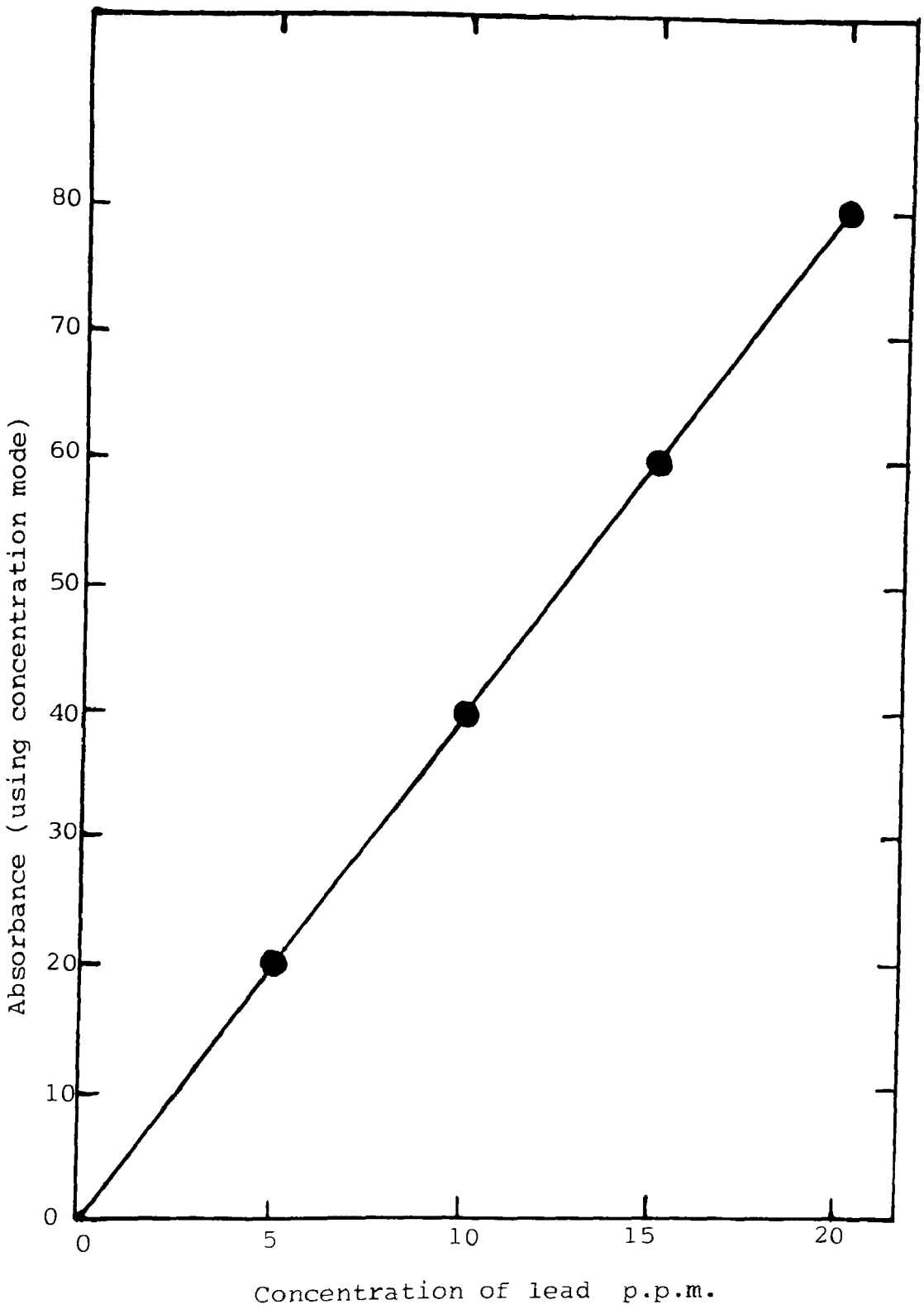

Figure A3.4 Calibration curve for lead analysis atomic absorption spectroscopy

Atomic Absorption Spectrophotometer 1275

This instrument gives the concentration of the metal ion directly and for the sake of simplicity, the operating instructions are numerated below.

(1) De-ionised water was used for aspiration.

(2) The required lamp was inserted and its current, band slit and wavelength were selected.

(3) The power was switched on and the instrument left to warm up for 15 minutes.

(4) The air was switched on and the pressure adjusted to 50 p.s.i. by holding the air trap nozzle with a finger and releasing it until stablized.

(5) The fan was switched on.

(6) The acetylene cylinder was turned on followed by pressing SET FLOW and observing the Oxidant/Fuel readings (oxidant was 20 and Fuel 5).

(7) The flame was ignited by touching FLAME ON.

(8) The wavelength was adjusted to read maximum transmission with the two knobs on the lamp. The deflection was brought back on the scale by pressing GAIN.

(9) The flame was optimized with the 2 p.p.m. standard to

give a reading value of approximately 0.5 by adjusting the horizontal, vertical and the X-Y plane position of the burner.

(10) The standards were aspirated in ascending order followed by pressing CONC. They were then recalled by pressing CAL STD 1, STD 2 and STD 3 and the calibration was checked with the 1.5 p.p.m. standard. During measurement, the instrument was checked with the 1 p.p.m. standard and if its reading value was higher or lower than 1, CAL RESLOPE was pressed thus automatic calibration.

(11) When the background was noisy (i.e. the read value was fluctuating), the buttons RUN MEAN, TIME SEC, and READ were pressed thus giving mean read values over a period of 1 second or more as required. The read was then returned to zero by pressing INT REPEAT.

(12) At the end of measurement, approximately 50ml. de-ionised water was aspirated followed by switching off the flame.

(13) The acetylene cylinder was turned off(on the small gauge acetylene read 5).

(14) The air was switched off followed by pressing the AIR button until the reading indicated a zero value (also the air gauge read zero).

(15) Finally the fan and power were switched off.

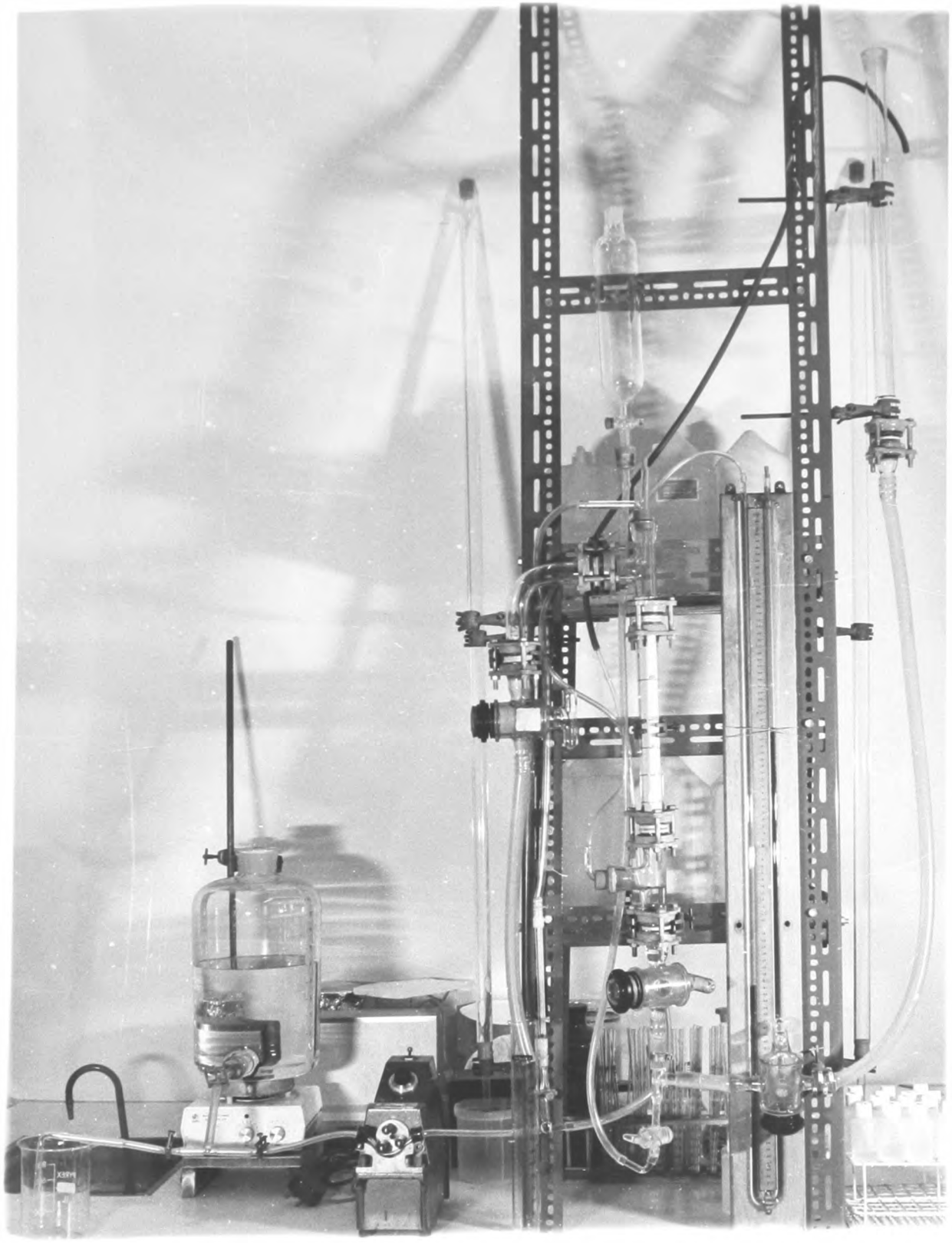

MOVING BED
APPARATUS